

**CONVERSION OF EUCALYPTUS WOOD CHIP TO SUGARS AND CHEMICALS:  
DEVELOPMENT OF ORGANOSOLV FRACTIONATION, HYDROLYSIS  
AND DEPOLYMERIZATION PROCESSES**

**MR. THEPPARAT KLAMRASSAMEE**

**ID: 53920009**

**A THESIS SUBMITTED AS A PART OF THE REQUIREMENTS  
FOR THE DEGREE OF DOCTOR OF PHILOSOPHY  
IN ENERGY TECHNOLOGY**

**THE JOINT GRADUATE SCHOOL OF ENERGY AND ENVIRONMENT  
AT KING MONGKUT'S UNIVERSITY OF TECHNOLOGY THONBURI**

**1<sup>ST</sup> SEMESTER 2014**

**COPYRIGHT OF THE JOINT GRADUATE SCHOOL OF ENERGY AND ENVIRONMENT**

Conversion of Eucalyptus Wood Chip to Sugars and Chemicals: Development of Organosolv Fractionation, Hydrolysis and Depolymerization Processes

Mr. Thepparat Klamrassamee

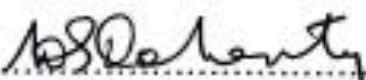
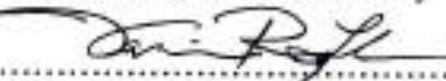
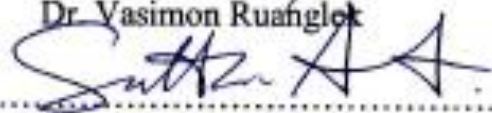
ID: 53920009

A Thesis Submitted as a Part of the Requirements  
for the Degree of Doctor of Philosophy  
in Energy Technology

The Joint Graduate School of Energy and Environment  
at King Mongkut's University of Technology Thonburi

1<sup>st</sup> Semester 2014

Thesis Committee

 ..... ( Assoc. Prof. Dr. Navadol Laosiripojana )	Advisor
 ..... ( Prof. Dr. William O.S. Doherty )	Co-Advisor
 ..... ( Dr. Vasimon Ruanglek )	Member
 ..... ( Prof. Dr. Suttichai Assabumrungrat )	Member
 ..... ( Dr. Verawat Champreda )	Member
 ..... ( Dr. Wisitsree Wiyaratn )	Member
 ..... ( Prof. Dr. Motonobu Goto )	External Examiner

**Thesis Title:** Conversion of Eucalyptus Wood Chip to Sugars and Chemicals:  
Development of Organosolv Fractionation, Hydrolysis and Depolymerization Processes

**Student's name, organization and telephone/fax numbers/email**

Mr. Thepparat Klamrassamee  
The Joint Graduate School of Energy and Environment (JGSEE)  
King Mongkut's University of Technology Thonburi (KMUTT)  
126 Pracha Uthit Rd., Bangmod, Tungkru, Bangkok 10140, Thailand  
Telephone: 0-91-551-2329  
Email: [deknaw8989@gmail.com](mailto:deknaw8989@gmail.com)

**Advisor's name, organization and telephone/fax numbers/email**

Assoc. Prof. Dr. Navadol Laosiripojana  
The Joint Graduate School of Energy and Environment (JGSEE)  
King Mongkut's University of Technology Thonburi (KMUTT)  
126 Pracha Uthit Rd., Bangmod, Tungkru, Bangkok 10140, Thailand  
Telephone: 02-872-6736 ext 4146  
Email: [navadol\\_1@jgsee.kmutt.ac.th](mailto:navadol_1@jgsee.kmutt.ac.th)

**Co-Advisor's name, organization and telephone/fax numbers/email**

Prof. Dr. William O.S. Doherty  
Centre for Tropical Crops and Biocommodities  
Queensland University of Technology (QUT)  
GPO Box 2434, Brisbane Q4001, Australia  
Telephone: + 61 7 3138 1245  
Email: [w.doherty@qut.edu.au](mailto:w.doherty@qut.edu.au)

**Topic:** Conversion of Eucalyptus Wood Chip to Sugars and Chemicals: Development of Organosolv Fractionation, Hydrolysis and Depolymerization Processes

**Name of student:** Mr. Thepparat Klamrassamee

**Student ID:** 53920009

**Name of Advisor:** Assoc. Prof. Dr. Navadol Laosiripojana

**Name of Co-Advisor:** Prof. Dr. William O.S. Doherty

## ABSTRACT

This research focuses on the fractionation, hydrolysis and lignin depolymerization of woody eucalyptus. Fractionation of lignocellulosic biomass is a primary step for converting multi-structure biomass into biofuels and other industrial products in integrated biorefinery processes. Here, the effects of homogeneous and heterogeneous acid promoters ( $\text{HNO}_3$ -,  $\text{HCl}$ -,  $\text{H}_2\text{SO}_4$ -, and  $\text{H}_3\text{PO}_4$ -activated carbons) on a single-step aqueous organosolv fractionation of eucalyptus wood chips were studied and optimized. The optimized process contained 16.7% w/v biomass in a ternary mixture of methyl isobutyl ketone:methanol:water (25:42:33) with 5% AC- $\text{H}_3\text{PO}_4$  and incubated at 180 °C for 60 min. Under these conditions, 41.2 wt.% cellulose was obtained in enriched solid pulp with the average glucan content of 75.9%. The majority of the hemicelluloses was hydrolysed into the aqueous-methanol phase, which contained 17.8 wt.% monomeric xylose and xylooligomers while 13.7 wt.% lignin was separated into the organic phase. The heterogeneous acid-promoter process is a potent alternative to corrosive homogeneous acids for lignocellulose fractionation in integrated biorefineries. Then, catalytic hydrolysis of woody eucalyptus with sulfonated carbon-based (SCB) catalysts prepared from three different carbon precursors (*i.e.* xylose, glucose, sucrose, and activated carbon) was studied under hot-compressed water (HCW). It was found that the reaction with sulfonated-sucrose shows the greatest performance, from which highest  $\text{C}_5$  and  $\text{C}_6$  sugar yields with less formation of unwanted by-products (*i.e.* furans, and 1,6-anhydroglucose (AHG)) were achieved at 200°C with 5 min reaction time. Furthermore, alkaline pretreatment and/or organosolv fractionation prior to the catalytic hydrolysis in the presence of SCB catalyst significantly improved the catalytic hydrolysis activity due to efficiently remove lignin, reduce hemicellulose and destroy the structure of cellulose. Apart from SCB catalysts, AC- $\text{H}_3\text{PO}_4$  (an acid promoter for organosolv fractionation) also showed great hydrolysis performance under HCW, from which high sugar yields with low unwanted by-product

formations can be achieved at 220°C with 5 min reaction time. The great benefit of AC-H<sub>3</sub>PO<sub>4</sub> is its possible use for both organosolv fractionation (as acid promoter) and hydrothermal hydrolysis (as acid catalyst), which provides potential for combining fractionation and hydrolysis processes without intermediate material treatment required.

For the lignin proportion, organosolv lignin (OL) obtained from the fractionation was further purified and the solubility upgraded by the alkaline precipitation process (as called treated organosolv lignin; TOL). From the study, TOL was found to enhance higher solubility in organic solvents (*i.e.* tetrahydrofuran (THF), dimethyl sulfoxide (DMSO), and methanol) than OL. Furthermore, the results of the compositional analysis revealed that OL contained small amounts of contaminations (*e.g.*, sugars, ash and sulfur), which came from the degradation of eucalyptus wood chips and H<sub>2</sub>SO<sub>4</sub> during the fractionation. After alkaline precipitation treatment, most of these contaminations were efficiently removed without causing any significant structural change, as confirmed by XPS and solid-state NMR analyses. The results of molecular weight and TGA analyses indicated high molecular weight and high residue solid of OL and TOL, which probably specifies the presence of condensed lignin. Lastly, FTIR spectra proved the presence of base insoluble lignin (BIL) contaminants in OL and also confirmed that the alkaline re-precipitation process enables removal of these contaminants without causing significant structural change to the lignin. Then, the depolymerization of TOL was studied at several temperatures and solvent systems (water and methanol-water) with and without the presence of several mesostructured silica catalysts (*i.e.* SBA-15, MCM-41, ZrO<sub>2</sub>-SBA-15 and ZrO<sub>2</sub>-MCM-41) and phosphate-based catalysts (*i.e.* CoP<sub>2</sub>O<sub>6</sub>, and CaP<sub>2</sub>O<sub>6</sub>) The optimum conditions were observed at 300°C using water/methanol (50:50, wt/wt) as solvent in the presence of high acidity SBA-15, from which total syringol yield of 23 wt.% (7.2 wt.% in aqueous fraction and 15.8 wt.% in residual lignin) can be achieved. From GC/MS analysis, the main components in aqueous fraction from the reaction in the presence of SBA-15 included high proportion of syringol (72.1 wt.%) with slight formations of 1,2-benzenediol, benzaldehyde, and ethanone, whereas the main components extracted from residual lignin were syringol (17.2 wt.%) with other multi-compound mixture of polymeric phenolic compounds and high molecular weight of lignin. For the reaction catalyzed by phosphate based catalysts, the optimize condition can be achieved by using CaP<sub>2</sub>O<sub>6</sub> at 300 °C for 1 h with methanol/water mixture (50/50, wt/wt), from which total syringol yield of 16.7 wt.% can be obtained without char formation. The phenol

products mainly consisted of five phenols: syringol, 1,2-benzendiol, benzoic acid, benzaldehyde, and ethanone.

**Keywords:** Organosolv fractionation, Hydrolysis, Depolymerization, Hot compressed water, Phosphate based catalyst, Mesostructured silica

## ACKNOWLEDGEMENTS

This thesis would never have been completed without the help and support of many others who are gratefully acknowledged here. Firstly, I would like to express my sincere gratitude to Assoc. Prof. Dr. Navadol Laosiripojana and Prof. Dr. William O.S. Doherty, my advisor and my co-advisor, respectively, for their suggestions, guidance, warm encouragement and generous supervision throughout my graduate studies. I also would like to thank Dr. Verawat Champreda, Dr. Vasimon Ruanglek, Prof. Dr. Suttichai Assabumrungrat, and Dr. Wisitsree Wiyaratn who are my committee members for their comments, and also to the external examiner, Prof. Dr. Motonobu Goto. I acknowledge the financial support from Thailand Research Fund (TRF), the Royal Golden Jubilee scholarship, and the Joint Graduate School of Energy and Environment (JGSEE).

Finally, I would like to thank the Centre for Tropical Crops and Biocommodities at Queensland University of Technology (QUT), Brisbane, Australia for providing the services and facilities during my stay there.

## CONTENTS

CHAPTER	TITLE	PAGE
	ABSTRACT	i
	ACKNOWLEDGEMENT	iv
	CONTENTS	v
	LIST OF TABLES	xii
	LIST OF FIGURES	xiv
1	INTRODUCTION	1
	1.1 Rationale	1
	1.2 Research objectives	6
	1.3 Overview of Chapters	7
2	LITERATURE REVIEW	9
	2.1 Physical and chemical characteristics of lignocellulosic biomass	9
	2.1.1 Composition	9
	2.2 Internal structure - physical and chemical properties	11
	2.2.1 Cellulose	11
	2.2.2 Hemicellulose	12
	2.2.3 Lignin	14
	2.3 Chemical interaction	16
	2.3.1 Intrapolymer linkages	16
	2.3.2 Functional groups/linkages in lignocellulosic structure	16
	2.3.3 Functional groups in lignocellulosic structure	17
	2.4 Lignocellulose biorefinery	18
	2.5 Lignocellulose pretreatment techniques	20
	2.5.1 Physical pretreatment	21
	2.5.2 Physicochemical pretreatment	21
	2.5.2.1 Steam explosion	21
	2.5.2.2 Liquid hot water (hydrothermal)	21
	2.5.3 Chemical pretreatment	22

**CONTENTS (Cont')**

<b>CHAPTER</b>	<b>TITLE</b>	<b>PAGE</b>
	2.5.3.1 Diluted acid pretreatment	22
	2.5.3.2 Alkali pretreatment	22
	2.5.4 Oxidative pretreatment	23
	2.5.4.1 Alkali peroxide	23
	2.5.4.2 Wet oxidation	23
	2.5.4.3 Ozonolysis	24
	2.5.5 Biological pretreatment	24
	2.5.6 Organosolv pretreatment	24
	2.5.6.1 Solvents and catalysts	25
	2.5.6.2 Mechanisms of organosolv delignification	27
	2.6 Summary of biomass pretreatment	29
	2.7 Lignocellulose hydrolysis techniques	30
	2.7.1 Acid hydrolysis	32
	2.7.1.1 Dilute acid hydrolysis	32
	2.7.1.2 Concentrated acid hydrolysis	32
	2.7.1.3 Acid hydrolysis by solid catalysts	32
	2.7.1.4 Alkaline hydrolysis	36
	2.7.1.5 Enzymatic hydrolysis	36
	2.7.1.6 Hot-compressed water (HCW)	36
	2.7.1.7 Comparison of various hydrolysis processes	43
	2.8 Isolation of lignin from lignocelluloses	45
	2.9 Lignin conversion process overviews	47
	2.10 Lignin depolymerization techniques	48
	2.10.1 Base-catalyzed lignin depolymerization	48
	2.10.2 Acid-catalyzed lignin depolymerization	50
	2.10.3 Solid catalyzed lignin depolymerization	50
3	<b>METHODOLOGY</b>	52
	3.1 Raw materials	52

**CONTENTS (Cont')**

<b>CHAPTER</b>	<b>TITLE</b>	<b>PAGE</b>
	3.2 Preparation of solid acid promoters for fractionation process	52
	3.3 Preparation of sulfonated carbon-based catalysts for hydrolysis process	53
	3.4 Preparation of acid catalysts for lignin depolymerization process	54
	3.4.1 Mesoporous silica	54
	3.4.2 Phosphate-based catalyst	54
	3.5 Experimental method	55
	3.5.1 Procedure for fractionation	57
	3.5.2 Procedure for hydrolysis reaction in HCW	58
	3.5.3 Procedure for lignin solubility testing and upgrading by alkaline precipitation process	58
	3.5.4 Procedure for lignin depolymerization	59
	3.6 Liquid product analysis	61
	3.6.1 Sugar products	61
	3.6.2 Phenolic compound products	61
	3.7 Characterization of promoters and catalysts	62
	3.7.1 BET surface area	62
	3.7.2 Temperature-programmed desorption (TPD)	62
	3.8 Characterization of isolated lignins	62
	3.8.1 Elemental analysis	62
	3.8.2 Klason lignin determination	63
	3.8.3 Mannich Reaction	63
	3.8.4 Molecular weight determination	63
	3.8.5 Thermal gravimetric analysis (TGA)	64
	3.8.6 X-ray photoelectron spectroscopy (XPS) analysis	64
	3.8.7 Solid-state nuclear magnetic resonance (NMR)	64
	3.8.8 Fourier transform-Infrared spectroscopy	64

**CONTENTS (Cont')**

<b>CHAPTER</b>	<b>TITLE</b>	<b>PAGE</b>
4	SINGLE-STEP AQUEOUS-ORGANOSOLV FRACTIONATION OF WOODY EUCALYPTUS WITH AND WITHOUT THE PRESENCE OF HOMOGENEOUS AND HETEROGENEOUS ACID PROMOTERS	66
	Chapter highlights	66
	4.1 Background	67
	4.2 Results and discussion	69
	4.2.1 Solid promoter characterization	69
	4.2.2 Effects of solvents and acid promoters on fractionation of eucalyptus wood chips	70
	4.2.3 Effect of operating conditions on fractionation of eucalyptus wood chips	72
	4.2.4 Solid acid promoters for fractionation of eucalyptus wood chips	77
	4.2.5 Stepwise fractionation and recycling of solid acid promoter	81
	4.3 Conclusion	86
5	ACTIVITIES OF CARBON-BASED ACID CATALYSTS TOWARD HYDROTHERMAL HYDROLYSIS OF RAW, PRETREATED, AND FRACTIONATED EUCALYPTUS	87
	Chapter highlights	87
	5.1 Background	88
	5.2 Results and discussion	89
	5.2.1 Hydrolysis of eucalyptus under HCW with sulfonated carbon-based catalysts	90
	5.2.2 Effect of hydrolysis conditions catalyzed by sulfonated carbon-based catalysts	91

**CONTENTS (Cont')**

<b>CHAPTER</b>	<b>TITLE</b>	<b>PAGE</b>
	5.2.3 Hydrolysis of pretreated and fractionated eucalyptus by H <sub>2</sub> SO <sub>4</sub> -Sucrose	95
	5.2.4 Effect of acid catalysts on the hydrolysis of Eucalyptus	98
	5.2.5 Sequential fractionation/hydrolysis with and without acid promoters	99
	5.2.6 Effect of hydrolysis conditions on the performance/activity of AC-H <sub>3</sub> PO <sub>4</sub>	100
	5.3 Conclusion	110
6	EXAMINE THE POOR SOLUBILITY OF LIGNIN PRODUCED BY A SINGLE-STEP AQUEOUS-ORGANOSOLV FRACTIONATION OF EUCALYPTUS WOOD CHIPS	111
	Chapter highlights	111
	6.1 Background	112
	6.2 Results and discussion	113
	6.2.1 Solubility of isolated lignin	113
	6.2.2 The elemental analysis	114
	6.2.3 Lignin compositions	115
	6.2.4 Mannich Reactivity	116
	6.2.5 Molecular weight distribution	117
	6.2.6 XPS analysis	117
	6.2.7 Thermal characteristics	121
	6.2.8 FTIR analysis of lignin samples	123
	6.2.9 Solid-state nuclear magnetic resonance (NMR)	125
	6.3 Conclusion	128

## CONTENTS (Cont')

CHAPTER	TITLE	PAGE
7	DEPOLYMERIZATION OF ORGANOSOLV LIGNIN FRACTIONATED WOODY EUCALYPTUS UNDER HYDROTHERMAL PROCESS WITH MESOSTRUCTURED SILICA AND PHOSPHATE-BASED CATALYSTS	129
	Chapter highlights	129
	7.1 Background	130
	7.2 Results and discussion	132
	7.2.1 Depolymerization of TOL under hydrothermal process in the presence of mesostructured silica catalysts	133
	7.2.1.1 Effect of catalyst on lignin depolymerization	133
	7.2.1.2 Effect of reaction temperature in the presence of MCM-41 and SBA-15	139
	7.2.1.3 Effect of solvent system in the presence of MCM-41 and SBA-15	143
	7.2.2 Depolymerization of TOL under hydrothermal process in the presence of phosphate -based catalysts	147
	7.2.2.1 Effect of catalyst on lignin depolymerization	147
	7.2.2.2 Effect of reaction temperature in the presence of CaP <sub>2</sub> O <sub>6</sub>	153
	7.2.2.3 Effect of solvent system in the presence of CaP <sub>2</sub> O <sub>6</sub>	158
	7.3 Conclusion	166

**CONTENTS (Cont')**

<b>CHAPTER</b>	<b>TITLE</b>	<b>PAGE</b>
8	SUMMARY AND RECOMMENDATIONS	167
	8.1 Summary	167
	8.2 Recommendations for further studies	171
	REFERENCES	172
	APPENDIX	183

## LIST OF TABLES

<b>TABLE</b>	<b>TITLE</b>	<b>PAGE</b>
2.1	The composition of lignocellulose from different plant origins on dry basis	10
2.2	The linkages between the monomer units in lignocelluloses	17
2.3	Functional groups in lignocellulosic structure	18
2.4	Methods for biomass lignocellulosic pretreatment	29
2.5	Comparison of catalytic properties and activities of solid acid catalysts for cellulose hydrolysis to glucose	34
2.6	The properties of water under different conditions	38
2.7	Comparisons of various hydrolysis techniques under various conditions	44
2.8	Properties of different technical lignins	46
2.9	Step involved in processing lignin	47
2.10	Base-catalyzed lignin depolymerization	50
4.1	N <sub>2</sub> physisorption results of solid acid catalysts	69
4.2	Results from NH <sub>3</sub> - and CO <sub>2</sub> -TPD measurements of carbon-based solid acid catalysts	70
4.3	Composition (wt.%) of the solid fraction	78
5.1	N <sub>2</sub> physisorption (BET) results and acid properties of sulfonated carbon-based catalysts prepared by different carbon precursors	91
5.2	Hydrolysis degradation of substrate (biomass and cellulose) to glucose with solid acid catalysts	109
6.1	Solubility of OL and TOL in organic solvents	114
6.2	Elemental analysis of lignins (wt.%)	115
6.3	Lignin formula and protein content of lignins	115

**LIST OF TABLES (Cont')**

<b>TABLE</b>	<b>TITLE</b>	<b>PAGE</b>
6.4	Composition of lignin samples (wt.%)	116
6.5	Active site of lignins	117
6.6	Average molecular weight of lignin samples	117
6.7	XPS analysis of OL, TOL, and SL	118
6.8	Assignment of lignin samples of FT-IR absorption bands (cm <sup>-1</sup> )	125
6.9	Assignment of lignin signals in the CPMAS <sup>13</sup> C NMR spectra	127
7.1	Specific surface area and acidity of synthesized catalysts	134
7.2	Yield of phenolic monomers at 250°C	138
7.3	Yields of phenolic monomers at 300 °C with methanol/water mixture (50/50, wt/wt)	146
7.4	Yield of phenolic monomers at 250 °C	152
7.5	Solid catalyzed lignin depolymerization	164

## LIST OF FIGURES

FIGURE	TITLE	PAGE
1.1	The composition of lignocellulosic biomass	2
1.2	The pathway of reactions occurring during fractionation and hydrolysis of lignocellulosic material	3
1.3	The diagram of sugar and chemical production via fractionation of biomass, hydrolysis of cellulose and depolymerization of lignin reactions of this research for upgrading lignocellulosic processing industries	6
2.1	Structure of single cellulose molecule	11
2.2	An illustration of the arrangement of the cellulose molecules in parallel chains and the accompanying hydrogen bonding (intra- and inter-chain hydrogen bonding)	12
2.3	Schematic illustration of different types of monomeric sugar units in hemicelluloses structure	13
2.4	Schematic illustration of xylans: (a) Partial xylan structure from hardwood chain. (b) Partial xylan structure from softwood chain	14
2.5	Monolignol units of lignin and respective direct breakdown products of lignin	15
2.6	The linkages individually include $\beta$ -O-4, 4-O-5, $\beta$ - $\beta$ , $\beta$ -1, $\beta$ -5, 5-5, and dibenzodioxocin	15
2.7	Basic steps of biorefinery	19
2.8	Products from lignocellulose biorefinery	19
2.9	Schematic illustration of pretreatment for increasing the accessibility of cellulose to cellulolytic enzymes in subsequent enzymatic hydrolysis stage	20

## LIST OF FIGURES ( Cont' )

FIGURE	TITLE	PAGE
2.10	Schematic representation of an ethanol organosolv pretreatment process	26
2.11	Solvolytic cleavage of $\beta$ - and $\alpha$ -O-aryl ether linkages in lignin	27
2.12	Solvolytic cleavage of $\alpha$ -O-aryl ether linkages and condensation reaction in lignin structure	28
2.13	The products occurring during hydrolysis of lignocellulosic material	31
2.14	Diagram of various hydrolysis technologies	31
2.15	Selected properties of water at high temperature and high pressure. IP = ionic product, expressed as $\log[\text{H}_3\text{O}^+][\text{OH}^-]$ ; $\epsilon$ = relative dielectric constant; a higher $\epsilon$ reduces the activation energy of a reaction with a transition state of higher polarity compared to the initial stage ; $\rho$ = density, defined as mass per unit volume	37
2.16	Mechanism for the conversion of microcrystalline cellulose in subcritical and supercritical water at 25 MPa	39
2.17	Mechanism pathway of xylan in HCW (representative hemicellulose) decomposition	40
2.18	Main reaction pathways of glucose and fructose in HCW	42
2.19	Comparison the various hydrolysis methods to glucose; enzymatic (70 °C, 1.5 days), concentrated acid (30–70% $\text{H}_2\text{SO}_4$ , 40 °C, 2-6 h), diluted acid (<1% $\text{H}_2\text{SO}_4$ , 215 °C, 3 min), HCW (150–250 °C, 10–25 MPa, 0–20 min), and alkaline (18% NaOH, 100 °C, 1 h)	43
2.20	Different lignin isolation processes from lignocellulose and the corresponding productions of technical lignins	46

### LIST OF FIGURES ( Cont')

FIGURE	TITLE	PAGE
3.1	Apparatus setup for catalyst preparation instrument (1: round bottom 4-neck flask, 2: nitrogen inlet, 3: thermometer, 4: connection tube, 5: vacuum pump, 6: flask- contained the activated carbon)	52
3.2	Preparation of sulfonated amorphous carbon from sugars (sucrose, glucose, and xylose) by direct synthesis pathways	53
3.3	The diagram of experimental procedure	56
3.4	The experimental setup apparatus for fractionation and hydrolysis reaction	57
3.5	The diagram of separation the product after lignin depolymerization reaction	60
4.1	Effect of media on lignocellulose fractionation	71
4.2	Effect of H <sub>2</sub> SO <sub>4</sub> concentration (acid promoter) on lignocellulose fractionation	72
4.3	Effect of temperature on lignocellulose fractionation	73
4.4	Effect of time on lignocellulose fractionation	74
4.5	Effect of pressure on lignocellulose fractionation	75
4.6	Effect of ratio of solvent (MIBK:methanol:water) on lignocellulose fractionation	76
4.7	Effect of ratio of eucalyptus wood chips to solvent (g/mL) on lignocellulose fractionation	77
4.8	Effect of heterogeneous acid promoters on fractionation	78
4.9	Effect of promoter amount (% of substrate) on lignocellulose fractionation	79
4.10	Effect of ratio of eucalyptus wood chips to solvent (g/mL) on lignocellulose fractionation in the presence of AC-H <sub>3</sub> PO <sub>4</sub> promoter	80

### LIST OF FIGURES ( Cont' )

<b>FIGURE</b>	<b>TITLE</b>	<b>PAGE</b>
4.11	Stepwise fractionation of eucalyptus wood chips	82
4.12	Reusability of solid promoter of fractionation process	83
5.1	Yield of liquid products from the hydrolysis of eucalyptus at 200°C for 5 min with and without the presence of various catalysts	91
5.2	Effect of reaction temperature on the yield of liquid products from the hydrolysis of eucalyptus in the presence of various catalysts (with the reaction time of 5 min)	92
5.3	Effect of reaction time on the yield of liquid products from the hydrolysis of eucalyptus in the presence of various catalysts at 200°C	92
5.4	Effect of reaction temperature on the yield of liquid products from the hydrolysis of cellulose and xylan in the presence of H <sub>2</sub> SO <sub>4</sub> -Sucrose catalyst (with the reaction time of 5 min)	94
5.5	Effect of eucalyptus particle size on the yield of liquid products and TOC value from the hydrolysis reaction	96
5.6	Effect of eucalyptus pretreatment process (with alkaline) and fractionation on the yield of liquid products	97
5.7	Reusability testing of H <sub>2</sub> SO <sub>4</sub> -Sucrose toward the hydrolysis of pretreated eucalyptus in powder at 200°C	98
5.8	Effect of catalyst activity on the sugar yield and selectivity	99
5.9	Compare the hydrolysis reaction (with and without fractionation) under various conditions on the product yield and eucalyptus conversion	100

### LIST OF FIGURES (Cont')

<b>FIGURE</b>	<b>TITLE</b>	<b>PAGE</b>
5.10	Effect of temperature on the product yield and fractionated eucalyptus conversion via hydrolysis reaction	101
5.11	Effect of temperature on the product selectivity of the hydrolysis of fractionated eucalyptus	102
5.12	Effect of retention time on the product yield and eucalyptus conversion via hydrolysis of fractionated eucalyptus	103
5.13	Effect of retention time on the product selectivity of the hydrolysis of fractionated eucalyptus	104
5.14	Effect of pressure on the product yield and fractionated eucalyptus conversion via hydrolysis reaction	104
5.15	Effect of pressure on the product selectivity of the hydrolysis of fractionated eucalyptus	105
5.16	Effect of catalyst loading (g) on the product yield and fractionated eucalyptus conversion via hydrolysis reaction	105
5.17	Effect of catalyst loading (g) on the product selectivity of the hydrolysis of fractionated eucalyptus	106
5.18	Reusability of solid acid catalyst in consecutive batches process on the product yield and fractionated eucalyptus conversion via hydrolysis reaction	106
6.1	XPS survey scan spectra. (a) OL; (b) TOL; (c) SL	119
6.2	XPS high resolution spectra of the C1s. (a) OL; (b) TOL; (c) SL	120
6.3	TGA and DTG curves of lignins; (a) OL; (b) TOL; (c) BIL	122
6.4	FTIR spectra of lignins; (a) OL; (b) TOL; (c) BIL	124
6.5	Subtracted FTIR spectra of lignins; (a) OL; (b) TOL; (c) The spectra was obtained by subtracting the OL sample spectrum (normalized on 1109 cm <sup>-1</sup> peak) from that TOL sample (normalized on 1109 cm <sup>-1</sup> peak)	124

### LIST OF FIGURES (Cont')

<b>FIGURE</b>	<b>TITLE</b>	<b>PAGE</b>
6.6	<sup>13</sup> C CPMAS NMR spectra of lignins. (a) TOL; (b) OL; (c) SL	126
7.1	Lignin distribution after reaction with different catalysts at 250 °C for 1 h	135
7.2	Syringol contents in aqueous fraction and residual lignin after reaction at 250 °C for 1 h	136
7.3	FTIR spectra of TOL sample and residue lignins after lignin depolymerization with and without catalysts at 250 °C for 1 h	137
7.4	Lignin distribution after reaction at different temperatures for 1 h	140
7.5	Effect of temperature on syringol (a) yield and (b) content ,(reaction time, 1 h)	141
7.6	GC-MS analysis of phenolic compound products in (a) aqueous fraction and (b) in THF solvent from residual lignin after lignin depolymerization reaction in the presence of SBA-15 at 300 °C for 1 h	142
7.7	Lignin distribution after reaction at 300 °C for 1 h with different solvent systems	144
7.8	Syringol contents in aqueous fraction and residual lignin fraction with different solvent systems after reaction at 300 °C for 1 h	144
7.9	GC-MS analysis of phenolic compound products (a) in aqueous fraction and (b) in THF solvent from residual Lignin after lignin depolymerization reaction in the presence of SBA-15 with methanol/water mixture (50/50, wt/wt) at 300 °C for 1 h)	145
7.10	Diagram of product separation after lignin depolymerization with and without solid catalyst	147

### LIST OF FIGURES (Cont')

<b>FIGURE</b>	<b>TITLE</b>	<b>PAGE</b>
7.11	Lignin distribution after reaction with different catalysts at 250 °C for 1 h	149
7.12	FTIR spectra of TOL and residual lignin at 250 °C for 1 h	150
7.13	Lignin distribution after reaction in the presence of CaP <sub>2</sub> O <sub>6</sub> at different temperatures for 1 h	154
7.14	Effect of temperature in the presence of CaP <sub>2</sub> O <sub>6</sub> on syringol (a) yield and (b) content, Reaction time, 1 h	156
7.15	GC-MS-identified phenolic compounds in (a) aqueous fraction and (b) residual lignin fraction after reaction in the presence of CaP <sub>2</sub> O <sub>6</sub> with water at 300 °C for 1 h	157
7.16	Lignin distribution after reaction in the presence of CaP <sub>2</sub> O <sub>6</sub> at 300 °C for 1 h with different solvent systems	158
7.17	Effect of different solvents in aqueous fraction and residual lignin fraction in the presence of CaP <sub>2</sub> O <sub>6</sub> on syringol (a) yield and (b) content at 300 °C for 1 h.	159
7.18	GC-MS-identified phenolic compounds in (a) aqueous fraction and (b) residual lignin fraction after reaction in the presence of CaP <sub>2</sub> O <sub>6</sub> with methanol/water solution (50/50, wt/wt) at 300 °C for 1 h.	160
8.1	Simplified reaction scheme for the conversion of the eucalyptus into sugars and chemicals	170

# CHAPTER 1

## INTRODUCTION

### 1.1 Rationale

Currently, the world is faced with an energy and environmental crisis due to fossil energy depletion and climate deterioration. This has led the drive to develop several alternative clean energy resources *e.g.*, biomass, wind, hydro, and solar. Among these approaches, the conversion of biomass to clean fuel, such as bio-ethanol and other chemicals has received much attention. Bio-ethanol is one of the promising alternative fuels, and can be mixed with gasoline to form gasohol. Bio-ethanol is typically produced from starch and sugar, and is called as first-generation bio-fuel. Nevertheless, using starch and/or sugar-based feedstocks will cause rising food prices and shortage in the near future. Currently, many researchers have been developing technologies to produce second-generation biofuel which are derived from non-food crops. One important resource for second-generation biofuel production is lignocellulosic biomass (or cellulosic biomass), which can also be converted to chemicals.

Lignocellulosic biomass has been considered as a potent alternative energy resource for agricultural-based countries such as Thailand. Some important types of biomass that are generally used for energy production are rice husk, rice straw, corncob, coconut shell, palm shell, cassava pulp and sugarcane bagasse. Lignocellulosic biomass consists mainly of cellulose, hemicellulose and lignin (**Figure 1.1**) with various proportions of these compounds depending on the type and source of biomass. Cellulose and hemicelluloses can be hydrolyzed to form C<sub>6</sub> and C<sub>5</sub> sugars, which can be further converted to ethanol via the fermentation process. In detail, the main component of cellulose is β-1,4 linked chain of glucose molecules. Hydrogen bonds between different layers of the polysaccharides contribute to the resistance of crystalline cellulose to degradation. Hemicellulose, the second most abundant component of lignocellulose, is composed of various 5- and 6-carbon sugars such as arabinose, galactose, glucose, mannose and xylose. Lignin is composed of three major phenolic components, namely p-coumaryl alcohol (H), coniferyl alcohol (G) and sinapyl alcohol (S).

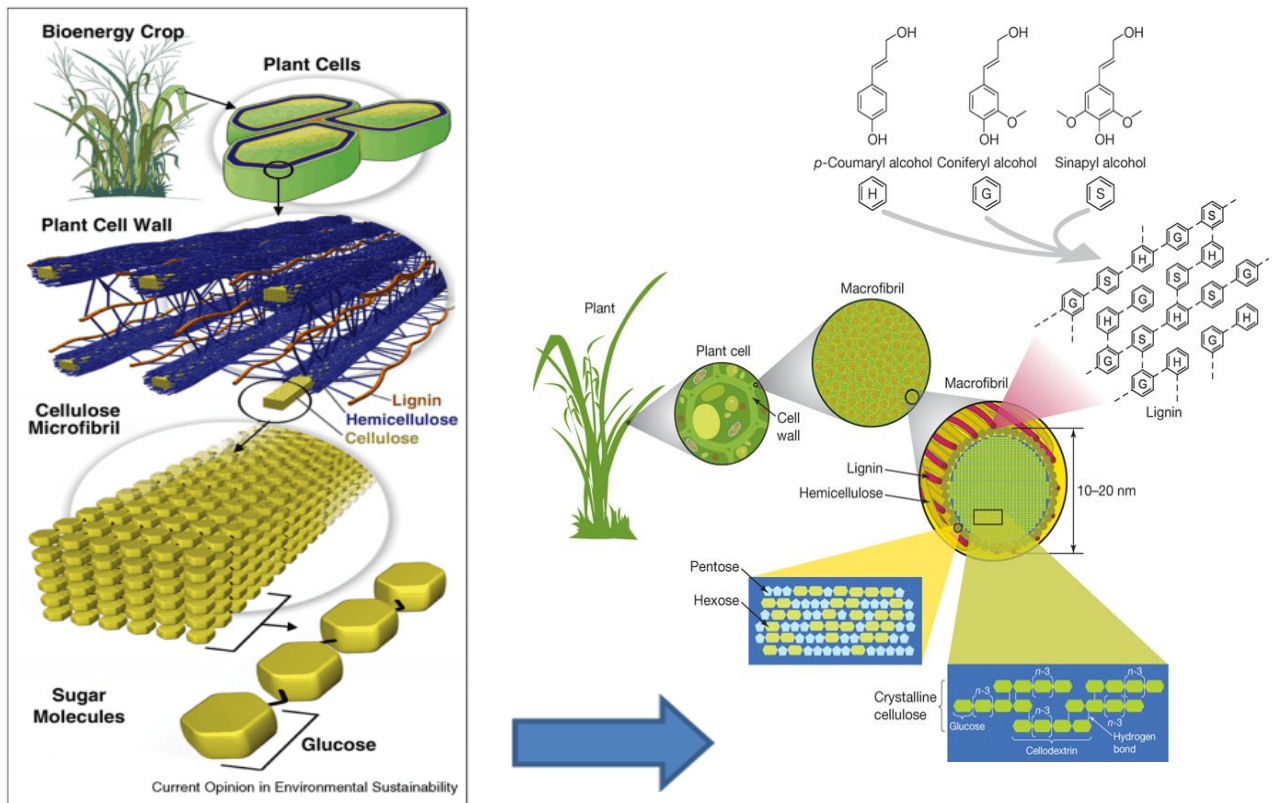


**Figure 1.1** The composition of lignocellulosic biomass (Rubin, 2008).

Technically, lignocellulosic biomass can also be converted into hydrocarbons, and building-block materials (**Figure 1.2**) for the production of polymers. Nevertheless, the crystalline and compact structure of lignocellulosic biomass makes it difficult to degrade to these compounds. To produce ethanol from lignocellulosic biomass, pretreatment process is required prior to subsequent saccharification and fermentation. The major aim of the pretreatment process is to break the structure of biomass into the form where hydrolysis is effectively achieved. In this process, there is cellulose substrate redistribution either to increase accessibility to the cellulose surface area and/or the solubilisation/removal of lignin. An alternative to the pretreatment process is the fractionation process, which aims not only to improve hydrolysis but also to isolate the core constituents of lignocellulosic biomass (*i.e.* cellulose, hemicelluloses, and lignin), as shown in **Figure 1.2**. From the fractionation process, cellulose and hemicellulose can be separately converted to sugars by hydrolysis reaction and which can then be further converted to chemicals *e.g.*, organic acids and furans. Lignin can be converted to phenolic compounds. The fractionation

process is expected to replace the conventional pretreatment processes and be applied for biorefinery technologies on an industrial scale in the near future (Bozell & Petersen, 2010).

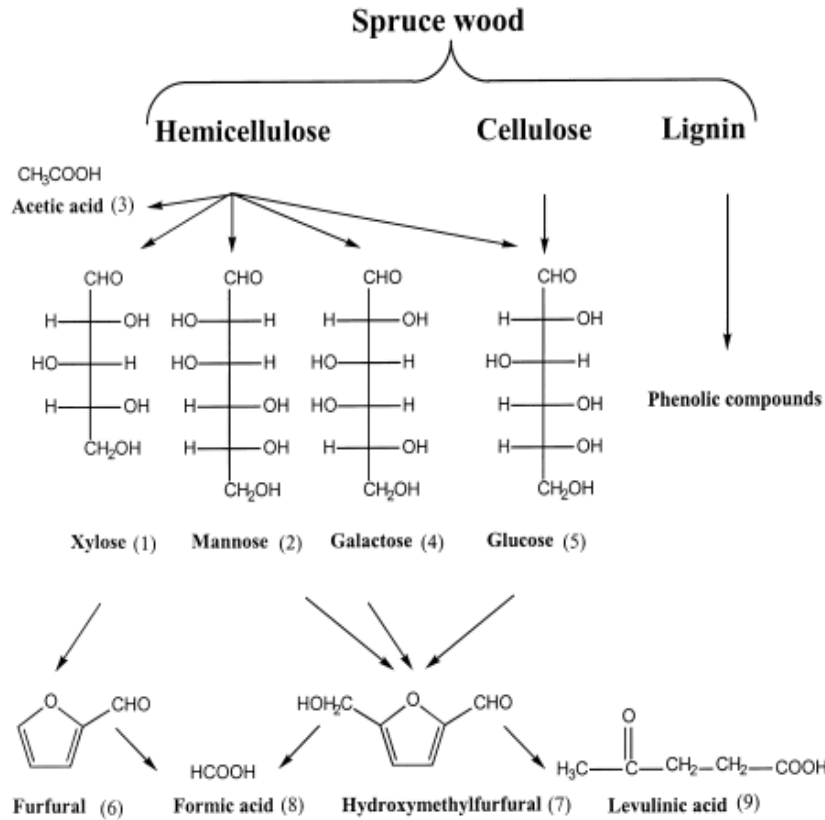


**Figure 1.2** The pathway of reactions occurring during fractionation and hydrolysis of lignocellulosic material (Palmqvist & Hahn-Hagerdal, 2000).

### Fractionation

In the fractionation process, toxic solvents are generally required to dissolve cellulose, hemicellulose and lignin. Current research and development is investigating the possible use of relatively less harsh conditions for biomass fractionation. Many fractionation methods are based on processes that are chemical (Sun & Cheng, 2002; Wang et al., 2012; Wildschut et al., 2013), thermal (Garrote et al., 2001; Imman et al., 2013), or combinations of the two (Amendola et al., 2012; Romaní et al., 2011). Among them, organosolv approaches have widely been investigated on hardwoods, softwoods and grasses (Brudecki et al., 2013; Lan et al., 2011; Pronyk & Mazza, 2012). Ethanol and methanol remain the primary solvents used in organosolv pretreatment, but many other solvents have been integrative employed including organic bases, ketones, and esters. In

addition, process design modeling for plants operating with ethanol-water, ethylene glycol-water, and acetosolv systems has been also carried out (Buranov & Mazza, 2012; González et al., 2008; Romani et al., 2013). Recently, a new organosolv technology, known as clean fractionation (CF), has been proposed (Bozell et al., 2011a). In the detail, biomass is treated with a ternary mixture of ketone, ethanol, and water in the presence of an acid promoter (*i.e.* H<sub>2</sub>SO<sub>4</sub>) that selectively dissolves the lignin and hemicellulose components leaving cellulose as an undissolved solid. The resulting single phase liquor is treated with water giving an organic phase containing lignin and an aqueous phase containing hemicellulose. This process offers high selectivity for separation of the primary biomass components and offers operational advantages for the production of both chemicals and fuels.

### **Hydrolysis**

In addition to the pretreatment and fractionation steps, another important process for biorefinery-based biomass conversion is the hydrolysis of cellulose and hemicellulose compounds into sugars. Various methods for hydrolysis of lignocellulosic materials have been reported. The conventional methods have been classified in two groups: chemical hydrolysis (dilute acid hydrolysis, concentrated acid hydrolysis and alkaline hydrolysis) and enzyme hydrolysis. Acid hydrolysis regarded as a cost-effective process, impacts on the environment and causes side reactions (*e.g.* dehydration to form hydroxymethylfurfural (HMF), furfural, levulinic acid, acetic acid, formic acid, and fructose (Chareonlimkun et al., 2010; Sasaki et al., 2008) and reduces sugar yields.

Enzyme hydrolysis is environmentally friendly and of high selectivity for sugar production. However, the cost of the enzyme remains expensive and the biomass must be intensively pretreated prior to the enzymatic hydrolysis process. Currently, many researchers have been widely developing the green and efficient hydrolysis technology for eliminating the above problems. The application of hot-compressed water (HCW) in the presence of a solid acid catalyst (heterogeneous reaction) is currently been recently developed for this application. As the solid acid catalyst, can easily be recovered compared to homogeneous acid catalyst it is more environmental friendly. Its repeated use results in reduced energy consumption. Some important examples of solid acid catalysts for this application are silica-alumina, zeolites, niobic acid, and strong ion-exchangeable resins. It is noted that the major problems of solid acid catalyst are low acid site concentrations, micro porosity, hydrophilic character of catalyst surfaces, and active site leaching.

These barriers need to be overcome before solid acid catalyst can be used in industrial scale. Therefore, several solid acid catalysts have been developed. For instance, (Hara, 2010; Suganuma et al., 2010; Yamaguchi & Hara, 2010) have developed a type of carbon-based solid acid with a high density of Brønsted acid sites (SO<sub>3</sub>H and COOH) by pyrolytically carbonizing sugars such as glucose, sucrose, or cellulose and subsequently sulfonating the carbons. The solid acid catalyst with a specific surface area of ~2 m<sup>2</sup>/g, at a low temperature (~100 °C), soluble sugar yield of 4%, glucose and 64% β-1,4-glucan 64%. On the basis of this result, this type of solid acid catalyst was of interest in the present work.

The reaction of lignocelluloses in HCW (with and without the presence of catalyst) can efficiently generate sugar-based compounds via hydrolysis reactions under various conditions (Ando et al., 2004; Karimi et al., 2006; Minowa & Inoue, 1999; Sun & Cheng, 2002). Ando et al. studied the decomposition behavior of plant biomass in HCW and found that hemicellulose decomposition commences at 180 °C, while cellulose decomposition would not start until the temperature is over 230 °C.

### **Lignin depolymerization**

Lignin conversion to phenolic compounds is difficult due to its structure. Therefore, the fractionation of the biomass prior to lignin conversion is regarded as a key enabling technology for lignin conversion into phenolics (Zakzeski et al., 2010). Generally, the strategies of lignin depolymerization can be achieved by various techniques; -oxidation, hydrolysis, hydrogenation, pyrolysis, and enzymatic reactions (Pandey & Kim, 2011). The fragmentation of lignin into smaller molecules has been reported frequently in literature (Deepa & Dhepe, 2014; Warner et al., 2014a; Xu et al., 2012) and recently reviewed by (Zakzeski et al., 2010). Since the weakest bonds in the lignin polymers are the α- and β-aryl-ether-bond followed by the aryl-aryl bond, thermal hydrodeoxygenation and hydrocracking have often been employed for depolymerization with or without the use of catalyst. Currently, there is still much to improve for lignin depolymerization in terms of the product yields and product separation. Several recent attempts have been focusing on new catalytic process to produce phenolic compounds. For instance, typical hydrotreating catalysts such as supported transition metal catalysts (sulfided NiMo, CoMo, etc.) have proven their efficiency for depolymerization reactions, but require severe operating conditions (Liguori & Barth, 2011; Zakzeski et al., 2010).

The project

This research focuses on the development of integrative processes, including the fractionation of biomass, hydrolysis of isolated cellulose and depolymerization of fractionated lignin for converting eucalyptus wood chips into sugar and chemicals in the biorefinery process, as shown in **Figure 1.3**.

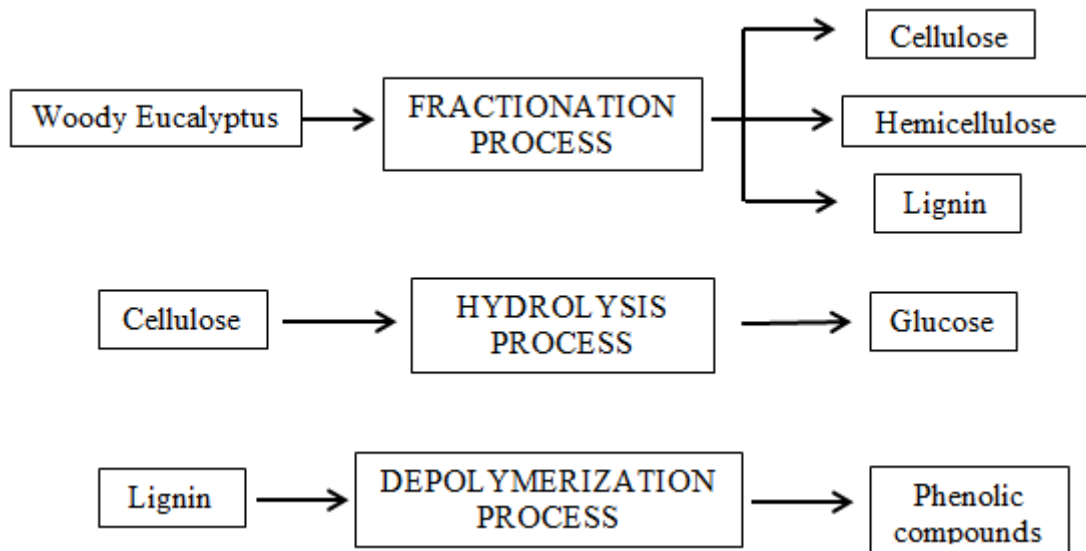


**Figure 1.3** The diagram of sugar and chemical production via fractionation of biomass, hydrolysis of cellulose and depolymerization of lignin reactions of in this study for the upgrading of lignocellulosic processing industries.

## 1.2 Research objectives

The main objective of this research is to study the concept of applying clean technology for sugar and high value chemical productions from eucalyptus wood chips. The technologies that were investigated: organosolv fractionation, hydrothermal hydrolysis and catalytic depolymerization. The specific sub-objectives are as follows:

- Investigate the effects of homogeneous and heterogeneous acid promoters and operating conditions (reaction temperature, retention time, amount of promoters, and ratio of solvent) on organosolv fractionation of eucalyptus wood chips.
- Study the hydrolysis of isolated cellulose and hemicellulose from eucalyptus fractionation in the presence of both homogeneous and heterogeneous catalysts

under a hot-compressed water (HCW) system at various reaction conditions, with the aim to produce C<sub>5</sub> and C<sub>6</sub> sugars.

- Determine the solubility characteristics, physico-chemical properties and structural features of fractionated lignin obtained by the HCW process.
- Investigate the conversion of lignin into phenolic compounds via depolymerization reactions in the presence of different types of catalyst (*i.e.* mesoporous silica-based and phosphate-based catalysts).

### 1.3 Overview of Chapters

The results and discussion are divided into 4 main parts. In the first part (Chapter 4), fractionation-based organosolv technology was intensively studied, from which several acid promoters, including homogeneous and heterogeneous acid promoters (HNO<sub>3</sub>-, HCl-, H<sub>2</sub>SO<sub>4</sub>-, and H<sub>3</sub>PO<sub>4</sub>-activated carbons), were applied to assist the fractionation. The fractionation performances with and without the presence of these promoters were compared under several operating conditions to understand the role of these acid promoters on eucalyptus fractionation. In the second part (Chapter 5), the hydrothermal hydrolysis of isolated cellulose and hemicellulose from eucalyptus fractionation for converting these compounds to C<sub>5</sub> and C<sub>6</sub> sugars was investigated and compared to that of raw eucalyptus and eucalyptus pretreated by the alkaline process. The effect of solid acid catalysts (*i.e.* carbon-based sulfonated catalysts) addition on the hydrolysis performance was also studied. Importantly, the integrative fractionation/hydrolysis by using acid promoter (*i.e.* H<sub>3</sub>PO<sub>4</sub>-activated carbon) as alternative hydrolysis catalyst was carried out for comparison. In the third part (Chapters 6-7), the isolated lignin from organosolv fractionation was characterized by several techniques (*i.e.* Klason lignin, elemental analysis, molecular weight, mannich reaction, thermal gravimetric analysis (TGA), X-ray photoelectron spectroscopy (XPS), Fourier transform-infrared spectroscopy (FT-IR) and solid-state nuclear magnetic resonance (NMR)) to determinate the physico-chemical properties and structural features (as presented in Chapter 6). Then, it was converted to phenolic compounds via catalytic depolymerization process, from which several acid catalysts *i.e.* MCM-41, ZrO<sub>2</sub>-MCM-41, SBA-15, ZrO<sub>2</sub>-SBA-15, CoP<sub>2</sub>O<sub>6</sub>, and CaP<sub>2</sub>O<sub>6</sub> were tested under several reaction conditions (as described

in Chapter 7). Finally, the summary of this work and recommendations for further studies are described in Chapter 8.

## CHAPTER 2

### LITERATURE REVIEW

Biomass is one of the sustainable resources that can be used to replace fossil fuels and assist in the reduction of the current energy and environmental crisis. Biomass is currently used for energy production in many sectors (transportation, industries, building, etc.) as it stores hidden energy in chemical bonds. Its main components consist of carbon, hydrogen, oxygen, and nitrogen while sulfur is also found in minor amounts. At present, most biofuels (*e.g.*, bio-ethanol) are largely produced from food crops in the forms of starch and sugar. There is concern that the use of food crops will cause rise in food prices and hence lead to food crisis in the future. Lignocellulosic biomass can be developed to replace food crops for biofuel production, particularly for cellulosic ethanol. Technologies have been developed to convert lignocellulosic biomass to ethanol with high efficiency. However, more research and development are required for cost reduction and design of value-added processes for co-products.

This chapter reviews the steps for the conversion of lignocellulosics into sugars and chemicals. A general overview of lignocellulosic biomass is first presented, followed by the fractionation and pretreatment, hydrolysis, and depolymerization reactions.

#### 2.1 Physical and chemical characteristics of lignocellulosic biomass

##### 2.1.1 Composition

Lignocellulosic biomass is the non-starch, fibrous part of plant material, and is the most abundant organic carbon on earth. Lignocellulosic materials consist of mainly three different types of polymers *i.e.* cellulose, hemicelluloses, and lignin, which are associated with each other in addition to low amounts of acids, salts, and minerals. The percentage compositions of these constituents vary but cellulose is generally the largest fraction, comprising of 30–50% while hemicellulose contributes approximately 20–40% while lignin presents for 15–25% of the total dry matter of the plant biomass (Boerjan et al., 2003). Cellulose exists as a polymer of D-glucose subunits, linked by  $\beta$ -1,4-glycosidic linkage. The cellulose in a plant consists of parts with a highly organized crystalline organized structure, which are connected by H-bond between the polysaccharide layers,

making it highly form to chemical or biological degradation. Hemicellulose, the second most abundant of lignocellulose, is a complex-branched carbohydrate that consists of pentoses (xylose and arabinose), hexoses (mannose, glucose, and galactose), and sugar acids. Hemicelluloses have lower molecular weights than cellulose and are easily hydrolysable. They serve as a connection between the lignin and cellulose fibers and give the whole cellulose-hemicellulose-lignin network more rigidity. Lignin is a heteropolymers of three different phenylpropane units that are held together by different kind of linkages. The main function of lignin is to give the plant structural support, impermeability and resistance to external microbial attack and oxidative stress. Lignin is non-water soluble and optically inactive. All these properties make the degradation of lignin very tough. The quantitative composition of the three main components (cellulose, hemicellulose, and lignin) in lignocellulose is dependent on its origins, as presented in **Table 2.1**.

**Table 2.1** The composition of lignocellulose from different plant origins on dry basis (Sun & Cheng, 2002)

<b>Lignocellulosic materials</b>	<b>Cellulose (%)</b>	<b>Hemicellulose (%)</b>	<b>Lignin (%)</b>
Hardwood stems	40–55	24–40	18–25
Softwood stems	45–50	25–35	25–35
Nut shells	25–30	25–30	30–40
Corn cobs	45	35	15
Grasses	25–40	35–50	10–30
Paper	85–99	0	0–15
Wheat straw	30	50	15
Sorted refuse	60	20	20
Leaves	15–20	80–85	0
Cotton seed hairs	80–95	5–20	0
Newspaper	40–55	25–40	18–30
Waste papers from chemical pulps	60–70	10–20	5–10
Primary wastewater solids	8–15	NA	24–29
Swine waste	6	28	NA
Solid cattle manure	1.6–4.7	1.4–3.3	2.7–5.7
Coastal Bermuda grass	25	35.7	6.4
Switchgrass	45	31.4	12

## 2.2 Internal structure - physical and chemical properties

### 2.2.1 Cellulose

Cellulose is typically the main component in lignocellulosic biomass. It is generally considered to be polymer of cellobiose, a dimer of D-glucose. As shown in **Figure 2.1**, the cellulose chemical formula is presented as  $(C_6H_{10}O_5)_n$ . The cellulose properties depend on the degree of polymerization (DP), *i.e.* the number of glucose units that make up the polymer. The number of glucose units per cellulose molecules can extend to a value of 17,000, although typically a number between 800-10,000 units are revealed (Gedon & Fengi, 2000).

$$DP = \frac{\text{Molecular weight of cellulose}}{\text{Molecular weight of one glucose unit}}$$

Cellulose is a crystalline polymer of glucose molecules that are arranged in long and straight chains linked by  $\beta$ -1,4 glucosidic bond. Hydrogen bonds in the structure help maintaining and supporting linear conformation of the cellulose chains, which are bungled together into microfibrils (Gedon & Fengi, 2000). Demonstration of hydrogen bonding that allows the parallel arrangement of the polymer chains of cellulose is shown in **Figure 2.2**.

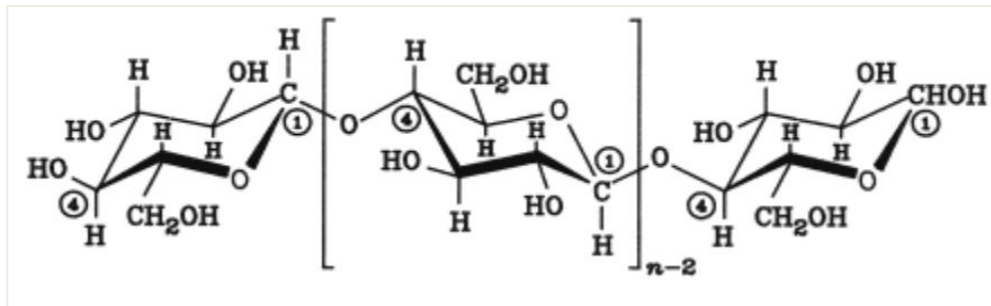


**Figure 2.1** Structure of single cellulose molecule (Gedon & Fengi, 2000).

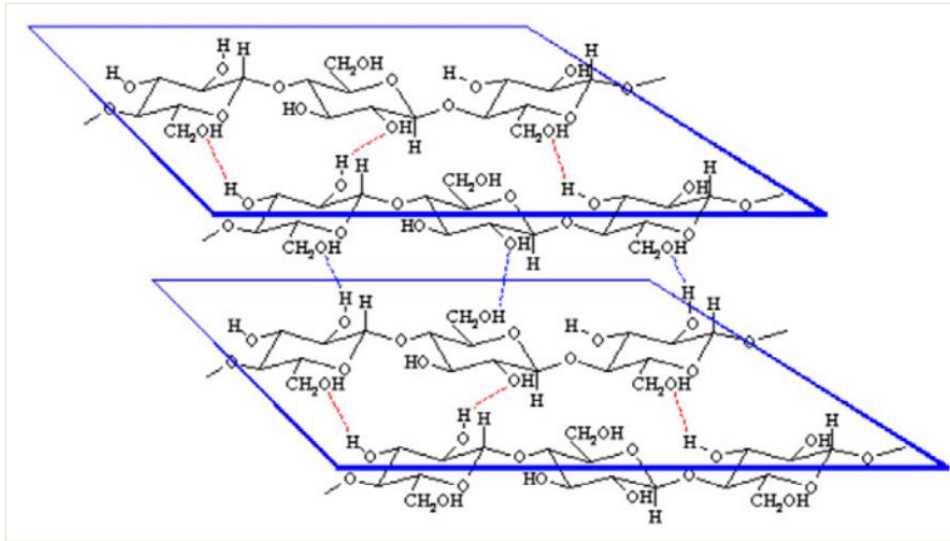


**Figure 2.2** An illustration of the arrangement of the cellulose molecules in parallel chains and the accompanying hydrogen bonding (intra- and inter-chain hydrogen bonding) (Gedon & Fengi, 2000).

### 2.2.2 Hemicellulose

Hemicelluloses are carbohydrate polymers with a complex heterogeneous structure. Due to their amorphous structure, they are readily soluble in water at medium temperatures more than 180 °C (Yu et al., 2008). The backbone chains of hemicellulose typically exist as homopolymers (same type of single sugar units) or heteropolymers (mixture of various sugars). The different types of sugars in the hemicelluloses structure is shown in **Figure 2.3**. Generally, the most common type of polymers that belongs to the hemicellulose family is xylan. Its degree of polymerization is relatively low (around 200 units), whereas the minimum limit can be around 150 monomers. The structures of hardwood xylan and softwood xylan are presented in **Figure 2.4(a)-(b)**, respectively. Sugars in hemicellulose are linked mainly by  $\beta$ -(1,4)-glycosidic bonds with  $\alpha$ -(1,2)-glycosidic bonds linking to 4-o-methylglucuronic acid. In addition, o-acetyl groups sometime replace the OH-groups in position C<sub>2</sub> and C<sub>3</sub> as presented in **Figure 2.4(a)**. In the case of softwood xylan, the acetyl groups are fewer in the backbone chain. Nevertheless, softwood xylan has additional branches consisting of arabinofuranose units linked by  $\alpha$ -(1,3)-glycosidic bonds to the backbone, as presented in **Figure 2.4(b)**.

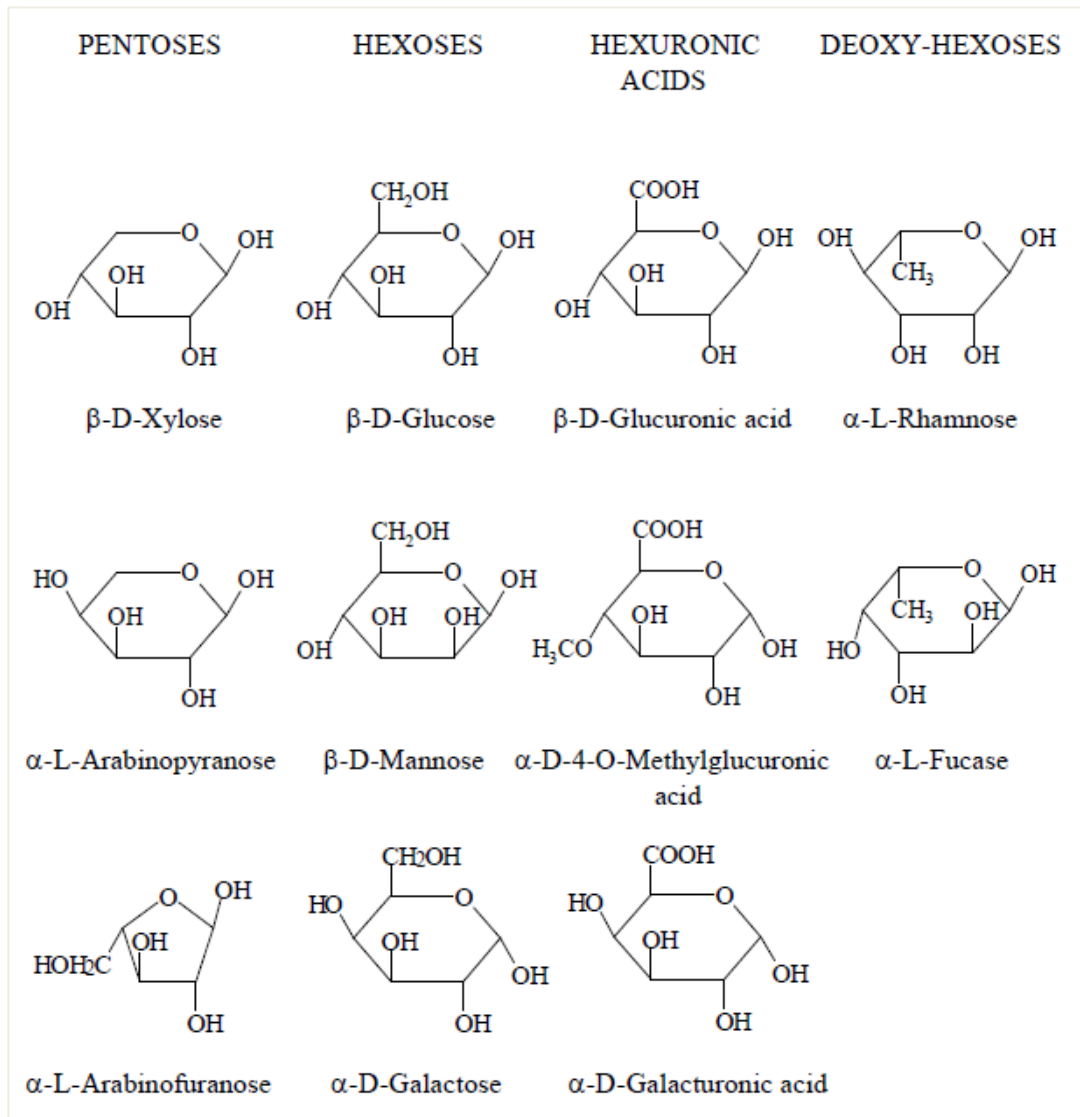


**Figure 2.3** Schematic illustration of different types of monomeric sugar units in hemicellulose structures (Gedon & Fengi, 2000).

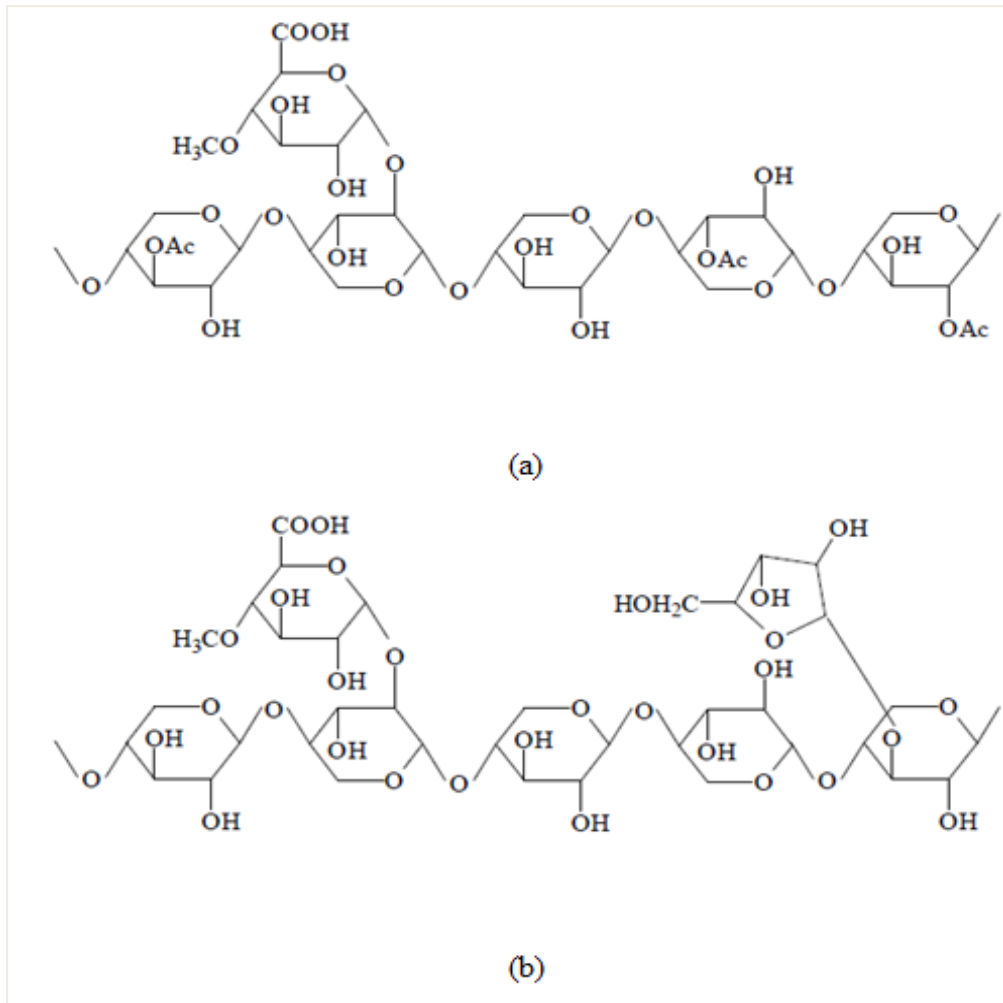


**Figure 2.4** Schematic illustration of xylans: (a) Partial xylan structure from hardwood chain. (b) Partial xylan structure from softwood chain (Gedon & Fengi, 2000).

### 2.2.3 Lignin

Lignin is the second most abundant natural polymer, which is typically deposited in nearly all vascular plants, and provides rigidity and strength to their cell walls. It is made up of three major monolignols (coniferyl alcohol (G), sinapyl alcohol (S) and *p*-coumaryl alcohol (H)) of lignin polymer, which were break down to provide the respective monophenolic product groups phenol, guaiacol and syringol, with different substitution patterns, as shown in **Figure 2.5**. Lignin from different plant origins contained different ratios of the monomeric phenolic units, linked together by various types of ether, aryl and carbon-carbon bonds such as  $\beta$ -O-4, 4-O-5,  $\beta$ - $\beta$ ,  $\beta$ -1,  $\beta$ -5, 5-5, and dibenzodioxocin as shown in **Figure 2.6**. The  $\beta$ -O-4 bond is the dominant linkage, consisting of more than half of the linkage structures of lignin (Zakzeski et al., 2010).

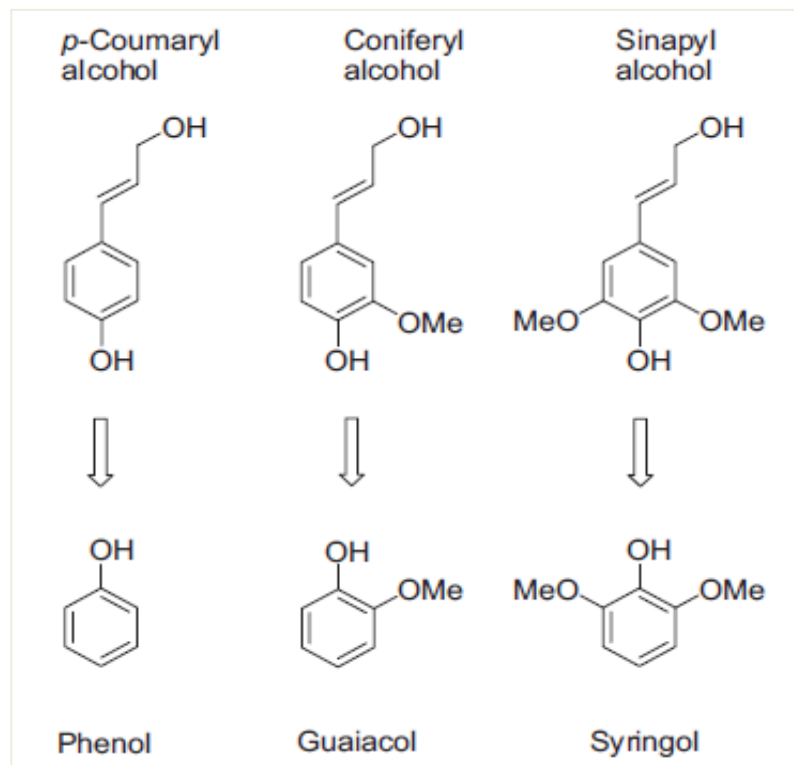


**Figure 2.5** Monolignol units of lignin and respective direct breakdown products of lignin (Boerjan et al., 2003).

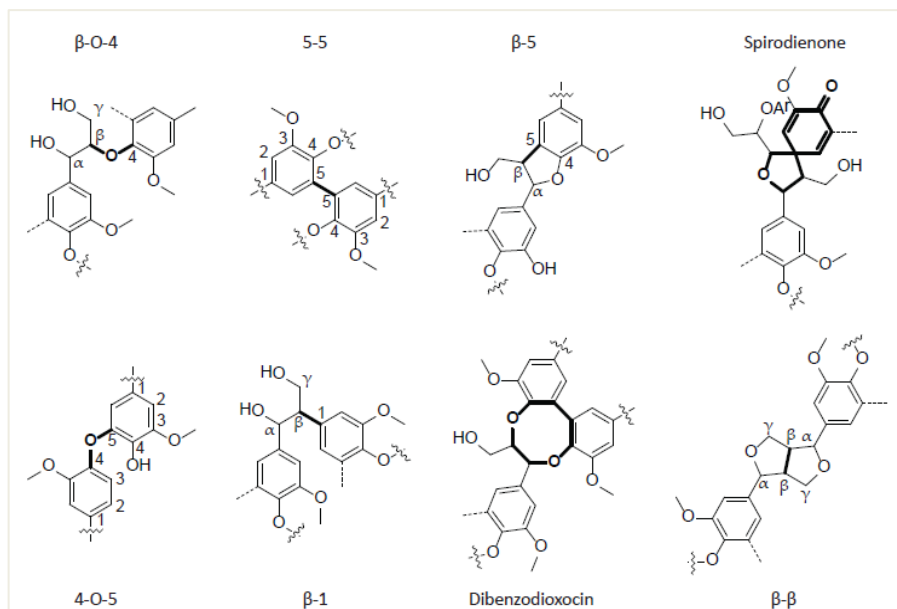


**Figure 2.6** The linkages individually include  $\beta$ -O-4, 4-O-5,  $\beta$ - $\beta$ ,  $\beta$ -1,  $\beta$ -5, 5-5, and dibenzodioxocin (Boerjan et al., 2003).

Recently, the value-added utilization of lignin generated from pulp and paper or biorefinery industry has attracted great interest as a rich source of phenols. Nevertheless, lignin depolymerization and conversion to value-added products are an issue of great cost and challenge because of its highly recalcitrant and complex structure.

## **2.3 Chemical interaction**

### **2.3.1 Intrapolymer linkages**

The structure of lignocellulose typically consists of four main types of bonds: ether bonds, ester bonds, carbon to carbon bonds and hydrogen bonds. The position of inter- and intrapolymer linkages in lignocellulose is summarized in **Table 2.2**. The lignin polymer contains mainly ether bonds and carbon-to-carbon bonds. The ether bonds in the lignin are estimated to be 70% of the total bonds between the monomer units, whereas the carbon-to-carbon bonds account for the remaining 30% (Zakzeski et al., 2010). The cellulose polymer is formed with two main linkages; ether linkage (or called as the glucosidic linkages) and hydrogen linkages. The heterogeneous hemicellulose contains various ether types of linkages such as fructosic and glucosidic bonds. The main difference with cellulose is that the hydrogen bonds are absent and that there is significant amount of carboxyl groups. The carboxyl groups can be present as carboxyl or as esters or even as salts in the molecule.

### **2.3.2 Functional groups/linkages in lignocellulosic structure**

The main interpolymer linkages between polymers in the lignocellulosic structure can be generally categorized into three types of bonds: ether, hydrogen, and ester bonds, as summarized in **Table 2.2**. In detail, the main linkages that connected cellulose with hemicellulose and lignin respectively are hydrogen bonds. Furthermore, lignin was connected with polysaccharides (*i.e.* cellulose-hemicellulose) with hydrogen bonds. Hemicellulose has linkages connected to lignin via ester bonds. Ether bonds between lignin and the polysaccharides are also identified.

**Table 2.2** The linkages between the monomer units in lignocelluloses (Gedon & Fengi, 2000; Harmsen, 2010)

<b>Bonds within different components (intrapolymer linkages)</b>	
Ether bond	Lignin, (hemi)cellulose
Carbon to carbon	Lignin
Hydrogen bond	Cellulose
Ester bond	Hemicellulose
<b>Bonds connecting different components (interpolymer linkages)</b>	
Ether bond	Cellulose-Lignin Hemicellulose lignin
Ester bond	Hemicellulose-lignin
Hydrogen bond	Cellulose-hemicellulose Hemicellulose-Lignin Cellulose-Lignin

### 2.3.3 Functional groups in lignocellulosic structure

The important factor of the functional groups that is applied to aspects of sugar and chemical production from lignocellulosic biomass are: (1) they are related to the hydrolysis of the carbohydrates (polymer of cellulose and hemicellulose) into monomer units, and the subsequent degradation of the monomer units into furans (*i.e.* furfural, hydroxymethylfurfural (HMF)); and (2) they are also involved with the depolymerization of lignin polymer (into fragments or phenolic compounds). As already mentioned, the cellulose fractions after broken down the structure becomes more accessible for enzyme hydrolysis because enzyme could go directly to main linkages (glucosidic bonds) of cellulose to break the bonds into sugar monomers. The lignin polymer contains most different functional groups involved in its depolymerization and degradation, eventually to derivatives that are soluble in water. All types of functional groups in lignocellulose structure are summarized in **Table 2.3**.

**Table 2.3** Functional groups in lignocellulosic structure (Harmsen, 2010)

Functional Group	Lignin	Cellulose	Hemicellulose
Aromatic ring	X		
Hydroxyl group	X		
Carbon to carbon linkage	X		
Ether (glucosidic) linkage	X	X	X
Ester bond			X
Hydrogen bond*		X	X

\*The hydrogen bond is not a functional group, as its reaction does not lead to chemical changes in the molecule. However, it changes the solubility of the molecule, and therefore it is important for the breakdown of lignocelluloses

## 2.4 Lignocellulose biorefinery

A biorefinery is a very interesting technology for converting the lignocellulose into valuable products and is a sustainable alternative to the conventional petroleum refinery. The basic concept of a biorefinery is presented in **Figure 2.7**. Firstly, the pretreatment step is required to open up the structure of lignocellulose which resulted in accessibility of enzymes to the cellulose fraction or separation of the lignocellulose components *i.e.* cellulose, hemicellulose, and lignin. Secondly, different technologies (*i.e.* physical, thermal, and chemical processes) can be used for the conversion processes such as extraction, gasification (syngas) and liquefaction of biomass. Biological or enzymatic conversion of the polysaccharide fraction is also considered an effective alternative. The final products *e.g.*, biofuels, chemicals, and materials can be obtained by either chemical or biological routes.

Lignocellulosic components can be the sources of several precursors for subsequent valorization: (1) glucose from cellulose, (2) pentoses, mainly xylose and arabinose, as well as some hexoses (*e.g.* mannose and glucose) and sugar acids, and (3) phenolic compounds from lignin. **Figure 2.8** presents a variety of products from lignocellulose by biorefinery processes. Cellulose can be hydrolyzed to glucose and further subsequently converted via fermentation processes to various products such as ethanol, propanol, acetone, and others. The hemicellulose can be also hydrolyzed to xylose (main C<sub>5</sub> sugar of hemicellulose) and further subsequently converted into xylite (sugar-substitute) (Kamm & Kamm, 2004). Chemical precursors such as furans can be obtained from dehydration of sugars. Furfural is

used for production of Nylon 6 and Nylon 6,6 while HMF is applied for production of lubricants, softener and others. Lignin fractions can be generally used as fuel and adhesive. Nevertheless, it can be converted to more valuable products, such as phenols, and aromatic hydrocarbons (including xylene, benzene, and toluene).

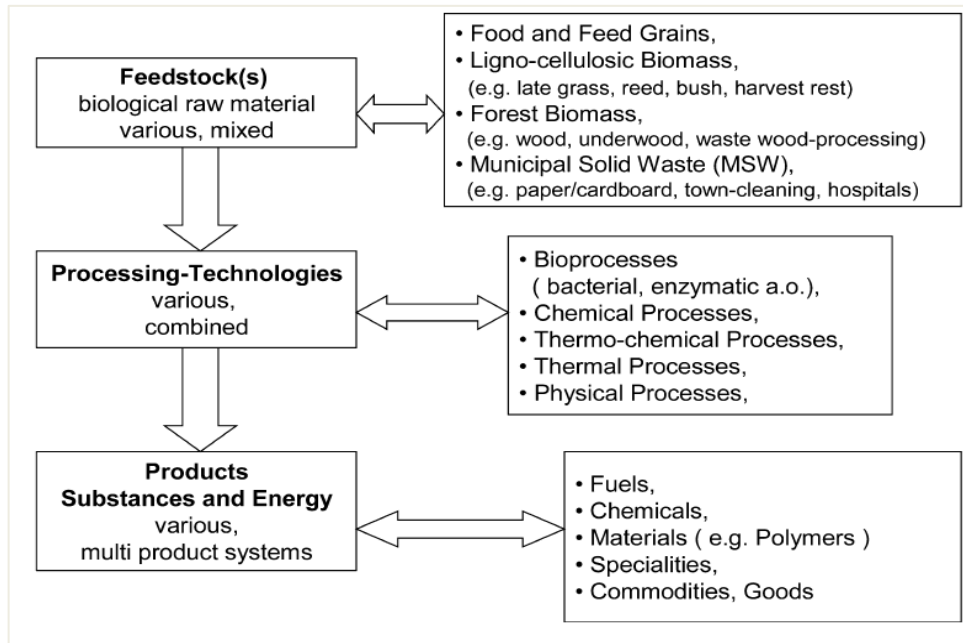


**Figure 2.7** Basic steps of biorefinery (Kamm & Kamm, 2004).

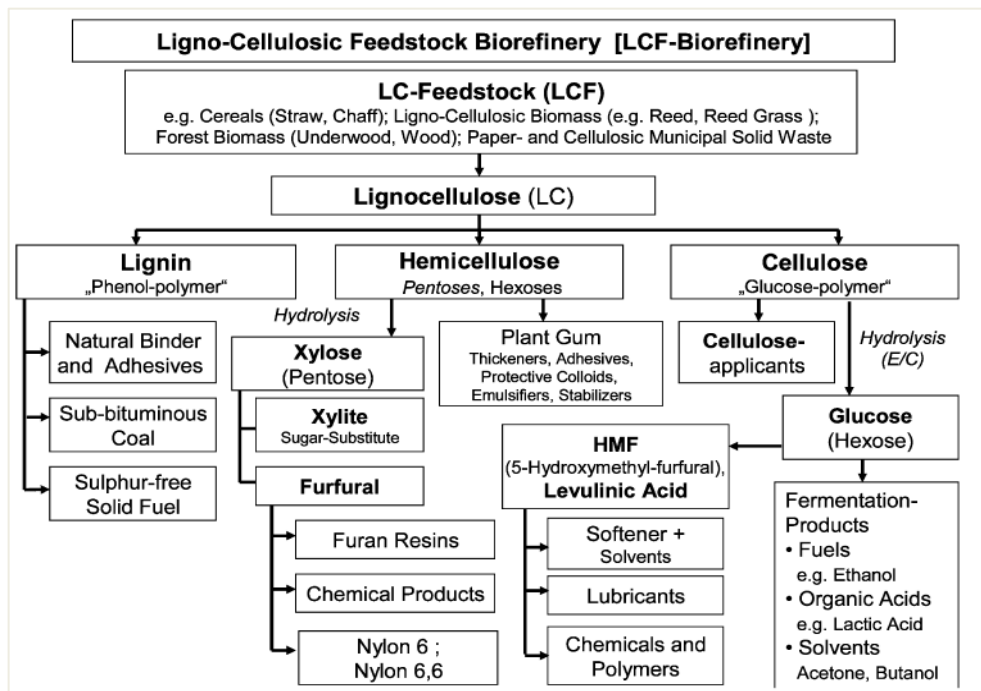


**Figure 2.8** Products from lignocellulose biorefinery (Kamm & Kamm, 2004).

## 2.5 Lignocellulose pretreatment techniques

Owing to its complex structure, lignocellulosic biomass is recalcitrant to physical, chemical, and biological attack. Hydrolysis of lignocellulosic biomass into sugars comprises two steps: the pretreatment of biomass and the enzymatic saccharification of the pretreated biomass into sugars for further conversion. The factors that have been identified to affect the hydrolysis of cellulose include porosity (accessible surface area) of the materials, cellulose fiber crystallinity, lignin and cellulose content and degree of polymerization (Kumar et al., 2009). The presence of lignin and hemicellulose makes the access of cellulase enzymes to cellulose difficult, thus reducing the efficiency of hydrolysis. Lignin can also interfere with the hydrolysis by irreversibly binding to hydrolytic enzymes. Pretreatment is a pre-requisite step to increase the enzymatic digestibility of lignocellulosic biomass in order to obtain a feasible sugar yield (**Figure 2.9**). The purpose of the pretreatment step is thus to remove lignin and hemicellulose, reduce crystallinity and increase the porosity of the materials. In general, the pretreatment must meet the following requirements: (1) improve the formation of sugars or the ability to subsequently form sugars by the downstream enzymatic hydrolysis; (2) avoid the degradation or loss of carbohydrate; (3) avoid the formation of by-products inhibitory to the subsequent enzymatic or conversion processes; and (4) be cost-effective to make the process viable (Kumar et al., 2009). Implementation of optimal pretreatment step will result in improved total yield of monomeric sugars in the hydrolysis step and the production of target fermentation products.

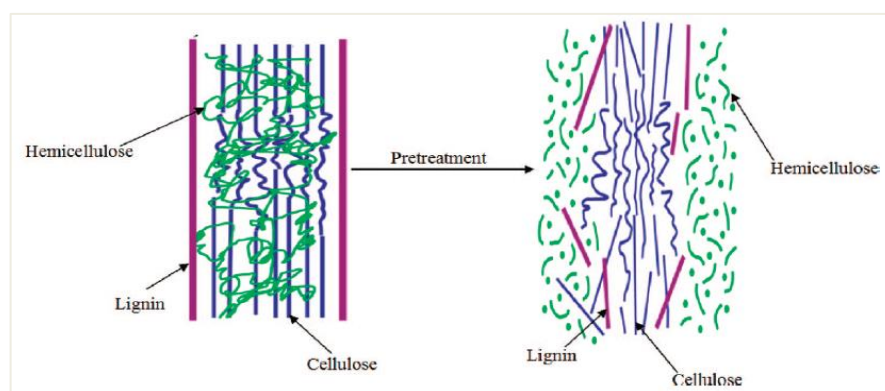


**Figure 2.9** Schematic illustration of pretreatment for increasing the accessibility of cellulose to cellulolytic enzymes in the subsequent enzymatic hydrolysis stage (Kumar et al., 2009).

Pretreatment technologies are generally categorized as follows: physical (*e.g.* chipping, milling or grinding), physicochemical (*e.g.* autohydrolysis/steam pretreatment, wet oxidation, and hydrothermolysis), chemical (*e.g.* acid hydrolysis, alkali, organic solvents, and oxidizing agents), biological, electrical, or a combination of these. Due to their differences in chemical composition, the pretreatment step for each biomass needs optimization in order to determine the optimal conditions and reaction parameters with the balance of saccharification efficiency, cost and energy consumption.

### **2.5.1 Physical pretreatment**

The physical pretreatment is generally based on mechanical actions such as cutting, milling, or grinding. The purposes of the physical pretreatment are to reduce the particle size and destroy the cell structure. Physical pretreatment is usually used as a first step in order to increase the accessible surface area before subsequent pretreatments by chemical or biological methods. Nevertheless, this method is energy intensive and also limited by its relatively high operating cost and scaling up of the equipment.

### **2.5.2 Physicochemical pretreatment**

#### **2.5.2.1 Steam explosion**

Steam explosion is one of the most effective methods for lignocellulose pretreatment. The process involves holding biomass under high temperature and pressure (160-260 °C, and 0.69-4.83 MPa) for several seconds to a few minutes before the material is exposed to atmospheric pressure (Kumar et al., 2009). This results in the explosive effects on the biomass structure. Majority of hemicellulose is solubilized which lead to increasing accessibility of enzymes to cellulose fibers while the lignin is not substantially solubilized in the absence of catalysts (Kumar et al., 2009). The effects of steam explosion can be enhanced by using acid catalysts which can increase solubility of hemicellulose under conditions with lower severity. Formation of inhibitory by-products from sugar degradation (*i.e.* 5-hydroxymethyl furfural and furfural) need to be avoided and optimization of the pretreatment condition is required.

#### **2.5.2.2 Liquid hot water (hydrothermal)**

Liquid hot water pretreatment is operated with water at high temperature and pressure. Other terms are hydrothermolysis, hydrothermal pretreatment, aqueous fractionation, solvolysis or aquasolv (Mosier et al., 2005). In non-catalytic liquid hot water processes, water is used as the sole solvent at high temperatures (160-230°C) under pressurized conditions for 5-30 min, which generates hydronium ions in situ by the ionization of water,

resulting in the release of acetic acid from hemicelluloses. This in turn auto-catalyzes the solubilisation of hemicelluloses in an acidic environment, whereas lignin is redeposited on the surface of the fiber. This resulted in an increasing accessibility to cellulose while avoiding the accumulation of inhibitory dehydration by-products. The major challenge of this process involves optimization of the process to minimize the amount of water and to on scaling-up of the reaction with economic feasibility.

### **2.5.3 Chemical pretreatment**

#### **2.5.3.1 Diluted acid pretreatment**

Dilute acid pretreatment is one of the most simple and effective pretreatment methods for lignocellulose. Sulfuric acid ( $\text{H}_2\text{SO}_4$ ) is commonly used in the range of 0.5-1.5% (Kumar et al., 2009). The method is relatively inexpensive and requires no costly equipment. Typically, the mixture of biomass and acid is held at 160-220°C for a few minutes (Harmsen, 2010; Mosier et al., 2005). The hemicellulose is hydrolysed and released in the forms of oligomeric and monomeric sugars into the liquid phase. However, the drawbacks of this method are high accumulation of inhibitory by-products from sugar dehydration. The use of acid also results in the corrosion of the equipment.

#### **2.5.3.2 Alkali pretreatment**

In alkaline pretreatment, the majority of the lignin fraction and some of the hemicellulose are removed, which leads to increasing accessibility of the enzyme to the cellulose fibers. The operating condition is relatively mild and cellulose degradation is minimal with low formation of inhibitory by-products. Conventional alkali catalyst used include minerals (*e.g.* NaOH, KOH, and  $\text{Ca}(\text{OH})_2$ ) and organic (*e.g.*  $\text{NH}_3$ ) catalysts as presented below;

##### **(a) Mineral alkaline pretreatment**

Sodium hydroxide (NaOH), potassium hydroxide (KOH), and calcium hydroxide ( $\text{Ca}(\text{OH})_2$ ) are commonly used for pretreatment due to their low cost, safety, and easy recoverability. (Chang & Holtzapple, 2000) reported that alkaline pretreatment of biomass using 1-5% alkali at high temperature between 85-135 °C and short reaction time between 1-3 h can lead to the maximal sugar yield from hemicellulose. However, at lower temperatures (50-65 °C) and longer reaction times (24 hrs), a substantially high sugar yield from hemicellulose (82%) can also be achieved (Kumar et al., 2009).

### **(b) Ammonia percolation**

(Kumar et al., 2009) reported that the ammonia percolation pretreatment of wheat straw effectively removes 60-70% of the lignin and around 50% of the hemicellulose, and leaves a highly digestible (up to 95%) solid fraction essentially free of fermentation inhibitors. This pretreatment is required to use at high temperature between 140-170 °C for effectiveness and to operate short time around 10-30 min.

### **(c) AFEX**

Ammonia Fiber Expansion (AFEX) is a unique method for the pretreatment of biomass, resulting in unique effects. (Chang & Holtzapfle, 2000) reported that the biomass is held to contact with the aqueous ammonia at temperature between 80-150 °C and pressure of 200-400 psi for 5-30 min followed by explosive decompression. The effects of this method included decreasing crystallinity of cellulose, opening structure of fiber, and hemicellulose removal. In contrast to other alkaline pretreatments, lignin in the biomass pretreated by AFEX is fragmented and remains in the material rather than removed and degraded.

#### **2.5.4 Oxidative pretreatment**

The delignification of lignocellulosic biomass can be carried out by pretreatment with oxidation, such as alkaline peroxide (hydrogen peroxide ( $H_2O_2$ )), wet oxidation (oxygen or air), and ozonolysis (ozone). This method can select lignin degradation to lead to loss of lignin and hemicellulose and obtain rich cellulose. Each oxidative pretreatment is presented below:

##### **2.5.4.1 Alkali peroxide**

Alkali peroxide pretreatment is one of the most effective methods of the pretreatment of lignocellulosic biomass at low temperature. Many studies (Harmsen, 2010; Kumar et al., 2009) have been reported that hydrogen peroxide under alkaline pH (pH 11.5 adjusted by NaOH) can lead to effective delignification of biomass. The process is generally performed using 2-5%  $H_2O_2$  at 25-30 °C for 2-8 h. This can result in the highly digestible solid fraction which can give high sugar yield up to 95%. The process is exothermic and requires no external heating; however, with relatively long reaction time.

##### **2.5.4.2 Wet oxidation**

In wet oxidation, air or oxygen is used as an oxidant in an aqueous medium at elevated temperature and pressure (Harmsen, 2010). The main decomposition products observed from lignin and hemicellulose oxidation are  $CO_2$ ,  $H_2O$ , and carboxylic acids.

(Klinke et al., 2002) reported that around 65% of lignin can be extracted from wheat straw at 180-185 °C for 15 min using carboxylic acids, CO<sub>2</sub>, and H<sub>2</sub>O as an oxidant.

#### **2.5.4.3 Ozonolysis**

Ozone pretreatment can extract the lignin from lignocellulose by attacking and cleaving the aromatic structures, while the cellulose and hemicellulose are slightly solubilized with the benefit of no formation of inhibitors. (Mosier et al., 2005) reported that pretreatment of wheat straw by ozonolysis can remove 35% of lignin and enhance its enzymatic hydrolysis up to 50% compared to the untreated biomass. The highest yield of sugar by enzymatic hydrolysis of 90% can be achieved.

#### **2.5.5 Biological pretreatment**

The biological pretreatment employed microorganisms, such as white, brown and soft rot-fungi, to degrade the lignin and hemicellulose (Mosier et al., 2005). The process required low energy and mild conditions. However, it has drawbacks related to its long residence time and slow reaction rate as well as controlling of efficiency in up-scaled process.

#### **2.5.6 Organosolv pretreatment**

The organosolv process is effective in the removal of hemicellulose and lignin from cellulose microfibrils. As opposed to other pretreatments, the lignin structure is not altered to a great extent which allows for isolation of high quality lignin. High-purity lignin is extracted by organic solvent for its use in many applications (*e.g.* used as biofuel or production of phenolic compounds) (Zakzeski et al., 2010). The common solvents such as alcohols, ketones, esters, glycols, and organic acids have been used. The organic solvent and water mixtures are used to extract the lignin and hemicellulose fractions, leaving reactive cellulose in solid fraction. The organosolv pretreatment is commonly carried out at high temperature (200 °C); however, it can operate at lower temperature (120-180 °C) with additional catalysts such as oxalic, salicylic, and acetylsalicylic acid, diluted common acids (*i.e.* H<sub>2</sub>SO<sub>4</sub>, HCl, HNO<sub>3</sub>, and H<sub>3</sub>PO<sub>4</sub>) (Brudecki et al., 2013; Buranov & Mazza, 2012). Moreover, the addition of catalysts in the organic solvent can also enhance the extraction of both hemicellulose and lignin (de la Torre et al., 2013).

The conventional organic solvents used are the low-molecular-weight alcohols (*i.e.* methanol and ethanol) because they have low boiling points and are easy to recover. Although alcohols can inhibit the enzymatic hydrolysis, it can easily be removed from the solid fraction prior to enzymatic hydrolysis. The main advantage of using the organic

solvents over other chemical pretreatment is that relatively pure and low-molecular-weight lignin is recovered (Laurichesse & Avérous, 2014). Nevertheless, the capital and operating costs associated with organic solvent recovery (*i.e.* evaporation and condensation) need to be considered. Removal of the solvent from the treated biomass is also very important because it can inhibit enzymatic hydrolysis and subsequent fermentation steps.

### 2.5.6.1 Solvents and catalysts

Various solvents and catalysts have been investigated for use in organosolv pulping and pretreatment. Methanol and ethanol are the conventional solvents used for organosolv pretreatment. The physico-chemical parameter of a solvent called Hildebrand solubility parameter or  $\delta$ -value of a solvent can be used for estimating the solubility of compounds in solvents. The Hildebrand solubility parameter can give the estimate of the interaction between various materials. The solvents with a  $\delta$  value close to 11 indicate good solubility of lignin. These include acetic acid ( $\delta=10.1$ ), formic acid ( $\delta=12.1$ ), ethanol ( $\delta=12.9$ ), and acetone ( $\delta=9.7$ ) (Sannigrahi & Ragauskas, 2013). Hence these compounds are used in the pulping of biomass.

A general schematic diagram of the ethanol organosolv pretreatment is shown in **Figure 2.10**. The ethanol pretreatment is generally carried out at 140-200 °C for 1-2 h at an ethanol concentration of 40-70%. These conditions can extract lignin and hemicellulose around 60-80%, and 70-90%, respectively. Moreover, the addition of H<sub>2</sub>SO<sub>4</sub> (0.5-1.75%) in the solvents can lead to greater degradation of lignin; however, greater hemicellulose degradation may occur as a side reaction (Sannigrahi & Ragauskas, 2013).

(Romaní et al., 2013) used a glycerol-water mixture (56 wt.%) at 200 °C for 69 min for eucalyptus fractionation. This resulted in the effective extraction of lignin and hemicellulose yields of 91%, and 82%, respectively. The cellulose was hydrolyzed by enzymatic hydrolysis, achieving 98% cellulose-to-glucose conversion. The glycerol-water mixture of lignocellulose fractionation has also been explored as an eco-friendly treatment. Nevertheless, the drawback of this method is high-energy costs in solvent recovery because the glycerol has high a boiling point (290 °C).

(Huijgen et al., 2010) investigated the pretreatment of wheat straw with 50%/50% acetone-water mixture at various reaction temperatures and times. Pretreatment under the suitable condition could remove 82% hemicellulose, 79% delignification and 93% cellulose recovery at 205 °C for 1 h. When the temperature was increased up to 200 °C, the content of residual lignin was increased due to condensation reaction. Nevertheless, the

amount of lignin recovery can be increased up to 100% after pretreatment at 220 °C for 120 min. Hemicellulose hydrolysis was auto-catalyzed by the pH drop resulting from the formation of acetic acid by dehydration of hemicellulose acetyl side groups.

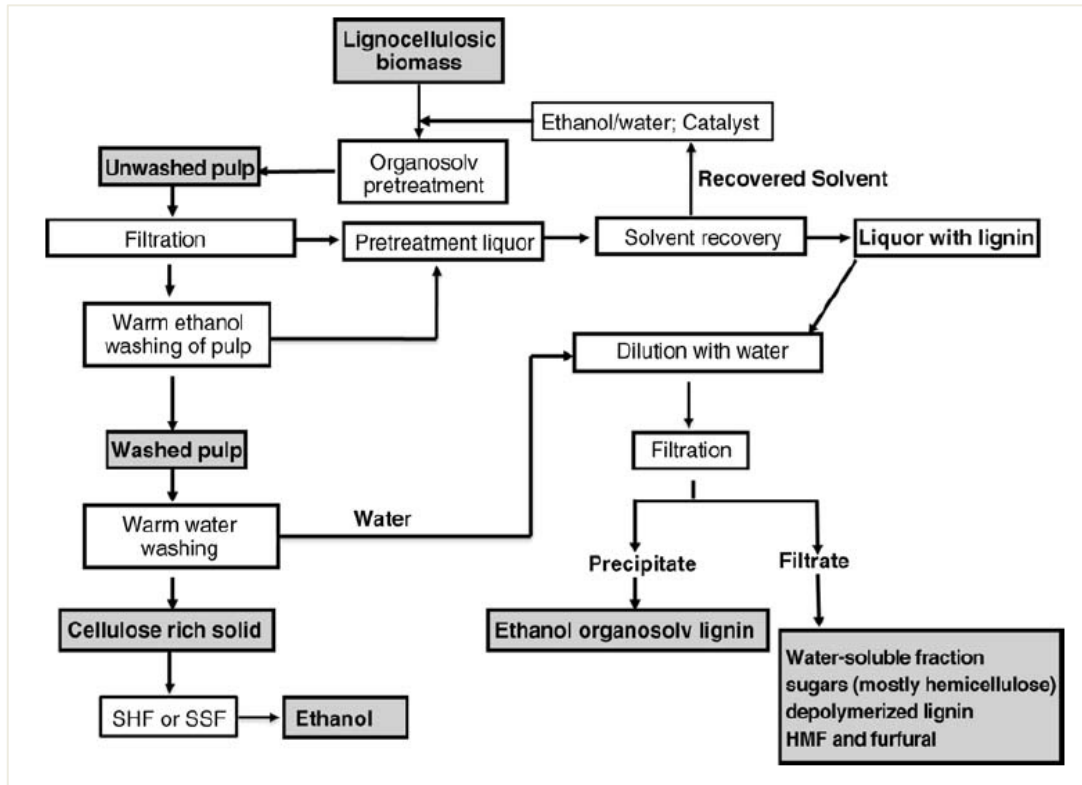


**Figure 2.10** Schematic representation of an ethanol organosolv pretreatment process (Sannigrahi & Ragauskas, 2013).

In a recent study, (Bozell et al., 2011a) developed an organosolv fractionation process to isolate lignocellulose with a ternary mixture of methyl isobutyl ketone (MIBK), ethanol and water in the presence of acid catalyst (sulfuric acid). This treatment can selectively extract hemicellulose and lignin, leaving cellulose in the solid phase. Separation of the organic phase containing lignin and the aqueous phase containing hemicellulose hydrolysis products can be achieved by adding more water to the liquid phase which resulted in phase disturbance. Pretreatment of biomasses (*i.e.* aspen, white poplar, tulip poplar, mixed oak and mixed southern hardwoods) with single-phase liquor at 140 °C for 56 min in the presence 0.05 M H<sub>2</sub>SO<sub>4</sub> resulted in the solid phase enriched in cellulose (92.7%). Moreover, the cellulose glucan content can approach 98% when using high acid concentration. It was reported that while the cellulose and lignin fractions isolated using

this technology were quite pure; however, downstream processing by ion exchange chromatography of the hemicellulose stream is required for removal of the impurities for subsequent processing.

### 2.5.6.2 Mechanisms of organosolv delignification

It is well known that the main linkages of lignin are aryl ether linkages (*i.e.*  $\alpha$ -O-aryl ether and  $\beta$ -O-aryl ether bonds). The  $\alpha$ -O-aryl ether bonds are readily cleaved while the  $\beta$ -O-aryl ether bonds are broken under more severe conditions (high temperature and pressure), especially at high acid concentration. The mechanisms of cleavage of  $\beta$ - and  $\gamma$ -O-aryl ether linkages are presented in **Figure 2.11**. The condensation reactions of lignin polymer can occur at severe conditions (high temperature, long residence time, and high acidic solvent). This reaction causes the formation of high-molecular-weight lignin which is difficult to dissolve in the organic solvents. The intermediate substance (benzyl carbocation) of  $\beta$ -O-aryl and  $\alpha$ -O-aryl ether cleavage can form a bond with another electron-rich carbon atom in a neighboring lignin unit, thus increasing lignin condensation as shown in **Figure 2.12**. Recently, (Roberts et al., 2011) have found that the method for preventing lignin condensation. It is found that the additional phenols in organosolv processes can prevent the condensation by reaction of the benzyl carbocations by electrophilic aromatic substitution on the aromatic ring of the solvent. This can block the reactive benzyl position, preventing it from undergoing condensation reactions with other lignin fragments.

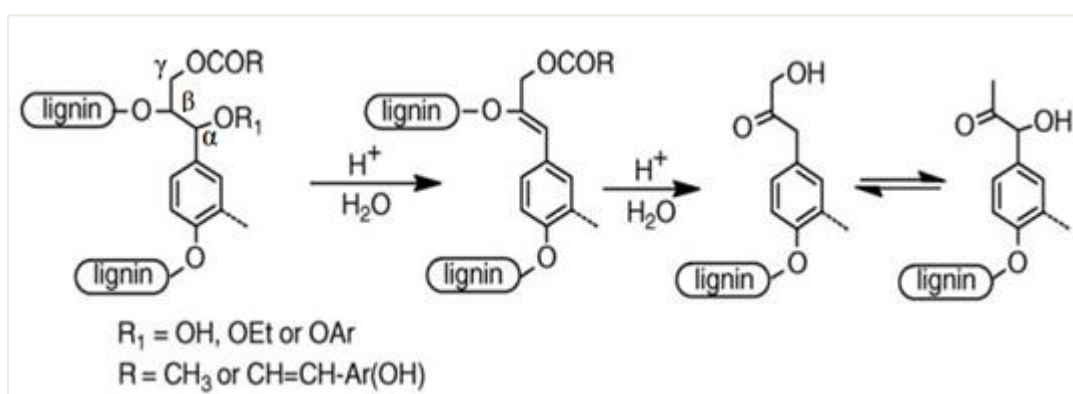


**Figure 2.11** Solvolytic cleavage of  $\beta$ - and  $\alpha$ -O-aryl ether linkages in lignin (Sannigrahi & Ragauskas, 2013).

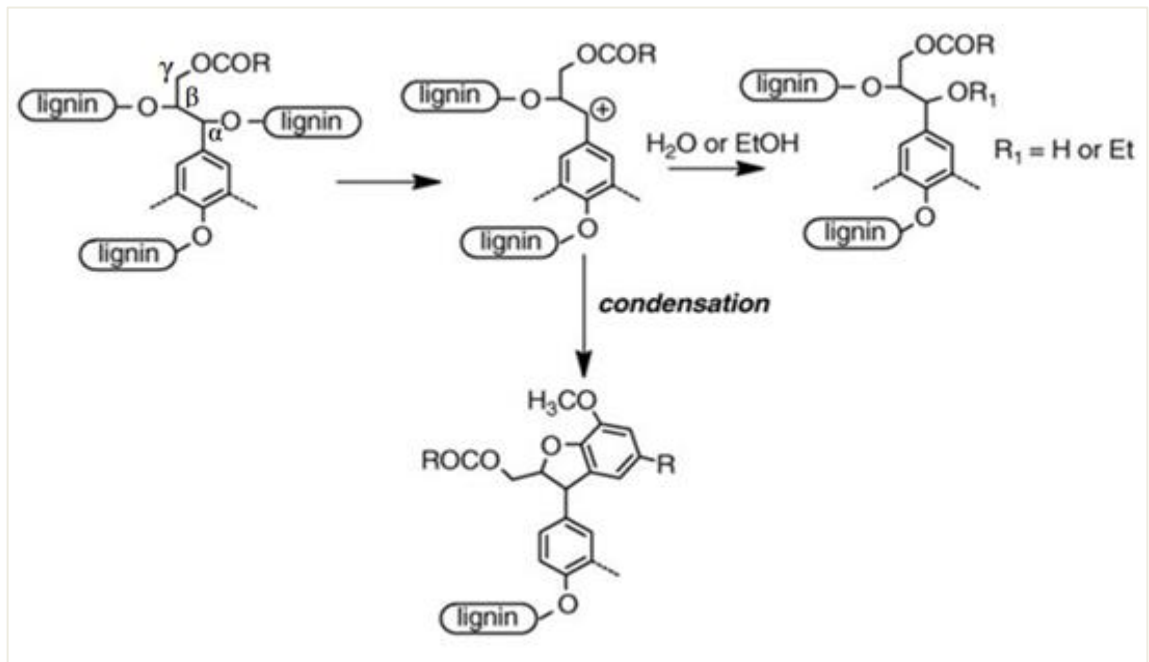


**Figure 2.12** Solvolytic cleavage of  $\alpha$ -O-aryl ether linkages and condensation reaction in lignin structure (Sannigrahi & Ragauskas, 2013).

## 2.6 Summary of biomass pretreatment

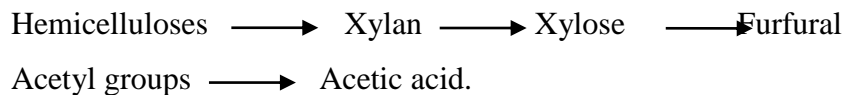
**Table 2.4** Methods for biomass lignocellulosic pretreatment (Harmsen, 2010; Mosier et al., 2005)

Pretreatment process	Advantages	Limitations and disadvantages
Physical pretreatment	Reduces cellulose crystallinity	Power consumption usually higher than inherent biomass energy
Steam explosion	Causes hemicellulose degradation and lignin transformation; cost-effective	Destruction of a portion of the xylan fraction; incomplete disruption of the lignin-carbohydrate matrix; generation of compounds inhibitory to microorganisms
AFEX	Increases accessible surface area, removes lignin and hemicelluloses to an extent; does not produce inhibitors for downstream processes	Not efficient for biomass with high lignin content
CO <sub>2</sub> explosion	Increases accessible surface area, cost-effective; does not cause formation of inhibitory compounds	Does not modify lignin or hemicelluloses
Ozonolysis	Reduces lignin content; does not produce toxic residues	Large amount of ozone required; expensive
Acid pretreatment	Hydrolyzes hemicelluloses to xylose and other sugars; alters lignin structure	High cost; equipment corrosion; formation of toxic substances
Alkali pretreatment	Removes hemicelluloses and lignin; increases accessible surface area	Long residence times required; irrecoverable salts formed and incorporated into biomass
Organosolv	Hydrolyzes lignin and hemicelluloses	Solvents need to be drained from the reactor, evaporated, condensed, and recycled; high cost
Biological	Degrades lignin and hemicelluloses; low energy requirements	Rate of hydrolysis is very low

As mentioned above, pretreatment methods were developed because of the requirements for various end uses of biomass feedstock. **Table 2.4** summarizes of each pretreatment method disadvantages and advantages.

## 2.7 Lignocellulose hydrolysis techniques

Hydrolysis processes are related to breaking down the  $\beta$ -1,4 glycosidic bonds in cellulose prior to fermentation. All products are converted from lignocellulosic biomass as presented in **Figure 2.13**. The hemicelluloses are hydrolyzed to xylose, mannose, acetic acid, galactose, and glucose are liberated. Hemicellulose hydrolysis can be generalized as:



The xylan can decompose into eight main products: water, methanol, formic, acetic, and propionic acids, hydroxy-1-propanone, hydroxy-1-butanone and 2-furfuraldehyde (Yu et al., 2008). Under strong severity conditions (*i.e.* high temperature and pressure), the xylose is further degraded into furfural (Ando et al., 2004). Similarly, 5-hydroxymethyl furfural (HMF) is formed from hexose degradation (Ando et al., 2004). Cellulose is broken down the structure to hydrolyze into glucose. The following reaction is proposed for hydrolysis of cellulose:



Different methods for the lignocellulosic hydrolysis have been recently developed. At present, there are various techniques for hydrolysis such as acid hydrolysis, alkaline hydrolysis, enzyme hydrolysis, hot-compressed water (HCW) hydrolysis and super solid acid catalyst hydrolysis. On the other hand, there are some other hydrolysis methods in which no chemicals or enzymes are applied. For instance, lignocelluloses may be hydrolyzed by gamma-ray or electron-beam irradiation, or microwave irradiation, nevertheless, those processes are commercially unfeasible. This review has divided the hydrolysis technologies into three main groups, as shown in **Figure 2.14**.

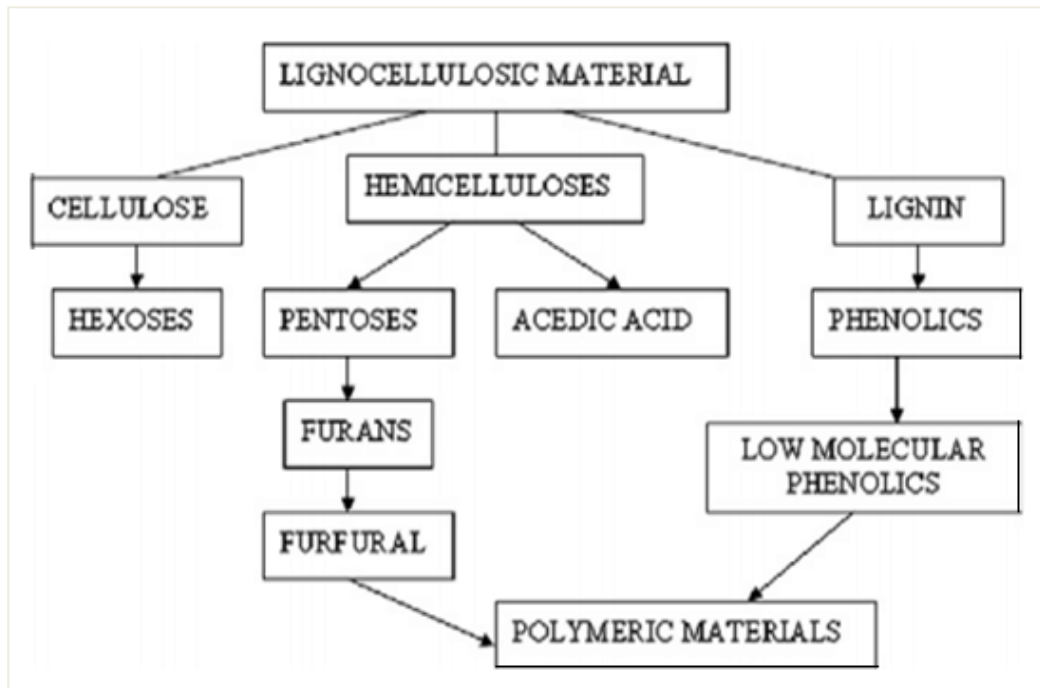


**Figure 2.13** The products formed during hydrolysis of lignocellulosic material.

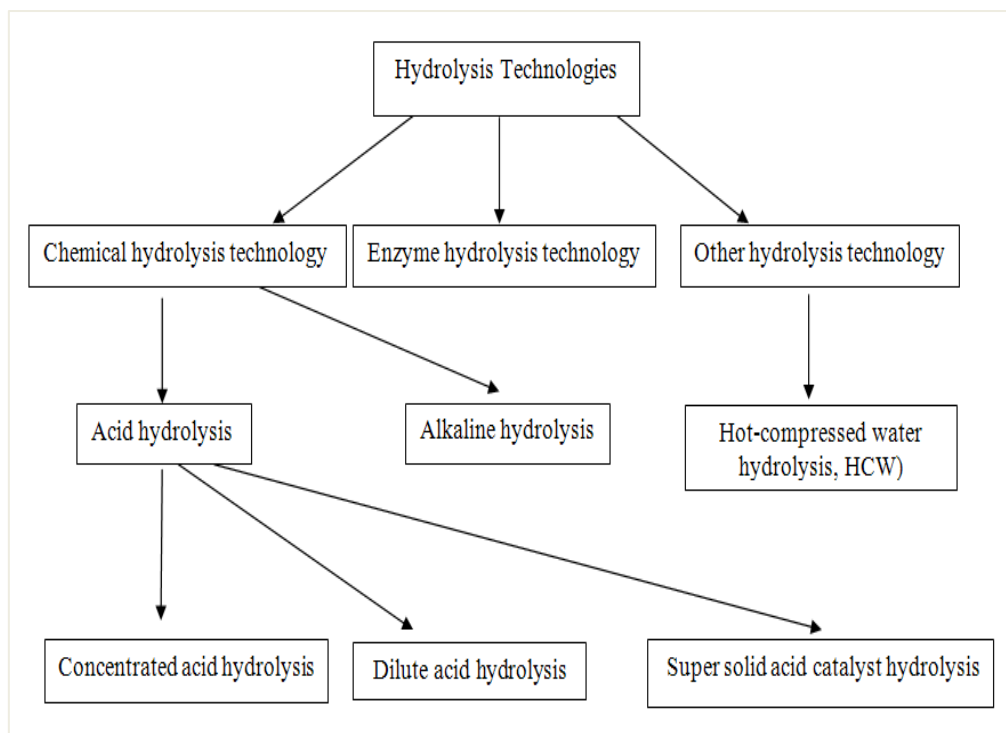


**Figure 2.14** Diagram of various hydrolysis technologies.

## **2.7.1 Acid hydrolysis**

### **2.7.1.1 Dilute acid hydrolysis**

Typically, dilute acid hydrolysis uses sulfuric acid of less than 1% for operating. It has been known for over 150 years that cellulose can be converted into glucose by dilute acid hydrolysis, which is feasible at a commercial scale and capable of providing a maximum glucose yield of 50% (Brethauer & Wyman, 2010). Higher glucose productions can be achieved by applying higher temperature for a shorter time. However, the degradation of glucose during dilute acid hydrolysis can lead to formation of inhibitory by-products (*i.e.* furans) at high temperature and long reaction time. (Yu et al., 2008) reported that countercurrent shrinking bed reactor technologies can be carried out for achieving more than 90% glucose yield from cellulose. Due to different structure between hemicellulose sugars (C<sub>5</sub> sugars) and cellulose sugars (C<sub>6</sub> sugars), the hemicellulose degrades faster than cellulose. One of classical methods that can increase the sugar yield and decrease degradation of sugar is a two-stage processes; first stage for recovering C<sub>5</sub> sugar, and second stage for recovering C<sub>6</sub> sugar (Sanchez et al., 2004).

### **2.7.1.2 Concentrated acid hydrolysis**

Concentrated sulfuric acid is commonly used to cleave the hydrogen bonding between cellulose chains and promote the conversion of cellulose into completely amorphous form. Compared to dilute acid hydrolysis, the concentrated acid hydrolysis operated under lower temperature (20-50°C) with longer time (2-6 h) can achieve almost 100% yield of sugars with lower sugar degradation. However, its drawbacks include environmental problem related to the use and treatment of acid, corrosion of equipment, and high cost of acid consumption (Guo et al., 2012).

### **2.7.1.3 Acid hydrolysis by solid catalysts**

The use of a homogenous catalyst or liquid acid hydrolysis is attractive due to its efficient reaction and mass transfer. Nevertheless, this method has encountered with many problems such as product separation, treatment of waste, catalyst recovery, and corrosion of equipment and reactor. Therefore, many researchers (Hara, 2010; Van de Vyver et al., 2011; Zhou et al., 2011) are recently interested in solid acid catalysts in order to overcome these problems related to the use of liquid acids. The solid acid catalysts have many advantages over liquid catalysts such as selectivity of product, catalyst activity, long operating time of catalysts, and ease of catalyst recycling. Moreover, they are more environmentally friendly compared to the liquid catalysts. Nevertheless, the development

of hydrothermal hydrolysis process in the presence of solid acid catalyst is challenging. Firstly, their acid strength and catalytic activities decrease when using water as the reaction media. Secondly, most of solid acid catalysts do not have strong acid sites enough to absorb the main linkages ( $\beta$ -1,4-glycosidic bonds) of cellulose for hydrolysis. These problems can be identified that solid acids with Bronsted acid sites (used for donating protons or accepting electrons during reaction) are very important to biomass hydrolysis. As a result, a good solid acid catalyst needs to be water-tolerant, has a strong acidity and has many acid sites for polysaccharides to access (Van de Vyver et al., 2011; Zhou et al., 2011). Recently, some studies reported have on the uses of cellulose hydrolysis using solid acid catalysts (Lanzafame et al., 2012; Van de Vyver et al., 2011; Yamaguchi et al., 2009). Several types of solid acid catalysts such as H-form zeolite, transition-metal oxide, cation-exchange resins, supported metal oxide solid acid catalysts, and supported carbonaceous solid acid catalysts, have been studied for their catalytic performances in the hydrolysis reaction of lignocellulose, as presented in **Table 2.5**. It is revealed that the Bronsted acid site on solid catalysts is important for the efficient hydrolysis lignocellulose. Sulfonated activated carbon showed a remarkably high yield of glucose (40%) and selectivity of higher than 90%. Moreover, integrating the use of ionic liquids for pretreatment prior to the hydrolysis with solid catalysts can enhance the glucose yield. However, the ionic liquid is expensive and is not economically feasible in large-scale processes.

**Table 2.5** Comparison of catalytic properties and activities of solid acid catalysts for cellulose hydrolysis to glucose (Guo et al., 2012)

Catalyst	Amount	Amount of acid sites (mmol/g)	Substrate	Amount	Pretreatment method	Water amount	Reaction temperature (°C)	Reaction time (h)	Glucose yield (%)	Selectivity
HSM-5B	0.2 wt%	0.3	Cellobiose	1 wt %	-	-	175	0.5	33.7	74.4
H-ZSM5	50 mg	-	Cellulose	45 mg	Milling	5 mL	150	24	12	-
HY	10 mg	-	Cellulose	100 mg	[BMIm][Cl]	10 mg	(240 W)	0.12	35	76
$\gamma$ -Al <sub>2</sub> O <sub>3</sub>	1.5 g	0.05	Cellulose	1.5 g	-	15 mL	150	3	-	-
Layered HNbMoO <sub>6</sub>	0.2 g	1.9	Cellobiose	1.0 g	-	10 mL	100	18	41	-
HT-OH <sub>Ca</sub>	0.5 g	1.17	Cellulose	0.45	Milling	150 mL	150	24	40	85
Nafion-50	0.1 g	-	Cellulose	0.2 g	[BMIm][Cl]	20 mL	160	4	35	-
Sulfated ZrNDSBA-15	50 mg	-	Cellobiose	250 mg	-	50 mL	160	1.5	55	65
FeCl <sub>3</sub> /Silica	0.47g	-	Cellulose	2.0 g	[BMIm][Cl]	30 mL	130	24	3	-
FeCl <sub>3</sub> /Silica	0.47g	-	Cellulose	2.0 g	[BMIm][Cl]	31 mL	190	24	9	-
Amberlyst-15	50 mg	1.8	Cellulose	45 mg	Milling	5 mL	150	24	25	-
Amberlyst-15	1.5 g	4.4	Cellulose	1.5 g	-	15 mL	150	3	15	-
Dowex 50wx8-100 ion-exchange resin	26 mg	-	Cellulose	50 mg	[BMIm][Cl]	270 mg	110	4	83	-
AC-SO <sub>3</sub> H	50 mg	1.25	Cellulose	45 mg	Milling	5 mL	150	24	40	95
AC-SO <sub>3</sub> H-250	0.3 g	2.23	Cellulose	0.27	-	27 mL	150	24	62	74
Fe <sub>3</sub> O <sub>4</sub> .SBA-SO <sub>3</sub> H	1.5 g	1.09	Cellobiose	1.0 g	-	15 mL	120	1	98	-
Fe <sub>3</sub> O <sub>4</sub> .SBA-SO <sub>3</sub> H	1.5 g	1.09	Cellulose	1.0 g	[BMIm][Cl]	16 mL	150	3	50	-
Fe <sub>3</sub> O <sub>4</sub> .SBA-SO <sub>3</sub> H	1.5 g	1.09	Starch	1.0 g	-	15 mL	150	3	95	-
Fe <sub>3</sub> O <sub>4</sub> .SBA-SO <sub>3</sub> H	1.5 g	1.09	Corn cob	1.0 g	-	16 mL	150	3	45	-

**Table 2.5** Comparison of catalytic properties and activities of solid acid catalysts for cellulose hydrolysis to glucose (continue) (Guo et al., 2012)

Catalyst	Amount	Amount of acid sites (mmol/g)	Substrate	Amount	Pretreatment method	Water amount	Reaction temperature (°C)	Reaction time (h)	Glucose yield (%)	Selectivity
PCP <sub>s</sub> -SO <sub>3</sub> H	0.2 g	1.8	Cellulose	25 mg	-	2.0 g	120	3	1.4	27
Ru-CMKs	50 mg	-	Cellulose	324 mg	-	40 mL	230	24	34	51
Cellulase-MSNs	4.5 mg	-	Cellulose	15 mg	-	-	50	24	90	-
HPA	0.08 mmol	-	Cellulose	0.1 g	-	5 mL	180	2	51	90
Cs-HPA	0.07 mmol	-	Cellulose	0.1 g	-	7 mL	170	8	39	89
Micellar HPA	0.07 mmol	-	Cellulose	0.1 g	-	8 mL	170	8	60	85

#### **2.7.1.4 Alkaline hydrolysis**

Alkaline catalysts are commonly used in lignocellulose hydrolysis process. The anomeric carbon atom can be attacked by OH<sup>-</sup> ions for cleaving the ether bonds (*i.e.* mainly glycosidic bonds). The cleavage of glycosidic bonds in water-soluble carbohydrates can be proved that alkaline hydrolysis can achieved the higher reaction rate than acid and hydrothermal hydrolysis. In addition, dilute alkaline pretreatment of lignocellulose can cause swelling, decreasing the crystallinity of cellulose, increasing internal surface area and cleavage of structural bonds between carbohydrates and lignin. However, the alkaline hydrolysis is difficult to achieve a high sugar yield since mono- and dimeric sugars (*i.e.* cellobiose, glucose, and fructose) can be degraded at low temperature (less than 100 °C) (Yu et al., 2008). It is found that the organic acids are formed during reaction due to severe attacking by alkaline. These organic acids lead to problems such as inhibition in fermentation process.

#### **2.7.1.5 Enzymatic hydrolysis**

Enzymatic hydrolysis is a classical method for breaking down the carbohydrate structure (starch or cellulose) to obtain high yield and high purity of sugars, but the main problems of this method are high capital cost and low reaction rate for use on a commercial scale (Kumar et al., 2009). Cellulases are a group of enzymes involved in hydrolysis of cellulose (Yu et al., 2008). The enzymatic process is operated under mild conditions *i.e.* 30-50 °C, pH 4-5. A pretreatment step is required prior to enzymatic hydrolysis in order to open the lignocellulose structure for increasing enzyme accessibility to the cellulose fibers.

#### **2.7.1.6 Hot-compressed water (HCW)**

##### **(a) Properties of HCW**

HCW has been used in many applications related to the pretreatment and hydrolysis of lignocellulosic biomass. Water in a sub- or super critical state have unique properties, such as relative dielectric constant ( $\epsilon$ ), density and interaction of hydrogen bonds, as shown in **Figure 2.15**. HCW can be defined as water at temperature above 150°C under self-generated or applied pressure (Toor et al., 2011). Compared to liquid water in normal state, HCW has a lower dielectric constant, weaker hydrogen bonds and high isothermal compressibility. The properties of sub- and supercritical water are summarized in **Table 2.6**.

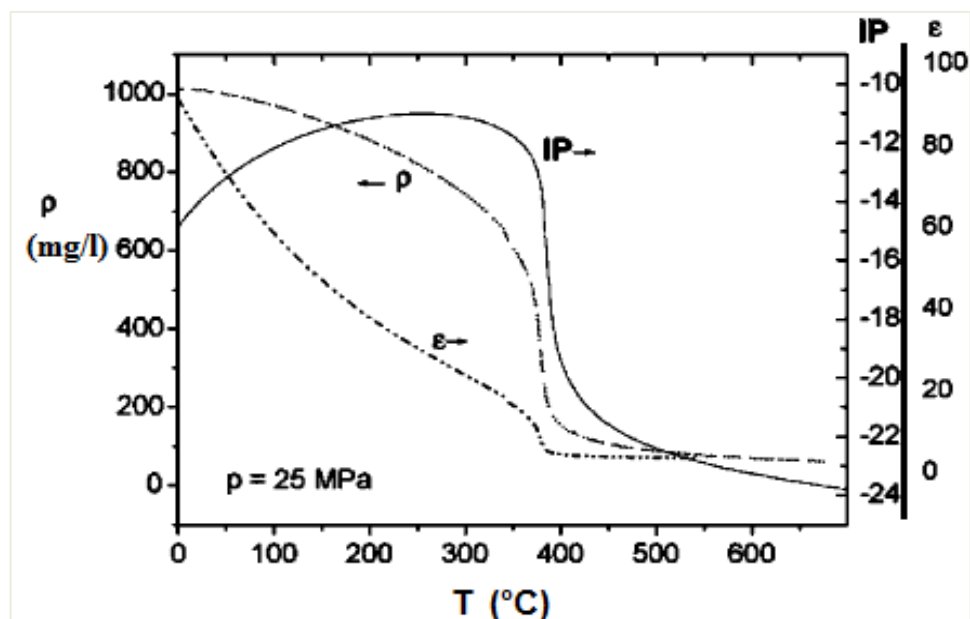


**Figure 2.15** Selected properties of water at high temperature and high pressure. IP = ionic product, expressed as  $\log[\text{H}_3\text{O}^+][\text{OH}^-]$ ;  $\epsilon$  = relative dielectric constant; a higher  $\epsilon$  reduces the activation energy of a reaction with a transition state of higher polarity compared to the initial stage ;  $\rho$  = density, defined as mass per unit volume (Yu et al., 2008).

Subcritical water is water that is under a pressurized condition at temperatures above its boiling point under ambient pressure, but below the critical point ( $T_c = 374\text{ }^\circ\text{C}$ ,  $P_c = 22.1\text{ MPa}$ ,  $\rho_c = 320\text{ kg/m}^3$ ). Subcritical water remains in the aqueous phase and has properties different from ambient water which are a low relative dielectric constant and a large ion product. The dielectric constant of water decreases when temperature increases. The ionic product (IP) for water near the critical temperature ( $\sim 250\text{ }^\circ\text{C}$ ) is about 3 orders of magnitude higher than that of ambient water (Toor et al., 2011). The concentrations of  $\text{H}^+$  and  $\text{OH}^-$  and their affinities are higher in HCW, which makes HCW an effective medium for acid and/or base catalysts for reactions such as hydrolysis of ether and/or ester bonds, and also as a solvent for extraction of low molecular-mass products. The supercritical water is water above the critical temperature of  $374\text{ }^\circ\text{C}$ . It is compressible and the properties depend strongly on pressure. Supercritical water is miscible with light gases and small organic compounds, and its dielectric constant varies in the range of  $3.7\sim 19.72$ , which has an influence on the rate of reactions with a polar-activated complex.

**Table 2.6** The properties of water under different conditions (Yu et al., 2008)

Fluid	Ordinary water	Subcritical water	Supercritical	
Temperature (°C)	25	250	400	400
Pressure (MPa)	0.1	5	25	50
Density (g·cm <sup>-3</sup> )	1	0.80	0.17	0.58
Dielectric constant	78.5	27.1	5.9	10.5
pK <sub>w</sub>	14.0	11.2	19.4	11.9
Heat capacity (kJ·kg <sup>-1</sup> ·K <sup>-1</sup> )	4.22	4.86	13.0	6.8
Dynamic viscosity (mPas)	0.89	0.11	0.03	0.07
Heat conductivity (mW·m <sup>-1</sup> ·K <sup>-1</sup> )	608	620	160	438

### (b) Cellulose and hemicellulose decomposition in HCW

The hydrolysis of cellulose has been studied under HCW conditions. (Toor et al., 2011) investigated a reaction mechanism for conversion of microcrystalline cellulose in super- and subcritical state of water as shown in **Figure 2.16**. For subcritical water, the crystalline part of cellulose is hydrolyzed only at the surface region without swelling or dissolving as shown in the upper part of this figure. Therefore, the overall conversion rate of microcrystalline cellulose is slow and there is no cellulose II crystal formed in the residue. Conversely, the crystallite can swell or dissolve around the surface region to form amorphous-like cellulose molecules in near- and supercritical water. These molecules are inactive; therefore, they can be readily hydrolyzed to lower DP celluloses and cellooligosaccharides. Some of the hydrolysate can pass from the polymer phase to the water phase by the cleavage of their hydrogen bond networks, while others remain on the crystallite surface of the residue. The released portion in the water phase is further hydrolyzed to water-soluble saccharides, or crystallized as water-insoluble cellulose after the reaction. In contrast, the amorphous-like portion remaining in the polymer phase is hydrolyzed to water-soluble saccharides, or swells further or dissolves and moves from the polymer phase to the water phase. As a consequence, the overall conversion rate of microcrystalline cellulose can increase more than that in near- and subcritical water.

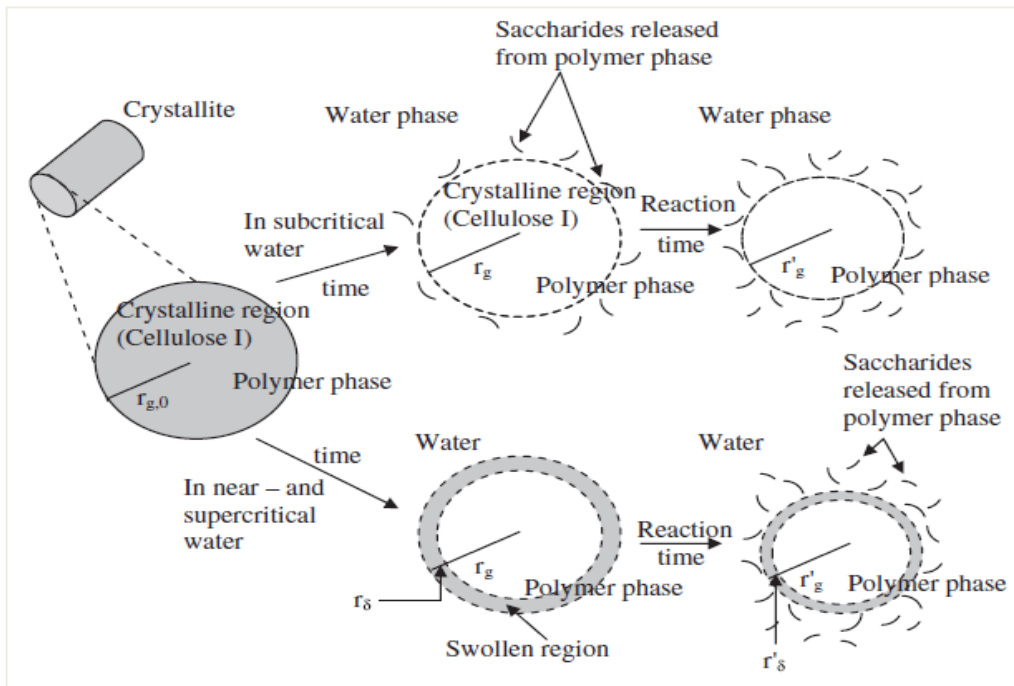


**Figure 2.16** Mechanism for the conversion of microcrystalline cellulose in subcritical and supercritical water at 25 MPa (Toor et al., 2011).

(Sasaki et al., 2008) studied the conversion of cellulose at temperatures between 290-400 °C with reaction times of less than 14 s. It is revealed that the main products of cellulose conversion in HCW were glucose, fructose, erythrose, dihydroxyacetone, glyceraldehyde, pyruvaldehyde, and oligomers (cellobiose, cellotriose, cellotetraose, cellopentaose, and cellohexaose). Furthermore, the main pathway of microcrystalline cellulose in sub- and supercritical water is also discovered. It is described that cellulose can be hydrolyzed by two main pathways of reaction, which are dehydration reaction of reducing-end glucose by cleavage of the glycosidic bond in cellulose fraction (or partly retro-aldol reaction) and hydrolysis of the glycosidic bond via the dissolution and swelling of cellulose. The factors that might have significant influence on cellulose hydrolysis in HCW include feedstock properties, heating rates, reactor configurations, and catalysts and other additives.

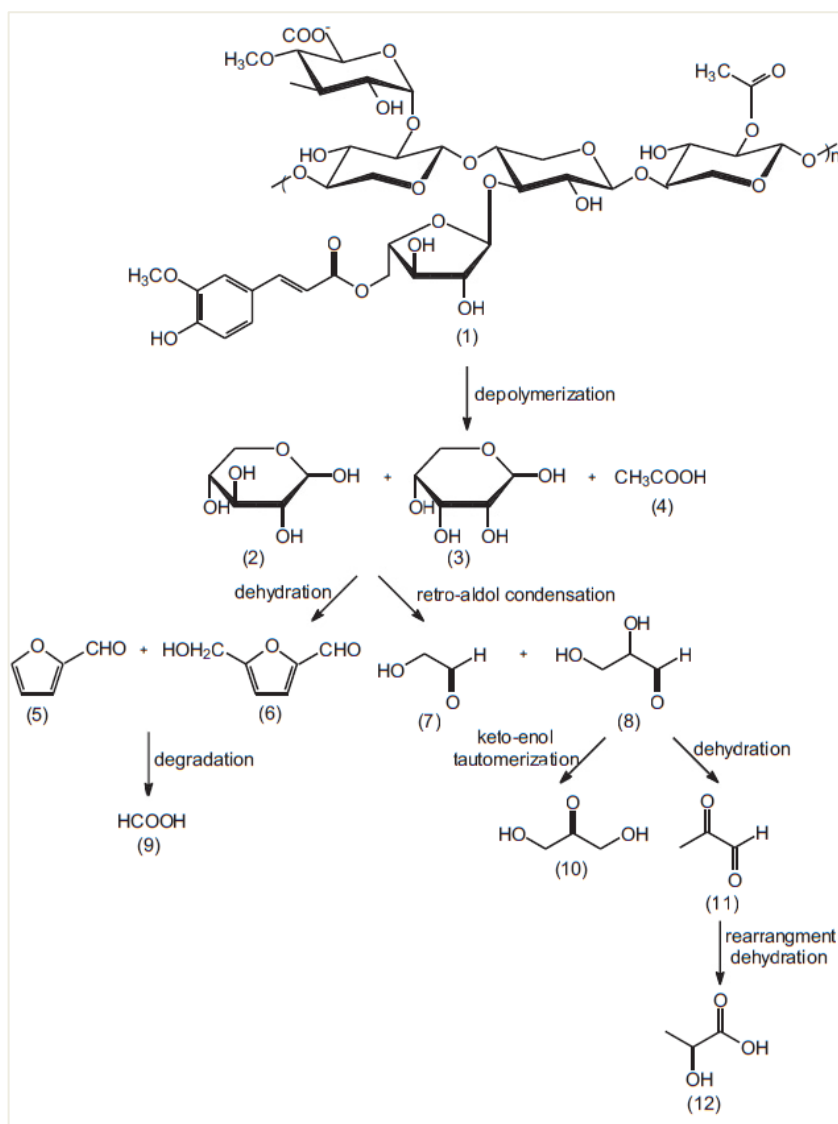


**Figure 2.17** Mechanism pathway of xylan in HCW (representative hemicellulose) decomposition (Aida et al., 2007; Piñkowska et al., 2011).

**Figure 2.17** shows the probable reaction pathway of xylan in HCW. The process of the decomposition of xylan starts from (1) its hydrolysis and the cleavage of acetyl groups and the formation of (2) xylose, (3) arabinose, and (4) acetic acid (Chareonlimkun et al., 2010). In the second stage of the reaction, the pentoses produced dehydrated and subjected to retro-aldol condensation. As a result of the dehydration of the pentoses, (5) furfurals (6) HMF are formed. Due to the consecutive reactions of hydration, dehydration, tautomerization and hydration, further intermediate products were produced, from which (9) formic acid and probably levulinic acid were obtained. As a result of retro-aldol condensation of xylose and arabinose, the liquid product fraction contained (7)

glycolaldehyde and (8) glyceraldehyde (Yu et al., 2008). Glyceraldehyde was further converted in tautomerization reaction to (10) dihydroxyacetone, and in dehydration reaction to (11) pyruvaldehyde (Ando et al., 2004). In turn, the regrouping and dehydration of pyruvaldehyde might have resulted in the production of (12) lactic acid.

### (c) Glucose decomposition in HCW

Sugars are the main products from the hydrolysis of lignocellulose. They are significant feedstocks for conversion into valuable chemicals. Therefore, understanding the mechanism of sugar decomposition is very important in biorefinery processes. Sugars such as glucose can be readily decomposed to stable form of product (5-hydroxymethyl furfural; HMF) in HCW. (Sasaki et al., 2008) studied the fundamental kinetics of glucose decomposition in HCW and found that the main products of glucose decomposition were fructose, erythrose, glycolaldehyde, dihydroxyacetone, glyceraldehyde, 1,6-anhydroglucose (AHG), and pyruvaldehyde. **Figure 2.18** shows the basic pathway of glucose decomposition as follows (1) glucose isomerization into fructose via keto-enol tautomerisation, (2) glucose dehydration into AHG, (Ando et al., 2004) and (3) glucose decomposition into aldehyde and ketone via retro-aldol condensation (Dedsuksophon et al., 2011). Further, (4) dehydration of the tautomerization intermediate and fructose produced 5-HMF (Aida et al., 2007). Moreover, the key reactions revealed that they were dehydration (C-O bond splitting) and retro-aldol condensation (namely C-C bond breaking). At temperature between 400-500 °C, the retro-aldol condensation became predominant. The dehydration reaction became significant at lower temperatures (250-350 °C).

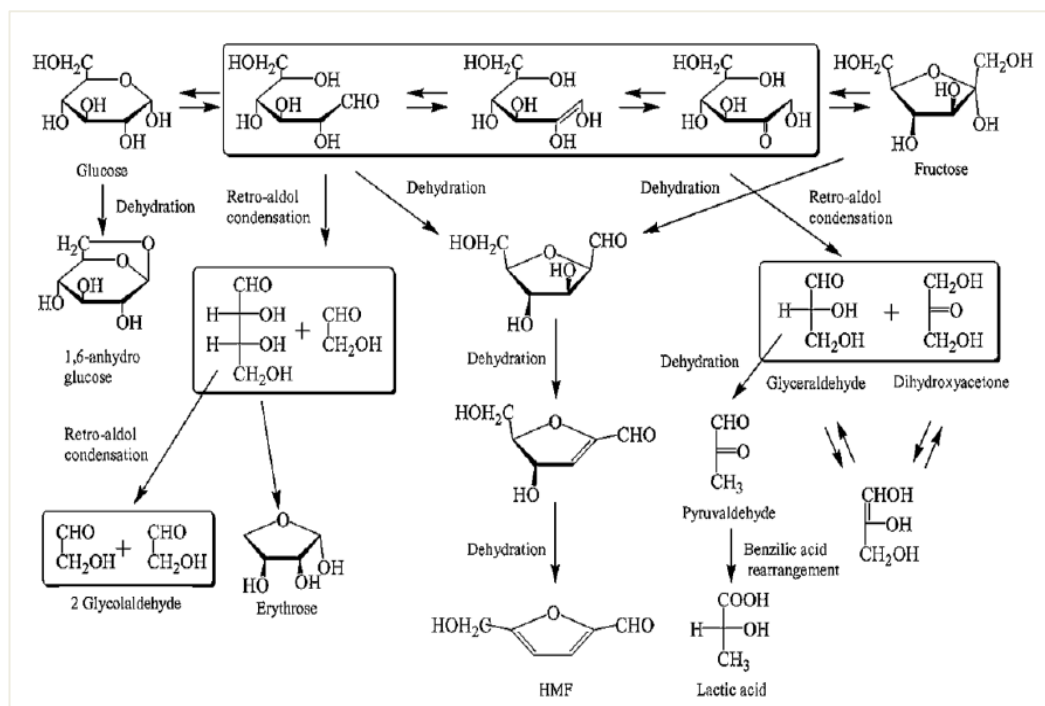


**Figure 2.18** Main reaction pathways of glucose and fructose in HCW (Yu et al., 2008).

#### (d) Lignocellulose decomposition in HCW

Many previous studies have focused on model compounds such as cellulose, glucose, and xylose. Few studies have been conducted so far on the detailed reaction mechanisms of the decomposition of lignocellulose in HCW due to the complicated structure of biomass. (Ando et al., 2004) studied the mechanism of biomass decomposition in HCW. The study revealed that hemicellulose starts to decomposition at 180 °C; whereas cellulose did not start to decompose until the temperature above 230 °C. Lignin was removed by HCW at relatively low temperature and flowed out with decomposed products of hemicellulose. Nevertheless, for the lignocellulosic biomass which has a large amount of lignin such as Japan cedar (33% lignin), a significant amount of lignin remained in the reactor after the obtained cellulose. Therefore, it is required to develop processes for isolating the components of lignocellulose and improving the sugar recovery. As the decomposition of hemicellulose starts at lower temperature (180 °C) than that of cellulose which rapidly increases at temperature higher than 230 °C, the degradation of glucose would be unavoidable if hemicellulose and cellulose are hydrolyzed together. As mentioned earlier, due to the complicated pathways of the HCW reaction, it is quite

difficult to find suitable conditions for lignocellulose in HCW system (Ando et al., 2004; Chareonlimkun et al., 2010; Jeong et al., 2012).

### 2.7.1.7 Comparison of various hydrolysis processes

Various hydrolysis methods of lignocelluloses are compared, as shown in **Figure 2.19** and **Table 2.7**. It can be seen that concentrated acid showed the highest performance based on the obtained glucose yield (90%). Dilute acid process can achieve the glucose yield of 70%. The enzymatic hydrolysis method can also give a glucose yield of 90%. In case of alkaline hydrolysis the lowest sugar yield (30%) was observed since the mono- and diametric carbohydrates, such as glucose, fructose, or cellobiose, are severely attacked by alkalis at temperature below 100 °C. However, it should be noted that the acid hydrolysis technologies have to high operating cost and various environmental and corrosion problem. In case of enzyme hydrolysis, the main problems are high cost of enzyme and long reaction time for hydrolysis.

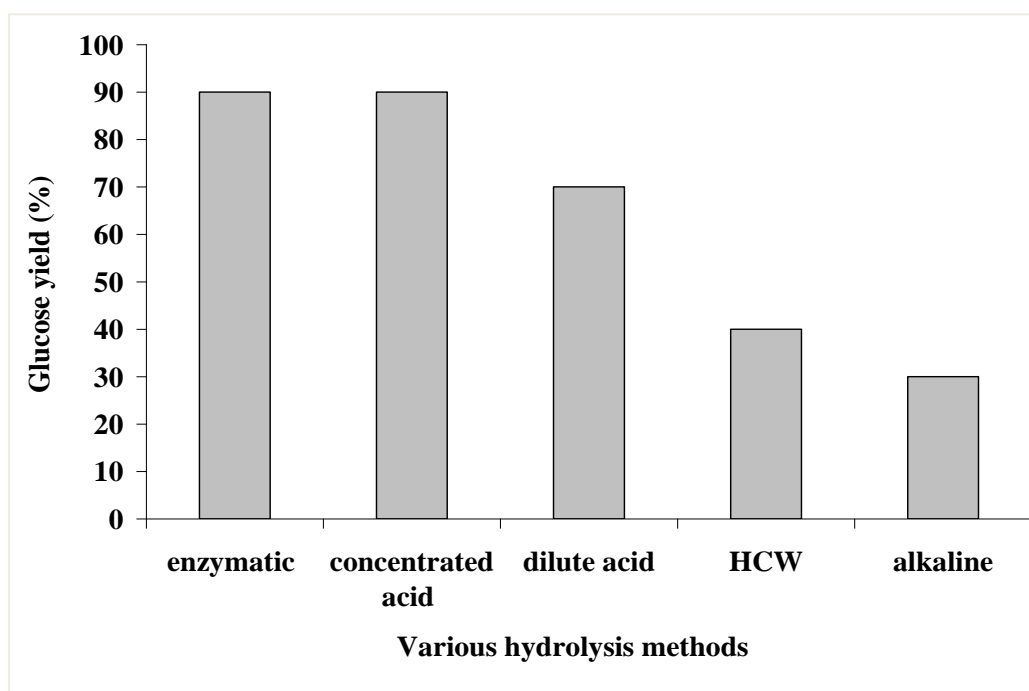


**Figure 2.19** Comparison of the various hydrolysis methods to glucose: enzymatic (70 °C, 1.5 days), concentrated acid (30–70% H<sub>2</sub>SO<sub>4</sub>, 40 °C, 2–6 h), diluted acid (<1% H<sub>2</sub>SO<sub>4</sub>, 215 °C, 3 min), HCW (150–250 °C, 10–25 MPa, 0–20 min), and alkaline (18% NaOH, 100 °C, 1 h) (Lenihan et al., 2010; Yu et al., 2008).

**Table 2.7** Comparisons of various hydrolysis techniques under various conditions (Yu et al., 2008).

Hydrolysis methods	Conditions	Sugar yield (%)	Advantages and disadvantages (A and D)
Concentrated acid	30–70% H <sub>2</sub> SO <sub>4</sub> 40 °C 2–6 h	90	A(i): high sugar recovery (ii): high reaction rate D(i): environmental and corrosion problems (ii): high costs for acid recovery
Dilute acid	<1% H <sub>2</sub> SO <sub>4</sub> 215 °C 3 min	50-70	A(i): high sugar recovery (ii) very high reaction rate D(i): environmental and corrosion problems (ii): sugar decomposition at elevated temperatures (iii): high utility cost for elevated temperatures (iv): high operating cost for acid consumption
Alkaline	18% NaOH 100 °C 1 h	30	A(i): high reaction rate D(i): low sugar yield (ii): sugar decomposition by alkali attack
Enzymatic	Cellulose 70 °C 1.5 days	90	A(i): high yield of relatively pure sugar (ii): mild environmental conditions (iii): no environmental and corrosion problems D(i): pretreatment of biomass required (ii): high cost of cellulase enzymes (iii): low hydrolysis rate (using long time of hydrolysis)
HCW	150–250 °C 10–25 MPa 0–20 min	40	A(i): no environmental and corrosion problems (ii): low maintenance costs (iii): relatively high reaction rates D(i): relatively low sugar yield

Therefore, alkaline hydrolysis should be used for the pretreatment of lignocellulosic biomass, which results in saponification of intermolecular ester bonds and cross-linking xylan hemicelluloses and other components, *e.g.* lignin and other hemicelluloses (Harmsen, 2010). Although the HCW achieved relatively low sugar yield of around 40%; however, the development of HCW process for hydrolysis and conversion of cellulose, hemicelluloses and lignocelluloses biomass has attract increasing interest as it is environmentally friendly.

## 2.8 Isolation of lignin from lignocellulose

The separation of lignin from cellulose and hemicellulose is an important technique as a primary step in biorefinery processes. Each method of separation processes obtains different lignin properties, such as purity, molecular weight, amount of linkage types, etc. The isolation processes are commonly based on the cleavage of ether and ester linkages, therefore the corresponding properties of lignin is very important to be considered before selecting a technique for lignin isolation. The classification of lignin isolation methods can be divided into two main groups, which are sulfur and sulfur-free processes as presented in **Figure 2.20**. The products from sulfur processes include Kraft and lignosulfonate lignins, which are primarily produced by pulp and paper industries, and mainly correspond to the lignin extraction from the cellulose. The sulfur-free processes can be divided into two main categories, which are lignins from solvent pulping (organosolv lignin) and from alkaline pulping (soda lignin). The primary properties of lignin are presented in **Table 2.8**, which show the effects of the different technical isolation techniques to chemical structure differences of lignins. Moreover, these properties have influences on further applications of the lignin products, such as in chemical modifications.

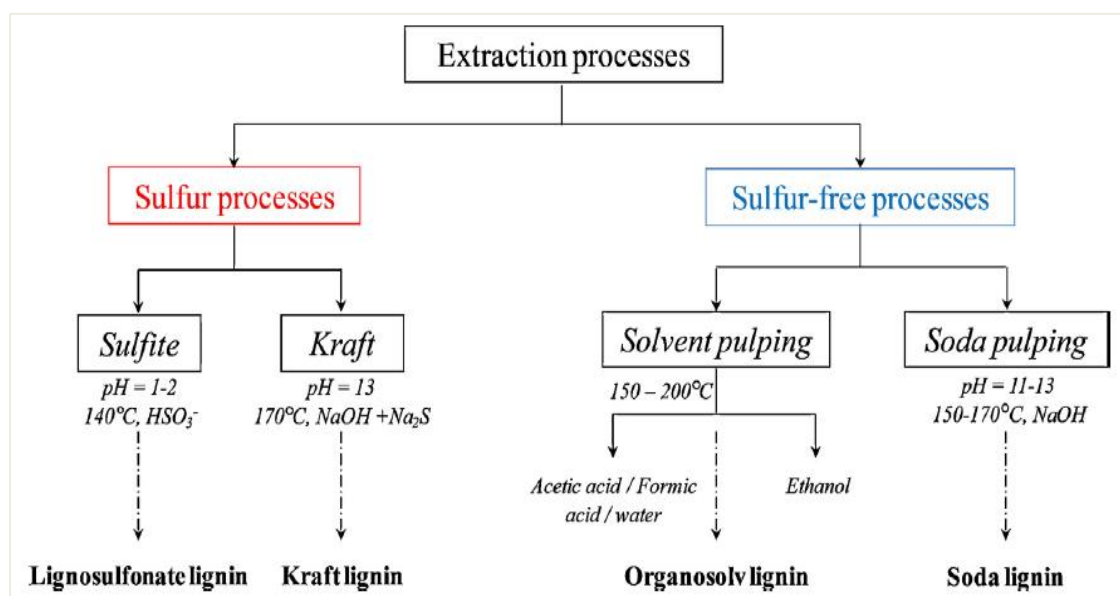


**Figure 2.20** Different lignin isolation processes from lignocellulose and the corresponding productions of technical lignins (Laurichesse & Avérous, 2014).

**Table 2.8** Properties of different technical lignins (Laurichesse & Avérous, 2014)

Lignin type	Sulfur-lignins		Sulfur-free lignins	
	Kraft	Lignosulfonate	Soda	Organosolv
Raw materials	Softwood Hardwood	Softwood Hardwood	Annual plants	Softwood Hardwood Annual plants
Solubility	Alkali Organic solvents	Water	Alkali	Wide range of organic solvents
Number-average molar mass ( $M_n$ g.mol <sup>-1</sup> )	1000–3000	15,000–50,000	800–3000	500–5000
Polydispersity	2.5–3.5	6–8	2.5–3.5	1.5–2.5
$T_g$ (°C)	140–150	130	140	90–110

## 2.9 Lignin conversion process overviews

The specific alternation of the conversion steps of lignin to fuels or bulk aromatic chemicals is presented in **Table 2.9**, though they may not necessarily occur independently or in this order. The requirements of each step are necessary to be considered when outlining technical and research needs for developing a feasible chemical process flow sheet. Typically, the processes of biofuel productions are required via deoxygenate lignin and avoid the formation of polyaromatic hydrocarbons. The fractionated lignin conversions to smaller molecules have been developed for lignocellulose (Laurichesse & Avérous, 2014). Generally, the suitable conditions for conversion to specific chemicals are different in operation. Therefore, each technical conversion process of lignocellulose is required to optimize chemistry, heat transfer, residence time, and quenching to form the desired product mixture.

**Table 2.9** Step involved in processing lignin (Harmsen, 2010; Laurichesse & Avérous, 2014; Pandey & Kim, 2011; Zakzeski et al., 2010)

Pre-treatment and fractionation	Isolation of lignocellulose into cellulose, hemicellulose, and lignin, or the separation of aromatics from processed whole biomass. Pretreatment may involve the removal of water, sulfur, alkali, or cellulosic impurities from lignin in order to prevent catalyst fouling. The fractionation of biomass may also reduce the molecular weight or alter the chemical bond linkages in lignin.
Depolymerization	Ether and alkyl linkages between the aromatic groups in lignin must be cleaved in order to produce aromatic monomers.
Modification of functional groups	Reduction of methoxy, hydroxyl, or alkyl groups to produce chemicals with lower oxygen to carbon ratios while protecting aromatic groups is necessary to produce valuable commodity chemicals or fuels. Oxidative modifications can be used to produce fine chemicals, such as vanillin, but highly selective processes for food-grade or pharmaceutical chemicals will not be considered in this study.
Product and catalyst/solvent separation	Catalysts, solvents, and untreated lignin will need to be separated from the final reaction products. Several separation steps may be necessary throughout the lignin conversion process in order to obtain purified products.

## 2.10 Lignin depolymerization techniques

Depolymerization is the primary method used to break down the lignin structure into phenolic compounds. Phenols are feedstock to produce many valuable products. Chemical depolymerization of lignin can be divided into five types, which includes base-catalyzed, acid-catalyzed, solid catalyzed, ionic liquids-assisted and supercritical fluids-assisted lignin depolymerizations. Generally, the use of homogenous catalysts (*i.e.* acid and base catalysts) for lignin depolymerization is straightforward, but the selectivity is low as different types of phenols and low purity are formed. Furthermore, the severe reaction conditions (high pressure, high temperature, and extreme pH) resulted in requirement of specially designed reactors, which led to high costs of facility and handling. Ionic liquids, and supercritical fluids-assisted lignin depolymerizations had high selectivity, but the high costs of ionic liquids recycling and supercritical fluid facility limited their applications on large-scale biomass treatment. Solid acid catalyzed depolymerization with selective bond cleavage is the major challenge for converting lignin to valuable chemicals under much milder reaction condition than base-catalyzed or acid-catalyzed depolymerizations (Pandey & Kim, 2011; Wang et al., 2013).

### 2.10.1 Base-catalyzed lignin depolymerization

The conventional base catalyst for lignin depolymerization is sodium hydroxide (NaOH). The method is operated at high temperature for converting lignin into phenolic compounds. (Lavoie et al., 2011) studied the depolymerization of softwood and hemp lignins obtained by the steam explosion of the respective biomass in the presence of 5 wt.% NaOH solution at the temperatures between 300 and 330 °C under pressures ranging from 9 to 13 MPa. The work identified 26 compounds by GC-MS, including guaiacol, catechol, and vanillin. The main contents of guaiacol, catechol, and vanillin are different because of the various amounts of ether linkages in the softwood and hemp lignins.

(Roberts et al., 2011) reported that NaOH can be used as a catalyst for the depolymerization of commercial organosolv lignin at 300 °C and 25 MPa. The main product from the study was catechol. Adding boric acid into the following treatment of base-catalyzed products led to significant increase in phenol products. Similar treatment was carried out by (Beauchet et al., 2012) for treatment of kraft lignin. The optimized conditions are at temperature 315 °C resulting in pyrocatechol as the major product with product selectivity up to 25.8%.

(Toledano et al., 2012) investigated different type of bases, including KOH, NaOH, Ca(OH)<sub>2</sub>, LiOH, and K<sub>2</sub>CO<sub>3</sub> in aqueous solutions for organosolv lignin depolymerization from olive tree pruning. The main product was catechol as identified by GC-MS. Experimental details in base-catalyzed lignin depolymerization are summarized in **Table 2.10**. Typically, lignin depolymerization by base catalysts were carried out at temperatures above 300 °C and at high pressures. The majorities of product consisted of catechol, syringol, and derivatives which were identified to be the most abundant components. The cleavage of the aryl-alkyl bond occurred at temperature over 270 °C. Majority of linkages in lignin is ether bonds ( $\beta$ -O-4 bond). Cation in sodium hydroxide can promote formation of the cation adducts, which catalyzed the formation of six-membered transition on  $\beta$ -O-4 bond during the reaction (Roberts et al., 2011). This result clearly showed that the concentration of base or the concentration ratio of lignin to base played an important role in the process. The base-catalyzed process seems to be easy; however, it can be carried out at severe conditions. However, it is difficult to control the process and the selectivity of desired products.

**Table 2.10** Base-catalyzed lignin depolymerization (Wang et al., 2013)

Lignin	Base catalyst aqueous solution	Reaction conditions		Major products	Yield (wt.%)
		<i>T</i> (°C)	<i>P</i> (MPa)		
Steam explosion hemp lignin	5 wt.% NaOH	300–330	3.5	Guaiacol	0.9–2.8
				Catechol	0.8–3.0
				Vanillin	0.50.08
Steam explosion softwood lignin	5 wt.% NaOH	300–330	3.5	Guaiacol	1.2–2.1
				Catechol	0.1–3.2
				Vanillin	0.3–0.5
Organosolv lignin	2 wt.% NaOH	300	25	Syringol	4.1
				Hydroxyacetophenone	1.6
				Guaiacol	1.1
Kraft lignin	5 wt.% NaOH	270–315	13	Pyrocatechol	0.5–4.9
Organosolv olive tree pruning lignin	4 wt.% NaOH, KOH, Ca(OH) <sub>2</sub> , LiOH, or K <sub>2</sub> CO <sub>3</sub>	300	90	Catechol	0.1–2.4

### 2.10.2 Acid-catalyzed lignin depolymerization

Acid catalysis has long been employed to depolymerize carbohydrates of plant cell walls, such as starch, cellulose, and hemicellulose. The effect of acid catalysts on carbohydrates has been extensively studied. Lignin depolymerization, however, is not as well understood, primarily due to the heterogeneity and reactivity of lignin. The acid catalyst for lignin depolymerization method was studied in a few literatures (Deepa & Dhepe, 2014; Kleinert et al., 2009).

(Kleinert et al., 2009) investigated lignin depolymerization of wheat straw lignin using a mixture of 10 wt.% of formic acid and 77 wt.% of ethanol under severe conditions (360 °C, 25 MPa). The main components of phenolic products consisted of methoxyphenols (1.3 wt.%), catechol (0.5 wt.%), and phenols (0.3 wt.%).

Recently, (Deepa & Dhepe, 2014) has reported on lignin depolymerization using the mineral acids (H<sub>2</sub>SO<sub>4</sub> and HCl) under 250 °C for 30 min with N<sub>2</sub> pressure at 7 bars. The initial pH of the solution was adjusted to pH 2. The H<sub>2</sub>SO<sub>4</sub> catalyzed reaction showed 39% yield and HCl catalyzed reaction gave 29% yield for THF soluble products. The acid-catalyzed depolymerization has been focused on the cleavage of the  $\beta$ -O-4 bond of the lignin, because it is the major ether linkage of lignin (more than 50%). The acid catalyst provided hydronium sources (H<sub>3</sub>O<sup>+</sup>) attacking the  $\beta$ -O-4 bond or the cationic aromatic rings to break down the bonds. However, the operation of acid-catalyzed depolymerization requires high temperature and pressure which leads to increasing capital cost for operation. Furthermore, due to severity conditions of operation, it would cause corrosive problem to the equipment and difficulty in controlling the system.

### 2.10.3 Solid catalyzed lignin depolymerization

Solid catalysts have been long developed for lignin conversions. The desirable properties of catalysts for lignin depolymerization include high conversion efficiency, stability under severity conditions, ease of recovery, and suppress char formation and condensation. Moreover, they are required to assist selective bond cleavage, leading to high selectivity values for a particular compound in the product stream. Various catalysts have been investigated for different processes and type of isolated lignin. (Zakzeski et al., 2010) conducted an extensive review of catalytic lignin valorization. For the catalytic process, heterogeneous acid catalysts (*e.g.* sulfided NiMo, CoMo, zeolites or amorphous silica-alumina with various compositions such as H-ZSM-5, H-mordenite, H-Y, silicate, and silica-alumina) are typical catalysts for lignin cracking and hydrolysis, which are the

primary step for disruption of the complex lignin polymer into smaller chemical molecules by breaking down the C-C bond. Several literatures (Deepa & Dhepe, 2014; Singh & Ekhe, 2014; Zakzeski et al., 2010) reported the catalytic cracking of lignin to bio-oil via liquefaction in the presence of MCM-41 and H-ZSM-5 at high temperature (340-410°C). Moreover, it has been reported that MCM-41, H-ZSM-5 and H-mordenite could produce more aromatics than using H-Y, silicate, and silica-alumina due to their high surface area and acidity, which led to the desirable environment of conversion of the long lignin polymer to high quality monomeric phenolic compounds.

(Sharma et al., 2004) reported on the catalytic depolymerization of lignin or bio-oil produced by liquefaction using H-ZSM-5 as a catalyst and temperatures in the range of 340-410 °C in a fixed bed reactor. The maximum amount of phenols accounting for 30 wt.% of the initial lignin and 60 wt.% of the total bio-oil were achieved.

## CHAPTER 3

### METHODOLOGY

#### 3.1 Raw materials

Eucalyptus (*Eucalyptus grandis*) wood chips were obtained from a local pulp mill in Ratchaburi Province, Thailand. The wood chip sizes were in the range of 1.5-2 cm x 1.5-2 cm with 0.25-0.5 cm thickness. The biomass was air-dried and used in the experiments without prior physical processing. Chemical compositions (% lignin, cellulose, hemicelluloses, and ash) were analyzed using the standard NREL method (Sluiter et al., 2010). The starting material contained 45.2 wt.% cellulose, 21.1 wt.% hemicelluloses, 30.4 wt.% lignin, and 3.3 wt.% other contents. Analytical grade organic solvents and chemicals were purchased from major chemical suppliers *i.e.* Sigma-Aldrich, Merck, and Fluka.

#### 3.2 Preparation of solid acid promoters for fractionation process

Solid acid promoters were prepared from activated carbon with various functional acid groups ( $\text{H}_2\text{SO}_4$ ,  $\text{H}_3\text{PO}_4$ ,  $\text{HNO}_3$ , and  $\text{HCl}$ ). The experiment was carried out by mixing 10 g of the sample (activated carbon) with 100 mL of concentrated acid in a 4-neck round bottom flask at temperatures typically between 220 and 250 °C under a flow of nitrogen through the apparatus as shown in **Figure 3.1**.

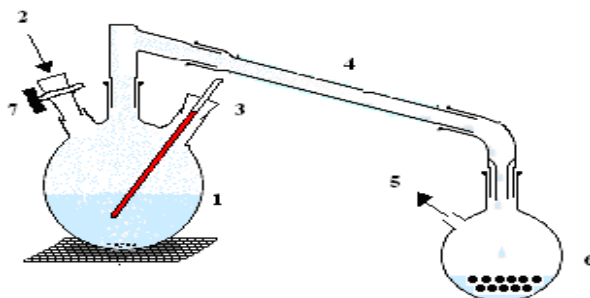


**Figure 3.1** Apparatus setup for catalyst preparation instrument (1): round bottom 4-neck flask, (2): nitrogen inlet, (3): thermometer, (4): connection tube, (5): vacuum pump, (6): flask- containing the activated carbon.

In detail, a 1-L flask containing 300 g of activated carbon was connected to the reaction flask to adsorb the acid vapor. The nitrogen inlet flow was switched off when the reaction reached the desired temperature and the sample was further heated until the acid solution was completely evaporated. The obtained solid was repeatedly washed with boiling water until no pH change was observed in the filtrate, which was used as solid acid promoter as described in (Suganuma et al., 2010).

### 3.3 Preparation of sulfonated carbon-based catalysts for the hydrolysis process

Sulfonated carbon-based (SCB) catalysts were prepared by direct sulfonation of sugars, as shown in **Figure 3.2**. In the detail, SCB catalysts were prepared by mixing 10 g of carbon materials (sucrose, glucose, and xylose) with 100 mL of concentrated  $\text{H}_2\text{SO}_4$  in a 4-neck round bottom flask. The mixture was heated at  $250^\circ\text{C}$  under  $\text{N}_2$  flow to produce a brown-black solid. A 1-liter flask containing the solid sample was connected to the reaction flask to adsorb the acid vapor. The nitrogen inlet flow was switched off when the reaction reached the desired temperature and the sample was further heated until the acid solution was completely evaporated. The obtained solid was repeatedly washed with boiling water until no pH change was observed in the filtrate and used as catalysts in this study.

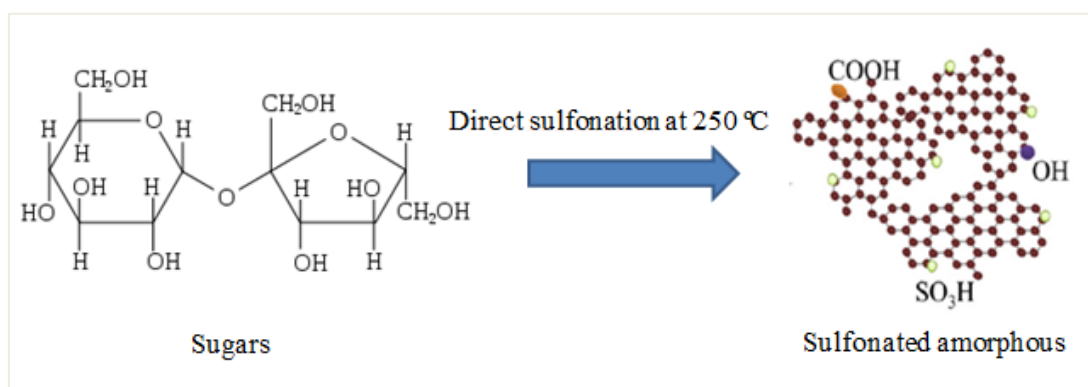


**Figure 3.2** Preparation of sulfonated amorphous carbon from sugars (sucrose, glucose, and xylose) by direct synthesis pathways.

### 3.4 Preparation of acid catalysts for lignin depolymerization process

#### 3.4.1 Mesoporous silica

SBA-15 was synthesized by using tetraethyl orthosilicate (TEOS, Sigma–Aldrich) as the silicon source and Pluronic P123 (Sigma–Aldrich) as the surfactant template. In detail, the solution of Pluronic P123 was heated before dispersing in 0.1 M HCl. After stirring, TEOS was slowly added and continuously stirred for 24 h. The mixture was then kept in autoclave at 120°C for 72 h. The obtained particles were filtrated and washed with deionized water until pH 5.0. Then, it was dried overnight and calcined in air at 600°C for 6 h. For MCM-41 synthesis, cetyltrimethylammonium bromide (CTAB) were dissolved in NaOH solution and followed by a dropwise addition of TEOS. The mixture was vigorously stirred and heated to 80°C for 2 h. Subsequently, the product powder was isolated, washed with water and methanol, and then freeze dried. Finally, it was calcined under the same condition as SBA-15. Mixed oxide ZrO<sub>2</sub>-SBA-15 and ZrO<sub>2</sub>-MCM-41 were prepared by incipient wetness impregnation of either SBA-15 or MCM-41 with solutions of zirconium (IV) propoxide (Sigma–Aldrich) in ethanol (Sigma–Aldrich). It is noted that the weight loading ratios of ZrO<sub>2</sub>/SBA-15 and ZrO<sub>2</sub>/MCM-41 were varied from 1/1, 1/2, and 1/3. The samples were dried and calcined in air at 600°C for 6 h.

#### 3.4.2 Phosphate-based catalyst

The phosphates of cobalt and calcium were synthesized using conventional precipitation in acetone–water mixtures. Then, CaCO<sub>3</sub> or CoCO<sub>3</sub> (1.0 g) was dissolved in 5 cm<sup>3</sup> of 70% H<sub>3</sub>PO<sub>4</sub> aqueous solution. Next, the solution was added by 30 cm<sup>3</sup> of acetone, and vigorously stirred at ambient temperature for 1 h. The precipitated products were filtered and washed with acetone until free phosphate ion. After that, the obtained samples were dried in an oven overnight, and then were calcined in air at 900 °C for 3 h (Daorattanachai et al., 2012). Surface areas of the samples were obtained using conventional N<sub>2</sub> sorption at 77 K (BELSORP-max, BEL, Japan) by conventional N<sub>2</sub> sorption at 77 K (BELSORP-max, BEL, Japan). The crystalline structure of CaP<sub>2</sub>O<sub>6</sub> was analyzed by X-ray diffraction (XRD, Bruker D8 Advance, Germany). The acid properties were analyzed by several indicators including neutral red (pKa = +6.8), methyl red (pKa = +4.8), dimethyl yellow (pKa = +3.3), crystal violet (pKa = +0.8), 4-(phenylazo)diphenylamine (pKa = +0.42), and dicinnamalactone (pKa = -0.3).

### 3.5 Experimental method

The experimental method can be divided into 4 main sections: (1) investigating of organosolv fractionation (with and without solid acid promoters), (2) testing of the hydrolysis reaction (with and without solid acid catalysts) in HCW, (3) upgrading of organosolv lignin (OL) solubility via alkaline precipitation process (called treated organosolv lignin; TOL), and (4) studying of lignin depolymerization for phenol productions. The details of these three experimental steps are explained in **Figure 3.3** and described further in the following sub-sections.

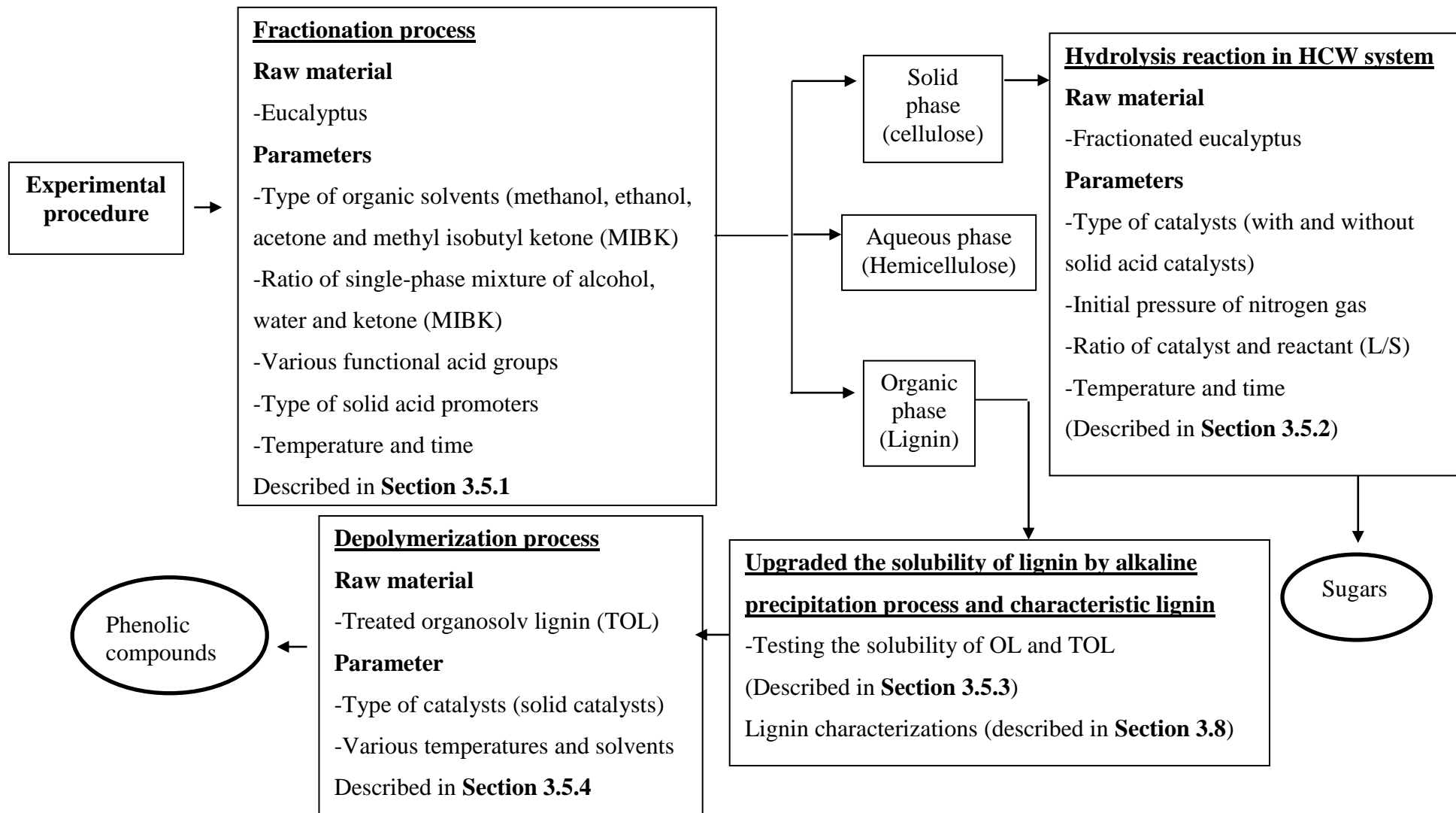


**Figure 3.3 The diagram of experimental procedure.**

### 3.5.1 Procedure for fractionation

The fractionation process was studied in a stainless steel reactor (1.27 cm. diameter and 13 cm in length with the wall thickness of 10 mm) equipped with a thermocouple to measure the temperature inside the reactor, as shown in **Figure 3.4**.

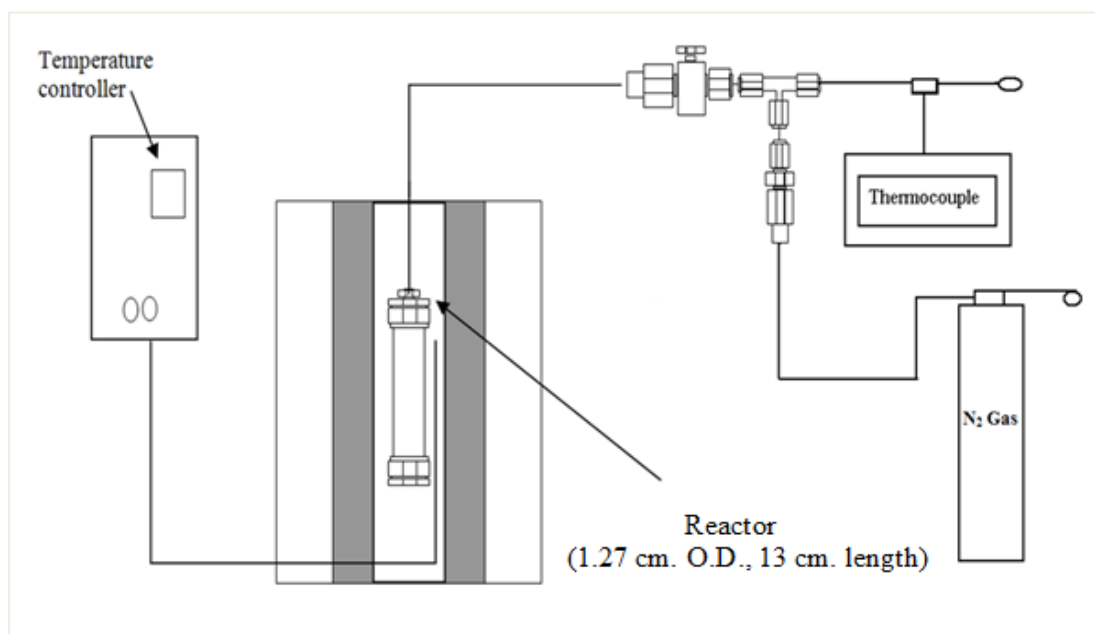


**Figure 3.4** The experimental setup apparatus for fractionation and hydrolysis reaction.

In the standard reaction process, 1 g of eucalyptus wood chips and 6 mL of the single-phase solvent mixture (methyl isobutyl ketone (MIBK):water: methanol) or other solvents as indicated with and without the homogeneous or heterogeneous acid promoters, in the reactor are heated to the desired temperature. Nitrogen was flowed into the reactor for purging and adjusting the initial pressure at 20 bars. The reactor was placed in a furnace and co-heated to 140-250°C for 10-180 min. Uniform heating was achieved by the use of a relatively small reactor size. There was no noticeable difference between the temperature measured inside the reactor and the furnace temperature. After that, the reaction was immediately stopped by quenching in a water bath. The solid cellulose-enriched fraction was separated by filtration on filter paper and washed with methanol then water, and dried at 60°C. The liquid fraction was combined with the rinsate and placed into a separating funnel. Water was added to the aqueous-organic fraction until phase separation was obtained. The mixture was stirred and then placed at room temperature for 20 min for complete phase separation. The aqueous phase containing hemicelluloses and

soluble products was recovered. The separated organic phase was dried at 105°C to obtain lignin. Yields of isolated products are reported as wt.% based on the amount of the starting biomass on a dried weight basis.

### **3.5.2 Procedure for hydrolysis reaction in HCW**

The hydrolysis reaction was also carried out in a stainless steel reactor (1.27 cm. diameter and 13 cm in length) equipped with a thermocouple to measure the temperature inside the reactor, as shown in **Figure 3.4**. The standard reaction contained 1 g of samples (*i.e.* eucalyptus wood chips, and fractionated eucalyptus) and 6 ml of water in the presence of heterogeneous acid catalysts (5% w/w) compared to that using an equal acid loading of homogenous catalyst (H<sub>2</sub>SO<sub>4</sub>). Nitrogen was flowed into the reactor for purging and adjusting the initial pressure (5-20 bars). The reactor was placed in a furnace and heated to 100-250°C for 5-40 min. The reaction was immediately stopped by quenching in a water bath. The solution was separated by a syringe filter (0.45 µm) for solid-liquid separation.

### **3.5.3 Procedure for lignin solubility testing and upgrading by alkaline precipitation process**

For solubility testing, 2 g of organosolv lignin (OL) from the organosolv fractionation of eucalyptus wood chips was dissolved in 100 ml of THF, DMSO, and methanol with the concentrations of 100 wt.%. These analytical-grade organic solvents were supplied by Sigma–Aldrich, Merck, and Fluka. After leaving overnight at room temperature, it was filtered under reduced pressure and dried at 70°C.

In order to upgrade the solubility of OL by the alkaline precipitation process, 20 g of OL was placed in a 600 mL beaker, to which 2 M NaOH was added dropwise until maximum dissolution was achieved. The mixture in beaker was then heated in a 35 °C water bath for at least 30 min. After heating, the solution was passed through a filter paper in order to separate the base-soluble lignin (bulk; called TOL), from the insoluble lignin material present. The base insoluble lignin (BIL) was then washed until a neutral filtrate was observed, and the base soluble lignin was left refrigerated overnight. The base soluble lignin was then re-precipitated via the drop-wise addition of 2 M H<sub>2</sub>SO<sub>4</sub> to a pH of 5.5. At around this point the appearance of the mixture began to change from dark black to murky brown, as a result of the initial stage of lignin precipitation. The addition of acid was then paused and the solution was continuously stirred for at least 30 min in a water bath at 65-67 °C. The addition of acid was then resumed until the pH was 3. The precipitated lignin was recovered via vacuum filtration and washed using hot water (70-80

°C). The washed lignin was then placed in a vacuum oven at 45 °C overnight to dry (Mousavioun et al., 2010). It is noted that soda lignin (SL) was also prepared and tested for comparison. The SL was extracted from sugarcane bagasse, obtained from Mackay Sugar Mill (Mackay, QLD, Australia) using 0.7 M NaOH. The procedure for this lignin isolation has been described elsewhere (Mousavioun et al., 2010).

### 3.5.4 Procedure for lignin depolymerization

The depolymerization reaction was carried out in a SS 316 stainless steel small tube reactor (3/8 inch O.D. and 12 cm. length), from which 35 mg of TOL was mixed with 2 ml of water or methanol with and without the presence of solid catalysts. For the solid catalysts are studied compared commercial catalyst (sulfide NiMo/Al<sub>2</sub>O<sub>3</sub>) to mesostructured silica catalysts (*i.e.* SBA-15, MCM-41, ZrO<sub>2</sub>-SBA-15 and ZrO<sub>2</sub>-MCM-41) and phosphate based catalysts (*i.e.* CoP<sub>2</sub>O<sub>6</sub>, and CaP<sub>2</sub>O<sub>6</sub>). The reactor was loaded into the heating sand bath at heated at 200, 250, 300, and 350°C for 60 min. At the end of the time, the reactor was removed and immersed in a room temperature water bath to quench the reaction. The product mixture was fractionated using a separation sequence described in **Figure 3.5**. In the first step, solid and liquid products were separated by centrifugation at 2000 rpm for 10-15 min. The solid phase was washed with distilled water mixed with tetrahydrofuran (THF). The THF-insoluble fraction contains the solid catalyst, high-molecular-weight products, and char (Nguyen et al., 2014; Toledano et al., 2012). The THF-soluble fractions containing a majority of the lignin residue (Nguyen et al., 2014; Toledano et al., 2012) was recovered after THF vaporization under vacuum at 45 °C, and weighed. The liquid phase was acidified to a pH of 2.5 with sulfuric acid (1 M) with slow stirring and then cooled to 0 °C. In this process, inorganic compounds (*e.g.*, sodium sulfate) were precipitated out as solids and were separated by filtration. The aqueous phase was passed through a column containing macroporous resin (DA201-C, Suqing, China) until a clear solution (almost colorless) was obtained. The phenolic products that were adsorbed on the resin were eluted with hot ethanol (70-80 °C). The phenolic solution (light yellow) was filtered through a 0.45 µm syringe filter, and was vacuum-dried at 45 °C to remove solvents and to recover phenolics. The phenolic solution was also characterized by GC-MS. The yields of the all dried fractions (aqueous fraction, residual lignin fraction and solid fraction) were determined gravimetrically and the yields were calculated in comparison to initial TOL weight.

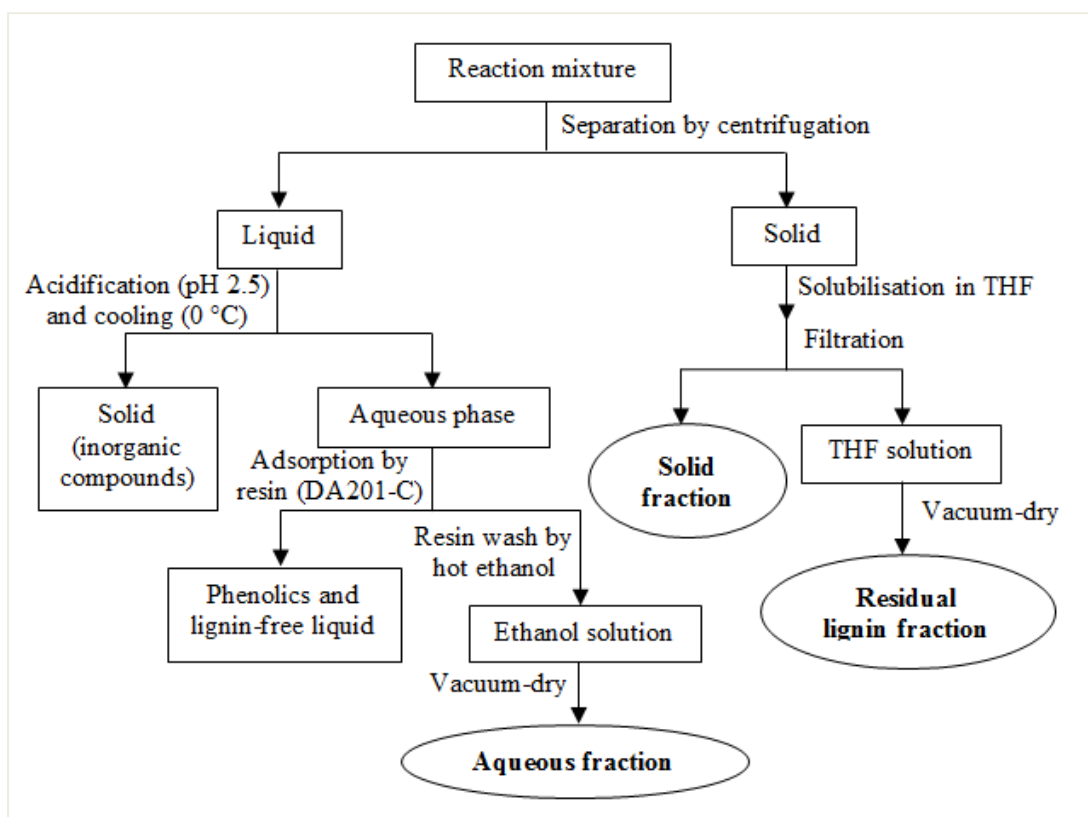


**Figure 3.5** Diagram of product separation after lignin depolymerization.

The fractions of the three main products: aqueous fraction, residual lignin fraction, and solid fraction, were calculated as follows:

- (1) Aqueous fraction (wt.%) = [weight of aqueous fraction (g)/weight of initial lignin (g)] × 100
- (2) Residual lignin fraction (wt.%) = [weight of THF-soluble fraction (g)/weight of initial lignin (g)] × 100
- (3) Solid fraction (wt.%) = [(weight of THF-insoluble fraction (g)-weight of solid catalyst (g))/weight of initial lignin (g)] × 100
- (4) Total yield of syringol product = (syringol in aqueous fraction + extracted syringol from residual lignin)

The promoters/catalysts performance for the fractionation, hydrolysis, depolymerization to products (sugars and chemicals) were quantified in terms of the conversion of feedstocks (woody eucalyptus, cellulose, and lignin). The yields of the products (cellulose, hemicellulose, lignin, sugars, phenolic compounds) highlighted the

performance of the catalysts for the fractionation, hydrolysis and depolymerization. The yields of the products (cellulose, hemicellulose, lignin, sugars, phenolic compounds), and the conversion of feedstocks (woody eucalyptus, cellulose, and lignin) were calculated using the following equations:

$$\text{Yield of product (\%)} = (\text{weight of product/weight of feedstock}) \times 100\%$$

$$\text{Selectivity of product (\%)} = (\text{weight of product/total weights of products}) \times 100\%$$

$$\text{Feedstock conversion (\%)} = \frac{(\text{weight of feedstock} - \text{weight of product})}{\text{weight of feedstock}} \times 100\%$$

### 3.6 Liquid product analysis

#### 3.6.1 Sugar products

The type and amount of sugar from the fractionation and hydrolysis processes were analyzed by a high performance liquid chromatograph (SPD-M10A DAD, Shimadzu) equipped with a refractive index detector using an Aminex HPX-87H column (Bio-Rad, Hercules, CA, USA) operating at 65°C with 5 mM H<sub>2</sub>SO<sub>4</sub> as the mobile phase at a flow rate of 0.5 ml/min.

#### 3.6.2 Phenolic compound products

GC-MS was used to characterize the phenolic products. The GC-MS system (Agilent J&W GC Columns 6890 app Hephaestus) was equipped with an Agilent 19091Z-012 capillary column (23.9 m × 0.32 mm × 0.17 μm; Agilent, USA). The temperature program of the oven was started at 90 °C for 10 min and then heated up at 3 °C/min to 250 °C. The NIST (National Institute of Standards and Technology) library of mass spectroscopy was used for the identification of the compounds). The products were quantified using the calibration curves of a number of lignin depolymerization products (syringol, phenol, guaiacol, 1-(4-hydroxy-3,5-dimethoxyphenyl)-ethanone, 4-hydroxy-3,5-dimethoxy-benzaldehyde, benzoic acid, 1,2-benzenediol, etc.).

### **3.7 Characterization of promoters and catalysts**

#### **3.7.1 BET surface area**

The specific surface areas, cumulative pore volumes, and average pore diameters of the solid acid promoter and solid catalysts were performed by a N<sub>2</sub> physisorption technique using the Brunauer-Emmet-Teller (BET) method. Solid promoters and solid catalysts were analysed for the BET surface area using a Belsorp-max TPD pro (BEL Japan, Tokyo, Japan) with thermal conductivity detector (Semi-diffusion type, 4-element W-Re filament) at the National Nanotechnology Center, Thailand.

#### **3.7.2 Temperature-programmed desorption (TPD)**

The acid-base properties of the solid promoter and solid catalysts were analyzed by temperature-programmed desorption techniques with ammonia and carbon dioxide (NH<sub>3</sub>- and CO<sub>2</sub>-TPD) carried out by a flow apparatus. In the detail, the samples (0.1g) was treated at 500°C in helium flow for 1 h and then saturated with 15% NH<sub>3</sub>/He mixture or pure CO<sub>2</sub> flow after cooling to 100°C. After purging with helium, the sample was heated to 650°C in helium flow. The amount of acid-base sites on the catalyst surface was calculated from the desorption amount of NH<sub>3</sub> and CO<sub>2</sub>. Then, it was determined by measuring the areas of the desorption profiles obtained from the Chemisorption System analyzer.

### **3.8 Characterization of isolated lignins**

#### **3.8.1 Elemental analysis**

A FLASHEA 1112 Elemental Analyzer instrument was used for the analysis of three lignin samples (OL, TOL, and SL). In preparation for analysis, the lignins were dried at 100 °C overnight, to remove any moisture. Samples (2 to 4 mg) were encapsulated in a tin container for analysis components (carbon, hydrogen, nitrogen, and sulfur). In order to determine the oxygen content, 2 to 4 mg samples were encapsulated in a silver container. The analysis results were obtained via gas chromatography, and compared with those of standard materials. The percentage of protein content was calculated as  $N (\%) \times 6.26$  (Mousavioun et al., 2010).

### 3.8.2 Klason lignin determination

Lignin samples (0.3 g) were added with 3 mL of 72% H<sub>2</sub>SO<sub>4</sub> in pressure tubes. The tubes were then immersed in a water bath at 30 °C for 1-2 h. The hydrolyzed lignin samples were then diluted to 4 % through the addition of water, then autoclaved at 121°C for 1 h (Mousavioun et al., 2010; Sluiter et al., 2010). The samples were filtered with porcelain crucibles to remove any solids and the liquid fraction was analyzed by HPLC for glucose, xylose and arabinose (Sluiter et al., 2010). The solid fraction, comprised of acid-insoluble lignin and the acid-insoluble ash, was placed in a muffle furnace at 575 ± 25 °C for 3 h. After cooling, the remaining acid-insoluble ash was weighted and calculated as a percentage of the original dry weight of the sample (Sluiter et al., 2010).

### 3.8.3 Mannich Reaction

The methodology of the Mannich Reaction has been previously reported and is associated with the substitution of the C-3 and C-5 aromatic positions of lignin (Mansouri & Salvadó, 2006). Paraformaldehyde (1.2 g) and diethylamine (2.92 g) were dissolved in 206 mL of 90% dioxane. This solution (25 mL) was added to new solution (0.5 g of lignin in 25 mL of 90% dioxane). The resultant mixture was left at room temperature for an hour and then refluxed at 80 °C for an additional hour. The mixture was then cooled down to room temperature then evaporated to dryness under vacuum at 30 °C. The dried residue was added to approximately 1 mL of 90% dioxane and 1 mL of water, then again evaporated to dryness, in order to remove the residual reagents. This step was repeated for three times. The dried residue was dissolved in small amount of 90% dioxane and freeze-dried. The final solid was subjected with elemental analysis. The nitrogen composition determined by elemental analysis was used to calculate number of free C-3 and C-5 positions.

### 3.8.4 Molecular weight determination

Size exclusion chromatography was used to determine the molecular weight of different lignins. Samples were prepared in eluent (0.1M NaOH) at a concentration of 0.2 mg/mL just prior to analysis and filtered through a 0.45 µm syringe to remove any residual solids. A high-performance liquid chromatography (HPLC) instrument was used with a Shodex Asahipak GS-320 HQ column and a Water 2487 UV detector (280 nm). The mobile phase was 0.1 M NaOH (adjusted to a pH of 12 with concentration HCl), with a flow rate of 0.5 mL.min<sup>-1</sup>. The temperature of column was maintained at 30°C. Sodium polystyrene sulphonate standards with molecular weights 1530, 4950, 16600, and 34700

g/mol were used to prepare a standard calibration curve. Lignin weight average molecular weight ( $M_w$ ) and number average molecular weight ( $M_n$ ) were calculated after comparison with standards.

### **3.8.5 Thermal gravimetric analysis (TGA)**

A Q500TGA instrument was used for the analysis with a flow rate of the purge gas ( $N_2$ ) of 20–35 mL/min. Approximately 30–50 mg of sample was weighed in an aluminum pan before it was heated at a rate of 5°C/min from room temperature to approximately 1000°C, for determination of total mass loss. A curve of weight loss against temperature was constructed from the data obtained. A derivative of this curve (DTG) was produced to indicate the temperatures at which the maximum rates of weight loss occurred.

### **3.8.6 X-ray photoelectron spectroscopy (XPS) analysis**

X-ray photoelectron spectroscopy (XPS) was used to analyze the surface chemistry and elemental composition of the lignin samples. The three lignin samples were analyzed using a Kratos Axis ULTRA X-ray Photoelectron Spectrometer (Kratos Analytical, UK) incorporating a 165 mm hemispherical electron energy analyzer. The incident radiation was monochromatic Al  $K_\alpha$  X-rays (1486.6 eV) at 150 W (15 kV, 10 ma). Photoelectron data were collected at a takeoff angle of  $\theta = 90^\circ$ . Survey (wide) scans were operated with pass energy of 160 eV and multiplex (narrow) high-resolution scans were operated at 40 eV. Survey scans were performed over a binding energy range of 1200 eV to 0 eV with 1.0 eV steps and a dwell time of 100 ms. Narrow high-resolution scans were run with 0.05 eV steps and 250 ms dwell time. The base pressure was  $1.0 \times 10^{-9}$  torr and  $1.0 \times 10^{-8}$  torr in the analysis chamber during sample analysis. Atomic contents (%) were calculated using the CasaXPS version 2.3.14 software (Manchester, UK). Peak fitting of the high-resolution data were also carried out using the CasaXPS software.

### **3.8.7 Solid-state nuclear magnetic resonance (NMR)**

The macromolecular structural of the lignin samples was studied using  $^{13}C$ -cross-polarization, magic-angle-spinning (CP/MAS) solid-state probe mounted on Inova 400 Varian (Agilent, US) operated at 100 MHz. Magic angle spinning was conducted at 13 kHz, a recycle time of 2 s, an acquisition time of 33 ms, and 4000 scans.

### **3.8.8 Fourier transform-Infrared spectroscopy**

Infrared (FT-IR) spectra of the solid lignin samples were obtained in an attenuated total reflectance (ATR) accessory on a Nicolet 5700 Diamond FT-IR spectrometer (Madison, WI, USA). The spectra were manipulated and plotted with the use of the

Galactic Industries Corporation GRAMS/32 software package (Salem, NH, USA). The measurement resolution was set at  $4\text{ cm}^{-1}$  with a mirror velocity of  $0.6329\text{ cm/s}$ , and the spectra were collected in the range  $4000\text{-}650\text{cm}^{-1}$  with 64 co-added scans. The final FTIR peaks were normalized with the respect to the distinct peak located at  $1109\text{ cm}^{-1}$ .

## CHAPTER 4

### SINGLE-STEP AQUEOUS-ORGANOSOLV FRACTIONATION OF WOODY EUCALYPTUS WITH AND WITHOUT THE PRESENCES OF HOMOGENEOUS AND HETEROGENEOUS ACID PROMOTERS

---

#### Chapter highlights

The fractionation of lignocellulosic biomass is a primary step for converting multi-structure biomass to biofuels and other industrial products in an integrated biorefinery processes. In this chapter, the effects of homogeneous and heterogeneous acid promoters ( $\text{HNO}_3^-$ ,  $\text{HCl}^-$ ,  $\text{H}_2\text{SO}_4^-$ , and  $\text{H}_3\text{PO}_4^-$ -activated carbons) on a single-step aqueous organosolv fractionation of eucalyptus wood chips were studied and optimised. The optimised process contained 16.7% w/v biomass in a ternary mixture of methyl isobutyl ketone:methanol:water (25:42:33) with 5% AC- $\text{H}_3\text{PO}_4$  and incubated at 180 °C for 60 min. Under these conditions, 41.2 wt.% cellulose was obtained in the enriched solid pulp with the average glucan content of 75.9%. The majority of the hemicelluloses was hydrolysed into the aqueous-methanol phase, which contains 17.8 wt.% monomeric xylose and xylooligomers; while 13.7 wt.% lignin was separated into the organic phase. The study demonstrated that a heterogeneous acid-promoter can replace homogeneous acid-promoters for effective fractionation of lignocelluloses.

---

## 4.1 Background

The fractionation of lignocellulosic components in plant biomass is a pre-requisite for an integrated biorefinery. Lignocellulosic fractionation entails disruption of lignocellulose's biopolymeric matrix and subsequent separation of its components into fractions according to selectivity of the media and process conditions (Bozell et al., 2011a). An optimised fractionation process exhibits selective separation of each component of a biomass feedstock with high recovery yield and minimal purification requirement before further processing as well as process economics as the main criteria. Many fractionation methods based on chemical (Buranov & Mazza, 2012; Sun & Cheng, 2002), thermal (Garrote et al., 2001; Imman et al., 2013), or their combination (Amendola et al., 2012; Romaní et al., 2011) processes have been studied for separation of biomass components. Among them, organosolv methods are generally versatile processes with respect to the raw materials and have been studied for fractionation of hardwoods, softwoods and grasses (Brudecki et al., 2013; Lan et al., 2011; Pronyk & Mazza, 2012). Ethanol and methanol remain the primary solvents used in organosolv pretreatment mixtures, but many alternative solvents have been employed including organic bases, ketones, and esters (Bozell et al., 2011a). Process design modeling for plants operating with ethanol-water, ethylene glycol-water, and acetosolv systems was carried out (Buranov & Mazza, 2012; González et al., 2008; Romaní et al., 2013). Recently, a new organosolv technology, termed Clean Fractionation (CF), has been reported (Bozell et al., 2011a). In this process, the lignocellulosic material is separated with a ternary mixture of ketone, ethanol, and water in the presence of an acid promoter (*i.e.*  $\text{H}_2\text{SO}_4$ ), which selectively dissolves lignin and hemicellulose, leaving cellulose as an undissolved solid. The resulting single phase liquor is treated with water giving an organic phase containing lignin and an aqueous phase containing hemicellulose. This process offers high selectivity for separation of the primary biomass components and offers operational advantages for the production of both chemicals and fuels.

In detail, (Bozell et al., 2011a) optimized the separation of woody feedstocks, grasses and agricultural residues, particularly on various hardwoods, *e.g.* aspen, poplar, and oak, focusing on yield and purity. The optimal process carried out in the presence of 0.1 M  $\text{H}_2\text{SO}_4$  or greater led to a cellulose-enriched fraction with an average yield of 47.7 wt.% with the Klason lignin of 5.1-6.8 wt.% and trace amounts of cross-contaminating

non-glucose sugars. A glucan content of 68.7% from batch separation was obtained under these conditions, which was marked improvement over the 89.9% under flow-through condition (Bozell et al., 2011a). High-purity lignin was obtained with an average yield of 17.8-19.5 wt.%. The hemicelluloses fraction obtained is 14.5 wt.% in average and comprises a complex mixture of monomeric sugar, *e.g.* xylose, mannose, uronic acids, and small amount of galactose and arabinose with dehydration products and the acid promoter.

In this study, the single-step aqueous-organosolv fractionation of eucalyptus wood chips based on the CF process was studied and optimised. The use of alternative environmental friendly heterogeneous activated carbon-based acid promoters to replace toxic and highly corrosive homogeneous  $\text{H}_2\text{SO}_4$  was investigated. This work highlighted the potential of efficient solid acid promoters for increasing the efficiency and selectivity of the fractionation process, and provides a basis for further development of the acid-catalysed aqueous-organosolv process in an integrated biorefinery.

## 4.2 Results and discussion

### 4.2.1 Solid promoter characterization

In this current work, four synthesized solid acid promoters were prepared. The specific surface area, cumulative pore volume, average pore diameter and pore size distribution of all synthesized promoters, determined by N<sub>2</sub> physisorption using Micromeritics ASAP 2020 surface area and porosity analyzer, are summarized in **Table 4.1**.

**Table 4.1** N<sub>2</sub> physisorption results of solid acid promoters

Catalysts	BET surface area (m <sup>2</sup> /g)	Cumulative pore volume (cm <sup>3</sup> /g)	Average pore diameter (nm)
H <sub>2</sub> SO <sub>4</sub> -Activated carbon	801	0.47	1.72
H <sub>3</sub> PO <sub>4</sub> -Activated carbon	853	0.49	1.66
HCl-Activated carbon	782	0.43	1.75
HNO <sub>3</sub> -Activated carbon	811	0.47	1.69

The NH<sub>3</sub>- and CO<sub>2</sub>-TPD techniques were then used to measure the acid-base properties of the promoters. The amounts of acid and base sites, which were calculated from the area below the curves of these TPD profiles, are listed in **Table 4.2**. Along with these values, the distribution of acid and base site on the promoter surface (namely the density of acid and base site;  $\mu\text{mol m}^{-2}$ ) and the strength of acid and base sites (the top peak of TPD spectra) are also given in the table since these parameters are important indicators to determine the catalytic reactivity of acid and base reactions.

For the base of the acid and base site densities, the values of these promoters are in the same ranges (from 1.09-1.24  $\mu\text{mol/m}^2$  acid density and from 0.36-0.52  $\mu\text{mol/m}^2$  base density). Among all catalysts, H<sub>3</sub>PO<sub>4</sub>-Activated carbon presents the highest total acid sites and acid density. The H<sub>3</sub>PO<sub>4</sub> is the most difficult to evaporate, indicating it could be adsorbed well on activated carbon.

**Table 4.2** Results from NH<sub>3</sub>- and CO<sub>2</sub>-TPD measurements of carbon-based solid acid promoters

Catalysts	Total sites (μmol/g)		Density of sites (μmol/m <sup>2</sup> )	
	Acid sites <sup>a</sup>	Base sites <sup>b</sup>	Acid sites	Base sites
H <sub>2</sub> SO <sub>4</sub> -Activated carbon <sup>c</sup>	873.1	344.4	1.09	0.43
H <sub>3</sub> PO <sub>4</sub> -Activated carbon <sup>d</sup>	1057.7	307.1	1.24	0.36
HCl-Activated carbon <sup>e</sup>	680.3	383.2	0.87	0.49
HNO <sub>3</sub> -Activated carbon <sup>f</sup>	721.8	421.7	0.89	0.52

<sup>a</sup> From NH<sub>3</sub>-TPD / <sup>b</sup> From CO<sub>2</sub>-TPD

#### 4.2.2 Effect of solvents and acid promoters on fractionation of eucalyptus wood chips

First, chemical compositions (% lignin, cellulose, hemicelluloses, and ash) were analyzed using the standard NREL method (Sluiter et al., 2010). The starting material contained 45.2 wt.% cellulose, 21.1 wt.% hemicelluloses, 30.4 wt.% lignin, and 3.3 wt.% other contents.

The efficiency and selectivity of various solvent systems, including water, methanol, ethanol, acetone, MIBK, and the single-phase aqueous-organic mixture, on the solubilisation of biomass components were investigated. The process was operated at 180°C for 60 min with a solid-to-liquid ratio of 1:6 (w/v) in the absence of acid promoter. The initial ratio of the single-phase solvent mixture was at 16:68:16 (MIBK: methanol:water) based on volume. Different pressurized solvent systems were tested, which varied in biomass solubilisation efficiency (**Figure 4.1**). It was found that the use of MIBK or acetone as the sole solvent did not show any significant solubilisation of biomass components from eucalyptus wood chips. Alcohols (methanol or ethanol) were similarly inefficient yielding 2.2 wt.% hemicelluloses as hydrolysis products in the form of xylose monomers and oligosaccharides to the liquid phase while > 90% of the solid pulp remained with no solubilisation of lignin under the experimental conditions. Markedly increased soluble sugar yield was observed when water was used as the sole solvent (15.1 wt.% xylose products and 4.4 wt.% glucose products in the aqueous phase), while no

solubilisation of lignin was observed. Applying a single phase water-organic mixture to eucalyptus wood chips in the absence of acid promoter led to partial solubilisation of the hemicellulose, mostly in the form of xylose (1.45 wt.%) and xylo-oligosaccharides (6.88 wt.%) with significant solubilisation of lignin (2.1 wt.%) into MIBK after phase separation. This condition gave the highest biomass solubilisation in this experiment, as shown by the lowest pulp yield (84.1 wt.%). The result thus suggested the potential of using the aqueous-organic solvent system on improving the efficiency of lignocellulosic component fractionation. Especially, the potential mechanistic of the fractionation using this multi-solvent, the aqueous phase solvent can fractionate both lignin and hemicellulose from eucalyptus wood chip, while MIBK is applied for dissolving and precipitating lignin from the aqueous phase solvent (Bozell et al., 2011a).

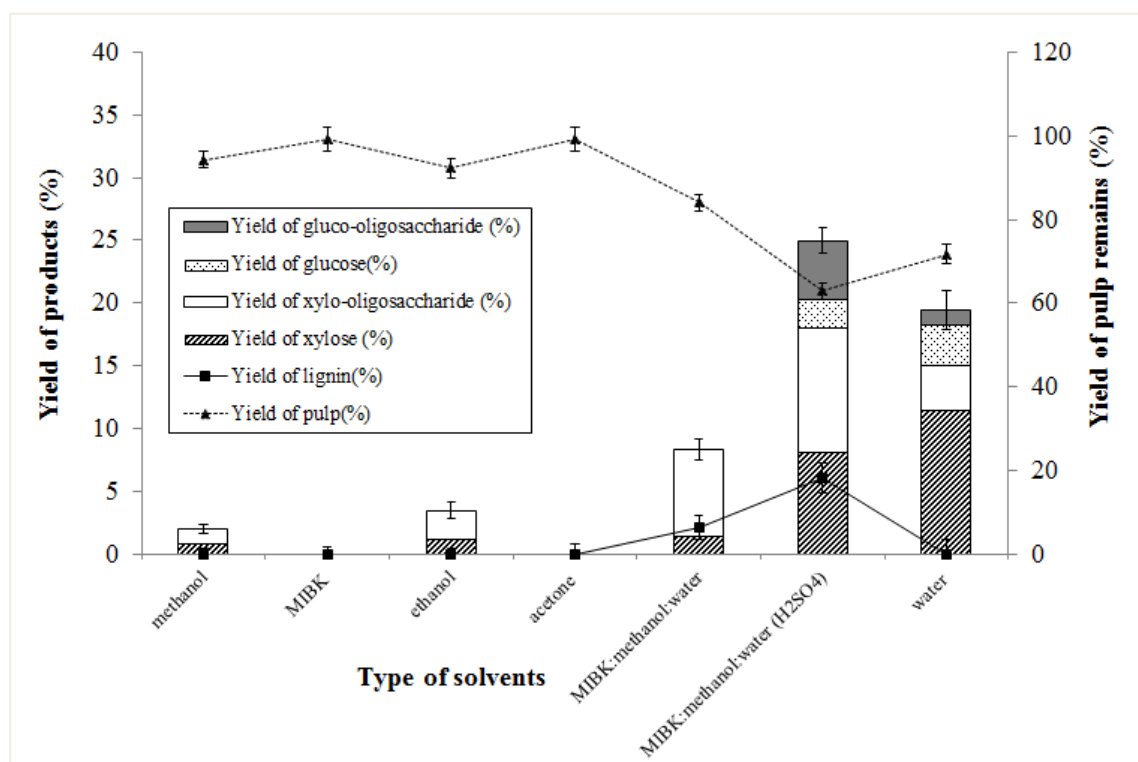


**Figure 4.1** Effect of media on lignocellulose fractionation.

Next, the effects of homogeneous acid promoters on biomass fractionation in the single-phase aqueous-organosolv system were tested at varying  $H_2SO_4$  concentrations (0-0.025 M), while other parameters were kept constant (*i.e.* in MIBK:methanol:water (16:68:16) at  $180^\circ C$  for 60 min; **Figure 4.2**). Clearly, the addition of a small amount of acid promoter (0.008 M  $H_2SO_4$ ) led to a remarkable increase in soluble hemicelluloses

hydrolysis product yield to 18.2 wt.% and lignin yield to 6.1 wt.%. Higher solubilisation of cellulose to glucose (2.2 wt.%) and cello-oligosaccharides (4.7 wt.%) into the aqueous phase was found under the acid catalysed conditions. Increasing acid concentration led to an increasing trend on solubilisation of the carbohydrate components. The maximum solubilisation of was found at 0.015 M  $\text{H}_2\text{SO}_4$  where 18.6 wt.% of the hemicelluloses was hydrolysed. Although cellulose decomposition to glucose and cello-oligosaccharides was higher at 0.025 M  $\text{H}_2\text{SO}_4$ , the sugar yield from hemicellulose hydrolysis was lower at the highest acid concentration owing to acid-catalysed sugar degradation to furans. No significant increase in lignin extraction was observed at acid concentration above 0.008 M. The acid dosage at 0.008 M is considered optimal for promoting fractionation efficiency and selectivity with minimal loss of cellulose fraction.

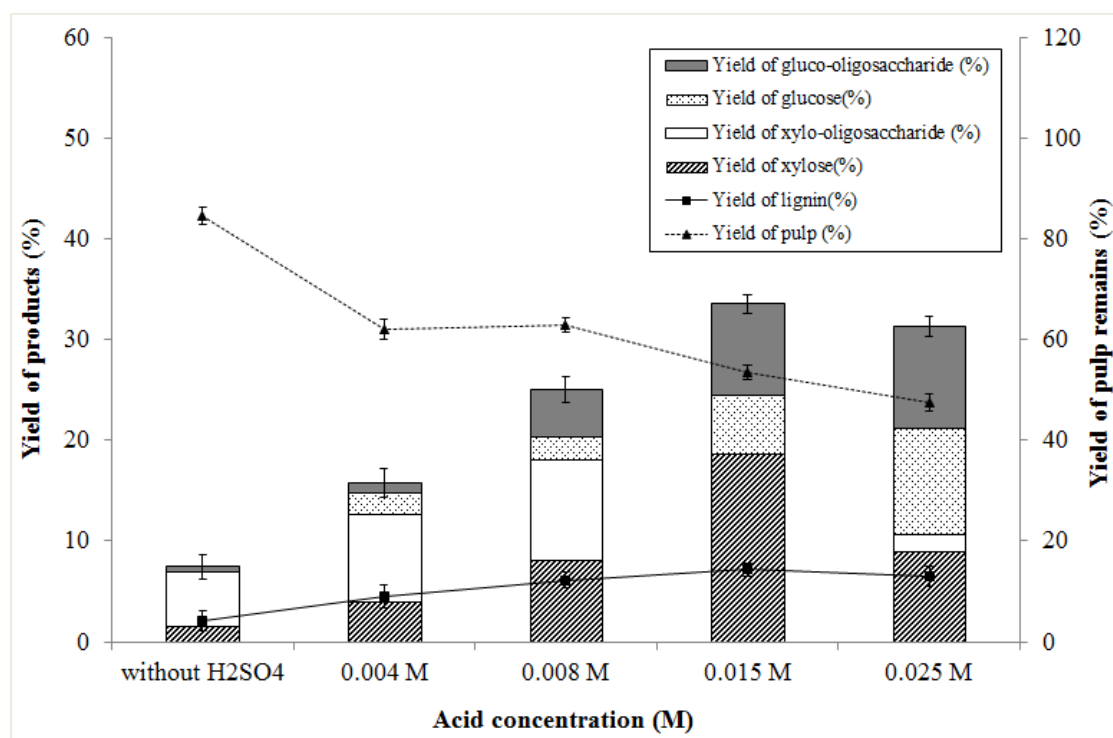


**Figure 4.2** Effect of  $\text{H}_2\text{SO}_4$  concentration (acid promoter) on lignocellulose fractionation.

#### 4.2.3 Effect of operating conditions on fractionation of eucalyptus wood chips

The influence of reaction temperature on biomass fractionation was studied by varying the fractionation temperature from 140 to 250°C while other operating conditions were kept constant in the presence of 0.008 M  $\text{H}_2\text{SO}_4$ . As shown in **Figure 4.3**, the total yield of soluble hemicellulose hydrolysis products increased sharply from 1.8 to 18.1%,

whereas the lignin yield was substantially increased from 0.05 to 6.1% when the reaction temperature increased from 140 to 180°C. Further increases in temperature to 200-220°C led to decreases in the total soluble hemicellulose hydrolysis product yield with increasing hydrolysis of cellulose to glucose and cello-oligosaccharides. The highest cellulose decomposition was observed at 220°C where 12.5 wt.% glucose hydrolysis products were found. The decrease in remaining pulp yield was found with increasing temperature. The optimal temperature was thus suggested at 180°C at which the highest yield of soluble hemicelluloses product was obtained with slight cross-contamination of cellulose decomposed products in the aqueous phase with the remaining pulp yield of 62.9 wt.%.

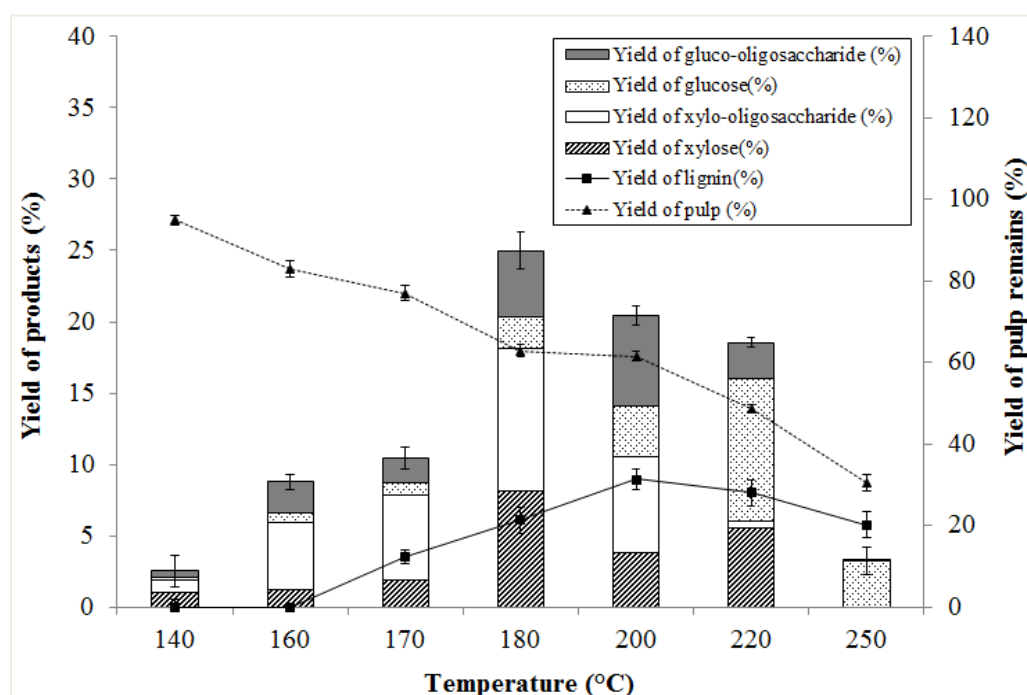


**Figure 4.3** Effect of temperature on lignocellulose fractionation.

The effect of fractionation time was investigated by varying the fractionation time from 10 min to 180 min while keeping the other parameters constant, *i.e.* eucalyptus wood chips of 1 g, amount of solvent mixture (MIBK:methanol:water;16:68:16) at 6 mL, fractionation temperature of 180°C, time at 60 min, pressure at 20 bars and catalyst promoter at 0.008 M H<sub>2</sub>SO<sub>4</sub>. As shown in **Figure 4.4**, it was observed that the fractionation time also affects the lignin yield and total sugar yield (xylose, xylo-oligosaccharide, glucose, and gluco-oligosaccharide). It can be revealed that C<sub>5</sub> sugar yield (xylose, xylo-oligosaccharide) and lignin yield increase rapidly with increasing the reaction time

until at 60 min. At longer fractionation time, the pulp yield and lignin yield were almost constant, whereas the total yield of C<sub>5</sub> sugar decreased due to converting into by-product at longer reaction times. As also shown in **Figure 4.4**, after 60 min, it was observed that C<sub>5</sub> sugar yield start to decompose into other products *i.e.* organic acid via dehydration reaction and cellulose from eucalyptus hydrolyzed to C<sub>6</sub> sugar (Ando et al., 2004). Hence, the optimal fractionation time seems to be at 60 min, from which the lignin yield of 6% and C<sub>5</sub> sugar yield (xylose, xylo-oligosaccharide) closed to 18% could be achieved.

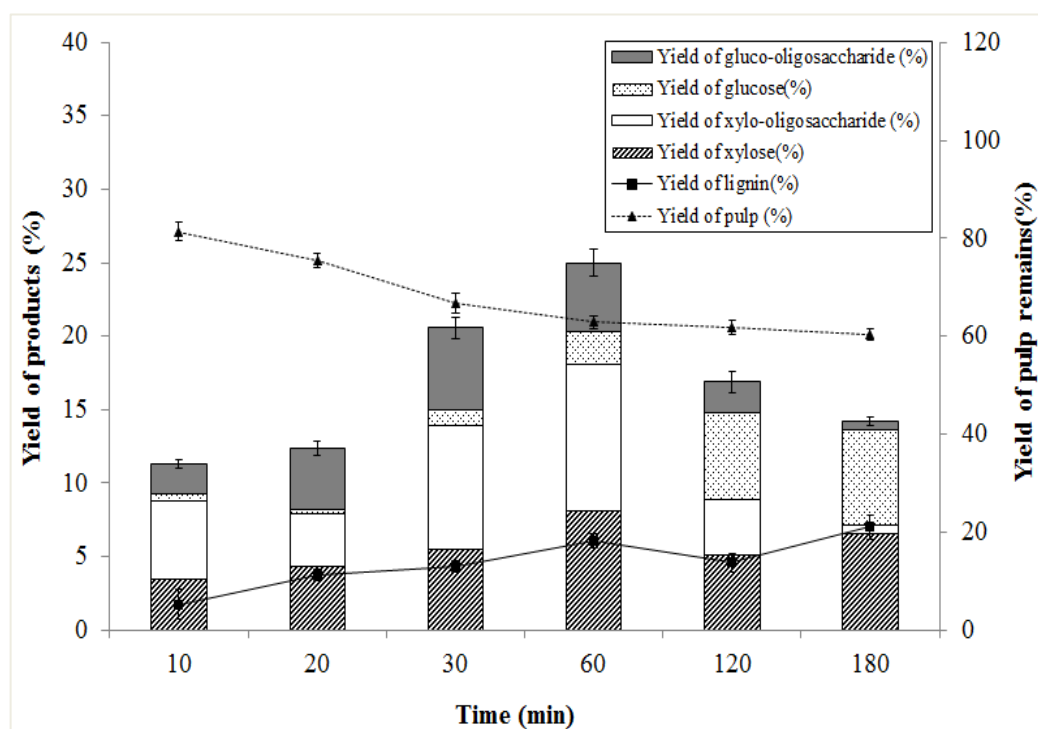


**Figure 4.4** Effect of time on lignocellulose fractionation.

Apart from the effect of times, the effect of pressure in the system was also studied by varying the pressure from 5 bars to 20 bars. The results are shown in **Figure 4.5**. It can be seen that the pressure shows insignificant impact on the fractionation process. In the present work, the fractionation pressure of 20 bars was chosen for further studies.

The effect of solvent ratio in the single-phase solvent mixture comprising MIBK, methanol, and water was also varied from 25/42/33, 33/42/25, 42/42/16, 34/50/16, and 16/68/16, while other components were kept constant under the optimal conditions in the presence of 0.008 M H<sub>2</sub>SO<sub>4</sub>. It can be seen from **Figure 4.6** that the low ratio of methanol/water promoted the isolation of lignin and hemicelluloses as xylose and other

hydrolysis products, while high MIBK ratio led to increased cellulose hydrolysis. Among all ratios studied, the solvent ratio of 25:42:33 (MIBK:methanol:water) led to the highest yield of lignin of 13.3 wt.% and hemicelluloses hydrolysate of 16.2 wt.% with the remaining pulp yield of 55.5 wt.%. This ratio was thus identified as the optimal solvent mixture in this study.

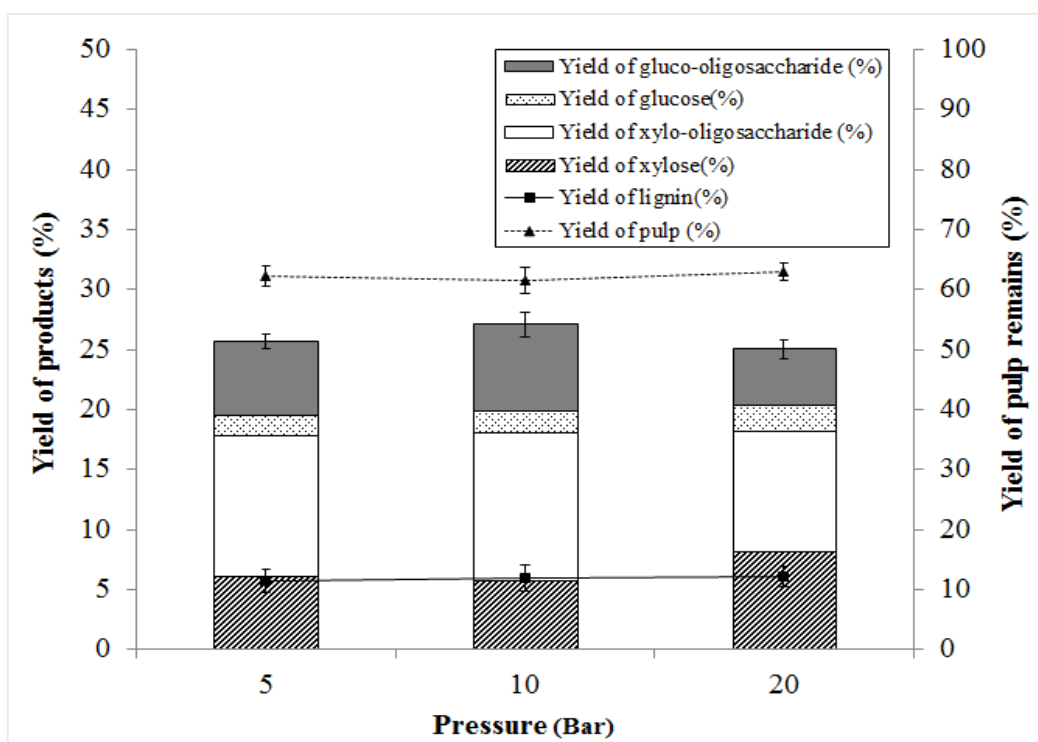


**Figure 4.5** Effect of pressure on lignocellulose fractionation.

Apart from the effect of ratio of solvent mixture, the amount of biomass in the system also plays an important role on the solid-liquid reaction performance since it can greatly impact the mass transfer limitation of the system. The effect of biomass weight to solvent amount on the fractionation performance was therefore studied under the conditions of 0.1-1 g eucalyptus in the presence of 0.008 M  $H_2SO_4$  promoter with 6 ml solvent mixture at the reaction pressure of 20 bars, reaction temperature of 180°C, and reaction time of 60 min. In detail, ratio of biomass weight to solvent were varied from 0.017 (0.1 g), to 0.042 (0.25 g), 0.083 (0.5 g), and 0.167 (1 g). The effect of weight to solvent amount on the yield of products (lignin, sugars) and yield of pulp remains are shown in **Figure 4.7**. It was found that the lower ratio of biomass weight to solvent can enhance higher sugars yield than the higher ratio of biomass weight to solvent, whereas

yield of lignin oppositely increased when the higher of biomass weight to solvent. It can be revealed that the lower ratio of biomass weight to solvent, the rate of hydrolysis reaction is faster than lignin extracting; therefore, it can achieve high yield of sugar with less lignin extraction. For the ratio of biomass weight to solvent at 0.017, the yield of sugar (closed to 40%) achieved the highest. Nevertheless, under this ratio, cellulose would decompose to C<sub>6</sub> sugar and the intensive liquid product separation is required to extract C<sub>6</sub> sugar from C<sub>5</sub> sugar. This disadvantage could possibly due to the further conversion of sugar to other by-products *i.e.* organic acid via the thermal cracking reaction. In case of using the ratio of biomass weight to solvent at 0.167, the highest yield of lignin (closed to 13%) can be achieved while high yield of total xyloses (xylose and xylo-oligosaccharide; closed to 16%) and relatively low yield of total glucoses (glucose and gluco-oligosaccharide; closed to 5%) were obtained. Therefore, we indicated here that the suitable ratio of biomass weight for biomass fractionation is 0.167.

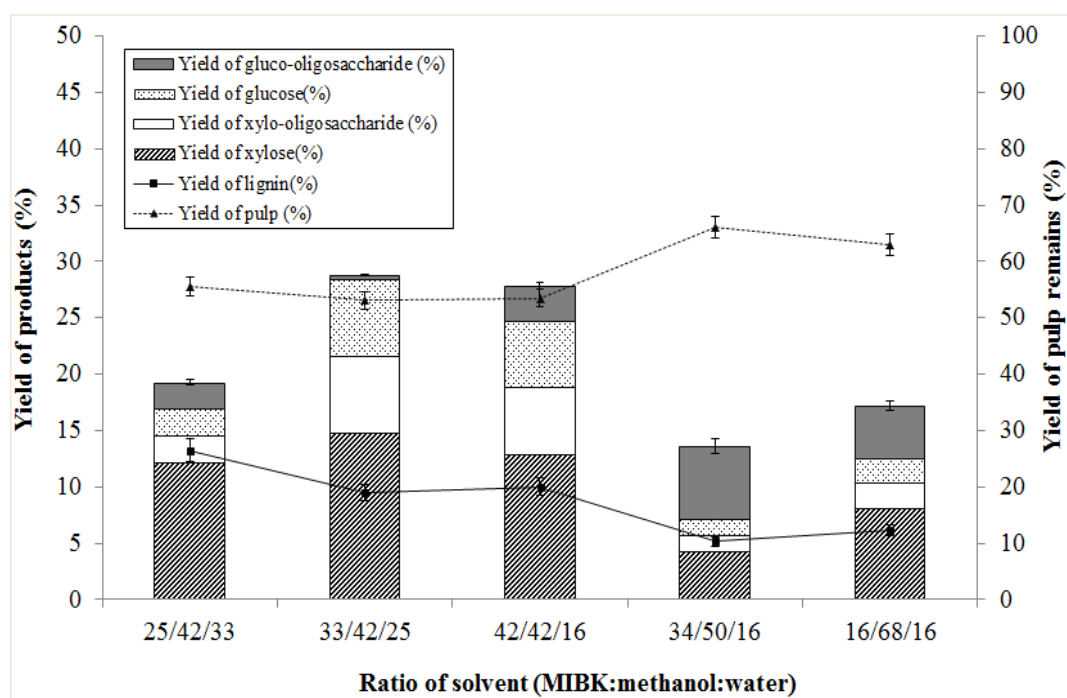


**Figure 4.6** Effect of ratio of solvent (MIBK:methanol:water) on lignocellulose fractionation.

Overall, the results indicated that the optimal condition for the single-phase organosolv fractionation process in the presence of homogenous acid promoter was at 180°C for 60 min with the initial pressure at 20 bars and the solid content of 16.7% w/v in

MIBK/methanol/water ratio of 25:42:33. Under these conditions, lignin is extracted in the organic phase at 13.3 wt.% and hemicellulose hydrolysate is obtained at 16.2 wt.% yield, mostly as xyloses (12.2 wt.%) and xylooligosaccharides (4.0 wt.%). Slight hydrolysis of cellulose was observed under the experimental conditions leading to the remaining pulp yield of 55.0 wt.% with partial loss of cellulose to glucose-based hydrolysis products (4.8 wt.%).

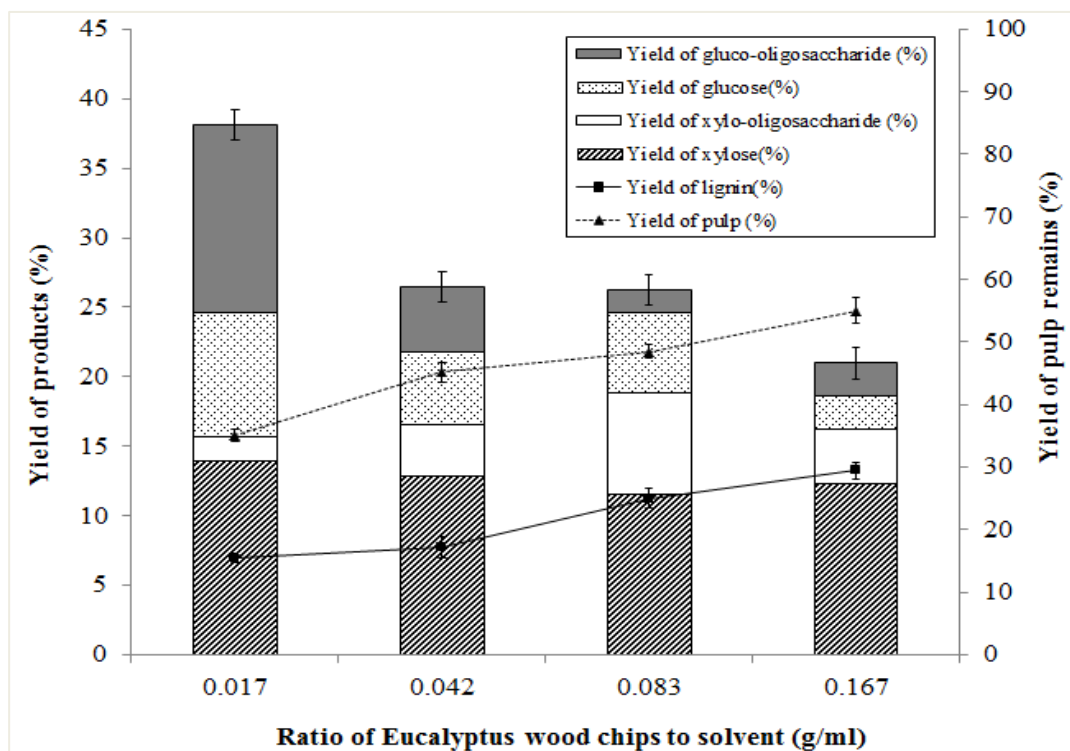


**Figure 4.7** Effect of ratio of eucalyptus wood chips to solvent (g/mL) on lignocellulose fractionation.

#### 4.2.4 Solid acid promoters for fractionation of eucalyptus wood chips

Heterogeneous acid promoters were synthesized as activated carbon with sulphonated (AC-H<sub>2</sub>SO<sub>4</sub>)/ phosphonated (AC-H<sub>3</sub>PO<sub>4</sub>)/nitrated (AC-HNO<sub>3</sub>)/ and hydrochlorated (AC-HCl) forms. The physical and chemical properties of the synthesized solid promoters were characterised. An analysis of the area by N<sub>2</sub> physisorption showed that the solid acid promoters had a high BET surface area in the range of 782-853 m<sup>2</sup>/g (Table 4.1). This corresponded to their high cumulative pore volume and average pore size. The NH<sub>3</sub>- and CO<sub>2</sub>-TPD techniques were then used to measure the acid-base properties of the promoters. The H<sub>3</sub>PO<sub>4</sub>-activated carbon promoter showed the highest

density per unit mass of acid sites ( $1057.7 \mu\text{mol/g}$ ) relative to basic sites ( $307.1 \mu\text{mol/g}$ ) (Table 4.2). The reactive site densities per unit area of all solid promoters were in the range of  $0.87\text{-}1.24 \mu\text{mol/m}^2$  for acid sites and  $0.36\text{-}0.52 \mu\text{mol/m}^2$  for basic sites. The data indicated that the phosphonated promoter exhibited superior performance on the activated carbon.

**Table 4.3** Composition (wt.%) of the solid fraction<sup>a</sup>

Acid promoter	Solid phase			Aqueous-alcohol phase			Organic phase
	Cellulose	Hemicellulose	Lignin	Cellulose	Hemicellulose	Lignin	Lignin
no promoter	43.18	17.22	25.77	1.57	8.5	-	1.75
H <sub>2</sub> SO <sub>4</sub>	38.67	4.88	14.88	4.87	16.18	-	13.25
AC-H <sub>2</sub> SO <sub>4</sub>	39.79	11.34	24.41	5.43	11.15	-	5.25
AC-HCl	42.77	15.02	27.45	2.01	8.05	-	0.75
AC-HNO <sub>3</sub>	42.55	17.04	28.99	3.03	4.11	-	0.35
AC-H <sub>3</sub> PO <sub>4</sub>	41.23	4.61	14.31	5.38	17.76	-	13.71

<sup>a</sup>Error of measurement =  $\pm 5\%$ .

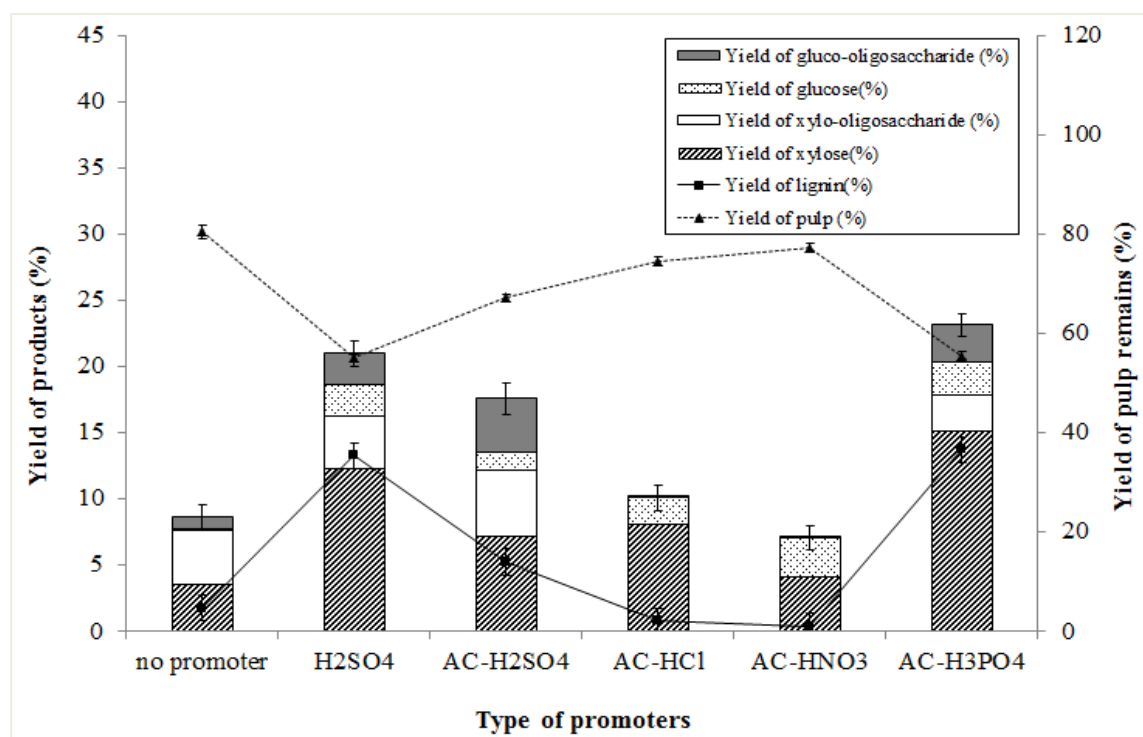


**Figure 4.8** Effect of heterogeneous acid promoters on lignocellulose fractionation.

The effects of various solid acid promoters on the fractionation of eucalyptus wood chips were evaluated under the optimal conditions for the  $\text{H}_2\text{SO}_4$  catalysed reaction. The fractionation process was performed at  $180^\circ\text{C}$  for 60 min with the initial pressure at 20 bars in the presence of 0.05 g (5% (w/w)) of the solid acid promoters. It was observed that AC- $\text{H}_3\text{PO}_4$  and AC- $\text{H}_2\text{SO}_4$  had led to increases in soluble product yield as compared to the control-lacking promoter while lower yields of soluble products were observed for the AC- $\text{HNO}_3$  and AC- $\text{HCl}$  catalyzed reactions (**Figure 4.8**). AC- $\text{H}_3\text{PO}_4$  showed the highest efficiency on enhancing the soluble products. This led to 17.8 wt.% hemicellulose hydrolysis products, mostly comprised of xylose monomer. High lignin solubilisation of 13.7 wt.% was obtained. Slight decomposition of cellulose to glucose-based products was found under this condition. The total hemicellulose, cellulose, and lignin products obtained from the AC- $\text{H}_3\text{PO}_4$  catalysed reaction were slightly higher than those obtained using homogeneous  $\text{H}_2\text{SO}_4$  or  $\text{H}_3\text{PO}_4$  under the experimental conditions. This led to comparable remaining pulp yield (55.5 wt.%) obtained with AC- $\text{H}_3\text{PO}_4$  compared to the homogeneous promoter. The result thus demonstrate improved efficiency and selectivity of the fractionation process using AC- $\text{H}_3\text{PO}_4$  compared with the conventional homogeneous acid promoter.

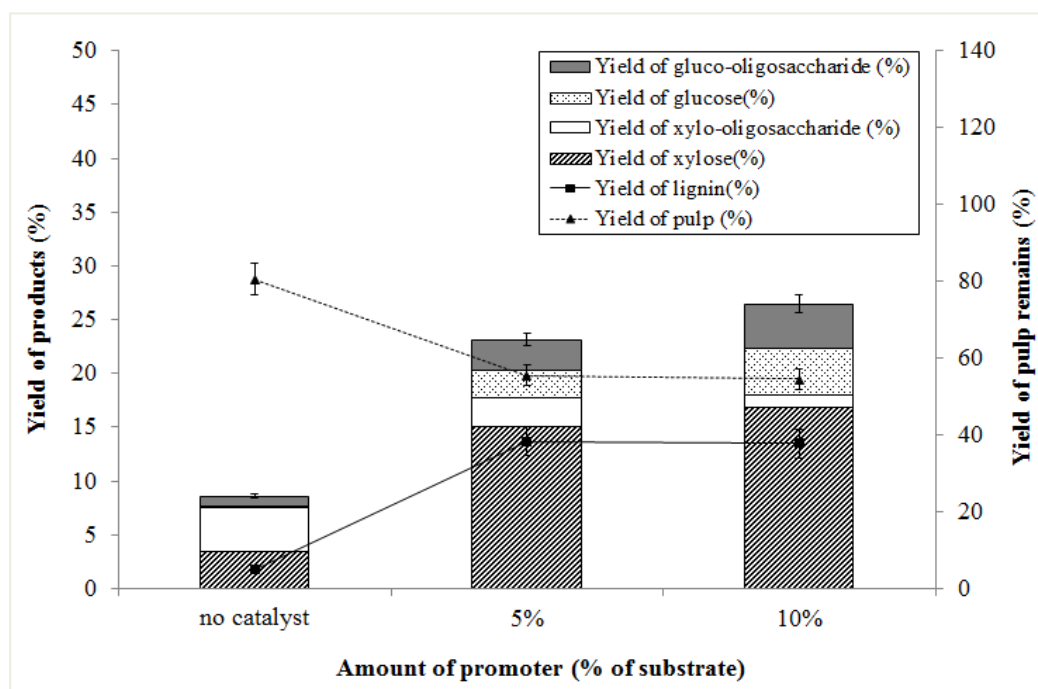


**Figure 4.9** Effect of promoter amount (% of substrate) on lignocellulose fractionation.

The effect of varying the amount of  $H_3PO_4$ -activated carbon on the reaction of eucalyptus was studied by varying the amount of promoter (% of substrate) from 0%, 5% to 10%, while keeping other parameters constant, *i.e.* fractionation temperature at  $180^\circ C$ , pressure reaction at 20 bars, and fractionation time at 60 min, amount of eucalyptus at 1 g, and amount of solvent mixture (MIBK:methanol:water; 25/42/33) at 6 mL. **Figure 4.9** shows that the use of a higher amount of  $H_3PO_4$ -activated carbon (5%) significantly promotes the total xylose yield (close to 18%) and lignin yield (close to 14%) compared to the reaction without catalyst, from which only total xylose yield of 8.5 % and a lignin yield of 1.75 % were obtained. By using 10% of  $H_3PO_4$ -activated carbon, the total xylose yield is higher than the use of 5%  $H_3PO_4$ -activated carbon but high proportion of  $C_6$  sugar (close to 8% of biomass) is also observed due to the decomposition of cellulose. This study revealed that the amount of acid promoter adding plays an important role on the fractionation performance as well as product distribution.

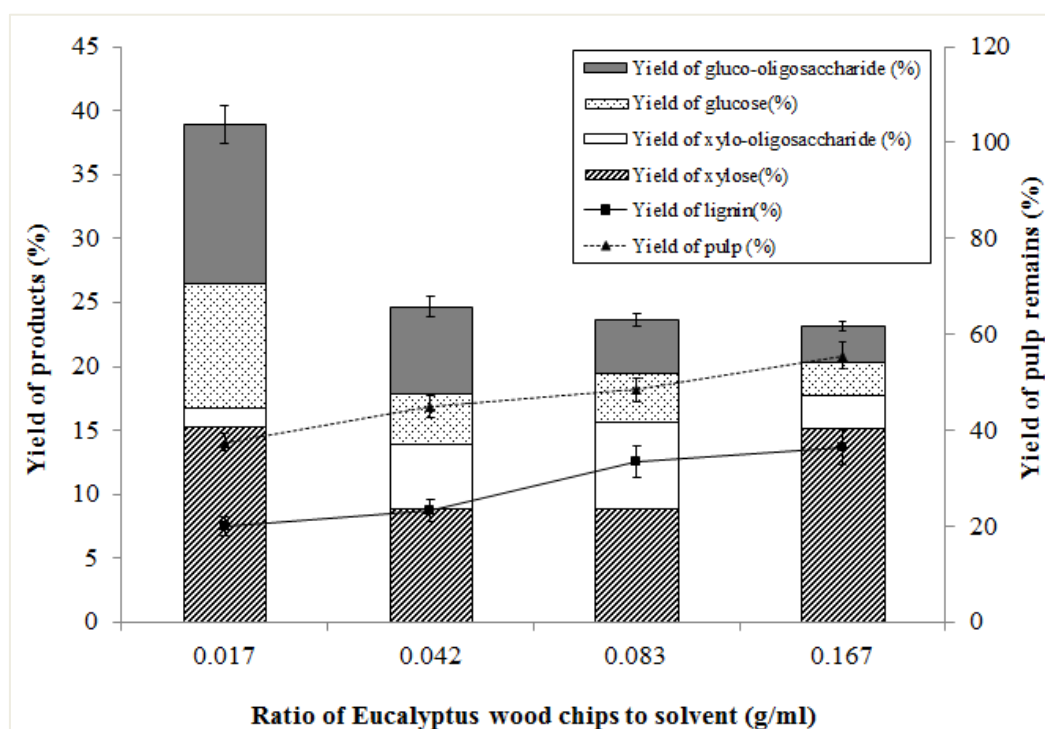


**Figure 4.10** Effect of ratio of eucalyptus wood chips to solvent (g/mL) on lignocellulose fractionation in the presence of AC- $H_3PO_4$  promoter.

The effect of biomass content to fractionation performance was then studied under the optimal reaction conditions at varying solid-to-liquid contents from 0.017-0.167 g/mL with 5% AC- $H_3PO_4$ . Increasing solubilisation of hemicellulose and cellulose was observed

at low solid content, which led to higher soluble sugar product yields (**Figure 4.10**). Nevertheless, an opposite trend was found for lignin solubilisation of which increasing lignin yield was obtained with increasing solid content. This could be due to the relatively faster rate of cellulose and hemicellulose hydrolysis to the rate of lignin extraction at low solid content. Overall, the changes in reaction selectivity led to increased remaining pulp yields at higher solid-to-liquid ratios. The highest soluble sugar product yield was observed at the solid ratio of 0.017 at which 16.7 % w/v of soluble hemicellulose hydrolysis products were obtained; however, with high cellulose decomposition as shown by high soluble glucan hydrolysis products (22.2 wt.%) and low lignin yield (7.5 wt.%). The solid-to-liquid ratio of 0.167 is thus considered optimal. At this ratio, high soluble hemicellulose hydrolysis products (17.8 wt.%) and lignin yield (13.7 wt.%) were obtained with slight hydrolysis of cellulose.

The compositions of the solid fraction from the fractionation with and without the presence of homogeneous or solid acid promoter were compared (**Table 4.3**). Fractionation under conditions with no acid promoter resulted in the solid fraction comprising 43.2 wt.%, 17.2 wt.%, and 25.8 wt.% cellulose, hemicellulose, and lignin, respectively, compared with 45.2 wt.%, 21.1 wt.% and 30.4 wt.%, respectively in the native biomass. Different solid promoters showed different efficiency and selectivity on biomass fractionation. Fractionation in the presence of AC-H<sub>3</sub>PO<sub>4</sub> showed high efficiency and selectivity compared with other activated carbon-based acid promoters and H<sub>2</sub>SO<sub>4</sub>. The solid fraction was highly enriched in cellulose (41.2 wt.%) with minor content of hemicellulose (4.6 wt.%) and lignin (14.3 wt.%) remaining which corresponded to the glucan content of 75.9%, showing higher glucan recovery compared to the reaction with H<sub>2</sub>SO<sub>4</sub>. The aqueous phase contained the majority of hemicellulose fraction (17.8 wt.%) with slight cross-contamination by cellulose hydrolysis products (5.4 wt.%). A lignin yield of 13.7 wt.% was obtained in the organic phase with no cross-contamination. The result thus highlighted the high potential of AC-H<sub>3</sub>PO<sub>4</sub> promoter on the aqueous-organosolv fractionation process.

#### **4.2.5 Stepwise fractionation and recycling of solid acid promoter**

The use of homogeneous and heterogeneous acid promoters on the stepwise fractionation of eucalyptus wood chips was studied using 0.008 M H<sub>2</sub>SO<sub>4</sub> and 5% AC-H<sub>3</sub>PO<sub>4</sub>. Stepwise fractionation of the biomass with fresh promoter led to further removal of hemicelluloses, cellulose, and lignin in the second and third reactions

(**Figure 4.11**). Hemicellulose remaining after the first reaction in the biomass was completely extracted in the second reaction. Further degradation of cellulose into the aqueous phase was observed in the second and third batch reactions. Overall, 19.8 wt.% hemicellulose hydrolysate and 16.3 wt.% lignin yields were obtained after three rounds of fractionation with 21.0 wt.% of cellulose hydrolysis product yield and the remaining pulp yield of 31.0 wt.% using AC-H<sub>3</sub>PO<sub>4</sub>. The performance of AC-H<sub>3</sub>PO<sub>4</sub> was slightly higher compared with H<sub>2</sub>SO<sub>4</sub> in terms of reaction efficiency and selectivity under the experimental conditions.

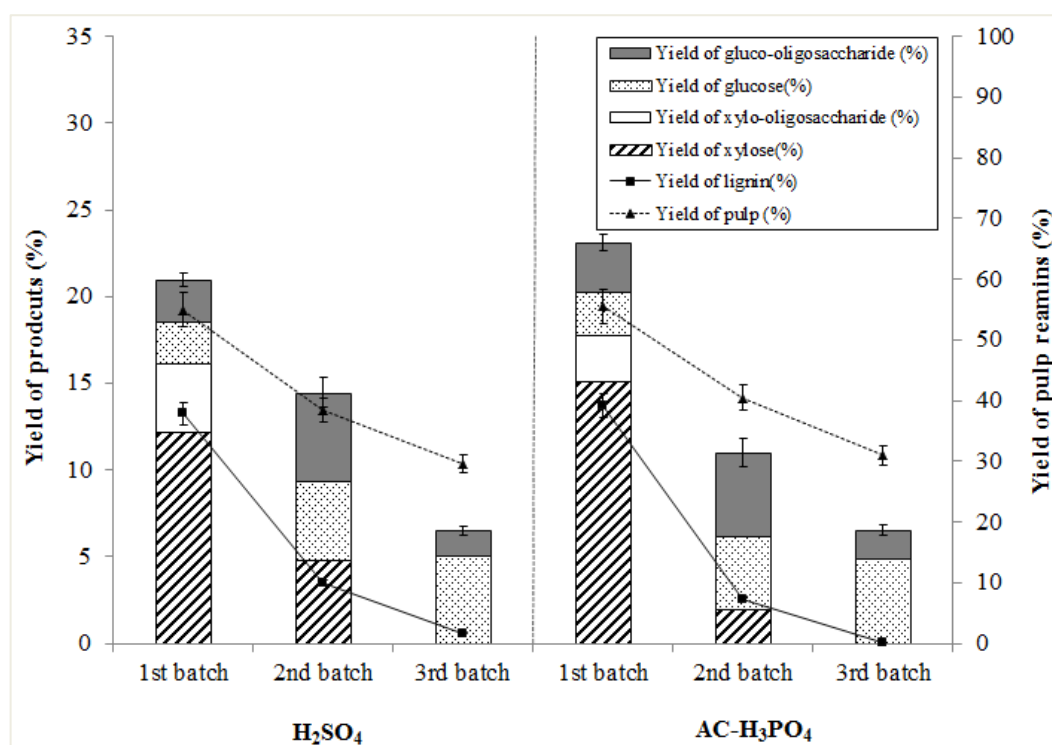


**Figure 4.11** Stepwise fractionation of eucalyptus wood chips.

The reusability of AC-H<sub>3</sub>PO<sub>4</sub> on sequential batch fractionation with fresh biomass was studied under the optimized reaction conditions. The results showed substantial decreases in fractionation efficiency after the first batch (**Figure 4.12**). This was shown by decreasing yields of pulp, xylose, and lignin content in subsequent reaction batches. The amount of remaining components remained constant from batch 2 to 6, which resulted in 70.0-73.0 wt.% solid pulp, 13.8-14.3 wt.% xylose and other hemicelluloses hydrolysis product yield, and 7.7-8.1 wt.% lignin yields. The reduced efficiency suggests that the leaching of solid promoter could occur at high temperature.

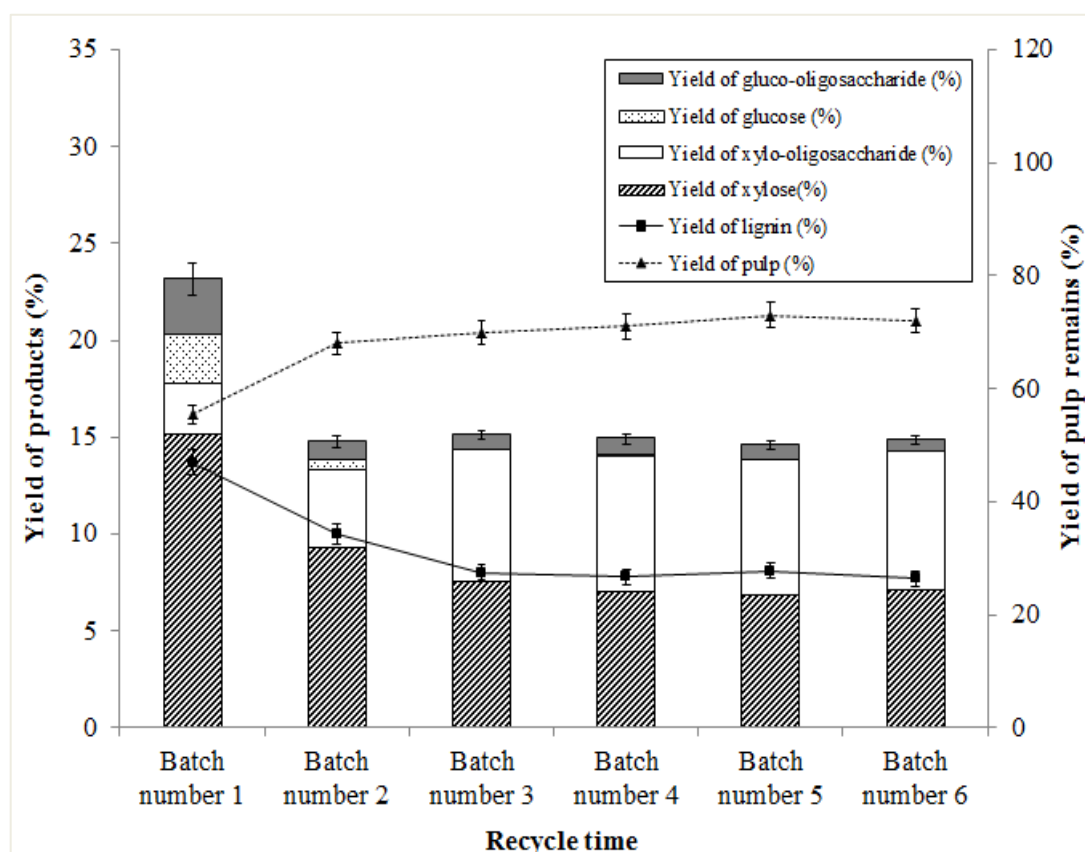


**Figure 4.12** Reusability of solid promoter of fractionation process.

The fractionation of lignocellulosic biomass components with high yield and selectivity is a prerequisite for the maximization of biomass in an integrated biorefinery. Cellulose-enriched fraction provides the major homogenous source of glucose for conversion to biofuels and chemicals while the hemicellulose fraction can be converted to wide range of commodity chemicals by fermentation or catalytic routes (Gírio et al., 2010). Currently, the use of lignin is still a challenge for biorefinery. With its high heterogeneity and structural complexity, lignin is conventionally used as a crude fuel for process energy; however, its conversion to high valued aromatics is promising (Zakzeski et al., 2010; Zakzeski et al., 2012). Various organosolv processes based on single organic solvents *e.g.* methanol, ethanol, propanol, and acetone have been studied for pretreatment and fractionation using different acids and bases as promoters (Bauer et al., 2012; Jiménez et al., 1998; Romání et al., 2013).

A recently developed organosolv process termed “Clean Fractionation” (CF) technology, allows efficient one-step separation of lignocellulosic addition to the MIBK

and methanol used in this study. Different ketones (*e.g.*, methyl ethyl ketone, methyl isopropyl ketone, and methyl butyl ketone) and alcohols (ethanol) have also been tested for this process; however, no significant difference in reaction selectivity was found (Bozell et al., 2011a). The use of ternary solvent mixture was also reported to enhance lignin solubilisation and retain its re-deposition on the cellulose solid pulp compared with the widely used aqueous ethanol process.

The CF process has been previously optimized for the separation of woody feedstocks, grasses and agricultural residues, particularly on various hardwoods, *e.g.* aspen, poplar, and oak, focusing on yield and purity. The optimal process carried out in the presence of 0.1 M H<sub>2</sub>SO<sub>4</sub> or greater led to a cellulose-enriched fraction with an average yield of 47.7 wt.% with the Klason lignin of 5.1-6.8 wt.% and trace amounts of cross-contaminating non-glucose sugars. A glucan content of 68.7% from batch separation was obtained under these conditions, which was marked improvement over the 89.9% under flow-through condition (Bozell et al., 2011a). High-purity lignin was obtained with an average yield of 17.8-19.5 wt.%. The hemicelluloses fraction obtained is 14.5 wt.% in average and comprises a complex mixture of monomeric sugar *e.g.*, xylose, mannose, uronic acids, and small amount of galactose and arabinose with dehydration products and the acid promoter.

The reaction medium and conditions in our work were substantially different from those previously reported (Bozell et al., 2011a). The optimised solvent mixture in our work *i.e.* MIBK:MeOH:H<sub>2</sub>O (25:42:33) is different to the reported optimal ratio for various hardwoods under batch and flow through conditions *i.e.* MIBK:EtOH:H<sub>2</sub>O (16:34:50). Cellulose-enriched solid fraction was obtained in this study with the typical yield of 41.3 wt.%, equivalent to 91.8% recovery of cellulose from the starting material. Typically, 17.8 wt.% hemicelluloses was recovered as soluble oligomeric and monomeric sugar products in the aqueous fraction with small molecular products *e.g.* organic acids, while 13.7 % lignin was efficiently extracted and recovered in the organic phase with no significant sugar cross-contamination. These were equivalent to 84.6% and 44.2% recoveries of hemicellulose and lignin from the native biomass.

The decrease of monomeric and oligomeric sugar products at high temperatures was due to their dehydration to furans at temperatures above 200°C in the presence of mineral acids (Chareonlimkun et al., 2010). Further conversion of sugars to other degradation products *e.g.*, organic acids was reported at 200°C. The results thus reflected

the optimal temperature at 180°C as observed in this study. It should be noted that the hydrolysis of hemicellulose and lignin in lignocellulosic biomass in the ternary solvent mixture started at 160°C while partial cellulose decomposition started at 180°C in the presence of acid promoter, which occurred at a lower temperature compared to that reported for non-catalytic hot compressed water (Ando et al., 2004).

Overall, higher enriched cellulose pulp and glucose recovery yields were obtained in our study, but with lower purity as compared to the previous work, which used conditions with higher strings (Bozell et al., 2011a). Hemicellulose was obtained with a greater fraction of xylooligosaccharides compared with the previous work (Bozell et al., 2011a), in which monomeric sugars were recovered while a substantially lower lignin content was extracted into the organic phase. These differences would be due to variation in biomass composition and structural characteristics and differences in solvent system and reaction conditions, in which less stringent conditions, *e.g.* lower acid concentration (0.008 M vs. 0.2 M H<sub>2</sub>SO<sub>4</sub>) was used in our study. Comparable performance of the Clean Fractionation process using low concentration of homogenous acid promoters was recently reported for fractionation of prairie cordgrass and switchgrass (Cybulska et al., 2012; Cybulska et al., 2013). The acid promoters were shown to have strong effects on selectivity, separation effectiveness, and component yield from the fractionation process while temperature and operating time exert less influence (Bozell et al., 2011b). Increasing acid concentration tends to result in higher levels of extracted lignin and hydrolysis of hemicelluloses, resulting in respectively higher purity of the pulp fraction, but with decreased pulp yield.

A typical barrier for the commercial-scale application of homogeneous promoters, particularly a strong acid, such as H<sub>2</sub>SO<sub>4</sub>, is the problem of acid recovery and waste treatment. Furthermore, it is well established that the use of homogeneous acid compounds is generally energy inefficient and leads to degradation of sugar monomers (by-product; *i.e.* furfural and hydroxy-methylfurfural) and equipment corrosion. Development of solid heterogeneous acid promoters as firstly demonstrated in this study provides a promising way to overcome these problems. Nevertheless, there are still limitations regarding catalyst deactivation, which could be due to the leaching of acid group (*e.g.* -SO<sub>3</sub>H, -PO<sub>3</sub>H<sub>2</sub>) from the surface of activated carbon after prolonged processing.

### 4.3 Conclusion

The single-step aqueous-organosolv process for the fractionation of eucalyptus wood chips was optimized in the presence of homogeneous and heterogeneous promoters. The fractionation process of eucalyptus wood chips for isolating products (including cellulose, hemicellulose, lignin) over liquid-state  $\text{H}_2\text{SO}_4$ , solid-state  $\text{H}_2\text{SO}_4$ -Activated carbon, and  $\text{H}_3\text{PO}_4$ -Activated carbon were studied under pressurized solvent conditions. It was found that the suitable condition for fractionation process was using eucalyptus wood weight to solvent mixture of 0.167, mixture of MIBK, methanol and water as solvent with the ratio of 25:42:33 (v/v), initial pressure of 20 bars, at  $180^\circ\text{C}$  for 60 min presence of 0.008 M  $\text{H}_2\text{SO}_4$ . In addition, in the presence of acid promoter *i.e.*  $\text{H}_2\text{SO}_4$ , higher fractionation performance was observed, from which 13.3% yield of lignin (43% of substrate), 12.2% yield of xylose, 4% yield of xylo-oligosaccharide (77% of substrate) can be extracted from eucalyptus wood chip. Importantly, synthesized solid acid catalyst (*i.e.* AC- $\text{H}_3\text{PO}_4$ ; activated carbon phosphonation) can be applied in the fractionation process instead of  $\text{H}_2\text{SO}_4$ ; from which the fractionation performance of AC- $\text{H}_3\text{PO}_4$  is comparable to that of  $\text{H}_2\text{SO}_4$ . More residual lignin (up to 16%) was extracted on the second and third times of fractionation under the same conditions, whereas all hemicellulose was obtained in the second round. The result showed the advantages of using AC- $\text{H}_3\text{PO}_4$  over the use of  $\text{H}_2\text{SO}_4$  including its reusability and less corrosive problem. The work leads to the development in efficient lignocellulose fractionation process for integrated biorefineries.

## CHAPTER 5

### ACTIVITIES OF CARBON-BASED ACID CATALYSTS TOWARD HYDROTHERMAL HYDROLYSIS OF RAW, PRETREATED, AND FRACTIONATED EUCALYPTUS

---

#### Chapter highlights

Catalytic hydrolysis of woody eucalyptus with sulfonated carbon-based (SCB) catalysts prepared from four different carbon precursors (*i.e.* xylose, glucose, sucrose, and activated carbon) was studied under hot compressed water (HCW) at 100-250°C with reaction times of 1-40 min. It was found that the SCB catalyst derived from sucrose gave the highest C<sub>5</sub> and C<sub>6</sub> sugar yields with reduced amounts of unwanted by-products (*i.e.* furans, and 1,6-anhydroglucose (AHG)), which were achieved at 200°C with 5 min reaction time. The alkaline pretreatment and/or organosolv fractionation prior to the catalytic hydrolysis in the presence of SCB catalyst significantly improved the catalytic hydrolysis process because of removal of lignin and hemicellulose.

In addition to SCB catalysts, AC-H<sub>3</sub>PO<sub>4</sub> (an acid promoter for organosolv fractionation of Chapter 4) also enhanced the hydrolysis resulting in high sugar yields and low proportions of unwanted by-products. This was achieved at 220°C with 5 min reaction time. The advantage of AC-H<sub>3</sub>PO<sub>4</sub> is that it can be used both for organosolv fractionation and acid hydrolysis. This provides the means to combine the fractionation and hydrolysis processes in one step.

---

## 5.1 Background

In a sugar platform biorefinery, lignocellulosic biomass is initially hydrolyzed into sugars which are then converted to targeted products by catalytic or biological processes. Enzymatic hydrolysis has advantages on its high selectivity and mild operational conditions. Nevertheless, high enzyme cost and enzyme deactivation due the presence of inhibitors from the prior chemical or thermal pretreatment step are the challenge for industrial implementation of the technology (Brethauer & Wyman, 2010). Alternatively, acid hydrolysis using mineral acids *e.g.*, H<sub>2</sub>SO<sub>4</sub>, HCl, and H<sub>3</sub>PO<sub>4</sub> overcome these problems. However, the corrosive nature of acids, the formation of unwanted by-products, and the requirement for an acid-containing waste treatment plant are the main concern (Karimi et al., 2006; Lenihan et al., 2010).

Recently, HCW has been proposed for the hydrolysis of lignocellulosic materials with the advantages on environmental friendliness and potential on reaction control through use of water density (Chareonlimkun et al., 2010; Dinjus & Kruse, 2007; Yu et al., 2008). In HCW, water is used as the sole solvent at subcritical temperatures under pressurized conditions. Under these conditions, hydronium ions are generated in situ by ionization of water, leading to the release of acetic acid from hemicelluloses, which in turn auto-catalyzes the solubilisation of hemicelluloses in an acidic environment (Ando et al., 2004; Toor et al., 2011). The main barrier to using HCW technology is the requirement of high energy input, which could be partially reduced by adding acids or alkali to help catalyze the reactions and control the decomposition of sugars to by-products, such as furans and organic acids (Chareonlimkun et al., 2010; Khemthong et al., 2012; Watanabe et al., 2003). However, the use of homogenous catalysts lead to difficulties in catalyst recovery, product contamination, and solvent recycling as well as increasing cost on waste water treatment. Heterogeneous acid-based catalysts have been studied for hydrolysis of lignocellulosic materials with the advantages on simple catalyst separation and recovery (Chareonlimkun et al., 2010; Guo et al., 2012; Van de Vyver et al., 2011). Among the currently developed solid acid catalysts *e.g.*, zeolites, transition-metal oxides, cation-exchange resins, supported solid acids and heteropoly compounds (Guo et al., 2012; Van de Vyver et al., 2011), carbonaceous solid acids (CSA) have several favorable characteristics such as high catalytic activity and selectivity, long catalyst life, and ease in recovery. CSA catalysts with SO<sub>3</sub>H, COOH and OH groups were studied for hydrolysis of

cellulose and its derived polysaccharides (Hara, 2010; Onda et al., 2009; Suganuma et al., 2010; Yamaguchi & Hara, 2010).

In this chapter, the hydrolysis of eucalyptus under HCW conditions was studied in the presence of sulfonated carbon-based catalysts prepared from different carbon precursors (*i.e.* sucrose, glucose, and xylose). The catalyst performance was evaluated based on C<sub>5</sub> and C<sub>6</sub> sugar yields, and the reaction selectivity was compared to the use of H<sub>2</sub>SO<sub>4</sub>. The effects of reaction temperature and time were also investigated to identify the optimum conditions for maximized sugar production. Effects of biomass particle size on the catalytic hydrolysis were also evaluated. Importantly, the effects of alkaline pretreatment (with NaOH) and organosolv fractionation prior to the hydrolysis on sugar yield and selectivity were carried out. The work provides the report on application of CSA and the influence of carbon precursor on catalytic hydrolysis of lignocellulosic materials. In addition to SCB catalysts, the potential use of AC-H<sub>3</sub>PO<sub>4</sub> (an acid promoter for organosolv fractionation in Chapter 4) was also examined since the possible use of AC-H<sub>3</sub>PO<sub>4</sub> for hydrolysis reaction will lead the good potential of combining the organosolv fractionation with the hydrothermal hydrolysis without acid promoter removal required.

## 5.2 Results and discussion

The experimental results are divided into two main sections: (1) hydrolysis of eucalyptus under HCW in the presence of sulfonated carbon-based catalysts including sucrose (S-Su), glucose (S-Gu) and xylose (S-Xy); (2) hydrolysis of pretreated and fractionated eucalyptus under HCW in the presence of selected H<sub>2</sub>SO<sub>4</sub>-Sucrose. The main product from the hydrolysis of eucalyptus is sugars (*i.e.* glucose, and xylose) with by-products (*i.e.* organic acid, furfural and hydroxymethylfurfural (HMF)) can also be formed via the dehydration of sugars, particularly at high reaction temperatures and long reaction times (Suganuma et al., 2010; Yu et al., 2008).

### 5.2.1 Hydrolysis of eucalyptus under HCW with sulfonated carbon-based catalysts

The hydrolysis of eucalyptus under HCW was first studied with and without the presence of synthesized sulfonated carbon-based catalysts (S-Su, S-Gu and S-Xy). The reaction using liquid  $\text{H}_2\text{SO}_4$  with the same acid content as the solid-acid catalysts was also tested for comparison. In the initial study, 0.1 g of eucalyptus in the presence of 0.005 g of catalyst and 1 mL of water was heated at  $200^\circ\text{C}$  for 5 min. As presented in **Figure 5.1**, the hydrolysis reaction led to release of glucose and xylose from hydrolysis of cellulose and hemicellulose into the liquid phase. A substantial amount of glucose was isomerized into fructose under the experimental conditions while side-products from sugar dehydration (furfural, HMF, and AHG) were found. S-Su showed the highest catalyst performance on hydrolysis efficiency, as shown by the highest sugar yield with the lowest proportion of HMF, furfural and AHG. This led to the  $\text{C}_6$  sugar yield of 15.5% and  $\text{C}_5$  sugar yield of 4.9% with 4.3% yield for the side-products. Slightly higher  $\text{C}_6$  sugar yield (16.6%) was obtained using liquid  $\text{H}_2\text{SO}_4$ ; however, with lower  $\text{C}_5$  sugar yield. A marked increase in formation of the side products (19.1%) were observed using  $\text{H}_2\text{SO}_4$  due to the strong promotion of dehydration reaction, suggesting higher reaction selectivity of the solid catalysts towards sugar production. The reaction with no catalyst showed noticeably lower sugar yields (6.2%) with relatively high furfural and HMF formations (7.2%). These results therefore reveal the benefit of sulfonated carbon-based catalyst, particularly S-Su, on the hydrolysis of eucalyptus in terms of sugar production yield and selectivity.

The properties of the SCB catalysts were determined in order to understand the differences in performance among the catalysts. The  $\text{NH}_3$ -TPD techniques were used to measure the acid properties of the catalysts. The amounts of acid sites were calculated from the area below the curves of the TPD profiles (**Table 5.1**). In addition to these values, the distribution of the acid sites on the catalyst surface (i.e. the density of acid sites) is also given in the table. This study found that the catalytic activity trend was in good agreement with the acid density of these catalysts, from which the catalyst with high acid site density, such as S-Su, was able to enhance the reactivity toward the hydrolysis reaction.

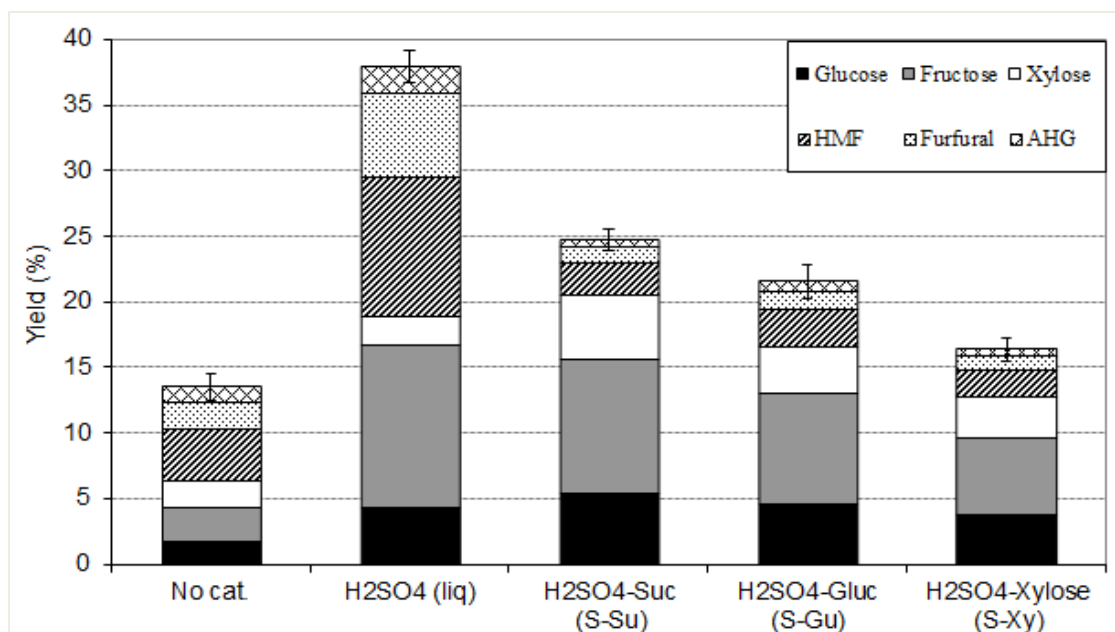


**Figure 5.1** Yield of liquid products from the hydrolysis of eucalyptus at 200°C for 5 min with and without the presence of various catalysts.

**Table 5.1** N<sub>2</sub> physisorption (BET) results and acid properties of sulfonated carbon-based catalysts prepared by different carbon precursors

Catalysts	BET surface area <sup>a</sup> (m <sup>2</sup> /g)	Amount of acid site (μmol/g)	Density of acid site (μmol/m <sup>2</sup> )
H <sub>2</sub> SO <sub>4</sub> -Sucrose	1.8	34.7	19.2
H <sub>2</sub> SO <sub>4</sub> -Glucose	1.5	18.3	12.2
H <sub>2</sub> SO <sub>4</sub> -Xylose	1.5	16.5	11.0

<sup>a</sup> Error of measurement = ±5%.

### 5.2.2 Effect of hydrolysis conditions catalyzed by sulfonated carbon-based catalysts

For the next step, the effects of reaction temperature and reaction time on the hydrolysis of eucalyptus in the presence of H<sub>2</sub>SO<sub>4</sub>-Sucrose, H<sub>2</sub>SO<sub>4</sub>-Glucose and H<sub>2</sub>SO<sub>4</sub>-Xylose were carried out by varying the reaction temperature from 200°C to 150, 175, 225 and 250°C (while keeping the reaction time constant at 5 min), and varying the reaction time from 5 min to 1, 3, 7, and 10 min (while keeping the reaction temperature constant at 200°C).

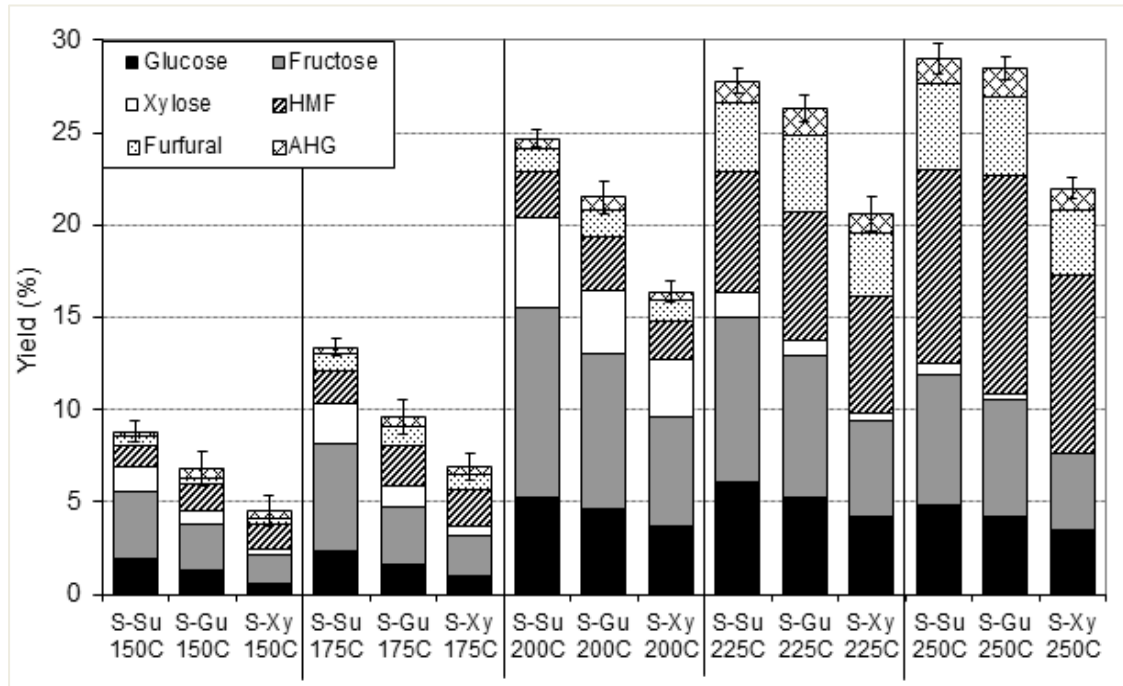


**Figure 5.2** Effect of reaction temperature on the yield of liquid products from the hydrolysis of eucalyptus in the presence of various catalysts (with the reaction time of 5 min).

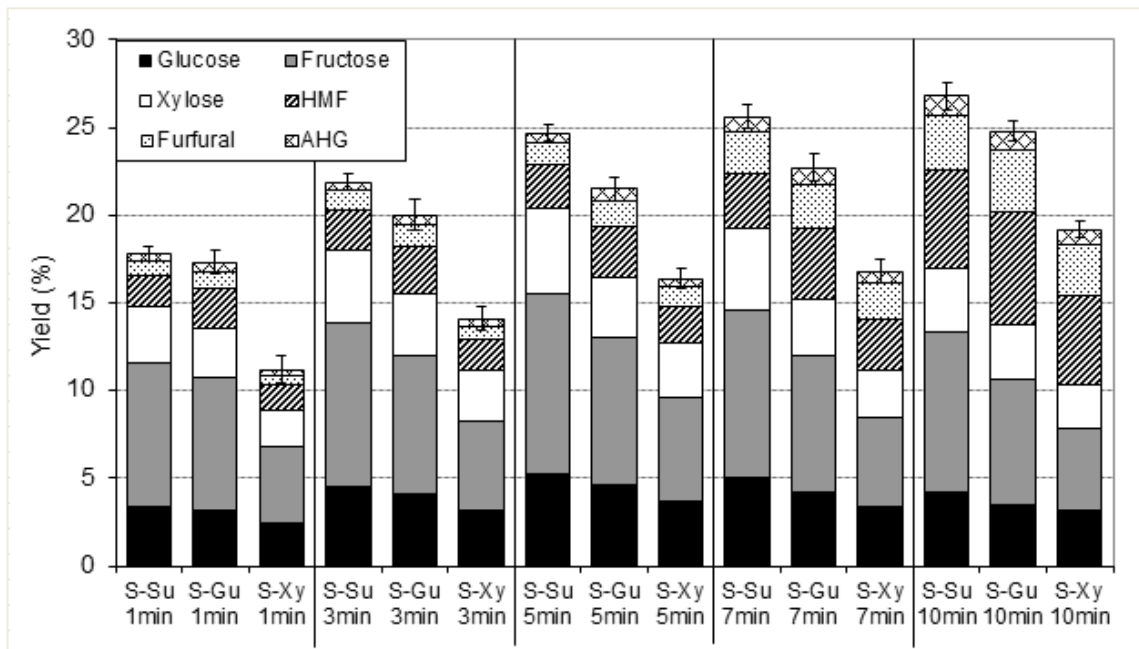


**Figure 5.3** Effect of reaction time on the yield of liquid products from the hydrolysis of eucalyptus in the presence of various catalysts at 200°C.

As shown in **Figure 5.2**, it can be seen that the reaction temperature shows significant effect on the feedstock conversion and yield of liquid products. In detail, the yield of C6 sugars (i.e. glucose and fructose) increased with increasing the reaction temperature from 150°C to 225°C and slightly dropped down at 250°C, while the yield of C5 sugar (xylose) increased with increasing the reaction temperature until 200°C and considerably decreased at higher temperatures (225-250°C). On the other hand, significant amounts of furfural, HMF and AHG were detected at temperatures above 200°C, and they dramatically increased with increasing the reaction temperature from 200°C to 250°C. The effect of reaction time is presented in **Figure 5.3**. It was found that the yield of sugars increase steadily with increasing the reaction time until at 5 min before oppositely decrease at longer reaction time. In addition, the formation of furans increased with increasing the reaction time, which is due to the occurring of dehydration reaction at longer reaction time.

From these studies, it can be concluded that at the temperatures between 150-200°C with the reaction time of 5 min, the rate of hydrolysis reaction is faster than the dehydration reaction, and achieved high yields of sugars with less formation of HMF and furfural. In contrast, above 200°C, monosaccharides can be decomposed into HMF and furfural via the dehydration reaction leading to decreasing sugar production at high temperature. It seems from the experiment that the suitable hydrolysis temperature for cellulose is at 200-225°C, which is slightly higher than that for hemicellulose where the sugar yield can be maximized at 200°C. For better understanding, the hydrolysis of single cellulose and xylan (as representative of hemicelluloses) in the presence of H<sub>2</sub>SO<sub>4</sub>-Sucrose were performed at 150-250°C, as shown in **Figure 5.4**. Clearly, the main products from the conversion of cellulose at the temperature below 200°C are glucose and fructose, while significant amount of HMF (along with a few furfural and AHG) was formed at higher temperatures. The maximum yield of glucose can be achieved at 225°C, while that of fructose is at 200°C.

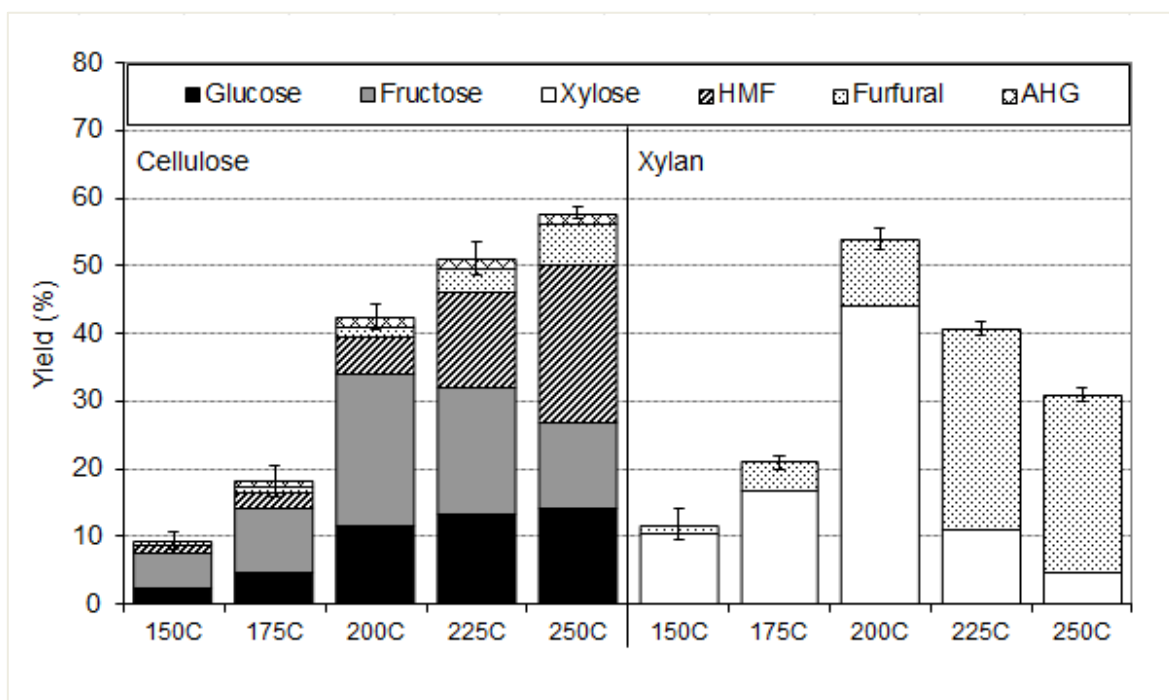


**Figure 5.4** Effect of reaction temperature on the yield of liquid products from the hydrolysis of cellulose and xylan in the presence of  $\text{H}_2\text{SO}_4$ -Sucrose catalyst (with the reaction time of 5 min).

Theoretically, it is known glucose is the main product from the hydrolysis of cellulose. The presence of fructose comes from the isomerization of glucose. HMF and furfural are produced from the further dehydration of glucose and fructose, whereas AHG is the by-product from the dehydration of glucose. In term of product yield and selectivity, the temperature of 200°C seems to be the optimum condition, where the hydrolysis and isomerization reactions are maximized while the dehydration reaction is minimized. For the xylan reaction, xylose is the main product at temperatures below 200°C while furfural (from the dehydration of xylose) is the major product at higher temperatures. Based on the studies over reaction temperature and time, the optimized condition for the hydrolysis of eucalyptus in the presence of  $\text{H}_2\text{SO}_4$ -Sucrose is at 200°C for 5 min, from which high total sugar yield (including glucose, fructose and xylose) with low furan and AHG formations can be achieved.

### 5.2.3 Hydrolysis of pretreated and fractionated eucalyptus by H<sub>2</sub>SO<sub>4</sub>-Sucrose

It is generally known that the pretreatment of biomass with alkaline (*i.e.* NaOH) can promote the hydrolysis reaction by degrading and removing the lignin from cellulose and hemicellulose (Harmsen, 2010). Therefore, the influence of alkaline pretreatment processes on the catalytic hydrolysis were carried out. For the initial wood chip size was in the range of 1.5–2×1.5–2 cm with 0.25–0.5 cm thickness. Prior to the pretreatment study, the effect of eucalyptus particle size on the hydrolysis performance was firstly determined by varying the average particle size of eucalyptus from less than 60 μm to 2-4 mm in the presence of H<sub>2</sub>SO<sub>4</sub>-Sucrose catalyst at 200°C with the reaction time of 5 min. It is noted that eucalyptus wood chip was also tested for comparison. As shown in **Figure 5.5**, smaller particle size of material can enhance higher sugars yield than the bigger particle size, which could be due to the improvement of mass transfer limitation in the system. Nevertheless, with the particle size of eucalyptus less than 60 μm, the yields of sugar and other liquid products oppositely decreased. This negative trend could possibly due to the conversion of eucalyptus to gaseous by-products via the thermal cracking reaction. As also presented in **Figure 5.5**, according to the measurement of the total carbon amount in the water solution after reaction, the TOC (total organic carbon) values for all experiments (except the reaction with less than 60 μm average particle size of eucalyptus) were always higher than 90% indicated that the quantity of gaseous products from the reactions were considerably less than that of liquid products. In contrast, the TOC value from the reaction with very fine particle sizes of eucalyptus (< 60 μm) was only 78%, which indicates the occurrence of gaseous carbon-containing products. Hence, eucalyptus with the average particle size between 60-100 μm, as well as the eucalyptus wood chip (as the reference case), was chosen for the pretreatment study.

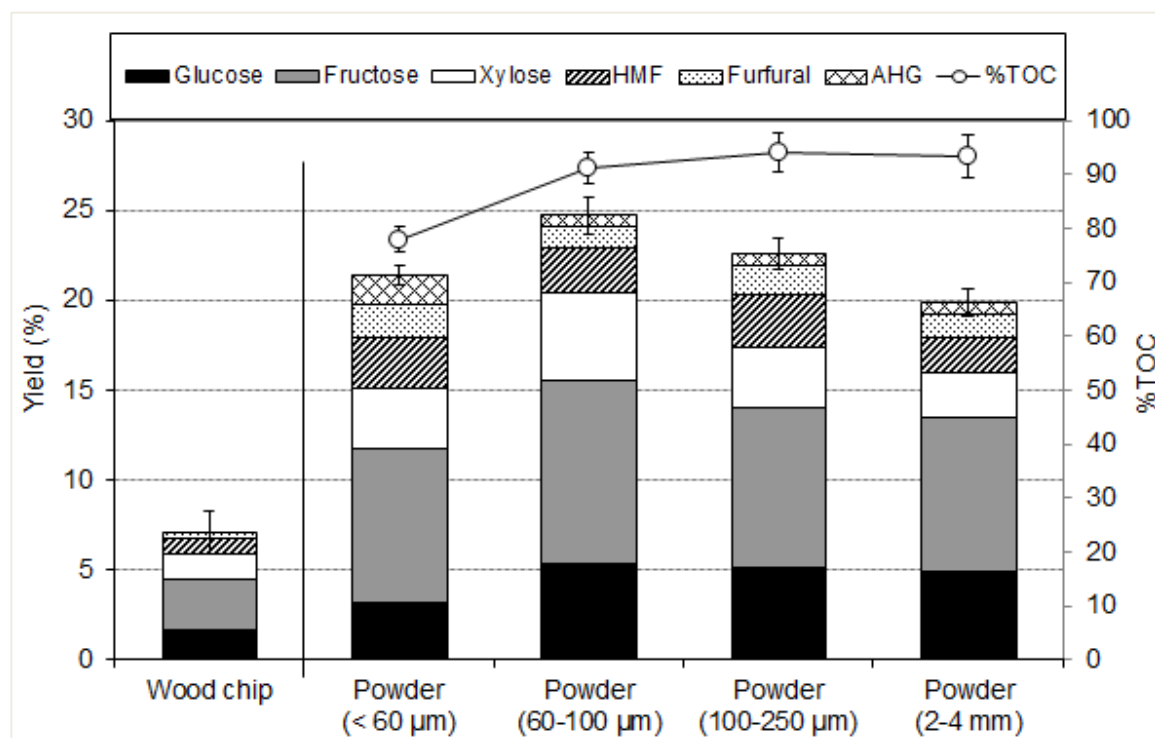


**Figure 5.5** Effect of eucalyptus particle size on the yield of liquid products and TOC value from the hydrolysis reaction.

In detail, eucalyptus samples were pretreated by either alkaline pretreatment or organosolv fractionation process prior to the hydrolysis. Based on our studies, the optimum condition for alkaline pretreatment is by mixing 5% w/v of NaOH solution with biomass at 10% solid content for 20 min at 90°C, while the condition for organosolv fractionation is using a ternary mixture of methyl isobutyl ketone (MIBK)/methanol/water in the presence with 0.008 M of H<sub>2</sub>SO<sub>4</sub> as an acid promoter at 180°C for 60 min. Then, the hydrolysis of the solid sample achieved from the pretreatments in the presence of H<sub>2</sub>SO<sub>4</sub>-Sucrose was performed at 200°C for 5 min. As shown in **Figure 5.6**, the hydrolysis of pretreated and fractionated eucalyptus exhibited significantly higher sugar yield and selectivity. More than 30% yield of total sugars can be achieved from the hydrolysis of eucalyptus in powder form, whereas 14% yield of total sugars were produced from the reaction with eucalyptus wood chips (compared to only 5.9% yield of total sugars achieved from the hydrolysis of non-pretreated eucalyptus wood chips). Therefore, this strongly indicates the importance of biomass pretreatment prior to the catalytic hydrolysis process.

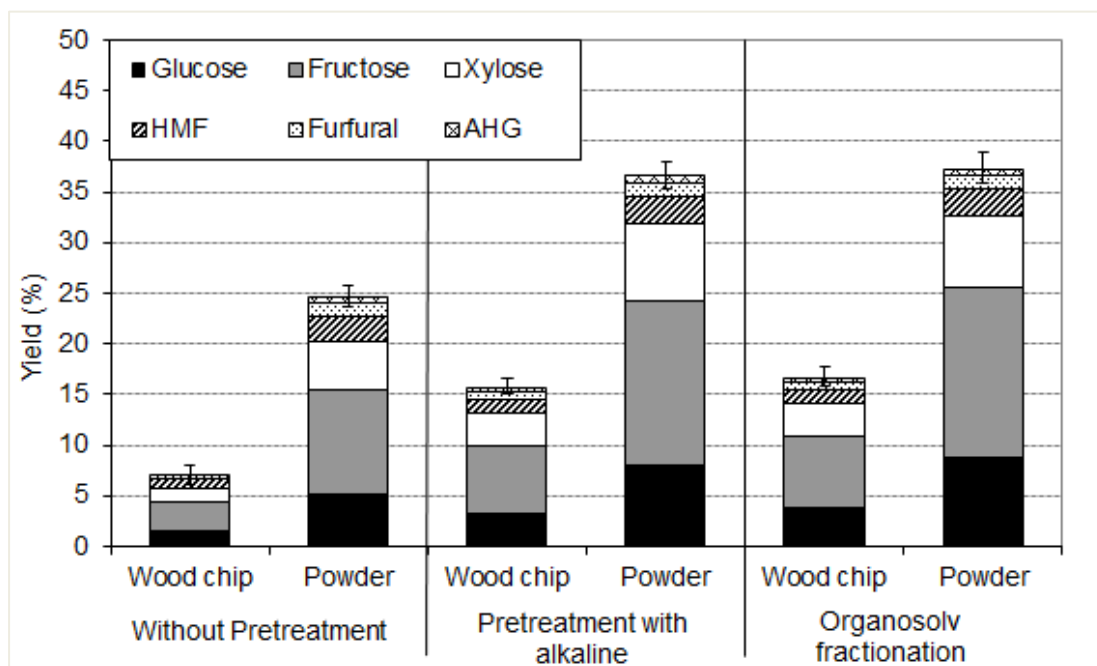


**Figure 5.6** Effect of eucalyptus pretreatment process (with alkaline) and fractionation on the yield of liquid products.

Next, the reusability of  $\text{H}_2\text{SO}_4$ -Sucrose on the sequential batch hydrolysis of pretreated eucalyptus in powder form was studied under the optimized reaction conditions. After separating the catalyst from the solution, the catalyst was washed and dried before re-testing the reaction under the same operating conditions. As shown in **Figure 5.7**, the result indicates high decrease in liquid product yield after the first recycle (with the deactivation percentage of 32.1%). Nevertheless, from the second to fifth catalyst recycling, the sugar yields from the reaction show only slight decrease (with the deactivation percentage of 8.8%). This catalyst deactivation suggested the partial leaching of acid sites from the surface of solid acid catalysts under the experimental condition. The results from  $\text{NH}_3$ -TPD techniques also confirm the leaching of acids since the total acid density decreased to  $12.2 \mu\text{mol}/\text{m}^2$  after fifth catalyst recycling. Therefore, to apply this  $\text{H}_2\text{SO}_4$ -Sucrose in the prolong hydrolysis application; the catalyst regeneration by re-sulfonation is required.

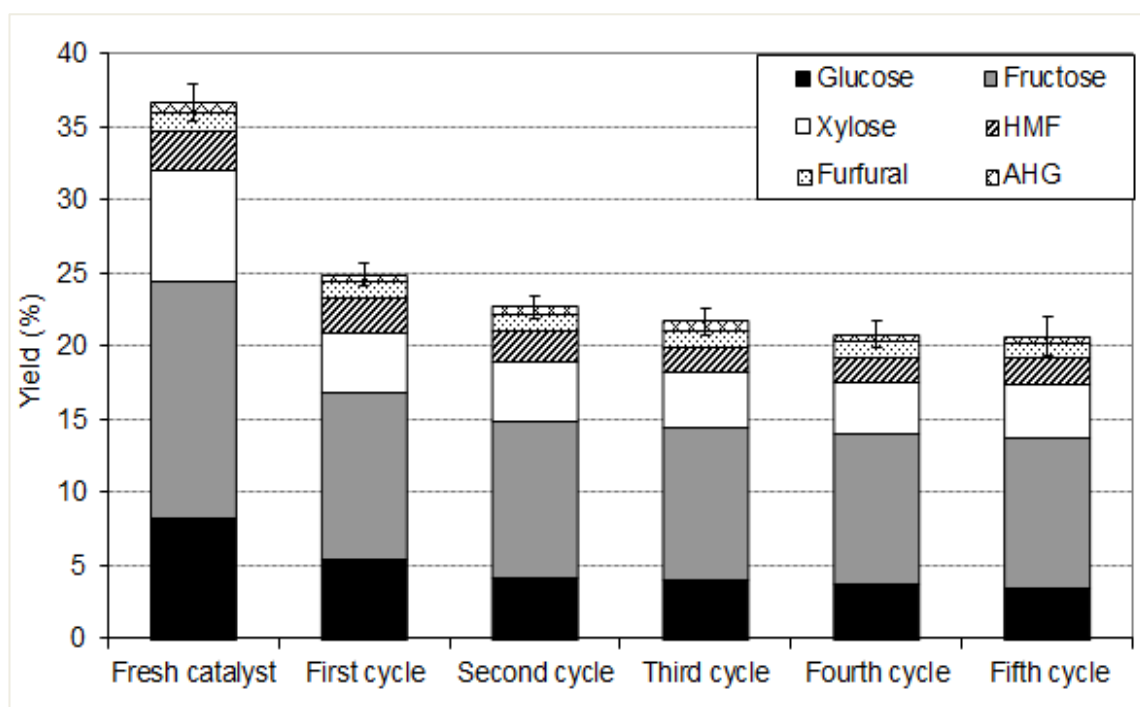


**Figure 5.7** Reusability testing of  $\text{H}_2\text{SO}_4$ -Sucrose toward the hydrolysis of pretreated eucalyptus in powder form at  $200^\circ\text{C}$ .

#### 5.2.4 Effect of acid catalysts on the hydrolysis of eucalyptus

As the next step, it aims to integrate the organosolv fractionation of eucalyptus with the hydrothermal hydrolysis. It was found from the results in Chapter 4 that  $\text{H}_3\text{PO}_4$ -activated carbon ( $\text{AC-H}_3\text{PO}_4$ ) is an alternative promoter for organosolv fractionation to replace  $\text{H}_2\text{SO}_4$ . In this section, further study was performed to determine the possibility of using  $\text{AC-H}_3\text{PO}_4$  as catalyst for the hydrothermal hydrolysis. The possible use of  $\text{AC-H}_3\text{PO}_4$  for hydrolysis reaction will lead the good potential of combining the organosolv fractionation with the hydrothermal hydrolysis without acid catalyst removal required.

The hydrolysis activities of acid catalysts (*i.e.*  $\text{AC-H}_3\text{PO}_4$ ,  $\text{AC-H}_2\text{SO}_4$ ,  $\text{AC-HCl}$ , and  $\text{AC-HNO}_3$ ) and carbon-based sulfonated catalysts (*i.e.*  $\text{Su-H}_2\text{SO}_4$  and  $\text{Gu-H}_2\text{SO}_4$ ) were compared as shown in **Figures 5.8**. It was found that the hydrolysis reactivity of carbon-based solid acid catalysts prepared from activated carbon and sugars are in the same range, from which  $\text{H}_3\text{PO}_4$ -activated carbon shows the highest activity and  $\text{H}_2\text{SO}_4$ -sucrose is the second best. These results are in good agreement with the acid site density of these

catalysts as presented in **Tables 4.2** and **5.1**; therefore, it can be concluded that the acid site density is one of the important key parameters indicating the hydrolysis performance.

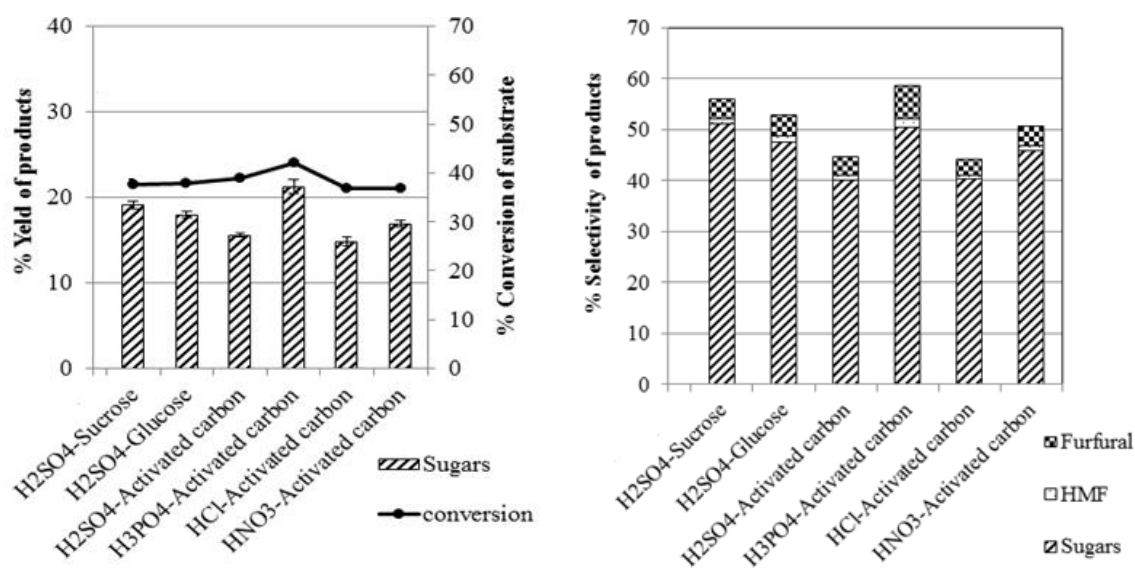


**Figure 5.8** Effect of catalyst activity on the sugar yield and selectivity.

### 5.2.5 Sequential fractionation/hydrolysis with and without acid catalysts

Since AC-H<sub>3</sub>PO<sub>4</sub> can be efficiently applied as a hydrolysis catalyst, the sequential fractionation/hydrolysis was further carried out under various operating conditions. All experiments were operated using solid residue from organosolv fractionation (with the weight of 0.55 g consisted of 41.23% cellulose, 4.61% hemicellulose, and 14.31% of lignin). The hydrolysis of the fractionated eucalyptus was performed under several conditions (*i.e.* reaction temperature, and reaction time) in the presence of AC-H<sub>3</sub>PO<sub>4</sub>. Firstly, the testing was performed over three groups of samples including (i) hydrolysis of raw eucalyptus with and without the uses of H<sub>2</sub>SO<sub>4</sub> and AC-H<sub>3</sub>PO<sub>4</sub> as hydrolysis catalyst, (ii) integrative fractionation/hydrolysis using H<sub>2</sub>SO<sub>4</sub> and AC-H<sub>3</sub>PO<sub>4</sub> as acid promoter and hydrolysis catalyst; and (iii) integrative fractionation/hydrolysis using H<sub>2</sub>SO<sub>4</sub> and AC-H<sub>3</sub>PO<sub>4</sub> as either acid promoter or hydrolysis catalyst, as shown in **Figure 5.9**.

It was observed that the first group of the sample had achieved the mixture of glucose and xylose in the liquid product, from which higher xylose yields than glucose yields were observed. For the second group of sample, the integration of fractionation and hydrolysis of eucalyptus in the presences of H<sub>2</sub>SO<sub>4</sub> and AC-H<sub>3</sub>PO<sub>4</sub> promoted the higher sugar yield with higher glucose proportion in the product. By integrating the fractionation

with hydrolysis, high proportion of xylose yield can be achieved from the fractionation step (as called first stage). Then, from the hydrolysis process (as called second stage), the glucose yield of 10% (35% of substrate) and xylose yield of 3.88% (19% of substrate) can be achieved. In the third group, it can be seen that the integration of fractionation (with  $H_2SO_4$  or  $AC-H_3PO_4$ ) and hydrolysis reaction (without catalyst) achieved lower sugar yields in second stage than did the second group (with  $H_2SO_4$  or  $AC-H_3PO_4$ ). Therefore, it is clear that  $AC-H_3PO_4$  can be efficiently used for both fractionation and hydrolysis without the removal required. Furthermore, this integrative operation also highlights the great benefit in terms of higher sugar yield achievement and the capability to separate glucose and xylose in the final product. Further studies to optimize the hydrolysis activity of  $AC-H_3PO_4$  *i.e.*, by varying reaction temperature, time, pressure, raw material to acid catalyst ratio were carried out as presented in the next section.

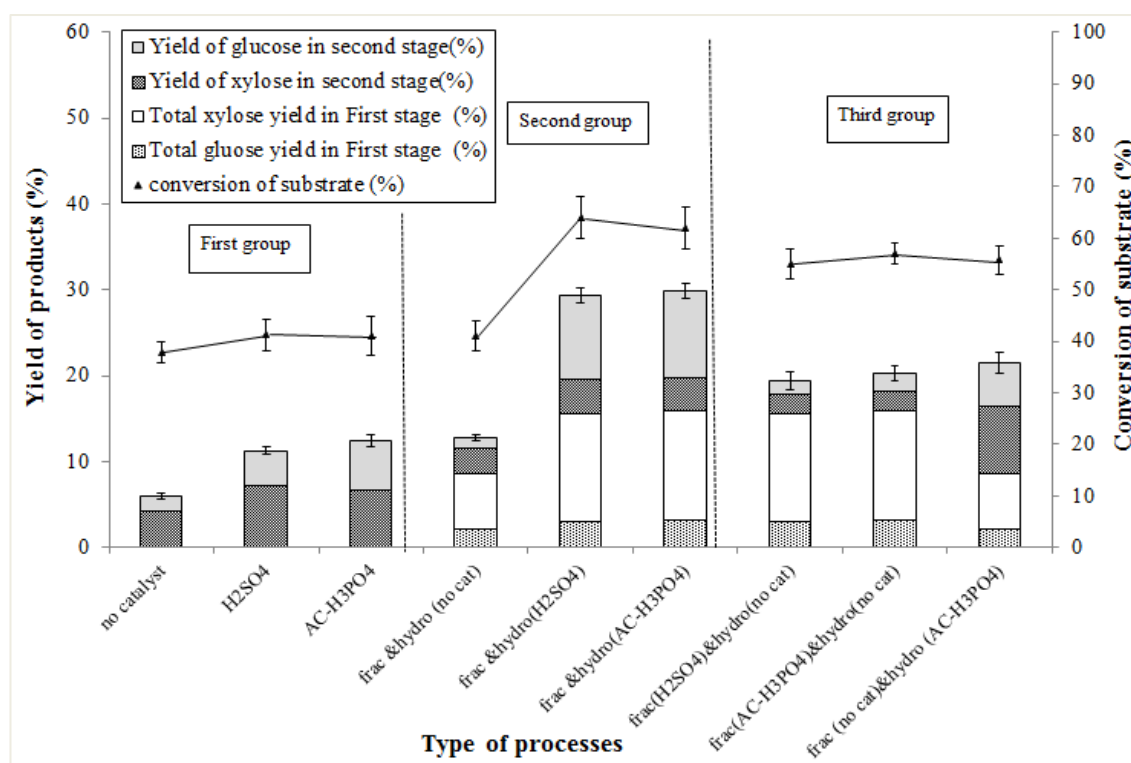


**Figure 5.9** Comparison of the hydrolysis reaction (with and without fractionation) under various conditions on the product yield and eucalyptus conversion.

### 5.2.6 Effect of hydrolysis conditions on the performance/activity of $AC-H_3PO_4$

First, the effect of hydrolysis temperature on the product yield and the conversion of eucalyptus were examined over fractionated eucalyptus in the presence of 0.05 g

AC-H<sub>3</sub>PO<sub>4</sub>, with 6 mL of DI water, initial pressure of 20 bars and reaction time of 5 min. The effect of reaction temperature on the yields of liquid product and eucalyptus conversion are shown in **Figure 5.10**, while **Figure 5.11** presents the product selectivity of the reaction. It can be seen that the temperature shows significant effect on the feedstock conversion and yield of liquid products. In detail, in the presence of AC-H<sub>3</sub>PO<sub>4</sub>, the conversion increased steadily with increasing the reaction temperature, whereas the yield and the selectivity of sugar also increased with increasing the reaction temperature from 100°C to 220°C; nevertheless, at the temperature above 220°C, the yield and the selectivity of sugar oppositely decreased. In addition, the formations of furfural and HMF were detected at the temperature above 220°C and they increased with increasing the reaction temperature from 200°C to 250°C.

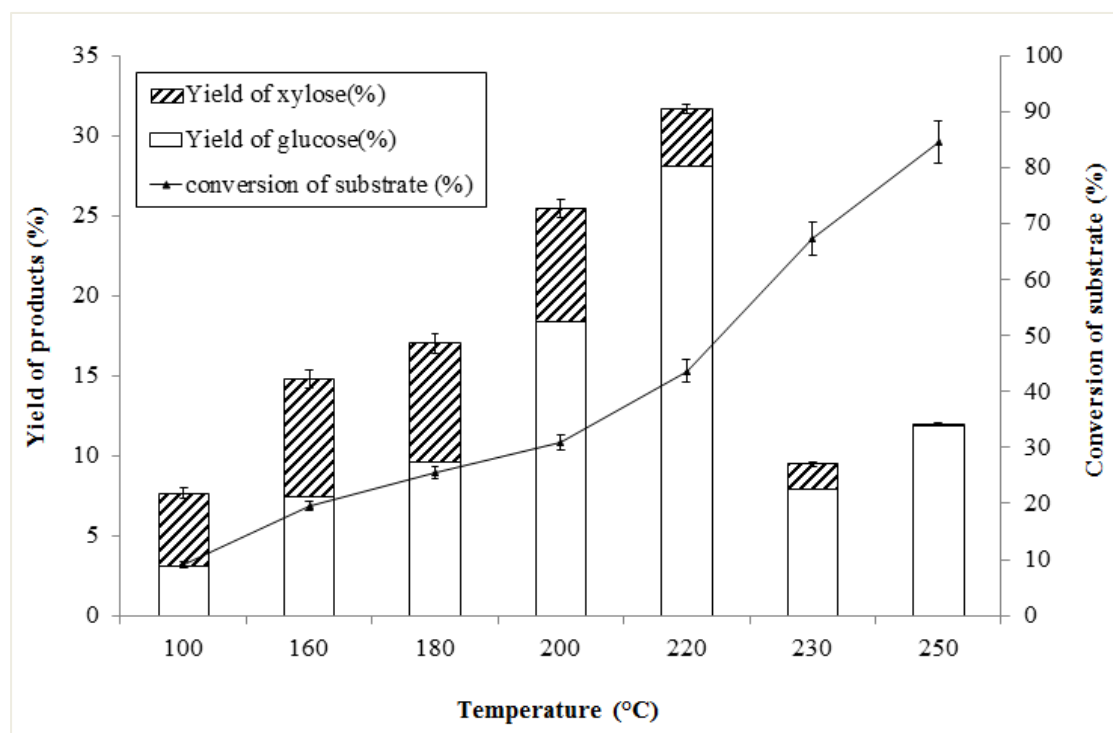


**Figure 5.10** Effect of temperature on the product yield and fractionated eucalyptus conversion via hydrolysis reaction.

It can be seen that at the temperature between 100-220°C, the rate of hydrolysis reaction is faster than dehydration reaction; therefore, high yield of sugar with less formation of HMF and furfural can be concluded. These results are good agreement with the report from (Tamthiengtrong N., 2011). In contrast, above 220°C, monosaccharides can

decompose into HMF and furfural via the dehydration reaction leading to the decreasing of sugar production at high temperature. Hence, based on this result, the reaction temperature of 220°C is the suitable temperature for the hydrolysis of eucalyptus wood chips. It is noted that the product and conversion profiles from the reaction without catalyst are in the same trend as those from the reaction in the presence of AC-H<sub>2</sub>SO<sub>4</sub>; nevertheless, noticeable lower sugar yields with higher furfural and HMF formations at high temperatures were observed that it are good agreement with (Tamthiengtrong N., 2011). This therefore highlights the benefit of heterogeneous acid catalyst on the hydrolysis of eucalyptus wood chips.

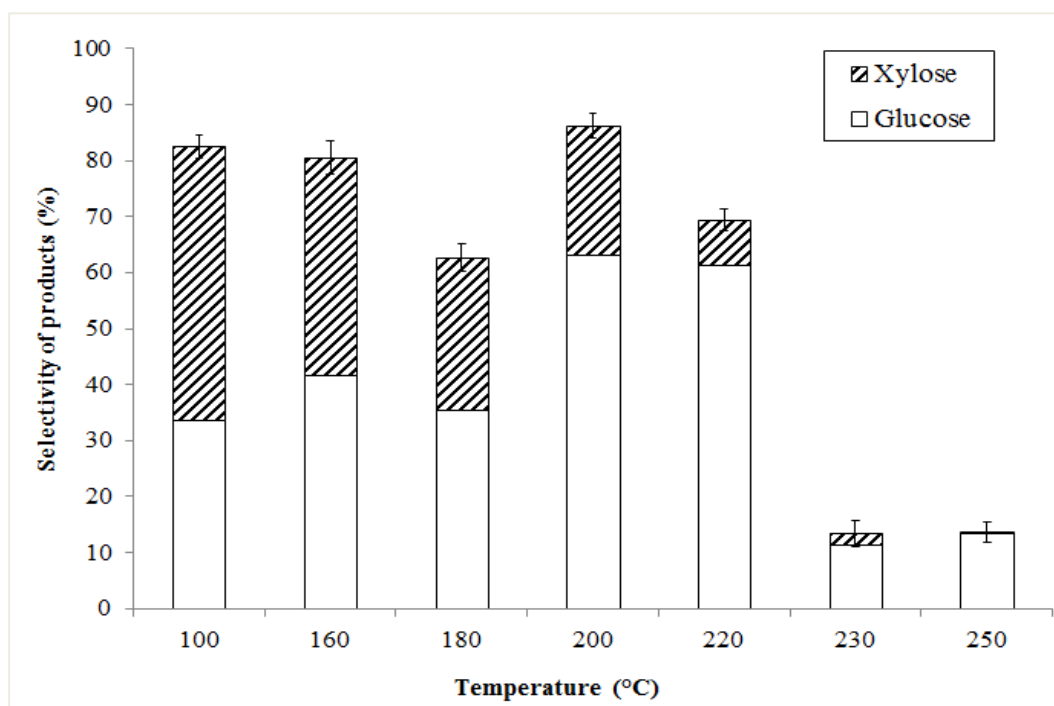


**Figure 5.11** Effect of temperature on the product selectivity of the hydrolysis of fractionated eucalyptus.

The effect of the reaction time was studied by varying the holding time from 5 min to 40 min, while other operating conditions were kept constant. As shown in **Figures 5.12** and **5.13**, it can be revealed that the yield of sugars increase steadily with increasing reaction time until after 5 min, the yield began to decrease at longer reaction times. In addition, the formation of furans (both HMF and furfural) increased with increasing the reaction time, which is due to the occurring of dehydration reaction at longer reaction time.

Therefore, the optimized condition for the hydrolysis of eucalyptus wood chips in the presence of AC-H<sub>3</sub>PO<sub>4</sub> is at 220°C for 5 min, from which the highest sugar yields of 31.68% can be achieved (glucose yield of 28.1%, and xylose yield of 3.58%). It is noted that the effect of hydrolysis pressure on the yield of liquid product and fractionated eucalyptus conversion, and product selectivity were also carried out as shown in **Figures 5.14** and **5.15**. It can be seen that the pressure shows slight positive impact on the hydrolysis reaction. In the present work, the hydrolysis pressure of 20 bars was therefore chosen for all studies. Lastly, the effect of increasing acid catalyst amount was examined. As shown in **Figures 5.16** and **5.17**, it was found that the addition of higher acid catalyst content (from 0.05 to 0.3 g) oppositely inhibits the yield of sugar production. This could be due to the use of too strong acid condition, which results in the further conversion of sugar to other unwanted by-products *i.e.* organic acids and aldehydes (Ando et al., 2004; Yu et al., 2008).

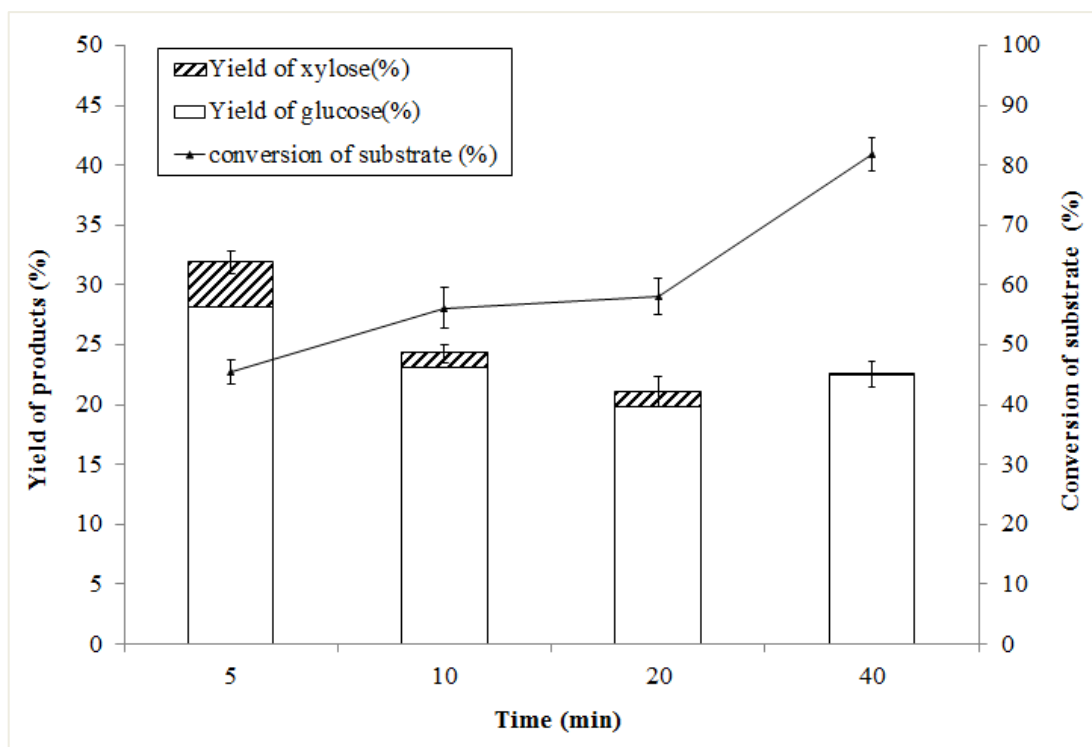


**Figure 5.12** Effect of retention time on the product yield and eucalyptus conversion via hydrolysis of fractionated eucalyptus.

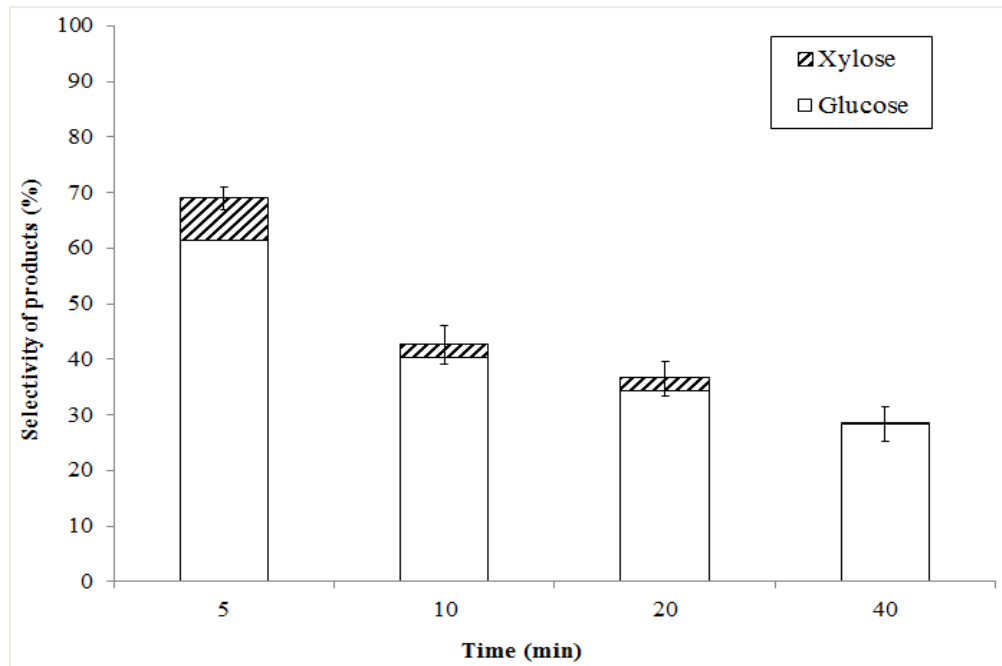


**Figure 5.13** Effect of retention time on the product selectivity of the hydrolysis of fractionated eucalyptus.

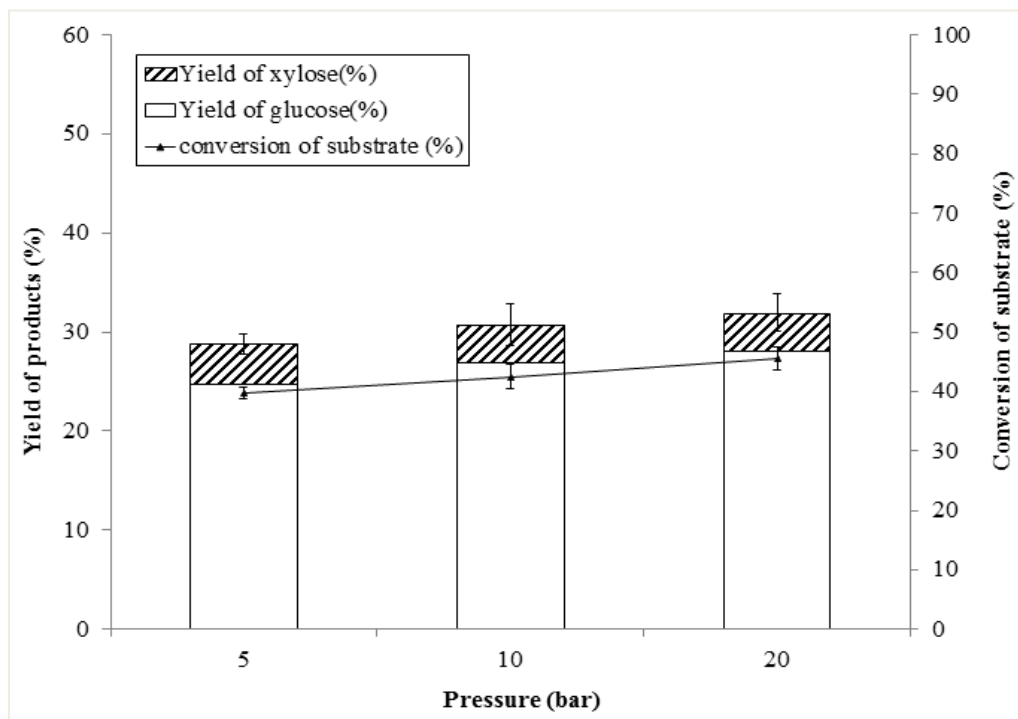


**Figure 5.14** Effect of pressure on the product yield and fractionated eucalyptus conversion via hydrolysis reaction.

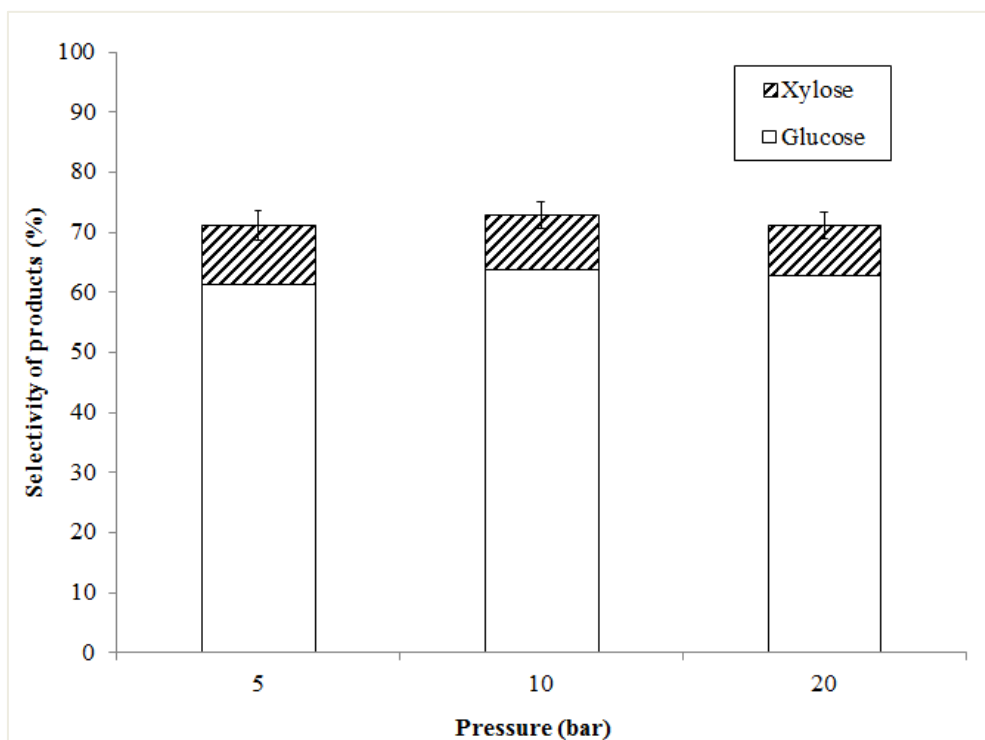


**Figure 5.15** Effect of pressure on the product selectivity of the hydrolysis of fractionated eucalyptus.

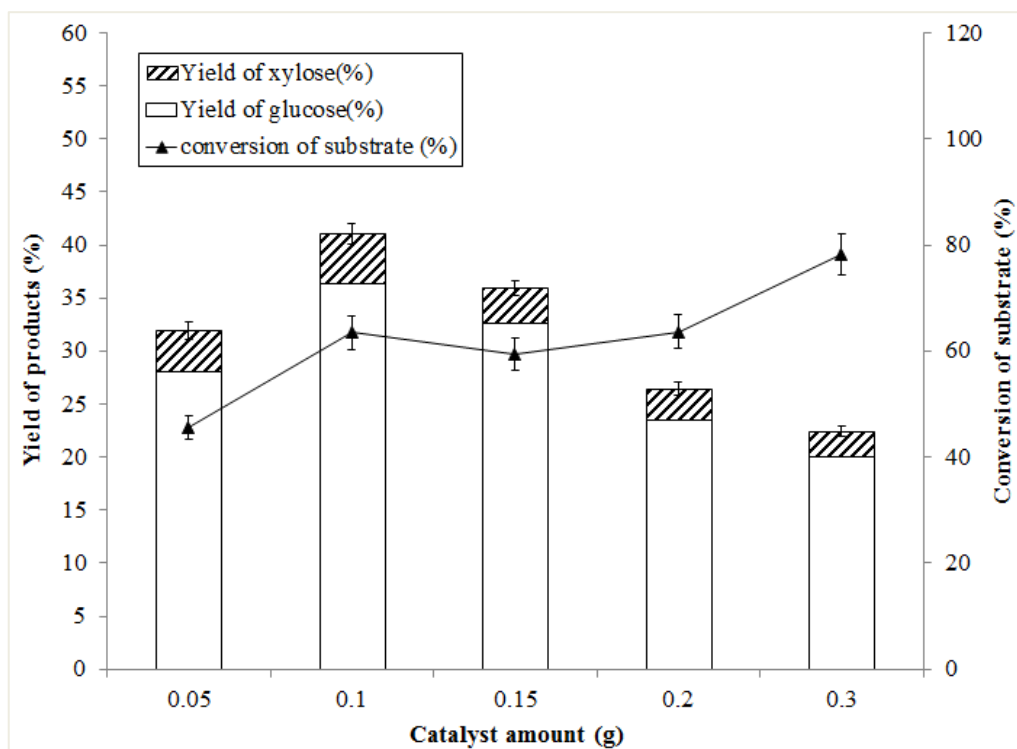


**Figure 5.16** Effect of catalyst loading (g) on the product yield and fractionated eucalyptus conversion via hydrolysis reaction.

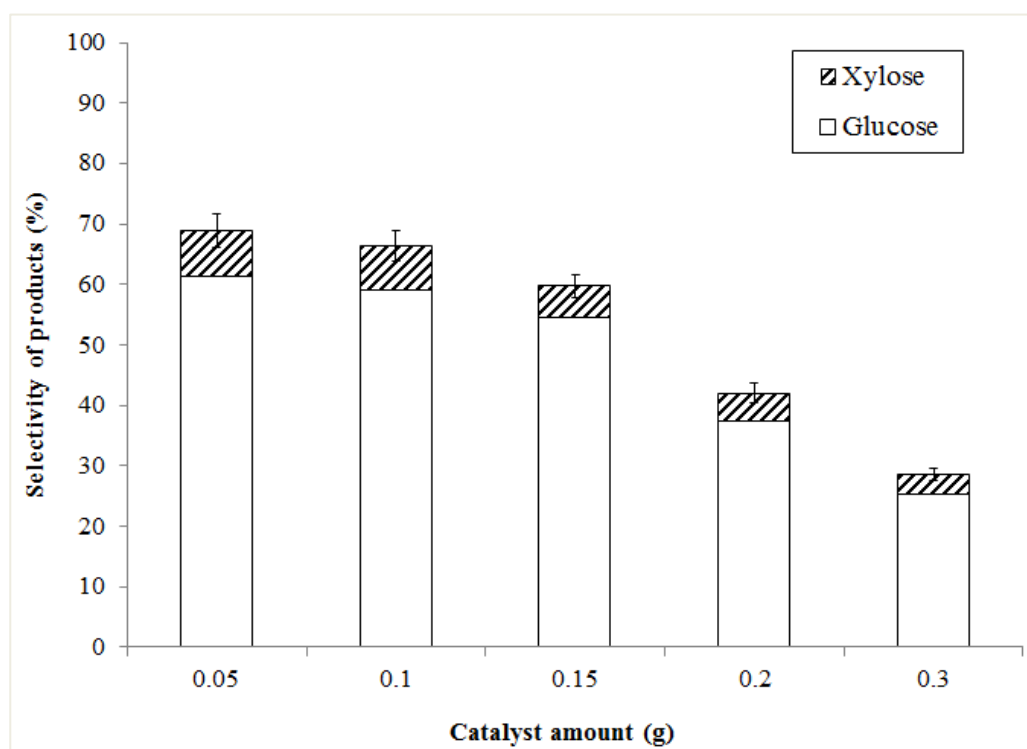


**Figure 5.17** Effect of catalyst loading (g) on the product selectivity of the hydrolysis of fractionated eucalyptus.

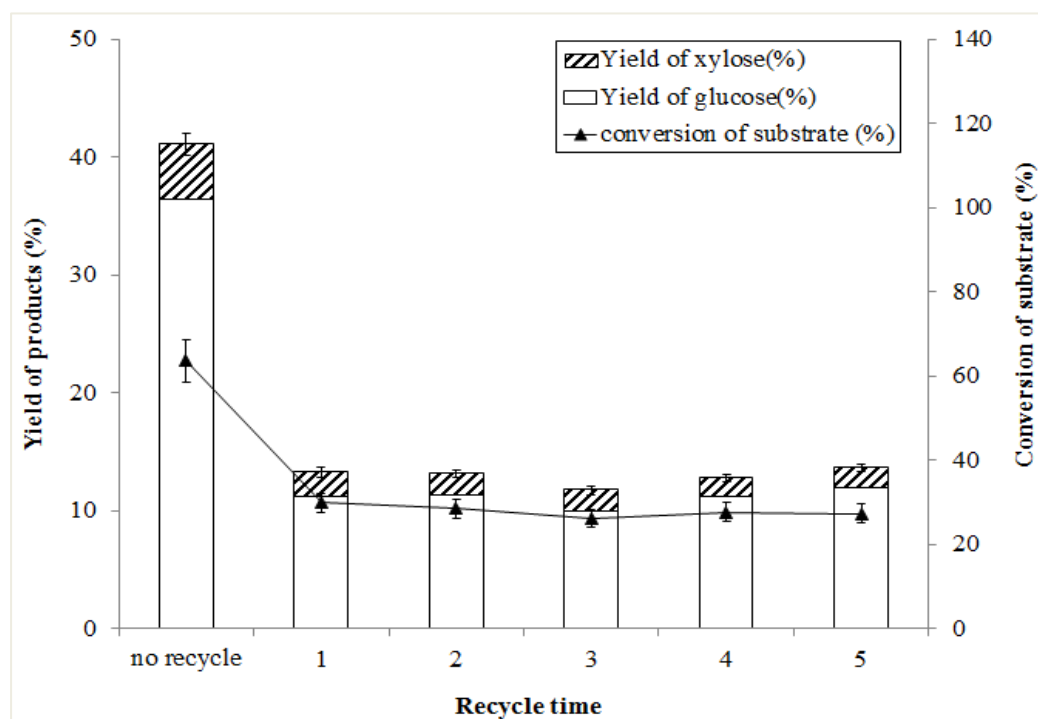


**Figure 5.18** Reusability of solid acid catalyst in consecutive batches processes on the product yield and fractionated eucalyptus conversion via hydrolysis reaction.

It is noted that the reusability of AC-H<sub>3</sub>PO<sub>4</sub> was also studied by filtering it out from the remaining solid residue after hydrolysis and reused again for fractionation/hydrolysis. As shown in **Figure 5.18**, substantial decrease in hydrolysis efficiency was observed after the first batch. Nevertheless, after second reused, the amount of glucose remained constant (25.8-30.5 wt.% decreasing of substrate conversion and 10.2-11.6 wt.% decreasing of glucose yield). The reducing of efficiency suggested leaching of the solid acid catalysts under the experimental condition.

Hydrolysis is a conventional method for converting cellulose into sugar in a biorefinery process, because sugar can be used as a substrate for producing industrial chemicals, ethanol, hydrocarbons and monomers. Up to now, the hydrolysis process has many techniques such as acid, alkaline, enzymatic and hot-compressed water (HCW). Each technique can generate various ranges of glucose yield as well as having its own advantages and disadvantages. This work focused on the use of HCW technology, from which the hydrolysis occurs efficiently under high temperature and pressure conditions in the presence of solid acid catalyst. It is noted that the use of solid acid catalysts has distinct advantages such as recycling, separation, and environmental friendliness. Here, synthesized carbon-based sulfonated catalysts (*i.e.* H<sub>2</sub>SO<sub>4</sub>-Sucrose, H<sub>2</sub>SO<sub>4</sub>-Glucose and H<sub>2</sub>SO<sub>4</sub>-Xylose) were synthesized and tested toward the hydrolysis reaction.

Typically, carbon-based sulfonated catalysts are prepared by a two-step process (Hara, 2010; Sukanuma et al., 2010; Yamaguchi & Hara, 2010). Firstly, the incomplete carbonized material (*i.e.* D-glucose, sucrose, cellulose) was heated for 1-5 h at 350-400 °C under N<sub>2</sub> flow to obtain amorphous carbon, which is ground into a powder, and boiled in 150 mL of concentrated H<sub>2</sub>SO<sub>4</sub> (>96%) or 150 mL of fuming sulfuric acid (15 wt.% SO<sub>3</sub>) at 150 °C under N<sub>2</sub> flow for 10-15 h, in a process called sulfonation (addition of -SO<sub>3</sub>H group on the surface area of amorphous carbon).

In this work, a one-step process was applied instead, from which the direct sulfonation of sugars (xylose, glucose, and sucrose) under N<sub>2</sub> flow at 230-250 °C was used. The benefit of a one-step preparation process is the simple and lower energy requirement. From the experiments, it was found that the best type of catalyst for hydrolysis is H<sub>2</sub>SO<sub>4</sub>-Sucrose. It has been known that the specific surface area, pore size and pore volume, the active site concentration and acidic type are typically important factors for solid acid performance. Solid acid catalysts being considered for cellulose hydrolysis should have a

large number of Brønsted acid sites, good affinity for the reactant substrates and good thermal stability.

In the present work, solid acid catalysts were characterized to determine their surface area and acid properties (*i.e.* amount of acid site ( $\mu\text{mol/g}$ ), and density of acid site ( $\mu\text{mol/m}^2$ )) to correlate their physical and chemical properties with their hydrolysis performance. It was found that the catalytic activity trend was in good agreement with the acid density of these catalysts, from which the catalyst with high acid site density like S-Su can enhance the great reactivity toward the hydrolysis reaction.

Since lignocellulosic biomass is a complex structure consisting of cellulose, hemicellulose, and lignin. Alkaline pretreatment and/or organosolv fractionation was found to improve the hydrolysis performance. More than 30% yield of total sugars can be achieved from the hydrolysis of eucalyptus in powder form, whereas 14% yield of total sugars were produced from the reaction with eucalyptus wood chip (compared to only 5.9% yield of total sugars achieved from the hydrolysis of non-pretreated eucalyptus wood chip). The aim of pretreatment and fractionation is to breakdown the lignin that binds the cellulose and to destroy the crystalline structure of cellulose and increase its surface area so that fragments become easy hydrolysis to sugar.

Regarding the use of AC- $\text{H}_3\text{PO}_4$  (acid promoter for organosolv fractionation) as hydrolysis catalyst, previously (Tamthiengtrong N., 2011) have reported that the suitable hydrolysis activities of sulphonated activated carbon (AC- $\text{H}_2\text{SO}_4$ )/ phosphonated activated carbon (AC- $\text{H}_3\text{PO}_4$ )/ nitrated activated carbon (AC- $\text{HNO}_3$ )/ and hydrochlorated activated carbon (AC-HCl), from which the highest sugars yield can be enhanced by applying  $\text{H}_3\text{PO}_4$ -activated carbon as a catalyst. These results are in good agreement with this study. It has been indicated that solid acid catalysts have several favorable characteristics to replace homogeneous acid catalysts (*i.e.*  $\text{H}_2\text{SO}_4$ , HCl,  $\text{H}_3\text{PO}_4$ ) for hydrolysis reaction such as high activity, high selectivity, long catalyst life and ease in recovery and reuse.

Recently, (Van de Vyver et al., 2011) studied the solid acid catalytic conversion of cellulose and summarized the performance of several solid chemocatalysts for the cellulose into glucose reaction, as shown in **Table 5.2**, which is compared to solid acid catalysts in this work. It can be revealed that the carbonaceous solid acid (CSA) catalysts are considered as the most promising catalyst for cellulose hydrolysis, since they provide good access of reactants to the acidic sites of  $\text{SO}_3\text{H}$  and  $\text{PO}_3\text{H}_2$  groups. The mechanism of lignocellulosic biomass hydrolysis with CSA catalysts is similar to that of homogeneous

acids, from which protons in  $\text{SO}_3\text{H}$  and  $\text{PO}_3\text{H}_2$  attack the  $\beta$ -1,4 glycosidic bonds in the solid crystalline cellulose. This is attributed to an increase in the acidity of  $\text{SO}_3\text{H}$  and  $\text{PO}_3\text{H}_2$  groups on the carbon material with a decrease in the amount of water.

**Table 5.2** Hydrolysis degradation of substrate (biomass and cellulose) to glucose with solid acid catalysts (Van de Vyver et al., 2011)

Catalyst	Type of substrates	Substrate conc. [wt.%] <sup>[a]</sup>	Time [h]	Temp. [K]	Conversion [%]	Yield of glucose [%]
This work (Phosphonated activated carbon)	Fractionated Eucalyptus wood chips	0.18	0.083	493	64	35.9 <sup>[b]</sup>
This work Amorphous carbon bearing from sucrose	Pretreated eucalyptus in powder form	0.05	0.083	473	65	8.3 <sup>[c]</sup>
Sulfonated activated carbon	Cellulose (Ball-milled)	0.9 (1.1)	24	423	43	41
Amorphous carbon bearing from cellulose $\text{SO}_3\text{H}$ , $\text{COOH}$ and $\text{OH}$ ( $\text{CH}_{0.62}\text{O}_{0.54}\text{S}_{0.05}$ )	Cellulose (Microcrystalline)	3.6 (12)	3	373	Up to 100	4 <sup>[d]</sup>
Silica/carbon nanocomposites	Cellulose (Ball-milled)	1 (1)	24	423	61	50
Layered $\text{HNbMoO}_6$	Cellulose (Microcrystalline)	2 (2)	12	403	n.r. <sup>[e]</sup>	1
10 wt.% Ru/CMK-3	Cellulose (Ball-milled)	0.8 (0.2)	0.25	503	68	34
Sulfonated CMK-3	Cellulose (Ball-milled)	1 (1.1)	24	423	94	75

[a] Catalyst/substrate ratios shown in parentheses; [b] the total sugar yields of 42 % (glucose yield of 35.9%, and xylose yield of 6.1 %) can be achieved; [c] the total sugar yields of 32.1% (glucose yield of 8.3%, xylose yield of 7.6%, and fructose yield of 16.2 %) can be achieved; [d] the main product in this reaction was water-soluble  $\beta$ -1,4-glucan (64% yield); [e] n.r.= not reported.

### 5.3 Conclusion

Sulfonated solid carbonaceous acid catalysts showed great hydrolysis performance as reflected by their high catalytic efficiency and selectivity under HCW conditions. Compared to the conventional homogenous acid catalysts, the developed Sucrose-SO<sub>3</sub>H can be recycled in consecutive batch process with lower loss of sugars via dehydration reaction and would be less corrosive to the system, resulting in improved overall economic feasibility of the process. This study also revealed the necessity for biomass pretreatment and/or fractionation prior to the hydrothermal hydrolysis, from which significantly higher yields of sugar can be achieved. AC-H<sub>3</sub>PO<sub>4</sub> also showed great hydrolysis performance under HCW, from which high sugar yields with low unwanted by-product formations can be achieved at 220°C with 5 min reaction time. Importantly, the great benefit of AC-H<sub>3</sub>PO<sub>4</sub> is its possible use for both organosolv fractionation (as acid promoter) and hydrothermal hydrolysis (as acid catalyst), which provides high potential for combining the fractionation and hydrolysis processes without intermediate material treatment required.

**CHAPTER 6**  
**EXAMINE THE POOR SOLUBILITY OF LIGNIN PRODUCED BY**  
**A SINGLE-STEP AQUEOUS-ORGANOSOLV FRACTIONATION OF**  
**EUCALYPTUS WOOD CHIPS**

---

**Chapter highlights**

Organosolv fractionation is known to be one of the promising techniques for isolating high purity lignin from lignocellulosic biomass. In the present study, organosolv lignin (OL) was obtained from the fractionation of eucalyptus wood chips using a ternary mixture of methyl isobutyl ketone (MIBK)/methanol/water in the presence of 0.008 M H<sub>2</sub>SO<sub>4</sub> as an acid promoter at 180°C for 60 min. It was further purified using the alkaline precipitation process (*i.e.* treated organosolv lignin, TOL). From the study, TOL was found to enhance higher solubility in organic solvents (*i.e.* tetrahydrofuran, dimethyl sulfoxide, and methanol) than OL. Both OL and TOL were then characterized by several techniques to understand their physico-chemical properties and structural features. It is noted that bagasse soda lignin (SL) was also prepared and examined for comparison.

The results of the compositional analysis revealed that OL contained small amounts of contaminations (*e.g.* sugars, ash and sulfur) that had come from the degradation of eucalyptus wood chips and H<sub>2</sub>SO<sub>4</sub> during the fractionation. After alkaline precipitation treatment, most of these contaminations were removed without causing any significant structural change, as confirmed by XPS, FTIR and solid-state NMR analyses. Moreover, FTIR spectra also proved the presence of base insoluble lignin (BIL) contaminants in OL. Elemental analysis indicated highest purity and highest molecular weight for TOL. Results from Mannich reactivity tests revealed that OL contains more active sites than TOL or SL. This may simply be because of the contaminants in OL reacting in the Mannich Process, and not with the free C-3 and C-5 lignin sites. Note however that SL is slightly more reactive than TOL, and therefore would be more useful in functionization reactions.

---

## 6.1 Background

Lignin is an aromatic polymer generally found in lignocellulosic biomass. This compound is typically deposited in nearly all vascular plants, and provides rigidity and strength to their cell walls. Lignin is traditionally considered as dehydrogenative polymers from three monolignols: p-coumaryl alcohol (H), coniferyl alcohol (G), and sinapyl alcohol (S). The major inter unit linkage within the lignin macromolecule is the ether linkage  $\beta$ -O-4, consisting of more than half of the linkage structures of lignin. It is different ratios, linked together by various types of ether, aryl and carbon-carbon bonds such as 4-O-5,  $\beta$ - $\beta$ ,  $\beta$ -1,  $\beta$ -5, dibenzodioxocin and 5-5 (Boerjan et al., 2003; Corma et al., 2007; Sarkanen et al., 1982; Zakzeski et al., 2010).

Recently, there have been several attempts to isolate lignin from lignocellulosic biomass for utilization as feedstock for value-added chemicals and fuels via depolymerization processes. The process employed in isolating lignin from its native lignocellulosic biomasses has significant influence on the structure, purity, and physicochemical properties of the obtained material (Zakzeski et al., 2010). Typically, lignin isolation methods belong to one of two main categories depending on the presence or absence of sulfur (*i.e.* sulfur and sulfur-free lignins). Sulfur lignins (or can be called Kraft and lignosulfonate lignins) are primarily produced by pulp and paper industries, from which sodium sulfide ( $\text{Na}_2\text{S}$ ) and aqueous sulfur dioxide ( $\text{SO}_2$ ) are applied to isolate lignin. Sulfur-free lignins can be classified into one of two main categories, lignins prepared via solvent pulping (*e.g.*, organosolv lignin), and those from alkaline pulping (*e.g.*, soda lignin). Among these isolated lignins, organosolv lignin (OL) is generally considered to be the highest quality lignin (El Hage et al., 2009; El Hage et al., 2010). They show high solubility in organic solvents and are practically insoluble in water, due to their highly hydrophobic nature. The solvents most commonly used in organosolv pretreatment are alcohols *i.e.* ethanol and methanol. Alternatively, other types of solvent can also be employed including organic acids (*i.e.* acetic acid, formic acid), organic bases, ketones, and esters. In addition, mixed-solvent systems have also been widely developed for example; ethanol and water, ethylene glycol and water, and acetosolv (González et al., 2008; Vila et al., 2002). Recently, a new organosolv technology has been applied for the selective dissolution of lignin and hemicellulose from lignocellulosic material, using a ternary mixture of ketone, methanol, and water in the presence of an acid promoter (*i.e.*

H<sub>2</sub>SO<sub>4</sub>) (Bozell et al., 2011a; Klamrassamee et al., 2013). This procedure is of particular interest because the resulting single phase solvent can be readily separated into two liquor fractions via the addition of water which produces an upper organic phase containing lignin, and an aqueous phase containing hemicellulose and its degradation products (Bozell et al., 2011a; Klamrassamee et al., 2013).

Referring to Chapter 4 and the organosolv process, the lignin obtained from that study was evaluated. Its solubility in organic solvents *i.e.* tetrahydrofuran (THF), dimethyl sulfoxide (DMSO), and methanol was also tested since it is one of the key important factors to enhance good lignin utilization. From the literature, poor solubility of lignin in organic solvent can lead to diffusion limitation problems in several reactions *i.e.* depolymerization and dehydrodeoxygenation (Deepa & Dhepe, 2014). On the other hand, lignin with good solubility in organic solvents can efficiently produce high quality of phenols and other value-added chemicals (Deepa & Dhepe, 2014).

In this study, OL was purified to improve its solubility in organic solvents by the alkaline precipitation process (treated organosolv lignin; TOL). The two lignins were characterized using elemental analysis, Klason lignin, Mannich reaction, molecular weight, X-ray photoelectron spectroscopy (XPS) analysis, Fourier transform-infrared spectroscopy (FT-IR), solid-state nuclear magnetic resonance (NMR), and thermal gravimetric analysis (TGA). Bagasse soda lignin (SL) obtained from conventional alkaline precipitation process was also examined for comparison.

## 6.2 Results and discussion

### 6.2.1 Solubility of isolated lignin

From the fractionation as described in Chapter 4, a lignin yield of 13.7% from feedstock (or 45.6% of original lignin substrate) was obtained. From the solubility test, this sample showed poor solubility in all organic solvents (**Table 6.1**). Typically, THF and DMSO are potent solvents to dissolve conventional lignins since they are polar aprotic solvents (Gosselink et al., 2004). The poor solubility of OL could be related to the use of MIBK during fractionation, which affects isolated lignin structure. Then, the OL sample was treated via an alkaline re-precipitation process. After re-precipitation, two fractions were obtained including the base soluble lignin (TOL), which accounted for approximately 85% of the OL sample, and base insoluble lignin (BIL), the remaining 15%. The solubility

of TOL sample was tested and it was revealed that the solubility in all organic solvents increased. This clearly highlights the improvement of lignin solubility by the alkaline re-precipitation process.

**Table 6.1** Solubility of OL and TOL in organic solvents

Type of solvents	Solubility (%)	
	OL sample	TOL sample
Acetone	10.1	30.9
Methanol	8.7	27.2
Ethanol	9.1	28.1
THF	15.0	40.0
DMSO	50.0	100.0

### 6.2.2 Elemental analysis

The results of the elemental compositions of OL, TOL and SL are shown in **Table 6.2**, and are used to calculate atomic ratios of the relevant atomic species. In lignin chemistry, the empirical formula of the macromolecule is commonly given as a hypothetical hydroxyphenyl structural unit. This is known as the C<sub>9</sub>-formula with six carbon atoms in the benzene ring and an additional three carbon atoms making up the propyl side-chain (Mousavioun et al., 2010). The results consisted of molecular weight of C<sub>9</sub> formulae, as well as the protein content of the various lignin samples from different extraction techniques, as presented in **Table 6.3**. The amount of carbon, oxygen, hydrogen and molecular weight of C<sub>9</sub> formulae for the three lignin samples were similar. The lignin with the highest nitrogen content is the SL, whereas the TOL sample had only trace amounts of nitrogen. This is due to the fact that the protein content of the OL sample was readily removed during the alkaline re-precipitation process (Mousavioun et al., 2010), as shown in **Tables 6.2** and **6.3**.

**Table 6.2** Elemental analysis of lignins (wt.%)

Lignin sample	C	O	H	N	S
OL	60.42	31.11	5.66	0.08	0.53
TOL	59.33	32.29	5.48	0.00	0.00
SL	59.72	29.22	6.14	0.61	0.00

The absence of sulfur in lignin is desirable, as it makes the material more amenable to chemical modification (Laurichesse & Avérous, 2014). It was also found that the OL sample contained a small amount of sulfur. It was expected that this contaminant would be presented as a result of the use of H<sub>2</sub>SO<sub>4</sub> as a catalyst in the extraction process. It is possible that the relatively high processing temperature (180°C), caused the H<sub>2</sub>SO<sub>4</sub> to degrade, resulting in a small amount of residual sulfur. The absence of sulfur in the TOL sample indicates the efficiency of the re-precipitation process as a purification treatment for this particular impurity.

**Table 6.3** Lignin formula and protein content of lignins

Lignin formulae	Empirical formula	C <sub>9</sub> formulae	Mw of C <sub>9</sub> formulae (g/mol)	Protein (%)
OL	C <sub>5.04</sub> H <sub>5.63</sub> O <sub>1.94</sub> N <sub>0.005</sub> S <sub>0.02</sub>	C <sub>9</sub> H <sub>10.08</sub> O <sub>3.47</sub> N <sub>0.009</sub> S <sub>0.04</sub>	175.01	0.51
TOL	C <sub>4.94</sub> H <sub>5.44</sub> O <sub>2.02</sub>	C <sub>9</sub> H <sub>9.9</sub> O <sub>3.68</sub>	176.78	0.00
SL	C <sub>4.98</sub> H <sub>6.11</sub> O <sub>1.83</sub> N <sub>0.04</sub>	C <sub>9</sub> H <sub>10.10</sub> O <sub>3.3</sub> N <sub>0.08</sub>	171.88	3.82

### 6.2.3 Lignin compositions

The result of the compositional analysis (sugars, Klason lignin, acid soluble lignin, and ash contents) of the various lignin samples are described in **Table 6.4**. The sugar analysis revealed that glucan and xylan had been dominant constituents of the three lignin samples, while arabinan had been only presented in minor quantities. The results show that the TOL sample contained significantly less sugars and ash than the OL sample, indicating the efficacy of the re-precipitation treatment as a purification process for removal of these contaminants. As a result the purity of this sample had slightly increased, to a value of

93.24%. The results clearly indicate that both sugars and ash content of the OL sample can be significantly reduced by applying the re-precipitation treatment process.

**Table 6.4** Composition of lignin samples (wt.%)

Lignin sample	Biochemical composition (wt.%)						
	Glucan	Xylan	Arabinan	Ash	AIL	ASL	Lignin purity (wt.%)
OL	0.03	0.91	0.05	0.12	92.59	0.04	92.63
TOL	0.01	0.29	0.02	0.04	93.14	0.10	93.24
SL	0.50	1.5	0.00	0.60	87.12	3.15	90.27

#### 6.2.4 Mannich Reactivity

The result for the number of active sites, described as the free C-3 and C-5 positions per C<sub>9</sub> unit in lignin, is presented in **Table 6.5**. These figures were determined by subtracting the amount of nitrogen in the C<sub>9</sub> formula of the untreated lignin (**Table 6.3**) from the amount of nitrogen in the C<sub>9</sub> formula of the treated lignin (**Table 6.5**). The OL extracted with MIBK/methanol/water showed the highest number of reactive sites/C<sub>9</sub> (0.36), followed by the SL and TOL samples, respectively. This may simply be because of the contaminants in OL reacting in the Mannich process, and not with the free C-3 and C-5 lignin sites. For the amount of sulfur contamination and the active sites, the use of TOL is suggested in the lignin hydrolysis process because the product can be free of sulfur, which is advantageous in many applications *i.e.* for producing low-molar mass phenol, aromatic compounds, and high quality commercialized lignin-based polymer (Laurichesse & Avérous, 2014). Therefore, the result of elemental analysis (**Table 6.2**) indicates that the OL sample contains a small amount of sulfur (0.5%), thought to be present due to the degradation of H<sub>2</sub>SO<sub>4</sub> and the sulfur content in eucalyptus chip. Nevertheless, this process not only removed the sulfur present but also some of the present nitrogen. For this reason the amount of active sites for the TOL sample was lower, as shown in **Table 6.5**.

**Table 6.5** Active site of lignins

Lignin sample	C	H	N	C <sub>9</sub> Formula	Reactive sites/C <sub>9</sub>
OL	57.7	6.89	2.8	C <sub>9</sub> H <sub>12.88</sub> N <sub>0.37</sub>	0.36
TOL	60.32	6.28	1.40	C <sub>9</sub> H <sub>11.17</sub> N <sub>0.18</sub>	0.18
SL	60.02	7.13	2.24	C <sub>9</sub> H <sub>12.74</sub> N <sub>0.29</sub>	0.21

### 6.2.5 Molecular weight distribution

The values of weight-average ( $M_w$ ), number average ( $M_n$ ) molecular weights, and polydispersity ( $M_w/M_n$ ) of lignin samples were calculated using the equation obtained from the trend line of the standard curve shown in **Table 6.6**. From this data, the high molecular weights were determined for the OL and TOL samples ( $M_w$ , 10940 and 10988 g/mol, respectively), and a lower molecular weight for the SL ( $M_w$ , 4028 g/mol). It is possible that the lignin isolated during the MIBK treatment at high temperature (180°C) and long residence time (60 min) may have significant alteration on the macromolecular structure due to more condensed aromatic skeleton and less  $\beta$ -O-4 linkage. However, the elution profiles showed a very broad distribution of molecular size of OL and TOL as indicated by its polydispersity ( $M_w/M_n$ ) value of 2-2.1.

**Table 6.6** Average molecular weight of lignin samples

Lignin sample	$M_w$ (g/mol)	$M_n$ (g/mol)	$M_w/M_n$
OL	10940	5163	2.1
TOL	10988	5518	2.0
SL	4028	2871	1.4

### 6.2.6 XPS analysis

The surface compositions of the OL, TOL, and SL samples were evaluated using XPS. The samples were irradiated with mono-energetic x-rays causing photoelectrons emitted from the sample surface and their binding energy was determined by an electron energy analyzer. An electron energy analyzer determines the binding energy of the photoelectrons. From the binding energy and intensity of a photoelectron peak, the elemental identity, chemical state, and quantity of an element are determined. The XPS survey scan of the lignin samples are shown in **Figure 6.1(a)-(c)**. Among all the elements

detected, carbon and oxygen were the main components, at 73-77 % and 23-26 %, respectively. Approximately 1 % sulfur was typically detected in OL. There is an evidence of OL surface contamination, indicated by the presence of the S2p signal and the amount of sulfur present (confirmed by the elemental analysis in **Table 6.2**). To observe any structural changes between the OL and TOL the XPS analysis was confirmed by a high-resolution XPS spectrum as presented in **Figure 6.2(a)-(c)**. According to the XPS data, it can be concluded that the alkaline re-precipitation process removed the sulfur impurity present in the OL sample without causing any significant structural change. High-resolution XPS spectra of OL, TOL, and SL are shown in **Table 6.7**. The C-C linkage was the major band associated with the lignins (33-38 of atomic %), followed by the C-O linkage (32-35 of atomic %), and finally the C-O-C and -OH linkage (23-26 of atomic %). The majority of amount linkage of lignin samples in this work was similar to the conventional lignin (Mousavioun et al., 2012). On the other hand, in addition the O=C linkage was detected around 1-1.4% for OL, and TOL to differ from the conventional lignin, indicating possibility on bonding association between lignin and MIBK.

**Table 6.7** XPS analysis of OL, TOL, and SL

Organosolv lignin (OL)			Treated organosolv lignin (TOL)			Soda lignin (SL)		
Linkage	Binding energy (eV)	Atomic %	Linkage	Binding energy (eV)	Atomic %	Linkage	Binding energy (eV)	Atomic %
O=C	531.749	0.9	O=C	531.814	1.4			
C-O*-			C-O*-			C-O*-		
C, OH	533.29	26.4	C, OH	533.508	23.7	C, OH	533.352	25.9
C-C	285	33.1	C-C	285	34.2	C-C	285	38.1
C-O	286.562	32.5	C-O	286.504	34.5	C-O	286.624	31.7
C=O	288.023	6.2	C=O	287.466	6.2	C=O	288.19	4.3
S2pSO4	169.712	1.1						

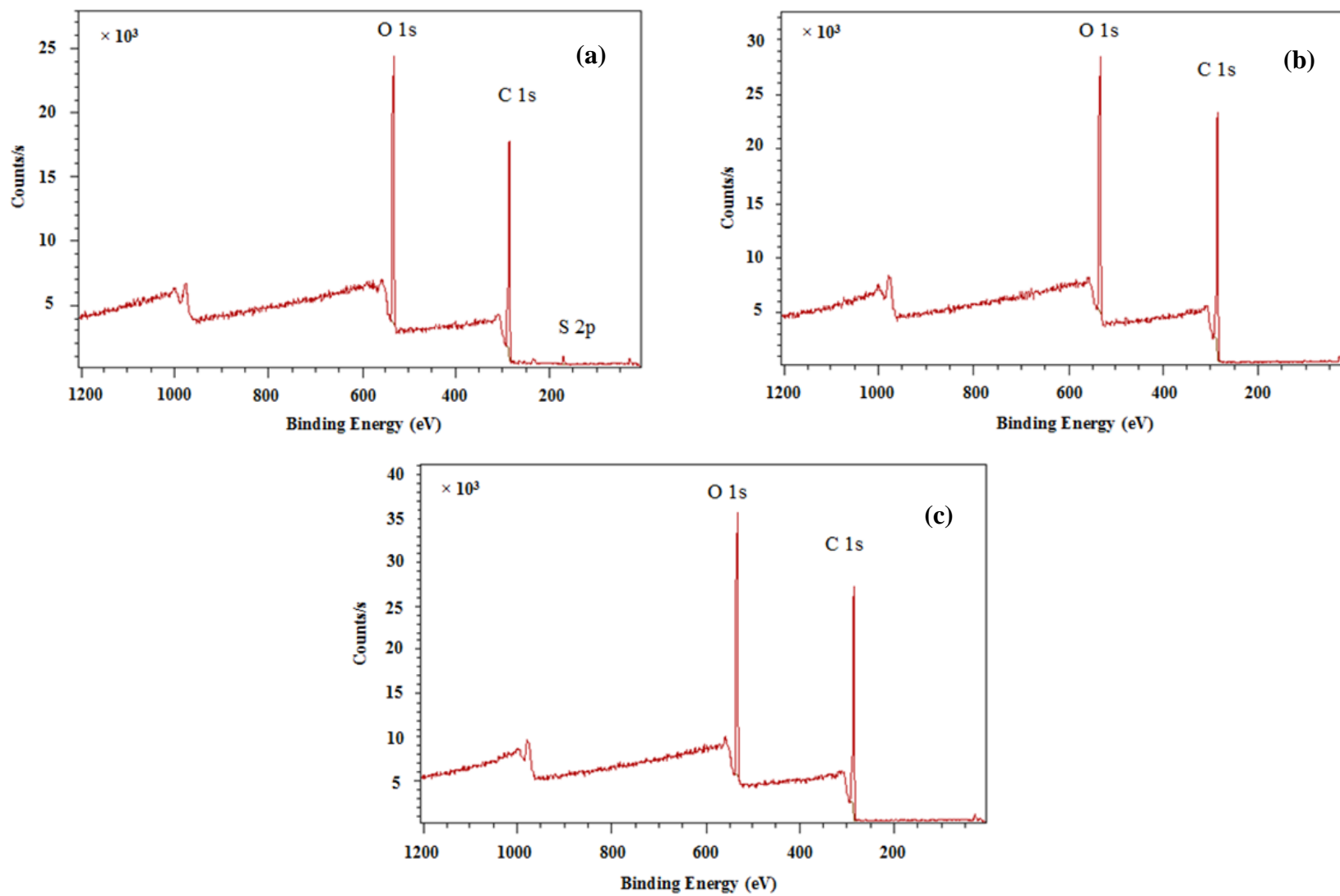


**Figure 6.1** XPS survey scan spectra. (a) OL; (b) TOL; (c) SL.

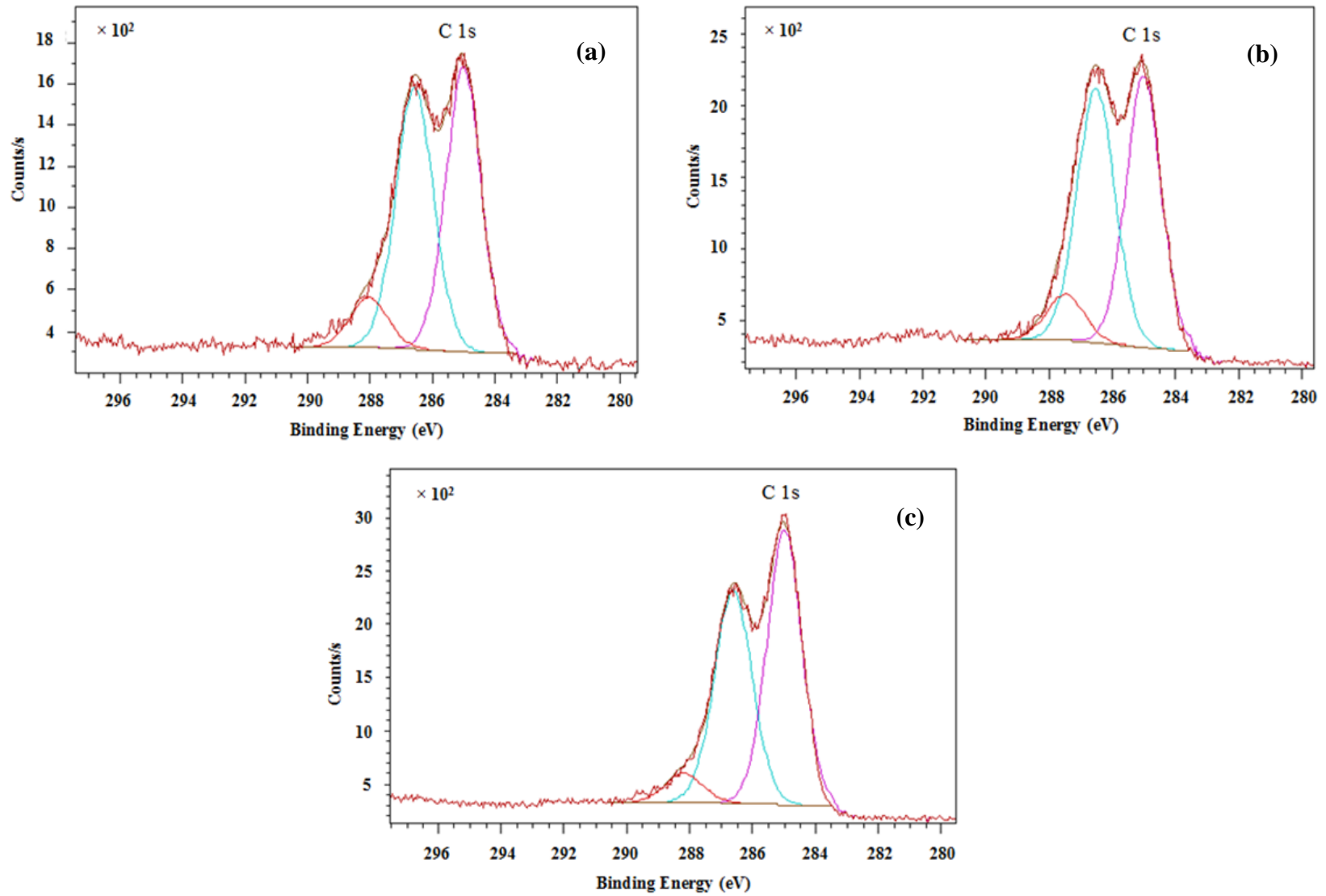


**Figure 6.2** XPS high resolution spectra of the C1s. (a) OL; (b) TOL; (c) SL.

### 6.2.7 Thermal characteristics

The thermal stability of the OL and TOL samples was analyzed via thermogravimetric analysis (TGA), the results for which are shown in **Figure 6.3(a)-(b)**. These materials are evidently prone to thermal degradation, and their thermal decomposition occurs in three stages. The first of these stages occurs at ~150 °C, which is assigned to the process of dehydration. The fact that the water content of the lignin is removed at temperatures higher than 100 °C indicates the strong interaction between water molecule and the hydroxyl groups in lignins (Domínguez et al., 2008). The maximum temperature at which the OL and TOL samples decomposed was approximately 351 °C and 325 °C, respectively.

For OL, and TOL, although 34-38% of them had decomposed at temperatures lower than 380°C, the remainder 62-66% decomposed at temperatures > 400°C. The second decomposition stage occurred when the temperature was increased to 500°C at which fragmentations of internal linkages between lignin units was found as shown in **Figure 6.3(a)-(b)**. The major products in this stage were coke, organic acid, and phenolic compounds together with gas products (Shukry et al., 2008). In the final stage (over 500 °C), the pyrolytic degradation of lignin, decomposition, and condensation of the aromatic rings occurred (Brebú et al., 2013; Yang et al., 2007) TGA showed that OL and TOL extracted with MIBK/methanol/water at high temperature (180 °C) with long treatment time (60 min) produced more residues (37-41%) at 800 °C) compared to classical solvent mixture (ethanol-water mixture) (Alriols et al., 2010; El Hage et al., 2009). This indicates that lignins at high temperature and long time may contain more condensed aromatic structures, which is more thermally stable. These results were strongly supported with the obtained molecular weight in **Table 6.6**. **Figure 6.3(c)** shows multi-stage thermal decomposition of base insoluble lignin (solid removed by alkaline precipitation process; BIL). The result of thermal decomposition of BIL is similar the thermal decomposition of hemicellulose (Amendola et al., 2012). This result may be related to the presence of carbohydrates (*i.e.* glucan, xylan, and arabinan) in the BIL as shown in **Table 6.4**. It can be concluded that the alkaline precipitation can be used to increase the purity of lignin and remove sugar contamination. In summary, the result of thermal composition of OL, and TOL was similar, indicating that the core structure of lignins is not changed by the alkaline precipitation process.

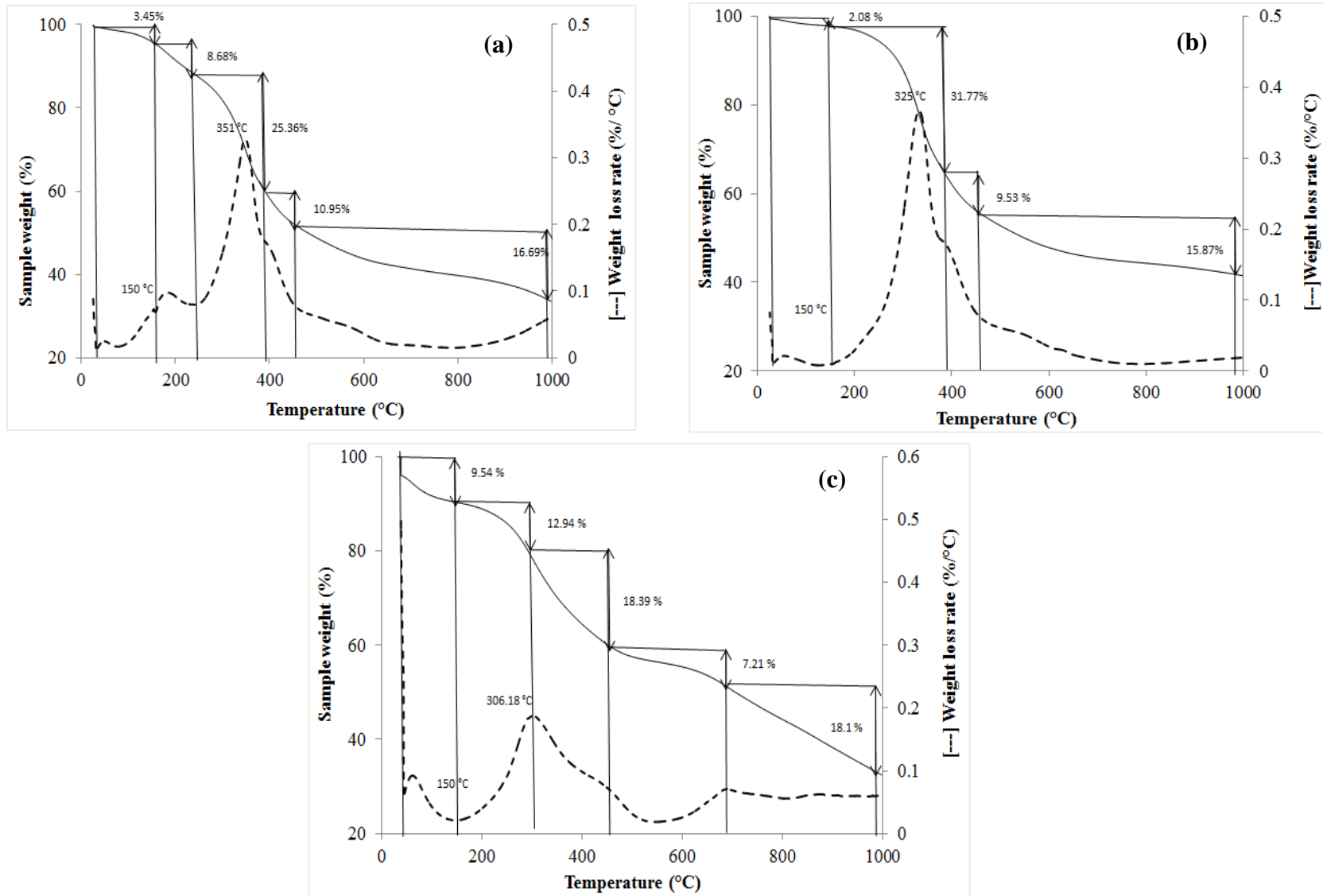


Figure 6.3 TGA and DTG curves of lignins: (a) OL; (b) TOL; (c) BIL.

### 6.2.8 FTIR analysis of lignin samples

The IR spectra of OL, TOL, and BIL are presented in **Figure 6.4**. As can be seen from the spectra, the two lignin fractions (OL and TOL) have similar IR spectra. The relative intensities of bands, assigned at 3400, 2936, 1705, 1599, 1511, 1456, 1423, 1351, 1310, 1260, 1210, 1110, 1029, 911, and 828  $\text{cm}^{-1}$  (**Figure 6.4(a)-(b)**) are rather similar, indicating the similar structure of the lignin in different fractions. In concordance with previous studies (Lora & Glasser, 2002), typical lignin peaks were identified and, consequently, the structure correspondences are shown in **Table 6.8**. These typical spectra of lignin revealed that the “core” of the lignin structure did not change significantly during the alkaline precipitation process. The IR spectra of the OL and TOL samples (**Figure 6.4(a)-(b)**) showed a strong hydrogen bonded O-H stretching absorption around 3400  $\text{cm}^{-1}$  and the bands centered around 2936  $\text{cm}^{-1}$  arising from C-H stretching in the aliphatic C-H and methoxy groups (Pandey, 1999). The bands at 1600, 1510, 1260, 1029  $\text{cm}^{-1}$  were due to aromatic skeleton vibrations (Billingham et al., 1997). The peak around 828  $\text{cm}^{-1}$  was related to the out of-plane C-H vibration in guaiacyl units (C2, C5 and C6) (Thring et al., 1990). Furthermore, the peak at 911  $\text{cm}^{-1}$  was attributed to C-H out of plane deformation (Heitner et al., 2010; Joseph & Aminul, 1999). As mentioned in re-precipitation alkaline method to treat the OL sample, the BIL sample was indicated that it seemed the contaminations (*i.e.* sugars, sulfur, and remaining MIBK in the OL sample). **Figure 6.4(c)** presents the spectrum of BIL with the major peaks assigned at 3400, 2936, 1705, 1210, 1110, and 1028  $\text{cm}^{-1}$ . All of the signals obtained remaining peaks, which indicated that some contaminations in OL have been removed by alkaline precipitation.

Therefore, to obtain insight into the OL and TOL sample spectra, the FTIR spectra of the lignin samples, the OL sample (**Figure 6.5(a)**) was subtracted from the TOL sample (**Figure 6.5(b)**) to obtain the subtract spectra, as presented in **Figure 6.5(c)**. Both spectra were normalized on the 1109  $\text{cm}^{-1}$  peak before spectral subtraction. **Figure 6.5(c)** shows the result of spectral subtraction, which indicates that the contaminations of OL (*i.e.* sugars, MIBK) were associated by the bonding interactions with the OL sample. The highest three peaks (1029  $\text{cm}^{-1}$ , 1109  $\text{cm}^{-1}$ , and 1210  $\text{cm}^{-1}$ ) of lignin were indicated after the OL sample spectrum was subtracted from TOL sample spectrum. Moreover, four enhanced lignin peaks at 1455  $\text{cm}^{-1}$ , 1510  $\text{cm}^{-1}$ , 1600  $\text{cm}^{-1}$ , and 1705  $\text{cm}^{-1}$  are presented (**Figure 6.5(c)**) indicating increased bond interactions between contaminations of OL (*i.e.* sugars)

and OL sample. In addition, all the peaks after the subtraction spectra showed positive peaks, indicating that further enhanced bonding had occurred between the contaminants in OL and the OL sample. In conclusion, the alkaline precipitation could remove the contaminants (*i.e.* sugars and MIBK) from OL. This finding agrees well with the compositions of lignins (**Table 6.4**).

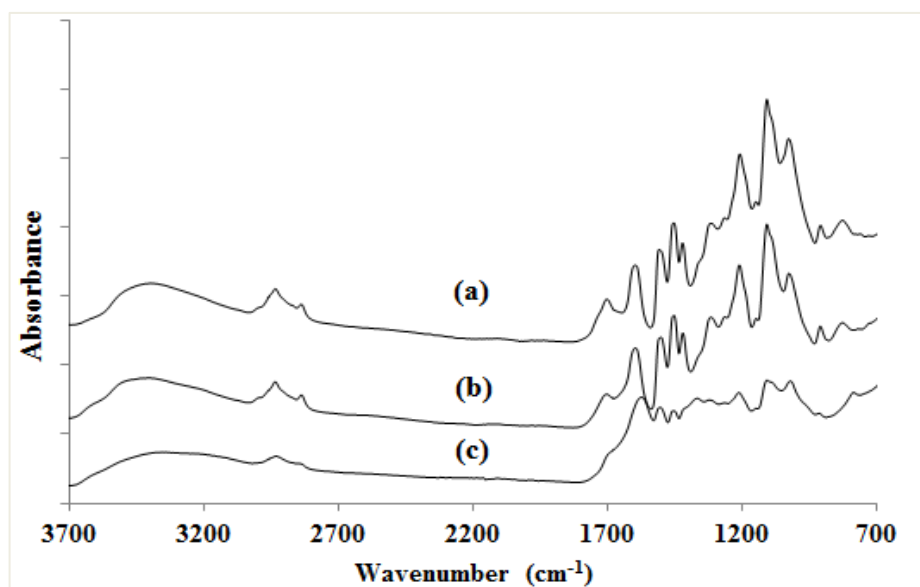


**Figure 6.4** FTIR spectra of lignins; (a) OL; (b) TOL; (c) BIL.

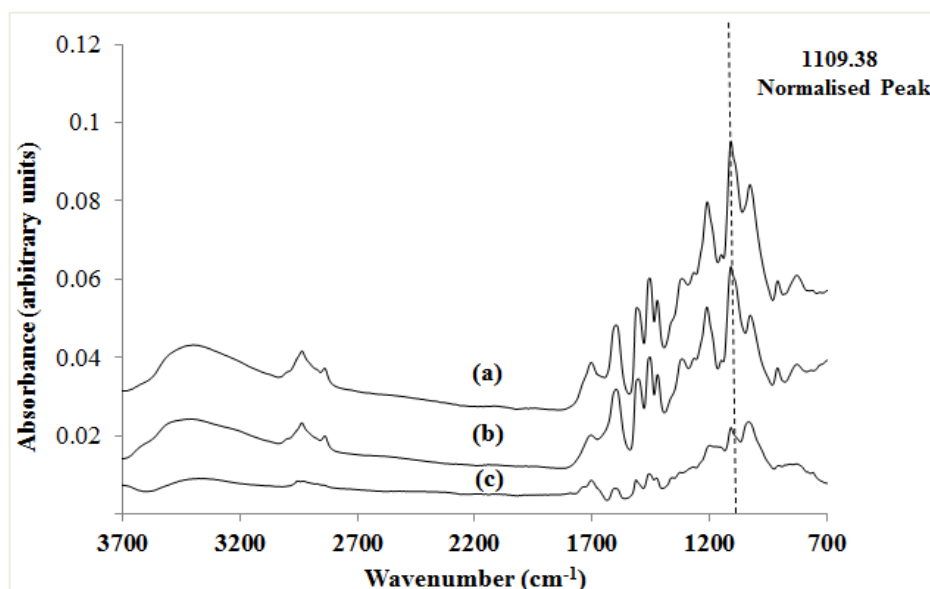


**Figure 6.5** Subtracted FTIR spectra of lignins: (a) OL; (b) TOL; (c) The spectra was obtained by subtracting the OL sample spectrum (normalized on  $1109\text{ cm}^{-1}$  peak) from that TOL sample (normalized on  $1109\text{ cm}^{-1}$  peak).

**Table 6.8** Assignment of lignin samples of FT-IR absorption bands ( $\text{cm}^{-1}$ ) (El Hage et al., 2009)

Wavelength ( $\text{cm}^{-1}$ )	Structure correspondence
3450–3400	O–H stretching
2940–2820	C–H stretching in methyl and methylene groups
1715–1700	Carbonyl stretching in unconjugated ketones and conjugated carboxylic groups
1675–1660	Carbonyl stretching in conjugated ketone groups
1605–1425	Aromatic skeletal vibrations
1330–1235	Syringyl ring breathing with C–O stretching
1275–1230	Guaiacyl ring breathing with C–O stretching
1100 approx.	C–H in plane deformation in guaiacyl and syringyl
835	Aromatic C–H out-of-plane deformation

### 6.2.9 Solid-state nuclear magnetic resonance (NMR)

The three lignin samples (OL, TOL, SL) were investigated by solid-state  $^{13}\text{C}$  NMR. The structural characteristics determined are shown in **Figure 6.6(a)-(c)**. The spectra of these samples can be divided into three regions; the aliphatic region (22–86 ppm), the aromatic region (106–153 ppm), and the carbonyls region (166–192 ppm) as shown in **Figure 6.6** and **Table 6.9**. The spectra of OL, TOL revealed that the “core” of the lignin structure did not change significantly during the OL treated alkaline re-precipitation process. This result was also confirmed with FT-IR analysis as shown in **Figure 6.6**. Nevertheless, several peaks of TOL (at 22, 35, 116, 128, and 134 ppm) were changed because the contaminations in the OL sample were separated from OL. The nature of these peaks of lignins is described in **Table 6.9**. The signal of SL sample (**Figure 6.6(c)**) contained different peaks at 74, 86, 116, 153, 170, and 175 due to the different isolation method and type of the starting materials. These solid-state spectra in this work were similar to those reported in literatures (Akim et al., 1993; Sharma et al., 2004; Wikberg & Liisa Maunu, 2004).

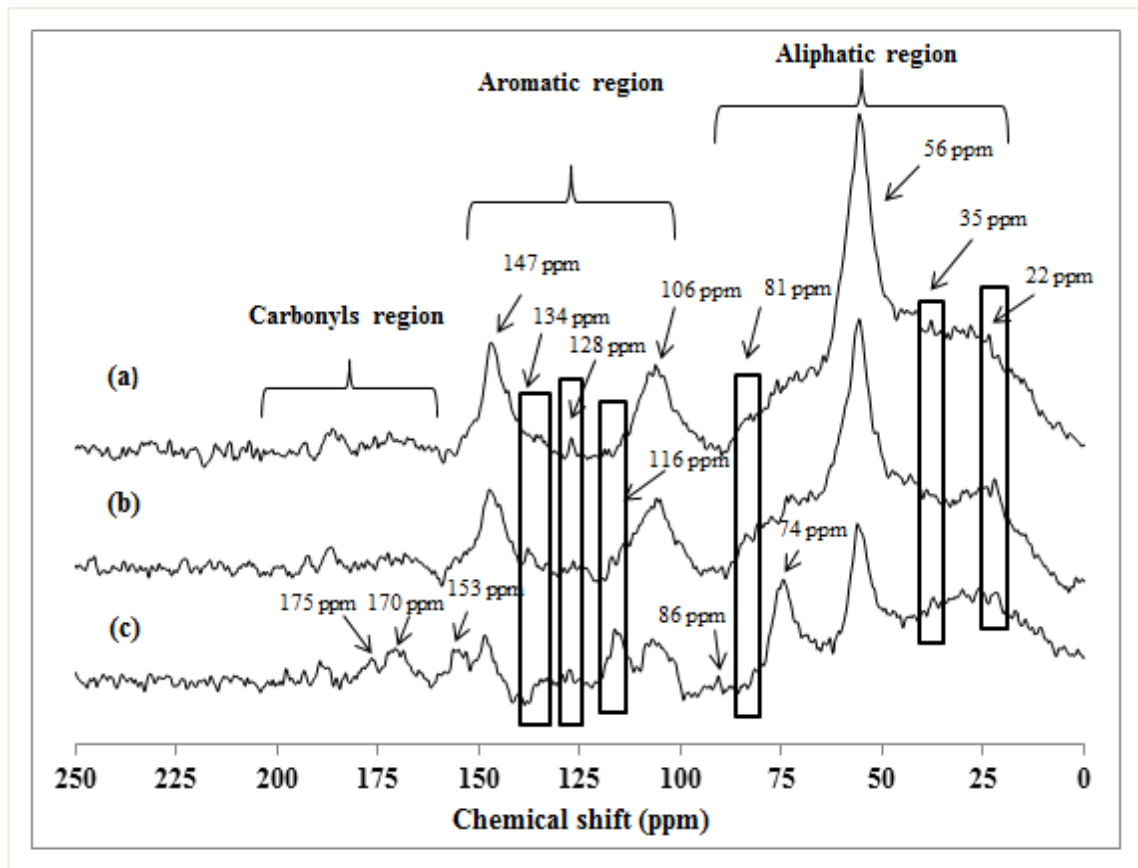


**Figure 6.6**  $^{13}\text{C}$  CPMAS NMR spectra of lignins. (a) TOL; (b) OL; (c) SL.

**Table 6.9** Assignment of lignin signals in the CPMAS  $^{13}\text{C}$  NMR spectra (Almendros et al., 1992; Sharma et al., 2004)

$^{13}\text{C}$ Shift, ppm	probable assignment
192	C=O in aromatic aldehyde
175	C=O in aliphatic acid
170	C=O in aliphatic ester
166	C=O in aromatic acid
153	C <sub>3</sub> and C <sub>5</sub> in etherified syringyl
147	C <sub>3</sub> and C <sub>4</sub> in etherified guaiacyl
134	C <sub>1</sub> in etherified syringil and guaiacyl
128	C <sub>2</sub> and C <sub>6</sub> in p-hydroxyphenyl
116	C <sub>5</sub> in guaiacyl and C <sub>3</sub> and C <sub>5</sub> in p-hydroxyphenyl
106	C <sub>1</sub> in carbohydrate and C <sub>2</sub> and C <sub>6</sub> in syringyl
86	C <sub>β</sub> in β-O-4-linked unit (threo) C <sub>β</sub> in β-O-4-linked unit (erythro) and C <sub>4</sub> in
81	4-O-methylglucuronic acid C <sub>2</sub> in xylose internal unit and C <sub>α</sub> in
74	β-O-4 linked unit
56	aromatic methoxy group
43	C <sub>α</sub> methyne with aliphatic substitution
35	C <sub>α</sub> , in arylpropanol
22	CH <sub>3</sub> group in acetylated xylan

### 6.3 Conclusion

Organosolv lignin (OL) was isolated from the fractionation of eucalyptus wood chips using a ternary mixture of methyl isobutyl ketone /methanol/water in the presence of 0.008 M H<sub>2</sub>SO<sub>4</sub> as an acid promoter at 180°C for 60 min. Further treatment by an alkaline precipitation process (treated organosolv lignin; TOL) enhanced higher solubility of this isolated lignin in organic solvents (*i.e.* tetrahydrofuran, dimethyl sulfoxide, and methanol). This gains great benefit for further conversion processes. In addition, the characterizations, revealed that OL contained small amounts of contaminations (*e.g.* sugars, ash, and sulfur), which was removed by alkaline precipitation treatment without causing any significant structural change.

## CHAPTER 7

### DEPOLYMERIZATION OF ORGANOSOLV LIGNIN FRACTIONATED WOODY EUCALYPTUS UNDER HYDROTHERMAL PROCESS WITH MESOSTRUCTURED SILICA AND PHOSPHATE-BASED CATALYSTS

---

#### Chapter highlights

Isolated and purified organosolv eucalyptus wood lignin was depolymerized at different temperatures with and without mesostructured silica catalysts (*i.e.* SBA-15, MCM-41, ZrO<sub>2</sub>-SBA-15 and ZrO<sub>2</sub>-MCM-41). It was found that at 300 °C for 1 h, the SBA-15 catalyst with high acidity had the highest syringol yield of 23.0% in a methanol/water mixture (50/50, wt/wt). Doping with ZrO<sub>2</sub> over these catalysts did not increase syringol yield, but increased the total amount of solid residue. Gas chromatography-mass spectrometry (GC-MS) also identified other main phenolic compounds such as 1-(4-hydroxy-3,5-dimethoxyphenyl)-ethanone, 1,2-benzenediol, and 4-hydroxy-3,5-dimethoxy-benzaldehyde, and the yields of these compounds depended on the reaction conditions, catalysts and solvents.

The reaction catalyzed by phosphate-based catalysts (*i.e.* cobalt polyphosphate (CoP<sub>2</sub>O<sub>6</sub>) and calcium phosphate (CaP<sub>2</sub>O<sub>6</sub>)) showed that the optimize condition can be achieved by using CaP<sub>2</sub>O<sub>6</sub> at 300 °C for 1 h with methanol/water mixture (50/50, wt/wt). Under these conditions, the highest syringol yield of 16.7 wt.% can be obtained without char formation. The good catalytic activity of CaP<sub>2</sub>O<sub>6</sub> is closely related to its high acidity, from which the acid strength of CaP<sub>2</sub>O<sub>6</sub> is in a range of  $+3.3 \leq H_0 \leq +4.8$ . From the reaction, the phenol products mainly consist of five phenols; syringol, 1,2-benzendiol, benzoic acid, 4-hydroxy-3,5-dimethoxy-benzaldehyde, and 1-(4-hydroxy-3,5-dimethoxyphenyl)-ethanone.

---

## 7.1 Background

Lignin is one of the major organic compounds in lignocellulosic biomass along with cellulose and hemicellulose. It consists of several complex and amorphous aromatic compounds comprised of variously linked phenylpropane units of hydroxyphenyl (H), guaiacyl (G), and syringyl (S) (Berlyn, 1972; Boerjan et al., 2003; Vanholme et al., 2010). Previously, lignin has been considered as an unwanted by-product, but is now generally utilized as low-grade fuel in industrial burner or boiler. Nevertheless, as the concept of integrative biorefinery has been widely proposed, lignin conversion to valuable fuels and chemicals is currently being intensively investigated. In order to isolate lignin from lignocellulosic biomass, two methods are used; one method uses ingredients containing sulfur, and the other method does not (Laurichesse & Avérous, 2014). Sulfur-derived lignins are primarily produced by the pulp and paper industries, where sodium sulfide ( $\text{Na}_2\text{S}$ ) and NaOH are used in the delignification process. Sulfur-free lignins can be classified into one of two main categories: lignins prepared via solvent pulping (*i.e.* organosolv lignin), and those from alkaline pulping (*i.e.* soda lignin). Among these, organosolv lignins (OLs) are generally considered to be the highest purity (El Hage et al., 2009; El Hage et al., 2010). They show high solubility in organic solvents and are sparingly soluble in water due to their hydrophobic nature.

Technically, lignin is a rich source of mono-aromatic compounds, particularly phenols. Nevertheless, due to its complex structure and high molecular weight, it is difficult to breakdown into phenol-based compounds in high yields. Recently, various techniques for the production of phenol and its derivatives from lignocellulosic materials have been reported, including solvolysis, hydrolysis, hydrocracking (or hydrogenolysis), pyrolysis, and alkaline oxidation (Pandey & Kim, 2011). The fragmentation of lignin into smaller molecules has been widely described in the literature (Kleinert & Barth, 2008; Pandey & Kim, 2011; Wang et al., 2013; Zakzeski et al., 2010). Since the weakest bonds in lignin polymers are the  $\alpha$ - and  $\beta$ -aryl-ether-bonds followed by the aryl-aryl bonds, thermal hydrodeoxygenation and hydrocracking have often been employed for depolymerization with and without a catalyst. For the catalytic process, heterogeneous acid catalysts (*e.g.*, sulfided NiMo, CoMo, zeolites or amorphous silica-alumina with various compositions such as H-ZSM-5, H-mordenite, H-Y, silicate, and silica-alumina) are typically used for hydrolysis and cracking. These processing steps are the primary steps necessary for

breaking down the C-C bond in the complex lignin structure (Kobayashi et al., 2012; Zakzeski et al., 2012). Several literatures (Deepa & Dhepe, 2014; Singh & Ekhe, 2014; Zakzeski et al., 2010) have reported the catalytic cracking of lignin to bio-oil via liquefaction in the presence of MCM-41 and H-ZSM-5 at high temperatures (340-410 °C). Moreover, it was reported that MCM-41, H-ZSM-5 and H-mordenite could produce a higher proportion of aromatic compounds than using H-Y, silicate or silica-alumina due to higher surface area and acidity, which provides a desirable environment for the conversion of long lignin polymer to monomeric phenolic compounds.

The metal phosphates, these materials are well known for their catalytic performance in converting sugar feedstocks (*i.e.* fructose, and sorbitol) to chemicals. Asghari et al. has reported the good dehydration activity of fructose to HMF in the presence of zirconium phosphates as catalysts under subcritical water condition. It was also revealed that zirconium phosphates were stable under subcritical water conditions, and they can easily be recovered, regenerated, and used several runs without changing their catalytic properties (Asghari & Yoshida, 2006). In addition, (Gu et al., 2009) studied the dehydration reaction for converting sorbitol to isosorbide in the presence of metal (IV) phosphates of tin, zirconium and titanium. It was found that tin phosphate shows the highest selectivity and lowest deactivation rate. (Bautista et al., 2003) studied the cyclohexanol dehydration reaction with a series of phosphates (Al, Fe, Ni, Ca and Mn). It was revealed that the additional aluminium in mixed  $\text{FeAl}(\text{PO}_4)_2$  and  $\text{Ca}_3\text{Al}_3(\text{PO}_4)_5$  shows the highest catalytic activity in conversion of cyclohexanol. Recently, (Daorattanachai et al., 2012) investigated the use of alkaline earth metal phosphates (calcium and strontium) for converting fructose, glucose, and cellulose to 5-hydroxymethylfurfural (HMF) under hot compressed water condition. It was found that both alkaline earth metals promote the production of HMF from fructose and glucose dehydration and cellulose hydrolysis/dehydration reaction, as compared with the non-catalytic system. Until now, no study has previously been done on the depolymerization activity of phosphate-based catalysts. The main types of heterogeneous catalyst that have been tested toward the lignin depolymerization were metal catalysts such as Pd, Pt, Ru, Ni, Co-Mo, and Ni-Mo supported on C,  $\text{Al}_2\text{O}_3$ ,  $\text{SiO}_2\text{-Al}_2\text{O}_3$ . The tests have been performed over several lignin sources (*e.g.* kraft lignin, organosolv switch grass lignin, acidic hydrolysis spruce lignin, enzymatic hydrolysis spruce lignin, kraft spruce lignin, lignosulfonate, birch sawdust lignin, enzymatic hydrolysis corn stalk lignin, and organosolv olive tree pruning lignin) at

the reaction temperature range of 150-300 °C. Several monomeric phenols such as guaiacol (1.7-10 wt.%), resorcinol (0.5-1.2 wt.%), pyrocatechol (1.3-4.9 wt.%), 4-ethylphenol (0.13-3.1 wt.%), 4-ethylguaiacol (0.06-1.4 wt.%), 4-propylguaiacol (7.8 wt.%), and 4-methylguaiacol (5 wt.%) were produced from the reaction (Pandey & Kim, 2011; Wang & Rinaldi, 2013; Zakzeski et al., 2012).

In this chapter, the depolymerization of treated organosolv lignin (TOL) was studied at several temperatures in different solvent systems (water and methanol-water) with and without the presence of solid acid catalysts. The evaluated catalysts included commercial sulfided NiMo/Al<sub>2</sub>O<sub>3</sub>, phosphate-based catalysts (*i.e.* CoP<sub>2</sub>O<sub>6</sub> and CaP<sub>2</sub>O<sub>6</sub>), and mesostructured silicas (*i.e.* SBA-15 and MCM-41) as well as mixed-oxide supports (*i.e.* ZrO<sub>2</sub>-SBA-15 and ZrO<sub>2</sub>-MCM-41). ZrO<sub>2</sub> was chosen as doping element due to its higher stability, while mesostructured silicas were selected due to their excellent textural characteristics (*e.g.*, pore volume and surface area). These catalysts have been reported to show good catalytic cracking of lignin to bio-oil via liquefaction, nevertheless, no study has previously reported the activities of these catalysts toward the depolymerization of lignin isolated from woody biomass. From the reaction, the depolymerized TOL was separated into three main fractions including aqueous fraction, residual lignin, and solid residue. These fractions were intensively characterized to understand the influences of catalyst, temperature and solvent on the product characteristics.

## 7.2 Results and discussion

The experimental results are divided into two main sections: (1) depolymerization of TOL under hydrothermal process in the presence of mesostructured silica catalysts (*i.e.* SBA-15, MCM-41, ZrO<sub>2</sub>-SBA-15 and ZrO<sub>2</sub>-MCM-41), and (2) depolymerization of TOL under hydrothermal processes in the presence of phosphate based catalysts (*i.e.* cobalt phosphate (CoP<sub>2</sub>O<sub>6</sub>) and calcium phosphate (CaP<sub>2</sub>O<sub>6</sub>)) under hydrothermal processes. Both sections were studied at several temperatures in different solvent systems (water and methanol-water) with and without the presence of solid acid catalysts compared to commercial sulfided NiMo/Al<sub>2</sub>O<sub>3</sub>.

## 7.2.1 Depolymerization of TOL under hydrothermal process in the presence of mesostructured silica catalysts

### 7.2.1.1 Effect of catalyst on lignin depolymerization

Firstly, the depolymerization of TOL with and without a catalyst was performed at 250 °C for 1 h with an initial pH of 7 and a reactor pressure of 1 bar (atmospheric pressure). It was found that the decomposition of TOL generated three main products: aqueous phenolic compounds fraction, residual lignin, and a solid fraction (containing char), as shown in **Figure 3.5**. The gaseous products generated from the reaction were not determined. **Figure 7.1** shows the proportion of the aqueous fraction, the residual lignin and solid residue. Although the presence of catalyst increased the proportion of the total phenolic compounds by a maximum of only 1.8%, the solid residue fraction decreased significantly with MCM-41 and SBA-15. The results also show that the higher proportion residual lignin was closely related to the lower proportions of solid residue and vice versa. This could be because the acidity of these mesostructured silica catalysts prevents char formation and promotes cleavage of the main linkages of lignin (*i.e.*,  $\beta$ -O-4 and  $\alpha$ -O-4) (**Table 7.1**). There was almost no solid fraction left with SBA-15. Without a catalyst, comparable amounts of residual lignin and solid fraction were obtained. The total amount of the three fractions obtained with water is 87.2%, lower than the amounts obtained with the catalysts (88.1-98.0%), which is possibly mainly due to the formation of gaseous products during the reaction and the formation of organic acids in the aqueous phase (in phenolics and lignin-free liquid shown in **Figure 3.5**). Three catalysts MCM-41, SBA-15 and NiMo/Al<sub>2</sub>O<sub>3</sub> gave similar amounts of aqueous fraction, whereas doping with ZrO<sub>2</sub> did not increase the amount of aqueous fraction. Although, NiMo/Al<sub>2</sub>O<sub>3</sub> gave the highest proportion of aqueous fraction, the post-reaction pH of the solvent reduced to 3.5, but did not change (pH 7.0) for the other catalysts. The change in the final pH may be due to leaching of NiMo/Al<sub>2</sub>O<sub>3</sub> and the formation of organic acids from lignin degradation. The leaching process would lead to deactivation of the catalyst.

**Table 7.2** shows the yields of the phenolic compounds in the aqueous fraction and syringol in the residual lignin fraction at 250 °C. The use of mesostructured silicas resulted in the formation of diversified products, including syringol, as well as small amounts of butylated hydroxytoluene, 4-hydroxy-3,5-dimethoxy-benzaldehyde, 1-(2,4,6-trihydroxy-3-methylphenyl)-1-butanone, and benzoic acid, although not all of these monomers were detected in the same reaction. Besides increasing the proportion of the aqueous fraction

(**Figure 7.1**), the presence of the catalysts also increased the proportion of syringol in the residual lignin. The increase in syringol and other phenolic monomers in the aqueous fraction was accompanied by the decrease in 1-(4-hydroxy-3,5-dimethoxyphenyl)-ethanone. The highest syringol yield in aqueous fraction was achieved with MCM-41 catalyst while the highest syringol in residual lignin fraction and the highest total syringol were achieved with SBA-15 catalyst. The total syringol content with MCM-41 and SBA-15 were 6.6% and 7.3% respectively.

**Table 7.1** Specific surface area and acidity of synthesized catalysts<sup>a</sup>

Catalysts	BET surface area (m <sup>2</sup> /g)	Total acid sites (μmol/g)	Density of acid sites (μmol/ m <sup>2</sup> )
SBA-15	564	1974	3.5
MCM-41	592	1768	2.9
ZrO <sub>2</sub> -SBA-15	442	1193	2.7
ZrO <sub>2</sub> -MCM-41	489	1027	2.1

<sup>a</sup> Error of measurement = ±5%.

**Figure 7.2** shows the proportions of syringol present in an aqueous fraction and in a residual lignin fraction. Besides the reduction in solid residue (**Figure 7.1**), the use of MCM-41 and SBA-15 catalysts significantly increased the proportion of syringol present in the aqueous fraction. The highest proportion of syringol in aqueous fraction was achieved with MCM-41-based catalysts. The syringol contents in residual lignin are very low, but generally showed a reversed trend compared to the proportion present in aqueous fraction.

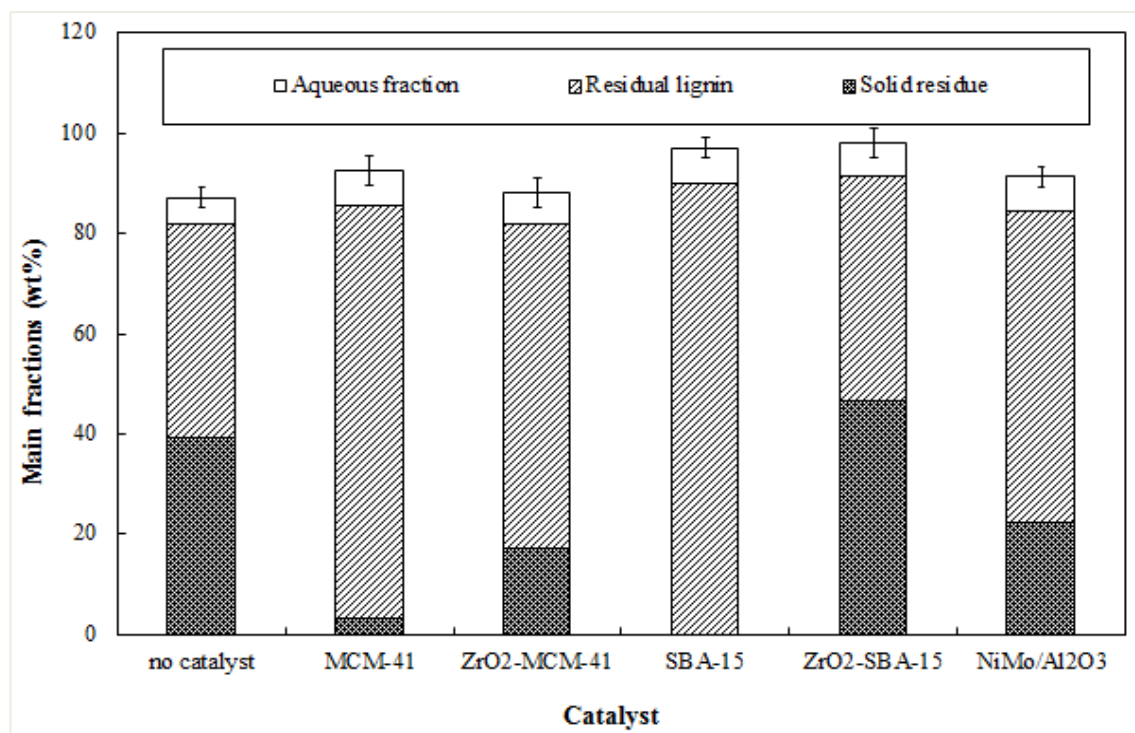


**Figure 7.1** Lignin distribution after reaction with different catalysts at 250 °C for 1 h.

The residual lignin fraction was also characterized by FT-IR spectroscopy in the wavenumbers region of 4000-700  $\text{cm}^{-1}$ . As shown in **Figure 7.3**, the intensity of the band at 3445  $\text{cm}^{-1}$  assigned to the OH groups (Boeriu et al., 2004) is present in the starting lignin material, the residual lignin from the reaction without a catalyst, the residual lignin from the reactions with MCM-41 and SBA-15, but absent in the spectra of residual lignins of NiMo/Al<sub>2</sub>O<sub>3</sub>, ZrO<sub>2</sub>-MCM-41, and ZrO<sub>2</sub>-SBA-15. This may be due to the fact that the use NiMo/Al<sub>2</sub>O<sub>3</sub>, ZrO<sub>2</sub>-MCM-41, and ZrO<sub>2</sub>-SBA-15 result in strong oxidation and the degradation of the aliphatic chain of phenyl propane units of lignin (Casas et al., 2012). Moreover, the decrease of the intensity of the band at 1225  $\text{cm}^{-1}$  assigned to 2<sup>nd</sup> OH group also confirms the loss of OH group during depolymerization process (Zhou, 2014). The absorption of the C-H stretching in the methyl and methylene groups (around 2950 and 2820  $\text{cm}^{-1}$ ) (Boeriu et al., 2004), increased during the depolymerization reaction of all the samples (Bai et al., 2013). The intensity of band at 1715  $\text{cm}^{-1}$  associated with carbonyl stretching in unconjugated ketones and conjugated carboxylic groups, which was observed in all samples. The aromatic skeletal vibration bands of 1600, 1500, and 1426  $\text{cm}^{-1}$ , typically found in lignin (Bai et al., 2013; El Mansouri & Salvadó, 2007) were relatively smaller for the samples derived from NiMo/Al<sub>2</sub>O<sub>3</sub>, ZrO<sub>2</sub>-MCM-41, and ZrO<sub>2</sub>-SBA-15. For

the TOL sample, the absorption bands of C-O stretching of syringyl ring (at  $1325\text{ cm}^{-1}$ ) and aromatic C-H deformation of syringol unit (at  $1120\text{ cm}^{-1}$ ) were stronger than those of the stretching of the guaiacyl ring (at  $1265\text{ cm}^{-1}$ ). This is due to the strong predominance of the syringol unit in isolated lignins from woody eucalyptus (Beauchet et al., 2012; Ibarra et al., 2005). After depolymerization, the absorption bands of C-O stretching of syringyl ring and aromatic C-H deformation of syringol unit decrease, whereas the intensity bands of stretching of guaiacyl ring increases. This is in good agreement with the GC/MS results, which detected syringol as the main product from the reaction (Rencoret et al., 2011; Zakzeski et al., 2012).

The doping of  $\text{ZrO}_2$  on MCM-41 and SBA-15 did not appear to promote the depolymerization reaction, and as a consequence, the amount of solid residue from these reactions increased compared to those without  $\text{ZrO}_2$ . On the basis of the reaction studies, it seems that the Bronsted acid property of the catalysts is closely related to the catalytic activity toward lignin depolymerization reaction. The main linkages between lignin are the  $\alpha$ - and  $\beta$ -aryl-ether-bonds, which are readily cleaved during the degradation of lignin in the presence of high acidity catalysts. As MCM-41 and SBA-15 gave the highest yields of phenolic products and they are relatively stable compared to  $\text{NiMo/Al}_2\text{O}_3$ , they were chosen for further analysis.

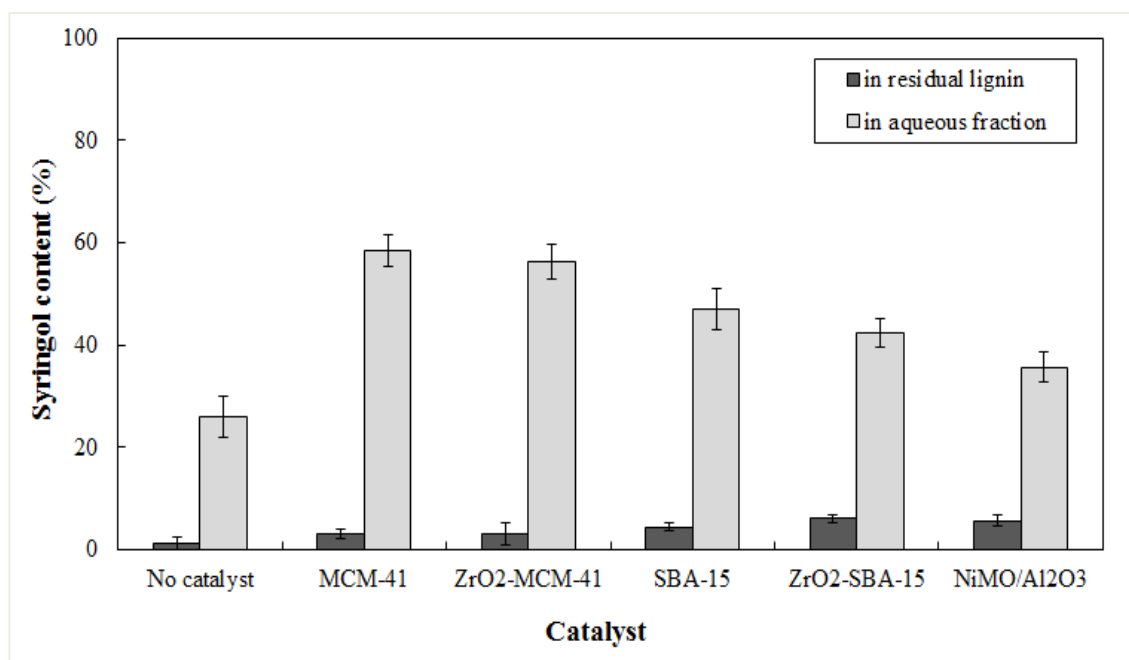


**Figure 7.2** Syringol contents in aqueous fraction and residual lignin after reaction at  $250\text{ }^\circ\text{C}$  for 1 h.

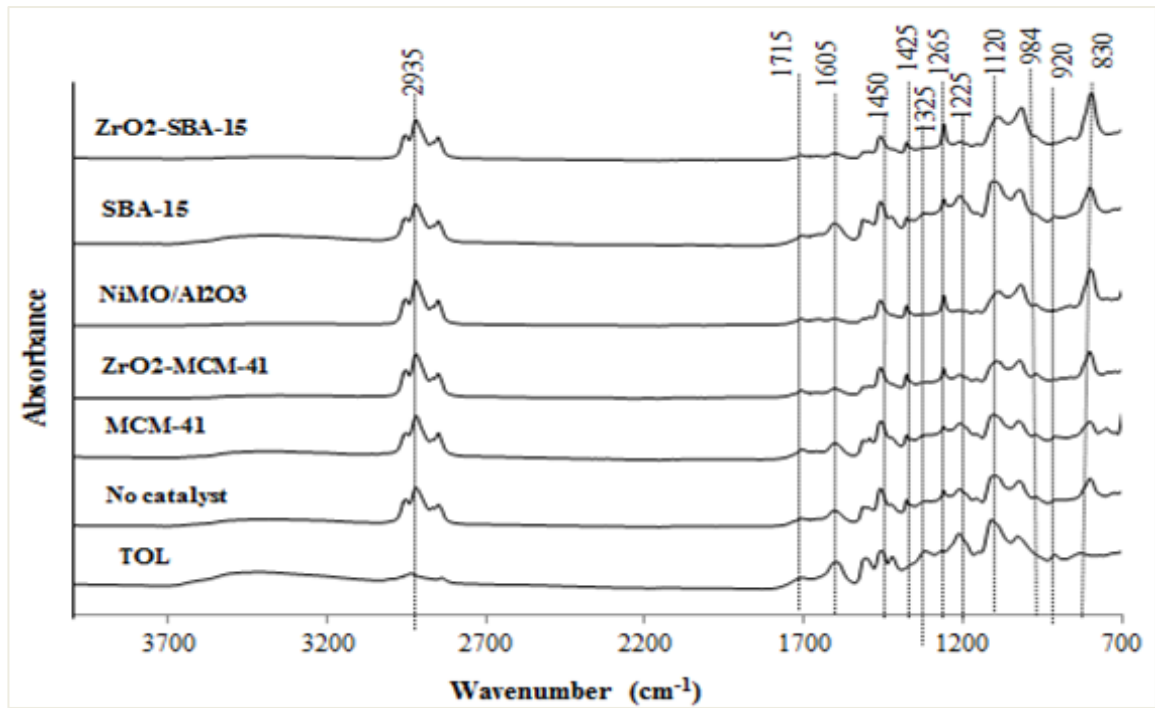


**Figure 7.3** FTIR spectra of TOL sample and residue lignins after lignin depolymerization with and without catalysts at 250 °C for 1 h.

**Table 7.2** Yield of phenolic monomers at 250°C<sup>a</sup>

Catalysts	Monomers in aqueous fraction (wt.%)						Syringol in residual lignin fraction (wt.%)	Total syringol (wt.%)
	Syringol	1-(4-hydroxy-3,5-dimethoxyphenyl)-ethanone	Butylated hydroxytoluene	4-hydroxy-3,5-dimethoxy-benzaldehyde	1-(2,4,6-trihydroxy-3-methylphenyl)-1-butanone	Benzoic acid		
No catalyst	1.32	2.55	-	-	-	-	0.53	1.85
MCM-41	4.01	0.23	0.48	-	-	1.97	2.57	6.58
ZrO <sub>2</sub> -MCM-41	3.54	0.45	-	-	0.77	0.11	3.05	6.59
SBA-15	3.23	0.85	-	-	-	-	4.05	7.28
ZrO <sub>2</sub> -SBA-15	2.78	0.97	-	-	-	-	2.73	5.51
NiMO/Al <sub>2</sub> O <sub>3</sub>	2.45	0.47	-	0.09	-	2.11	3.51	5.96

<sup>a</sup>All the yields were calculated in comparison to the initial amount of lignin.

### 7.2.1.2 Effect of reaction temperature in the presence of MCM-41 and SBA-15

The effect of the reaction temperature on the yield of phenolics in the presence of MCM-41 and SBA-15 were studied at a fixed reaction time of 1 h. The results in **Figure 7.4** show that the reaction temperature had an impact on TOL conversion, the proportions of aqueous fraction, and the residual lignin and solid residue fractions. The proportion of the solid residue was highest at 200 °C for both catalysts. This is possibly due to the formation of THF-insoluble high molecular weight compounds. The total mass balance of the main fractions considerably decreased to less than 80% (referred to initial TOL) at 350°C. This could be due to a higher proportion of gaseous products at high temperature and the formation of organic acids from the side chain of phenolic propanoid units (Barbier et al., 2012; Beauchet et al., 2012; Kang et al., 2013; Roberts et al., 2011). The yields of the solid residues increased at 350 °C compared to those at 250 and 300 °C, possibly due to the formation of char.

The amount of the aqueous fraction increased to a maximum (9.7%) with MCM-41 at 350 °C, but the maximum (7.0%) was achieved at 300 °C for SBA-15 (**Figure 7.4**). The amount of aqueous fraction generally increased with a decrease in the total solid (including residual lignin) (**Figure 7.4**). This may be related in part, to the fact that increasing the reaction temperature promotes the rate of breaking down the main linkages ( $\beta$ -O-4 ether bonds) in lignin to monomeric units (Deepa & Dhepe, 2014). However, working temperatures above 300 °C can result in decomposition of phenolic products to organic acids and char formation (Barbier et al., 2012; Kang et al., 2013). It was revealed that ether linkages in syringyl units (mainly  $\alpha$ - or  $\beta$ -O-4 bonds) were readily cleaved during depolymerization reaction at high temperatures. The addition of MCM-41 or SBA-15 may have inhibited condensation reactions and increased the amount of phenolics formed. However, re-polymerization and cross-linking between the reactive sites of the phenolics and the side chains of the degraded lignin could occur at high temperatures, hence increasing char formation (Roberts et al., 2011). The char formed could deposit on the surface of solid catalyst leading to a decrease of the specific area, and loss of active sites (Kang et al., 2013).

**Figure 7.5a** shows the syringol yields in aqueous fraction and in residual lignin. Syringol yields increased significantly with increasing temperature from 200 °C to 300 °C, then remained unchanged with MCM-41, but decreased with SBA-15 at 350 °C. On the

basis of this study, the reaction temperature of 300 °C was the optimum condition, where the syringol yields with MCM-41 and SBA-15 was 15.1% and 18.8% respectively. Furthermore, as shown in **Figure 7.5b**, increasing the reaction temperature from 200 °C to 250 °C significantly increased the syringol content in aqueous fraction. Further increases in temperature to 300 °C did not increase the syringol content in the aqueous fraction with MCM-41, but increased to 90.3% at 300 °C with SBA-15. The syringol contents in residual lignin fractions increased with increasing reaction temperature. The highest syringol contents in residual lignin were achieved at 350 °C with both catalysts.

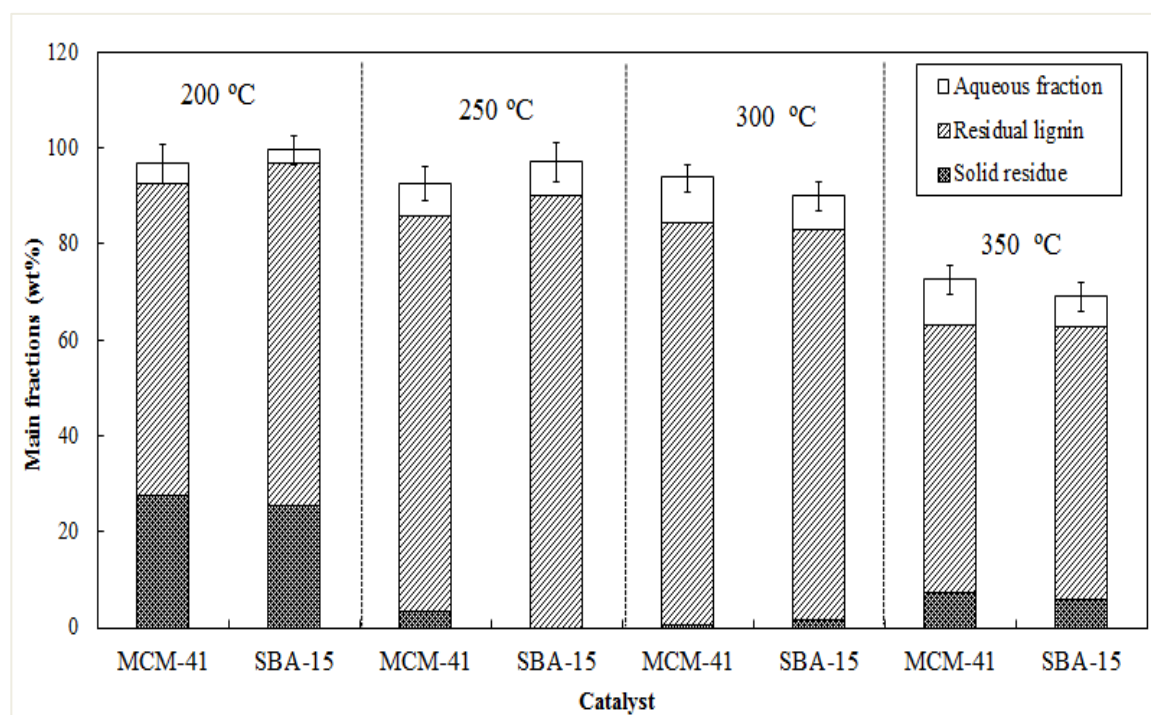


**Figure 7.4** Lignin distribution after reaction at different temperatures for 1 h.

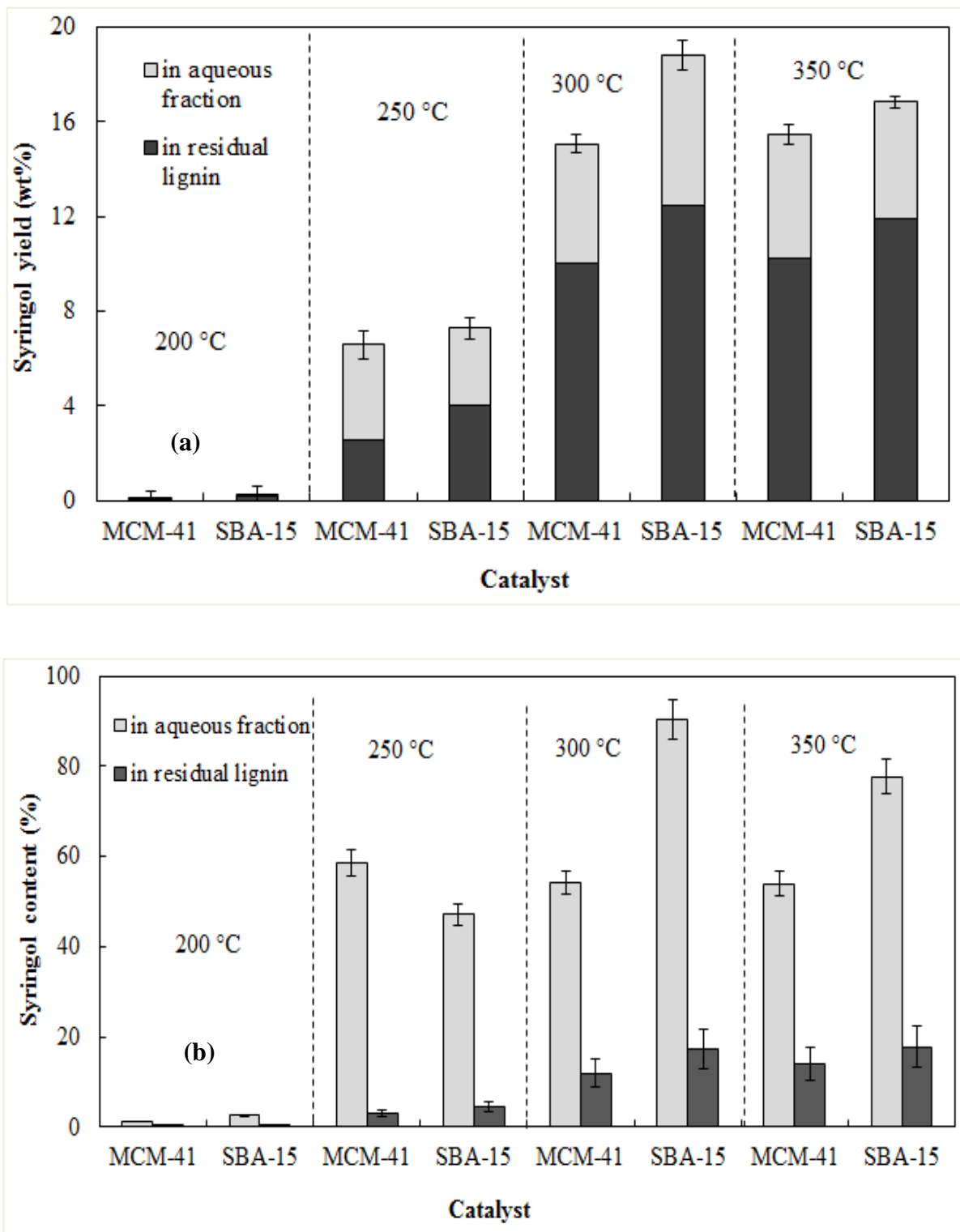


**Figure 7.5** Effect of temperature on syringol (a) yield and (b) content, (reaction time, 1 h).

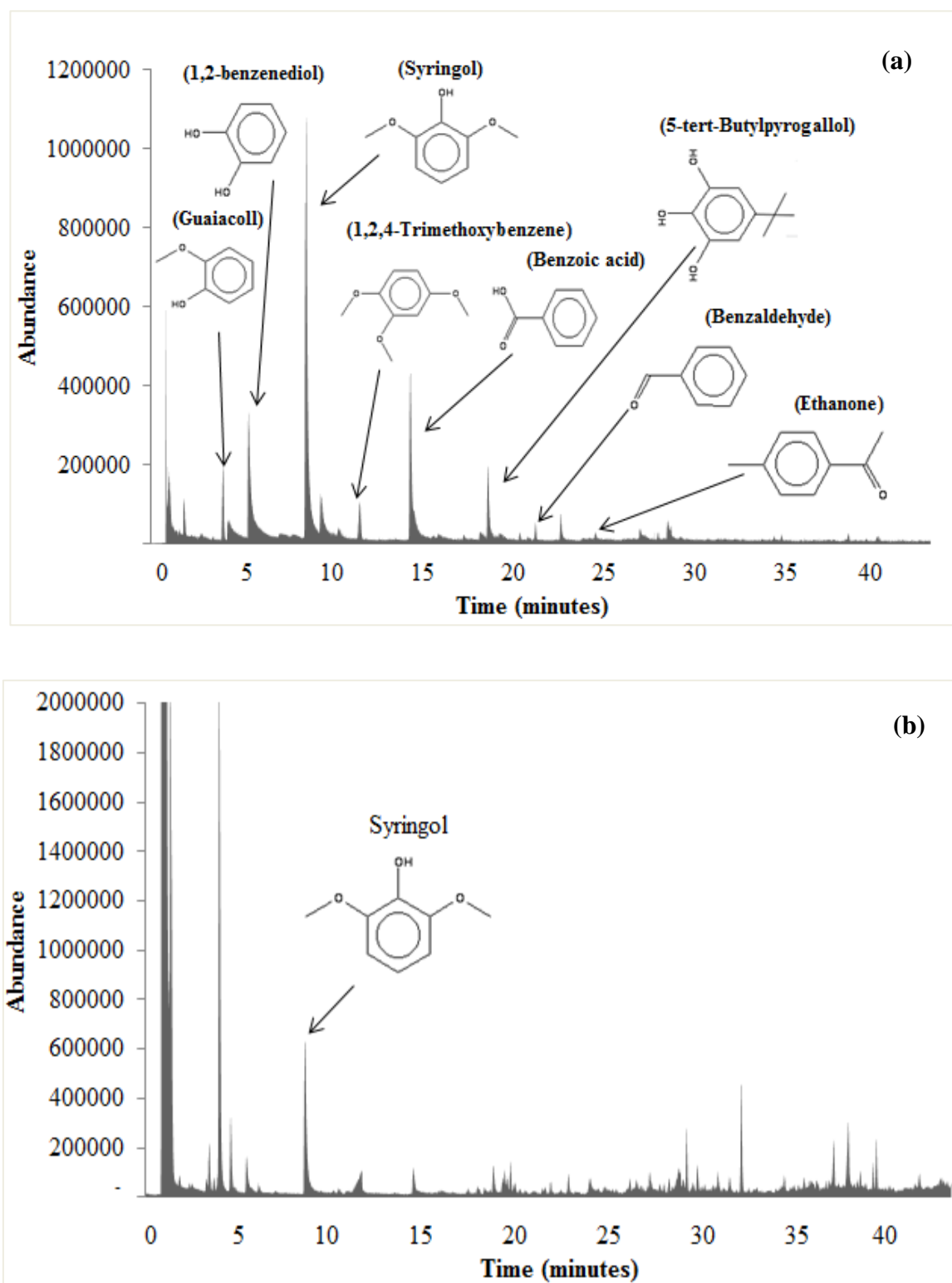


**Figure 7.6** GC-MS analysis of phenolic compound products (a) in aqueous fraction and (b) in THF solvent from residual lignin after lignin depolymerization reaction in the presence of SBA-15 at 300 °C for 1 h.

The GC/MS analysis results (**Figure 7.6(a)**), show that the main monomeric phenolic components present in the aqueous fraction from the reaction at 300 °C in the presence of SBA-15 were syringol, guaiacol, 1,2-benzendiol, 1,2,4-trimethoxybenzene, benzoic acid, 5-tert-butylpyrogallol, and 1-(4-hydroxy-3,5-dimethoxyphenyl)-ethanone. It seems that guaiacyl and syringyl structural lignin units are the precursors for the primary products from lignin depolymerization. For the phenolics in the residual lignin, as shown in **Figure 7.6(b)**, the dominant peak is syringol with a yield of 12.4% compared to TOL (**Figure 7.5a**) and a content of 17.2% in residual lignin fraction (**Figure 7.5b**).

### 7.2.1.3 Effect of solvent system in the presence of MCM-41 and SBA-15

The use of alcohol-water solvent mixture has been reported to limit diffusion effects in lignin depolymerization since lignin shows high solubility in polar organic solvents (*e.g.* methanol-water mixture and ethanol-water mixture) (Deepa & Dhepe, 2014). In this study, a methanol-water solvent system (methanol/water weight ratio of 50/50) was used to investigate the influence of solvent on the phenolic product yields and syringol contents. **Figure 7.7** shows the compound distribution after reaction in methanol-water mixture. The amount of aqueous fraction increased slightly, while the amount of solid residue decreased compared to the water system. As shown in **Table 7.3** and **Figure 7.8**, several phenolic monomers were formed in aqueous fraction and the composition was different to that with aqueous fraction derived in water alone (**Figure 7.6**). Compared to water as a solvent (**Figure 7.5a** at 300 °C), syringol yields increased in both aqueous fraction and in residual lignin. The total syringol yields with MCM-41 and SBA-15 were 20.4% and 23.0% respectively, 4-5% higher than those with the reactions in water. As shown in **Figure 7.8**, the syringol content in residual lignin with MCM-41 increased from 11.9% (water) to 17.8% (methanol/water mixture) and with SBA-15 increased from 17.2% (water) to 19.5% (methanol/water mixture). The syringol content in aqueous fraction with MCM-41 increased but decreased with SBA-15. The syringol contents in aqueous fraction and residual lignin fraction with SBA-catalyst and methanol/water solvent were 72.1% and 19.5% respectively. As shown in **Figure 7.9(a)**, GC-MS analysis of phenolic compound products in aqueous fraction from the reaction with SBA-15 indicated that the main monomeric phenols were syringol, 1,2-benzendiol, 1,2,4-trimethoxybenzene, benzaldehyde, 5-tert-butylpyrogallol, and ethanone. For the phenolics in the residual lignin, as shown in **Figure 7.9(b)**, the dominant peak is syringol.

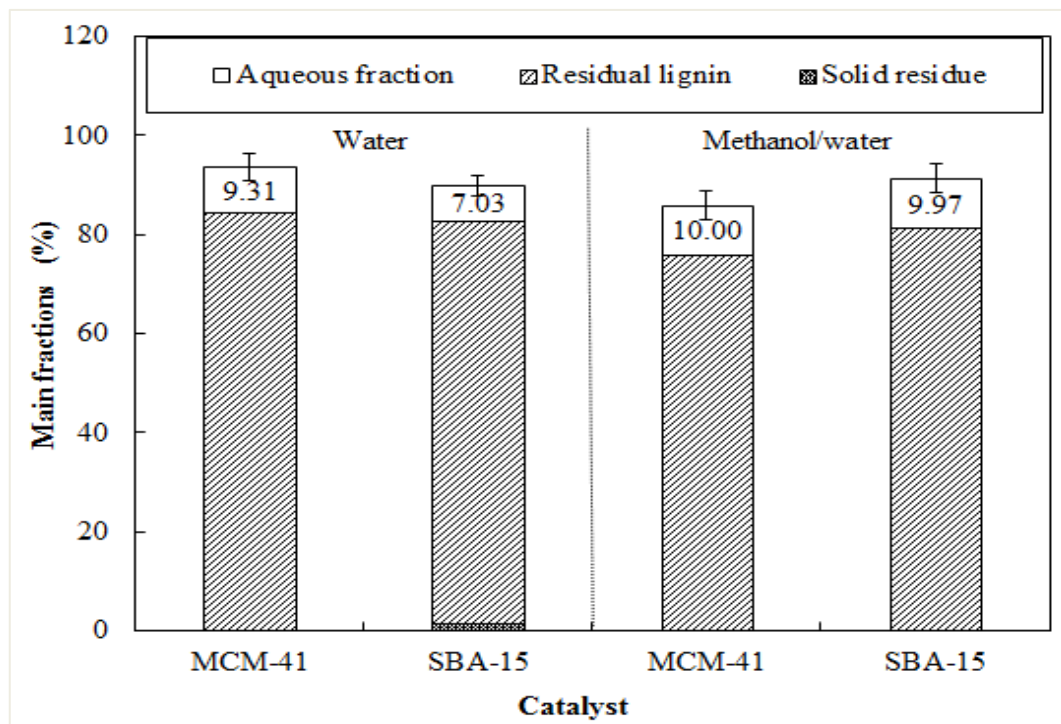


**Figure 7.7** Lignin distribution after reaction at 300 °C for 1 h with different solvent systems.

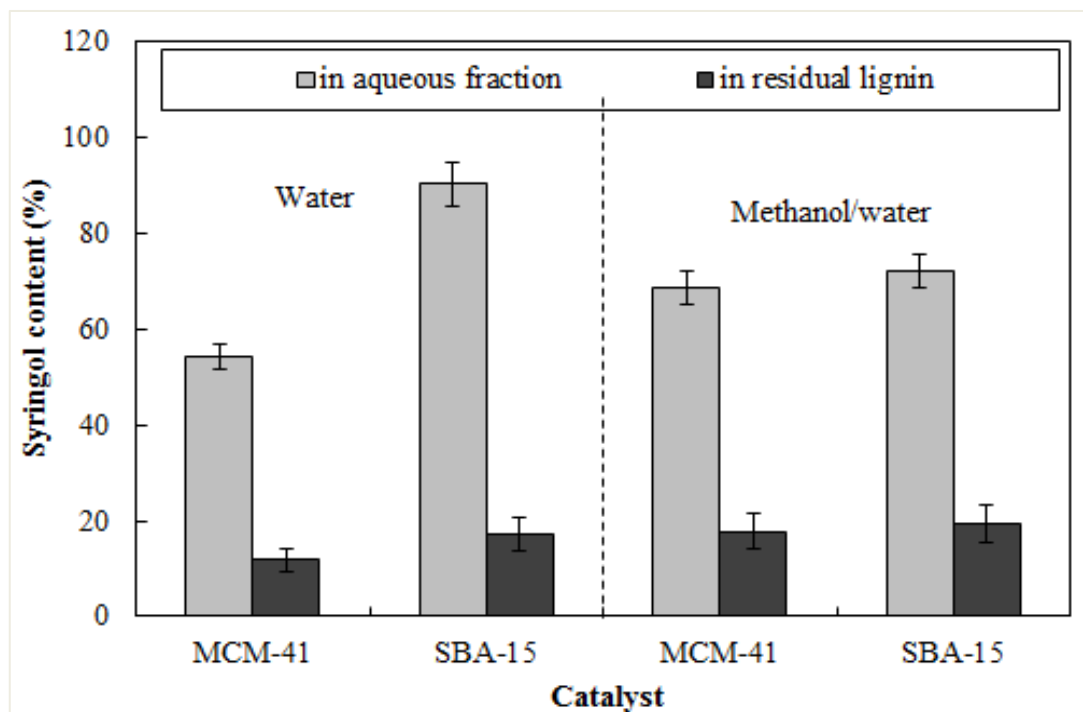


**Figure 7.8** Syringol contents in aqueous fraction and residual lignin fraction with different solvent systems after reaction at 300 °C for 1 h.

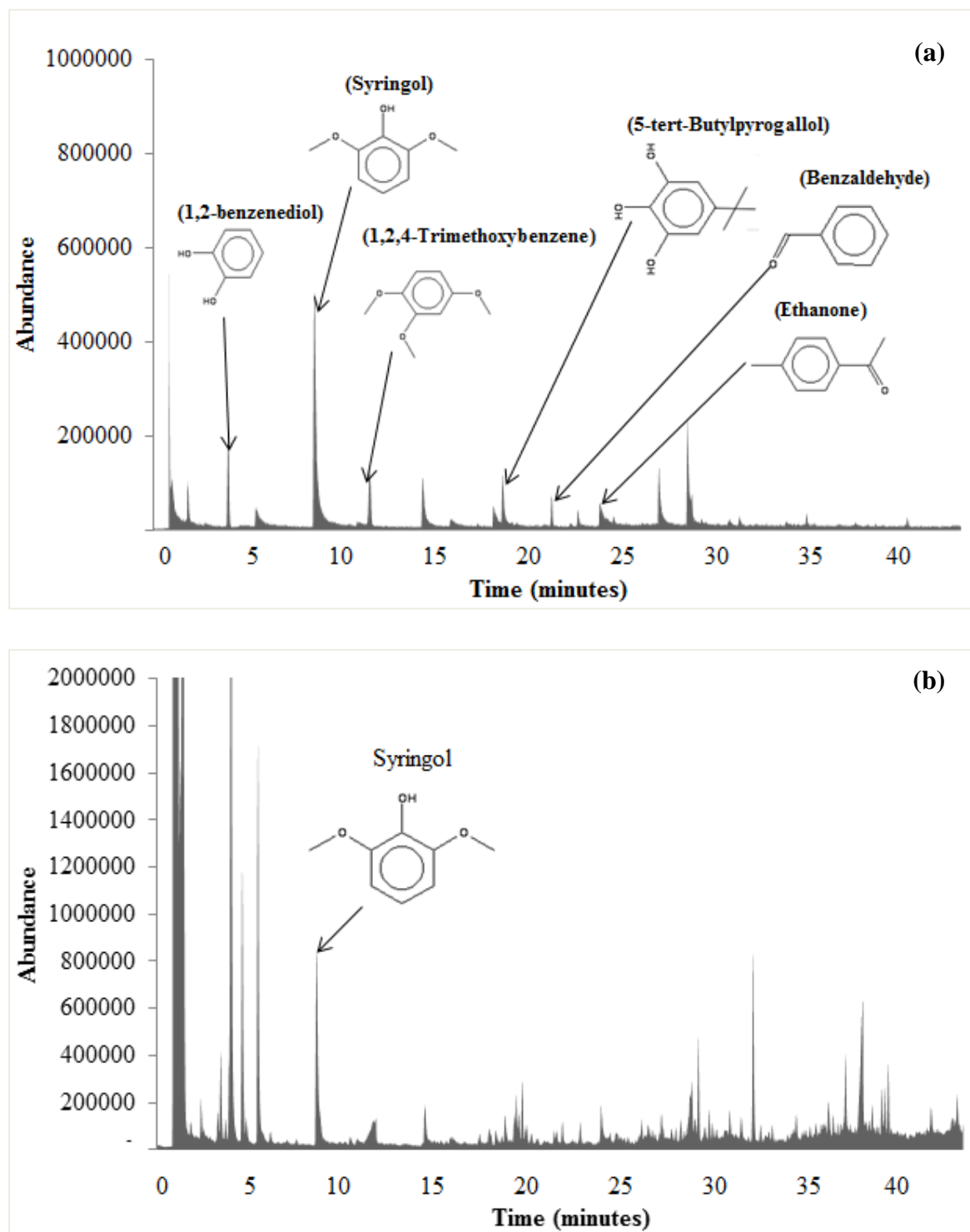


**Figure 7.9** GC-MS analysis of phenolic compound products (a) in aqueous fraction and (b) in THF solvent from residual lignin after lignin depolymerization reaction in the presence of SBA-15 with methanol/water mixture (50/50, wt/wt) at 300 °C for 1 h.

**Table 7.3** Yields of phenolic monomers at 300 °C with methanol/water mixture (50/50, wt/wt)<sup>a</sup>

Catalysts	Monomers in aqueous fraction (wt%)					Syringol in residual lignin fraction (wt.%)	Total syringol (wt.%)
	Syringol	1-(4-hydroxy-3,5-dimethoxyphenyl)-ethanone	1,2-benzenediol	4-hydroxy-3,5-dimethoxy-benzaldehyde	Phenol		
MCM-41	6.88	-	0.52	0.35	0.71	13.53	20.41
SBA-15	7.19	0.02	1.05	0.61	-	15.84	23.03

<sup>a</sup>All the yields were calculated by comparison with the initial amount of lignin.

## 7.2.2 Depolymerization of TOL under hydrothermal process in the presence of phosphate-based catalysts

### 7.2.2.1 Effect of catalyst on lignin depolymerization

The depolymerization of TOL under hydrothermal systems was firstly studied with and without the presence of solid catalysts ( $\text{CoP}_2\text{O}_6$  and  $\text{CaP}_2\text{O}_6$ ). The reaction using commercial sulfided  $\text{NiMo}/\text{Al}_2\text{O}_3$  was also compared. In this study, the reaction containing 35 mg of TOL in the presence of 35 mg of catalyst in 2 ml of water was initially tested at  $250^\circ\text{C}$  for 1 h with an initial pH of 7 and a reactor pressure of 1 bar (atmospheric pressure). As presented in **Figure 7.10**, the depolymerization reaction of TOL led to release of three main products: aqueous phenolic compounds fraction, residual lignin, and a solid fraction (containing char). It was noted that the proportion of gaseous products generated from the reaction was relatively low based on the amount collected; hence, it was not considered in this study.

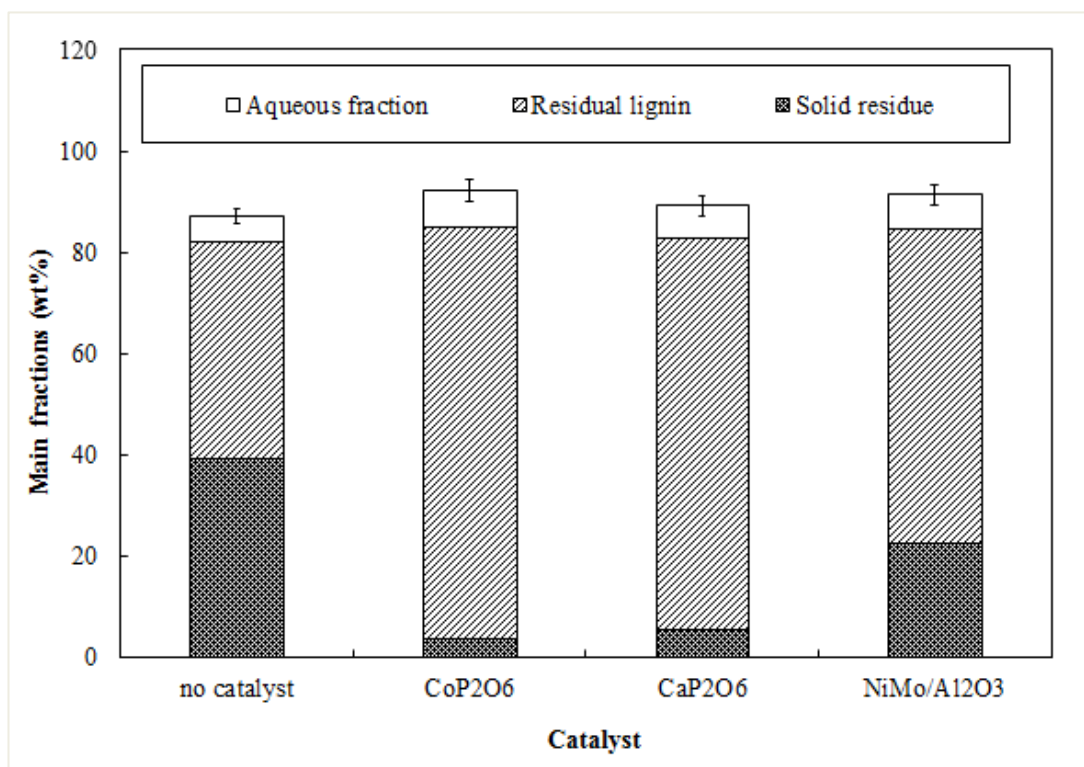


**Figure 7.10** Diagram of product separation after lignin depolymerization with and without solid catalysts.

Clearly, the presence of catalysts promoted the phenolics in the aqueous phase (4-5 wt.% compared to the reaction without catalyst). In addition, a higher proportion of residual lignin was closely related to a lower proportion of solid residue and vice versa. This could be due to the fact that the suitable acidity of these phosphate based catalysts prevents char formation and promotes cleavage of the main linkages of lignin (*i.e.*  $\beta$ -O-4 and  $\alpha$ -O-4). The total mass balance of the three fractions obtained with water is 87.2%, lower than the amounts obtained with the solid catalysts in the range of 89.3-92.3%, which is possibly due to the formation of gaseous products during the reaction and the formation of organic acids in aqueous phase (in phenolics and lignin-free liquid as earlier explained in **Figure 3.5**). For phosphate based catalysts (*i.e.*  $\text{CoP}_2\text{O}_6$  and  $\text{CaP}_2\text{O}_6$ ), they have low surface area around  $0.5 \text{ m}^2/\text{g}$ , while the acidity cannot analyze by  $\text{NH}_3$ -TPD techniques due to no internal pore to use analysis. Therefore, for the  $\text{CoP}_2\text{O}_6$  and  $\text{CaP}_2\text{O}_6$  catalysts were analyzed the acid property measurement giving the acid strength in the same range of  $+3.3 \leq \text{H}_0 \leq +4.8$ . It is well known that low value of  $\text{H}_0$  correspond to greater acid strength. Nevertheless, the range of acidity of phosphate based catalyzed still lower than homogeneous catalyst such as phosphoric acid in the range of +0.8 to +3.3 has been reported by (Daorattanachai et al., 2012).

The yields of monomeric phenols in the aqueous fraction and syringol in the residual lignin fraction were analyzed by GC-MS, as shown in **Table 7.4**. It can be seen that the additional the catalysts also increased the proportion of syringol in the residual lignin. Interestingly, a substantial amount of syringol was found associated with the lignin residue, particularly with the presence of catalysts. The syringol yield in the aqueous fraction increased, whereas the yield of ethanone decreased with the presence of catalysts. The use of  $\text{CoP}_2\text{O}_6$  promoted the spread of phenol products (*i.e.* syringol, ethanone, and benzoic acid); whereas the use of  $\text{CaP}_2\text{O}_6$  seemed more selectivity to syringol. The highest syringol yields in aqueous fraction and in residual lignin can be achieved from  $\text{CaP}_2\text{O}_6$  catalyst. The proportions of syringol observed in aqueous fraction and in residual lignin fraction are shown in **Figure 7.11**. It can be seen that the proportion of syringol in aqueous fraction significantly increased under a hydrothermal system. The highest proportion of syringol in aqueous fraction and the syringol contents in residual lignin were achieved with a  $\text{CaP}_2\text{O}_6$  catalyst.

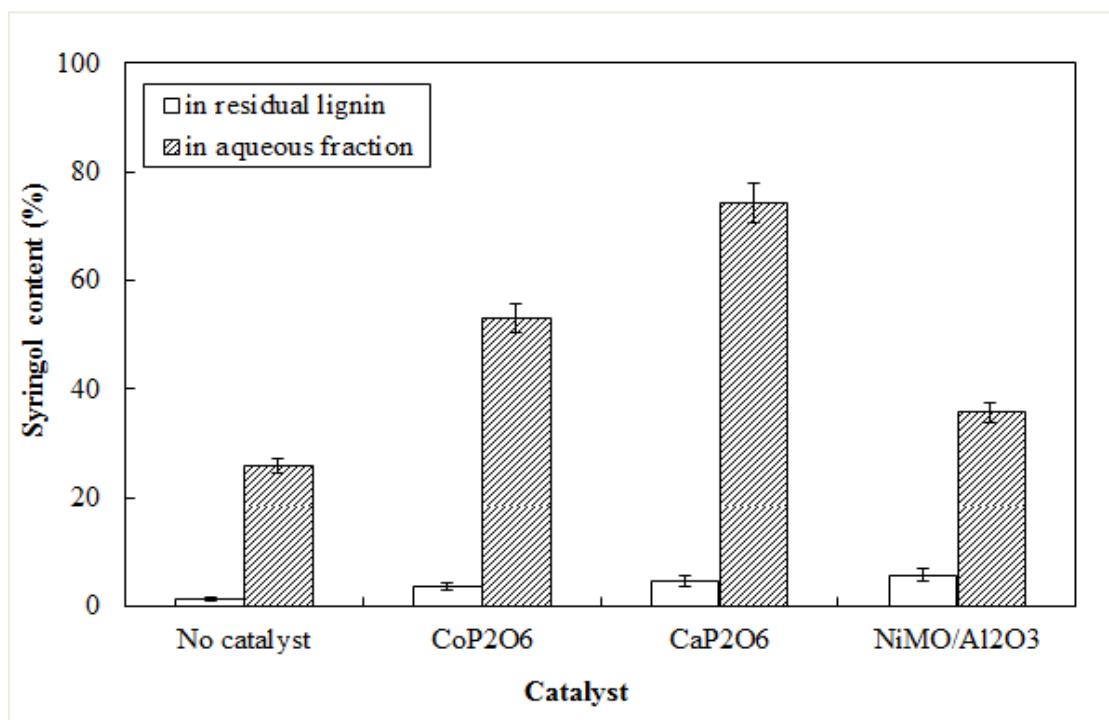


**Figure 7.11** Lignin distribution after reaction with different catalysts at 250 °C for 1 h.

The GC/MS analysis detected only monomeric phenolic compounds (mainly syringol). Other phenolic products were mainly in oligomeric forms and GC/MS could not obtain any peaks since the amount of unconverted lignin (residual lignin) could not be broken down to subunits and some of them were condensed. It is noted that residual lignins were also characterized by FT-IR spectroscopy in the wave numbers region of 4000-700  $\text{cm}^{-1}$ . As shown in **Figure 7.12**, the intensity of the band at 3445  $\text{cm}^{-1}$  assigned to OH groups appeared in the IR spectra of the TOL sample (Boeriu et al., 2004), residual lignin from the reaction without solid catalyst (no catalyst), and residual lignin from the reactions with CoP<sub>2</sub>O<sub>6</sub> and CaP<sub>2</sub>O<sub>6</sub>; on the other hand, it was absent in the spectra of residual lignin from the reactions with commercial sulfided NiMo/Al<sub>2</sub>O<sub>3</sub>. This could be due to the fact that sulfided NiMo/Al<sub>2</sub>O<sub>3</sub>, affect the strong oxidation and the degradation of the aliphatic chain of phenyl propane units of lignin (Casas et al., 2012). Moreover, the decrease of intensity of the band at 1225  $\text{cm}^{-1}$  assigned to 2<sup>nd</sup> OH group also confirms the loss of OH group during depolymerization process (Zhou, 2014). For the absorption of the C-H stretching in the methyl and methylene groups (around 2950 and 2820  $\text{cm}^{-1}$ ) (Boeriu et al., 2004), all residues lignin predominantly increased during the depolymerization reaction (Bai et al., 2013). The intensity of band at 1715  $\text{cm}^{-1}$  was carbonyl stretching in

unconjugated ketones and conjugated carboxylic groups, which was observed in all samples. At 1600, 1500, and 1426  $\text{cm}^{-1}$ , they refer to the adsorption of aromatic skeletal vibration bands, which are typically found in lignin (Bai et al., 2013; El Mansouri & Salvadó, 2007). These bands of residual lignin from the reaction with sulfided NiMo/Al<sub>2</sub>O<sub>3</sub> were relatively small. From TOL sample, the absorption bands of C-O stretching of syringyl ring (at 1325  $\text{cm}^{-1}$ ) and aromatic C-H deformation of syringol unit (at 1120  $\text{cm}^{-1}$ ) were stronger than those of stretching of guaiacyl ring (at 1265  $\text{cm}^{-1}$ ). Moreover, the intensity bands of aromatic C-H deformation of guaiacol unit were not observed. This could be due to the strong predominance of syringol unit in isolated lignins from woody eucalyptus (Beauchet et al., 2012; Ibarra et al., 2005). After depolymerization, the absorption bands of C-O stretching of syringyl ring and aromatic C-H deformation of syringol unit decrease, whereas the intensity bands of stretching of guaiacyl ring increases. This is in good agreement with the GC/MS results, which detected syringol as the main product of the reaction (Rencoret et al., 2011; Zakzeski et al., 2012).

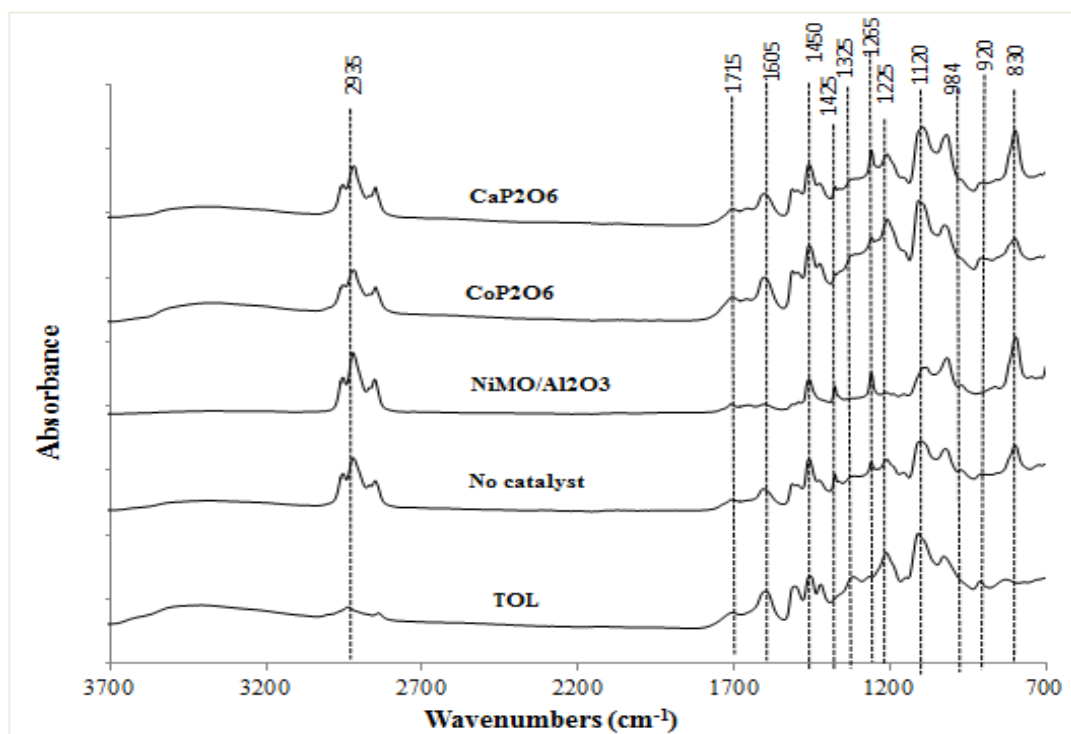


**Figure 7.12** FTIR spectra of TOL and residual lignin at 250 °C for 1 h.

The depolymerization reaction in the presence of  $\text{CaP}_2\text{O}_6$  achieved the highest purity of syringol (74.3 wt.%) in aqueous phenolics and the highest yield of total syringol product of 8.5 wt.% (referred to initial the TOL weight). The highest yield of total syringol product in residual lignin can also be achieved from the reaction with  $\text{CaP}_2\text{O}_6$  (3.59 wt.%) with small solid residue. In addition, the  $\text{CaP}_2\text{O}_6$  catalyst seemed to have prevented the char formation, and so, was chosen for further studies.

**Table 7.4** Yield of phenolic monomers at 250 °C<sup>a</sup>

Type of solid catalysts	250 °C						Syringol in residue lignin (wt.%)	Total syringol (wt.%)
	Monomers in aqueous phase (wt.%)							
	Syringol	1-(4-hydroxy-3,5-dimethoxyphenyl)-ethanone	Butylated hydroxytoluene	4-hydroxy-3,5-dimethoxy-benzaldehyde	1-(2,4,6-trihydroxy-3-methylphenyl)-1-butanone	Benzoic acid		
No catalyst	1.32	2.55	-	-	-	-	0.53	1.85
CoP <sub>2</sub> O <sub>6</sub>	3.79	0.05	-	-	-	2.09	2.88	6.67
CaP <sub>2</sub> O <sub>6</sub>	4.88	0.55	-	-	-	-	3.59	8.47
Sulfided NiMO/Al <sub>2</sub> O <sub>3</sub>	2.45	0.47	-	0.09	-	2.11	3.51	5.96

<sup>a</sup>All the yields were calculated in comparison to the initial amount of lignin.

### 7.2.2.2 Effect of reaction temperature in the presence of $\text{CaP}_2\text{O}_6$

The effect of the reaction temperature on the phenolic product yield and selectivity from TOL depolymerization in the presence of  $\text{CaP}_2\text{O}_6$  was studied at a fixed reaction time of 1 h. As shown in **Figure 7.13**, it was found that the reaction temperature shows significant impact on the formations of phenolic compounds in aqueous phase and lignin residue. It also affected the residual solid (char and high molecular weight compounds) and the overall TOL conversion. In detail, the lignin residue fraction increased with increasing reaction temperature from 200°C to 300°C and then dropped at 350°C. In case of phenolic compounds in aqueous fraction, the amount of them can be increased with the same trend of increasing temperature from 200°C to 300°C, particularly at 350°C seemed significantly increased. Nevertheless, the total mass balance of the main fractions at 350°C considerably decreased to less than 80% (referred to initial mass of lignin feedstock). This could be due to higher formation of gaseous products at high temperature and also formation of organic acids from side chain of poly-phenolic lignin. (Barbier et al., 2012; Beauchet et al., 2012; Kang et al., 2013; Roberts et al., 2011). For the lowest lignin, depolymerization was observed at 200°C because lignin could not break down at this temperature, which is in good agreement with (Deepa & Dhepe, 2014). Therefore, the increase in phenolic fraction with reducing residual solid (char and high molecular weight compounds) indicate that increasing reaction temperature promoted the rate on breaking down the main linkages ( $\beta$ -O-4 ether bonds) in lignin to be faster than on residual solid forming. It was revealed that ether linkages among syringyl units (mainly  $\alpha$ - or  $\beta$ -O-4 bonds) were readily cleaved during depolymerization reaction at high temperatures. The additional of  $\text{CaP}_2\text{O}_6$  could inhibit the condensation at active site of lignin during depolymerization reaction, whereas high temperature and/or long time (in this work at above 300 °C and 1 h) increased the monomeric phenolic product rate, but could lead to re-polymerization and cross-linking between the reactive sites of the combined phenol and the side chains of the degraded lignin, hence increasing the char formation composition in residual solid (Roberts et al., 2011). The characteristics such as XRD patterns, the SEM images of the  $\text{CaP}_2\text{O}_6$  catalyst has been also studied by (Daorattanachai et al., 2012). It was revealed that majority of peaks with the single phase of the phosphate can be obtained well-crystallized structures with XRD analysis and the samples are in the form of sintered materials of primary particles to achieve the size in the range of 100–500 nm. Typically, the char formation could deposit on the surface of conventional solid catalysts leading to decreasing of

specific area (Kang et al., 2013) until deactivation of solid catalysts. For  $\text{CaP}_2\text{O}_6$ , it seemed novel catalyst for preventing char formation with suitable acidity of catalysts ( $+3.3 \leq \text{H}_0 \leq +4.8$ ) and has also obtained a small surface area ( $0.5 \text{ m}^2 \cdot \text{g}^{-1}$ ).

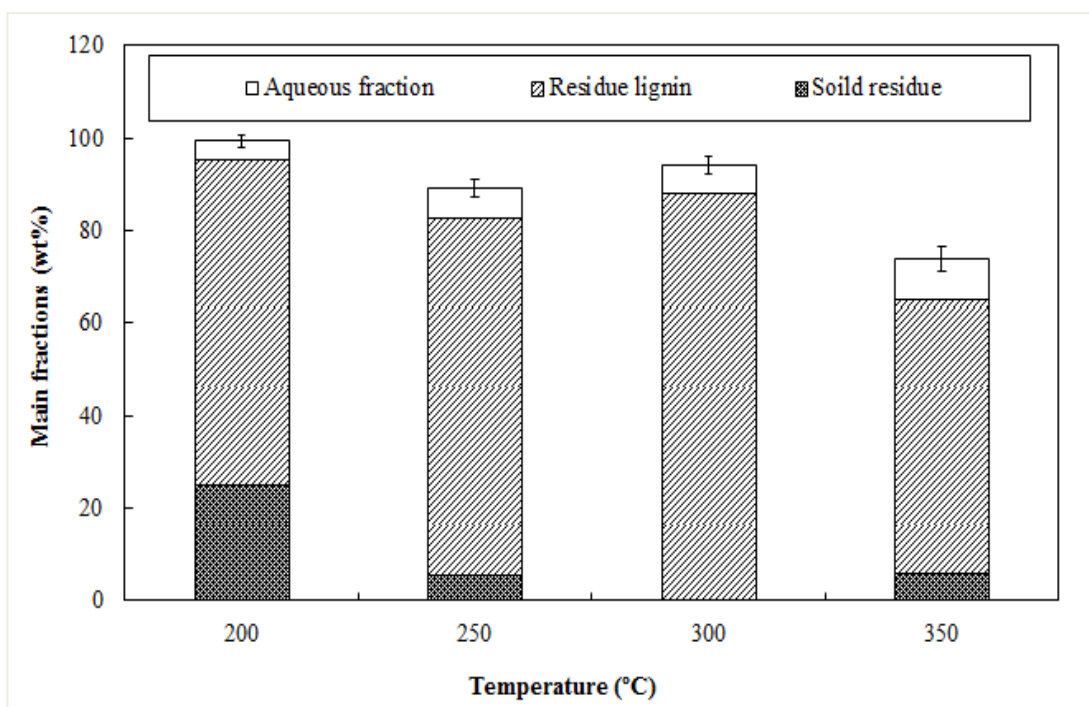


**Figure 7.13** Lignin distribution after reaction in the presence of  $\text{CaP}_2\text{O}_6$  at different temperatures for 1 h.

The syringol yields in the aqueous phase and in residual lignin with additional  $\text{CaP}_2\text{O}_6$  for the depolymerization reaction is shown in **Figure 7.14a**. Syringol yields increased significantly with increasing temperature from 200 °C to 300 °C, and became steady with  $\text{CaP}_2\text{O}_6$  at 350 °C. Based on this study, the reaction temperature of 300 °C was the optimum condition where the total syringol yields with  $\text{CaP}_2\text{O}_6$  were achieved 14 wt.% (yields in aqueous phase and in residual lignin around 4.1 wt.% and 9.8 wt.%, respectively). Furthermore, as shown in **Figure 7.14b**, the additional  $\text{CaP}_2\text{O}_6$  for depolymerization process increased reaction temperature from 200 °C to 250 °C significantly increased syringol content in aqueous fraction; whereas increase the temperature above 250 °C affect significantly to decrease syringol content in aqueous fraction. According to a higher temperature (250 °C), the syringol content decreased, which could be due to the further cracking of other compounds (Barbier et al., 2012). Therefore, the highest syringol content in aqueous fraction can be achieved 74.3 wt.% at 250 °C

for 1 h. The post-reaction pH of solvent with additional  $\text{CaP}_2\text{O}_6$  reduced to 3.5 at 300 °C. The change in final pH could be due to the leaching of acid from  $\text{CaP}_2\text{O}_6$  could lead to catalyst deactivation for the prolong reaction run. Therefore, the use  $\text{CaP}_2\text{O}_6$  for depolymerization reaction above 250 °C is possible catalyst starting to deactivation, which are good agreement with (Daorattanachai et al., 2012). The temperature of 300 °C was chosen for further study because this temperature can achieve the highest yield of total syringol after lignin depolymerization.

According to GC/MS analysis, as shown in **Figure 7.15(a)**, the main monomeric phenolic components in the aqueous fraction from the reaction at 300 °C in the presence of  $\text{CaP}_2\text{O}_6$  consist of syringol, guaiacol, 1,2-benzendiol, benzoic acid, benzaldehyde, creosol, 5-tert-butylpyrogallol, and ethanone. It seems that coniferyl and sinapyl alcohols being structural lignin units are the primary products from lignin depolymerization. For the phenols products in residue lignin after dissolving by THF, as shown in **Figure 7.15(b)**, the dominant peak is mainly syringol with the yield 9.8 % based on weight of initial lignin and 11.1 %wt based on the weight of total lignin residue.

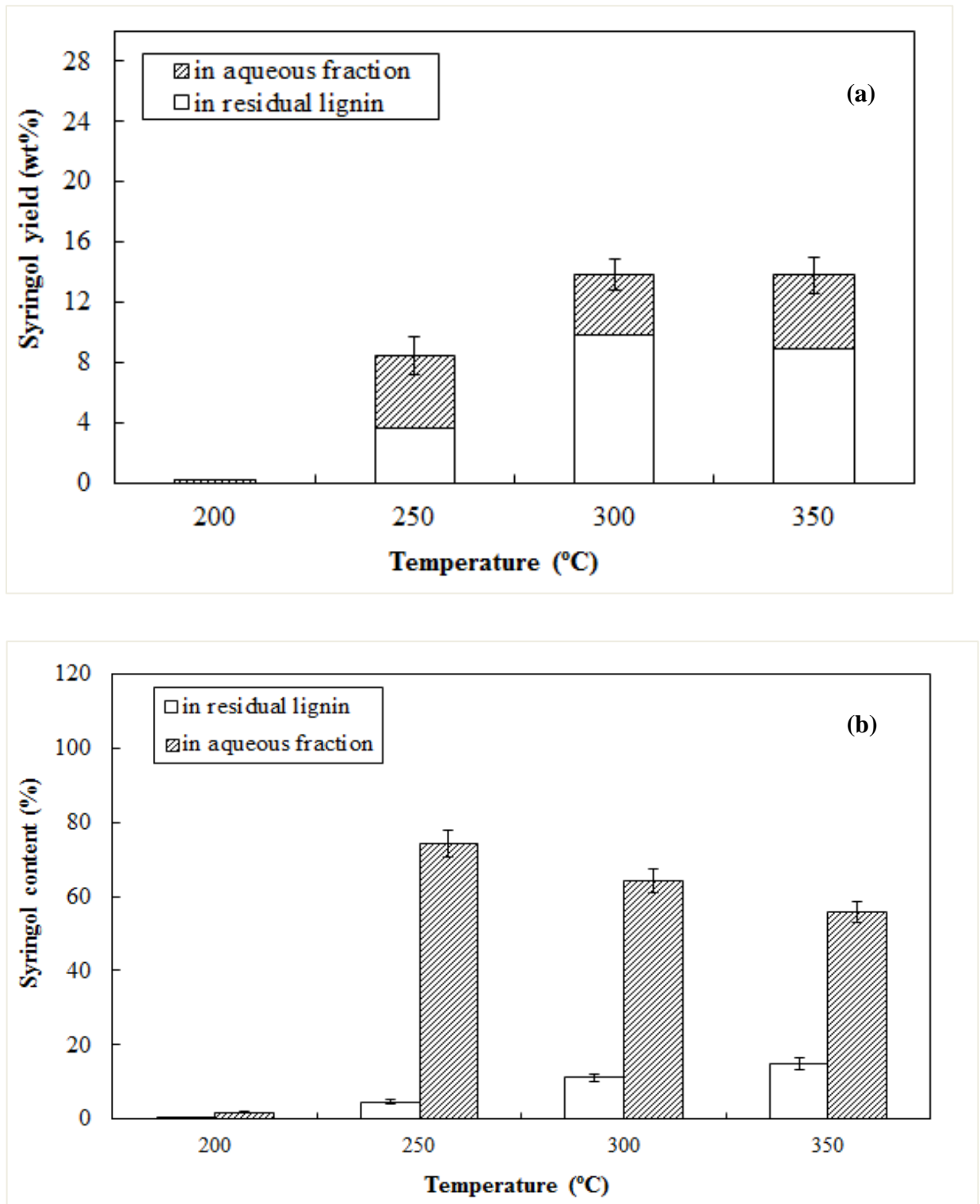


**Figure 7.14** Effect of temperature in the presence of  $\text{CaP}_2\text{O}_6$  on syringol (a) yield and (b) content. Reaction time: 1 h.

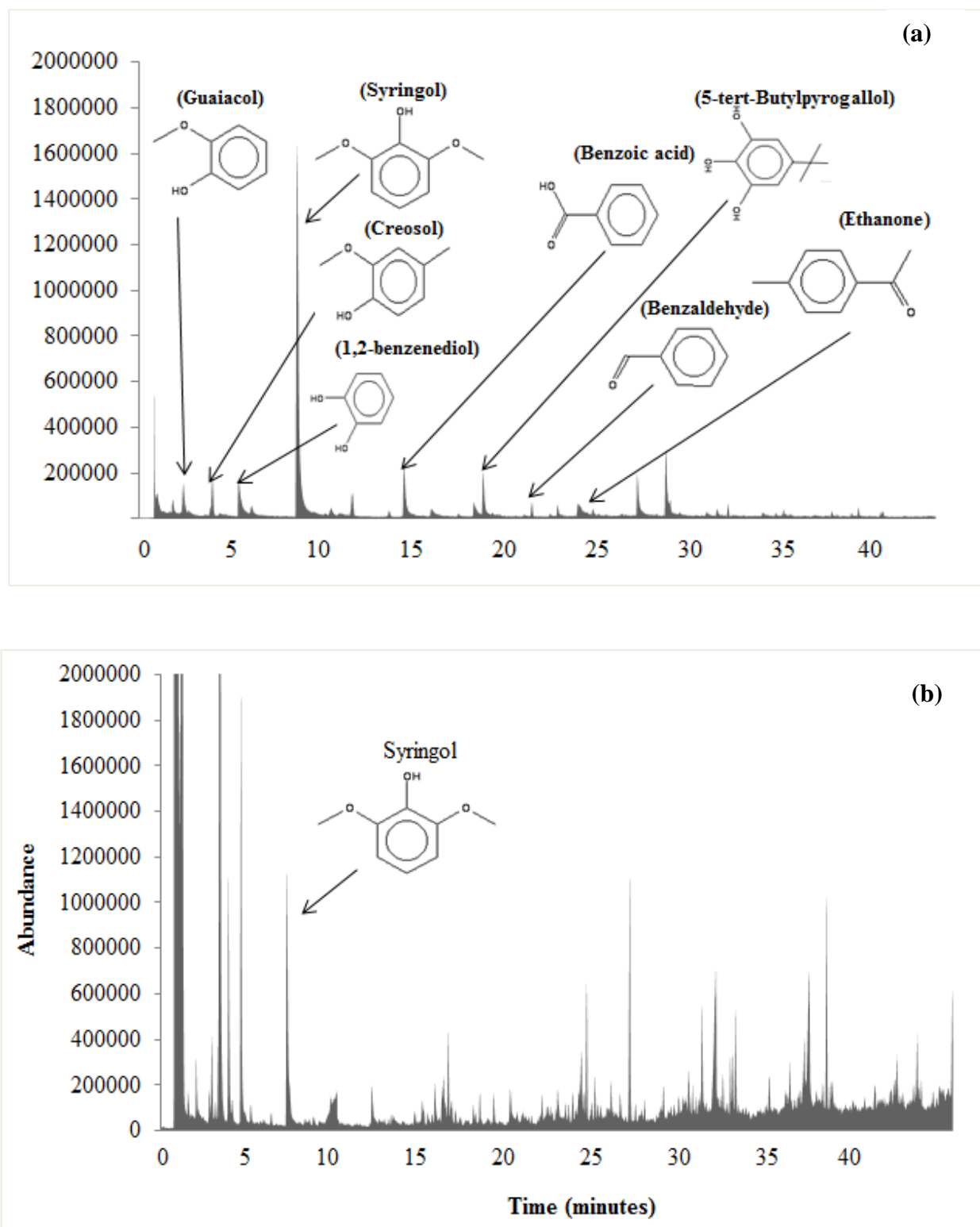


**Figure 7.15** GC-MS-identified phenolic compounds in (a) aqueous fraction and (b) residual lignin fraction after reaction in the presence of  $\text{CaP}_2\text{O}_6$  with water at  $300\text{ }^\circ\text{C}$  for 1 h.

### 7.2.2.3 Effect of solvent system in the presence of $\text{CaP}_2\text{O}_6$

The use of an alcohol-water solvent mixture solvent has been reported to solve the restricting of the diffusion limitation in lignin depolymerization, since lignin typically shows high solubility in organic solvents (*i.e.* methanol-water mixture and ethanol-water mixture) (Deepa & Dhepe, 2014), and could eventually lead to the achievement of high monomeric aromatic compound yield. In this study, methanol-water solvent system (methanol/water weight ratio of 50/50) was applied to determine its influence on the phenolic product yield and selectivity from TOL depolymerization in the presences of  $\text{CaP}_2\text{O}_6$  at 300 °C for 1 h. As shown in **Figure 7.16**, it was found that the use methanol-water solvent mixture promotes the formation of phenolic compounds in aqueous fraction and lignin residue, compared to the use of single water as solvent. It also showed positive effects on residual solid and overall TOL conversion. **Figure 7.17a** shows the syringol yield in residual lignin and aqueous fraction with use water for solvent compared to using methanol-water solvent. It was found that the use alcohol-water solvent can promote total syringol yield; whereas the syringol content in aqueous phase decreased, as shown in **Figure 7.17b**.

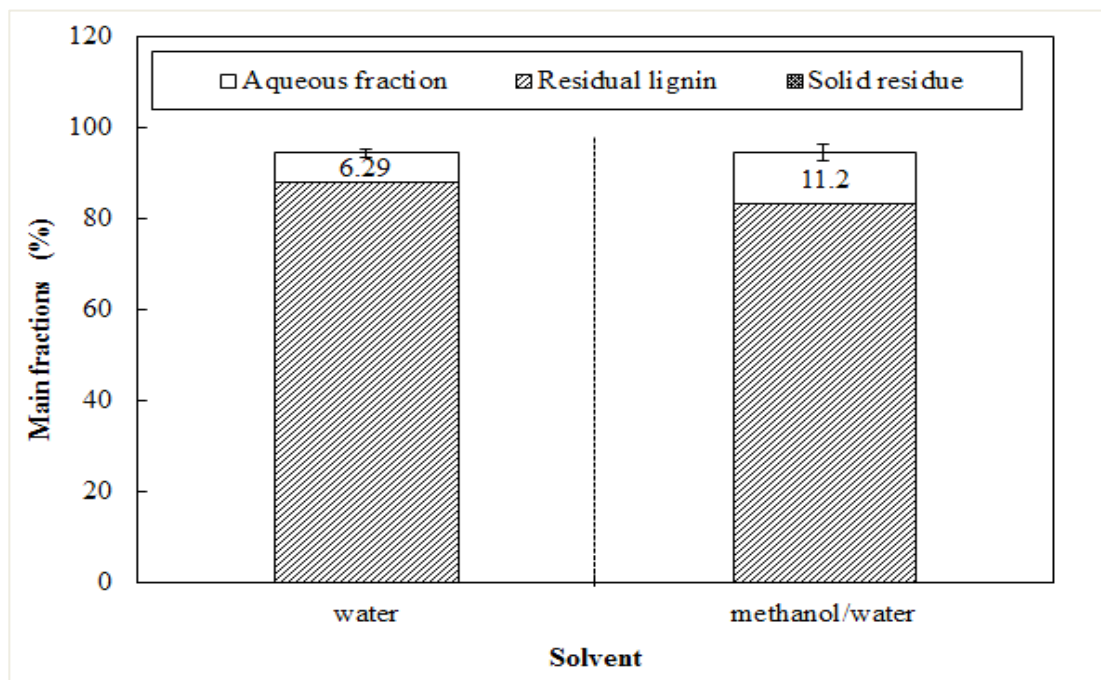


**Figure 7.16** Lignin distribution after reaction in the presence of  $\text{CaP}_2\text{O}_6$  at 300 °C for 1 h with different solvent systems.

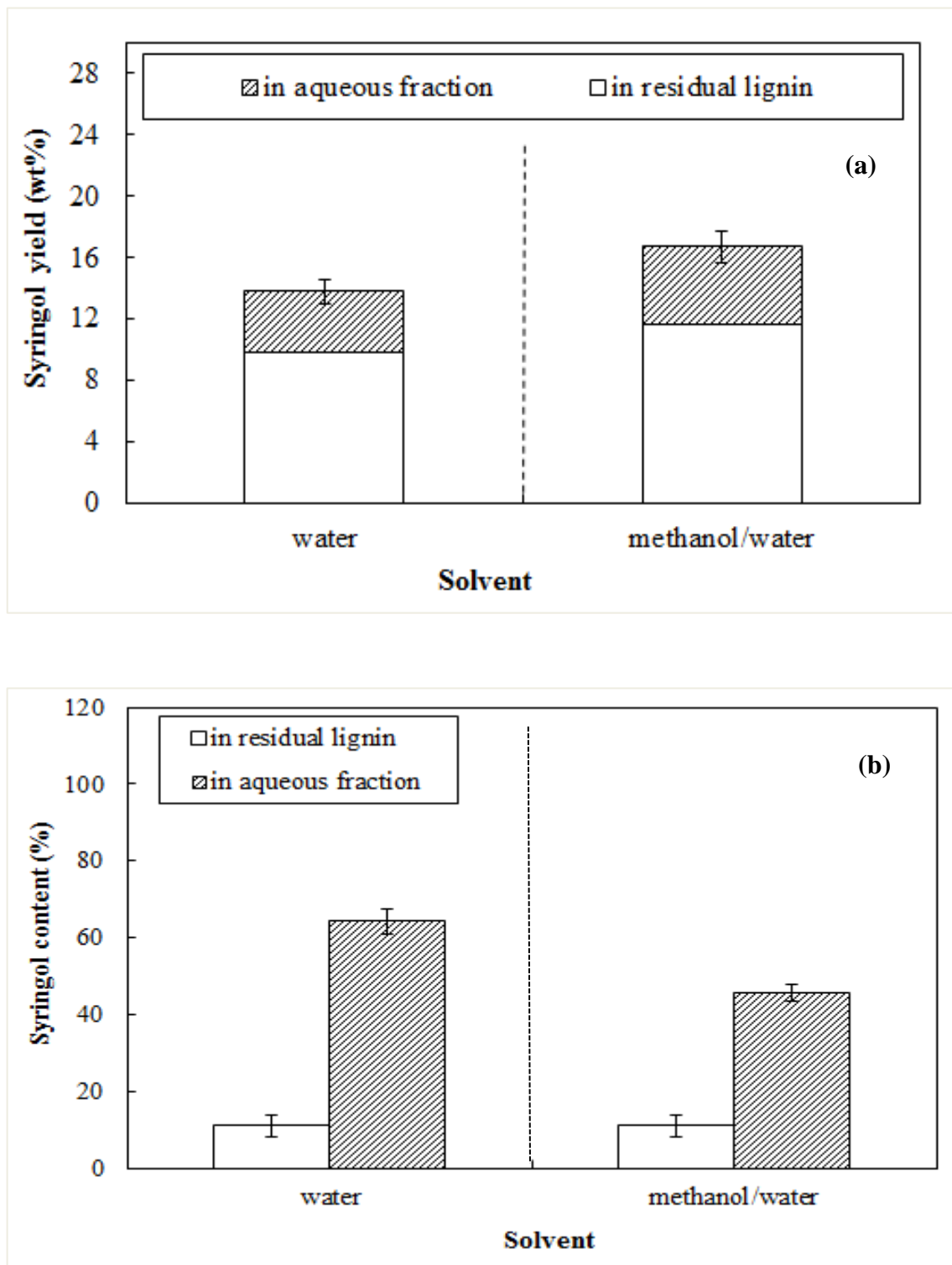


**Figure 7.17** Effect of different solvents in aqueous fraction and residual lignin fraction in the presence of  $\text{CaP}_2\text{O}_6$  on syringol (a) yield and (b) content at 300 °C for 1 h.

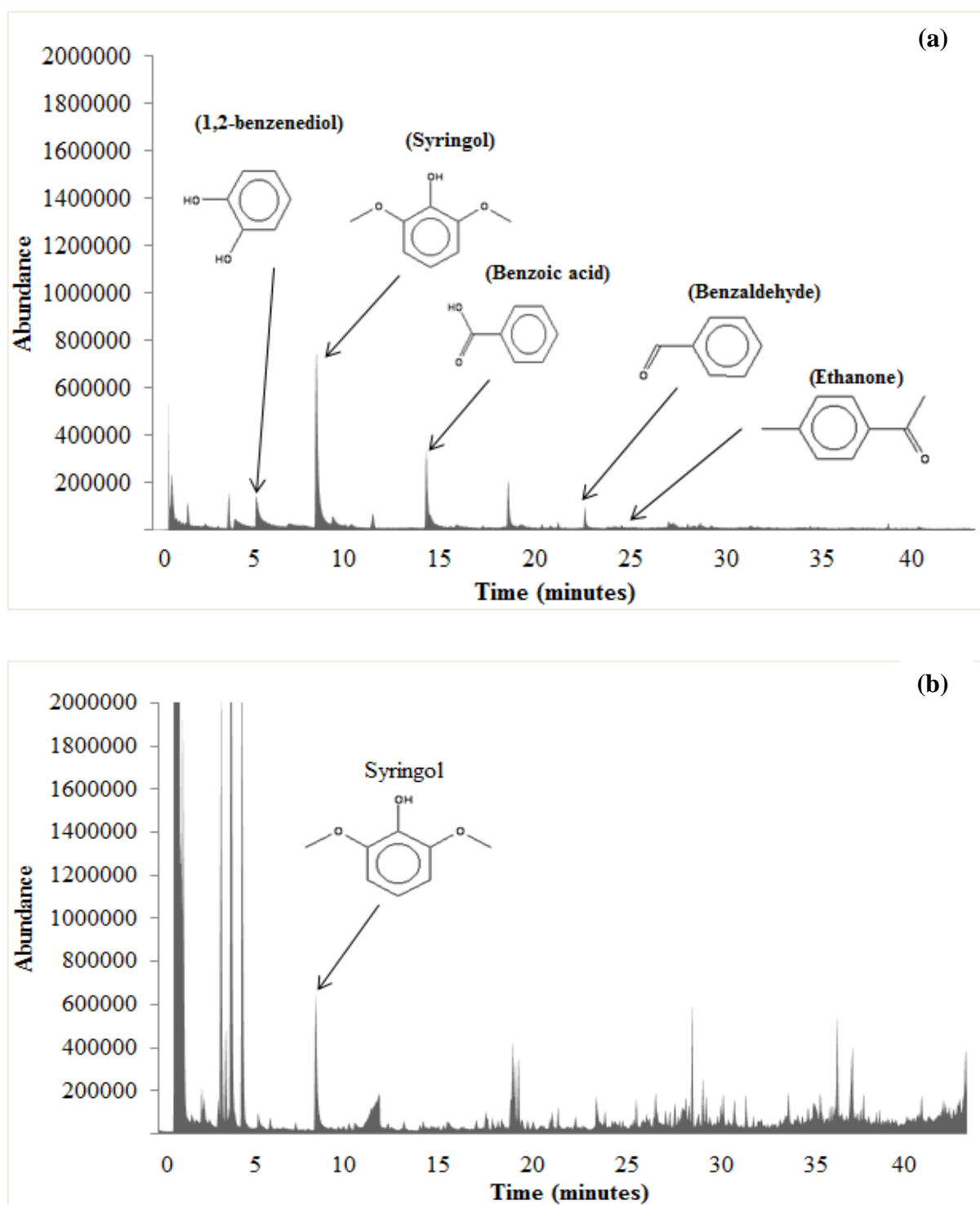


**Figure 7.18** GC-MS-identified phenolic compounds in (a) aqueous fraction and (b) residual lignin fraction after reaction in the presence of  $\text{CaP}_2\text{O}_6$  with methanol/water solution (50/50, wt/wt) at 300 °C for 1 h.

As shown in **Figure 7.18(a)**, GC-MS analysis of phenolic compound products in the aqueous fraction from the reaction with additional  $\text{CaP}_2\text{O}_6$  at 300 °C for 1 h, indicated that the main monomeric phenols were syringol, 1,2-benzendiol, benzoic acid, benzaldehyde, and ethanone. The highest composition in aqueous phase was syringol (45.7 % in aqueous phenolics or 5.12 % of initial lignin). For the phenol products in residue lignin, the dominant peak is also syringol with the total yield of 11.6 % based on weight of initial lignin and the syringol content in residual lignin 11.1 % based on the weight of total lignin residue (**Figure 7.18(b)**). Based on all studies, the reaction temperature of 300 °C using methanol-water solvent system (50/50 wt/wt) in the presence of  $\text{CaP}_2\text{O}_6$  was then optimum conditions to achieve the highest total syringol yield of 16.7 %w/w (including syringol in aqueous phase, and extracted syringol from residue lignin).

Depolymerization process is one of the primary methods for fragment lignin into monomeric phenolic products for the biorefinery process, because phenols can be used as feedstock for producing industrial mono-aromatic compounds (*i.e.* benzene, and xylene), liquid fuels and polymers. Up to now, the literature reviews (Pandey & Kim, 2011; Wang et al., 2013) have been reported many techniques, such as alkalines (*i.e.* NaOH,  $\text{CaOH}_2$ , KOH), acids (a few literature reviews), ionic liquids, and super critical fluids. Each technique can generate various ranges of phenol products as well as having its own advantages and disadvantages. This work focused on the use of hydrothermal technology, from which the depolymerization reaction occurs efficiently under high temperature and without initial any gas at atmosphere in the presence of solid catalysts. It is noted that the uses of solid acid catalysts have numerous advantages over liquid catalysts regarding activity, selectivity, catalyst life, and ease recovery and reuse. Here, synthesized two groups of solid catalysts; mesostructured silica catalysts (*i.e.* SBA-15, MCM-41,  $\text{ZrO}_2$ -SBA-15 and  $\text{ZrO}_2$ -MCM-41) and phosphate based catalysts (*i.e.*  $\text{CoP}_2\text{O}_6$  and  $\text{CaP}_2\text{O}_6$ ) were synthesized tested toward the depolymerization reaction.

Interestingly, in this study, the reaction was performed over organosolv lignin from woody eucalyptus under high temperature (300°C) without initial pressurization in the presence of mesostructured silica catalysts (*i.e.* SBA-15, MCM-41,  $\text{ZrO}_2$ -SBA-15 and  $\text{ZrO}_2$ -MCM-41). These catalysts have been reported to show good catalytic cracking of lignin to bio-oil via liquefaction; nevertheless, no study has previously reported the production of high yield and selectivity of syringol from the depolymerization of woody biomass. The benefits of SBA-15 are their high surface area and acidity, which lead to the

desirable environment for converting long lignin polymer to high quality monomeric phenolic compounds. It was observed in the present work that the reaction with SBA-15 in methanol-water mixture (50:50 wt/wt) produced relatively a high yield of syringol up to 23.0 % (in aqueous fraction and in residual lignin) with only small amounts of other phenolic compounds (*i.e.* ethanone, 1,2-benzenediol, and benzaldehyde) produced. In addition, high purity of syringol in the aqueous fraction (72.12 wt.%) was achieved. From the results of experiments, it was clearly found that the best type of catalyst for depolymerization was SBA-15. It has been known that the surface area, pore structure, and total acidity are typically important factors for solid acid performance. Solid acid catalysts being considered for lignin depolymerization should have a large number of Brønsted acid sites, good affinity for the reactant substrates and good thermal stability. In the present work, solid acid catalysts were characterized to determine their surface area and acid properties (*i.e.* amount of acid site ( $\mu\text{mol/g}$ ), and density of acid site ( $\mu\text{mol/m}^2$ )) to correlate their physical and chemical properties with their depolymerization performance. It was found that the catalytic activity trend is in good agreement with the acid density of these catalysts, from which the catalyst with the highest acid site density like SBA-15 can enhance the great reactivity toward depolymerization reaction. It can be revealed that the SBA-15 catalysts are considered as the most promising catalyst for lignin depolymerization, since they provide good access of reactants to the acidic sites. The mechanism of lignin depolymerization with SBA-15 catalysts is similar to that of homogeneous acids, from which protons attack the  $\beta$ -O-4 ether linkages in the lignin structure.

The depolymerization mechanistic route consists of the following steps: (1) a water molecule adsorbs onto the acid site of SBA-15 via an intermolecular hydrogen bond; (2) the soluble lignin diffuses into the internal pores of the SBA-15; (3) the lignin undergoes depolymerization over the acid site with adsorbed water; and (4) the depolymerization products diffuse out of the pores. So, these mechanisms for depolymerization over SBA-15 need to be dissolved in solvent and be converted into short phenolic chains to make full use of Bronsted acid sites internal channels of SBA-15. Deepa and Dhepe (Deepa & Dhepe, 2014) reported that the use of alcohol-water solvent mixture could efficiently minimize the diffusion limitation for lignin depolymerization due to the high solubility of lignin in this organic solvent system, and lead to the achievement of high monomeric aromatic compound yield. The suitable alcohol/water ratios have been reported to be in the range of

40-60 wt.% (Patil et al., 2014), which is in good agreement with the observation in this study.

In addition, for the phosphate-based catalysts (*i.e.*  $\text{CoP}_2\text{O}_6$  and  $\text{CaP}_2\text{O}_6$ ), the depolymerization reaction occurs efficiently under high temperature and without initial any gas at atmospheric pressure. Here, synthesized phosphate based catalysts were synthesized tested toward the depolymerization reaction. Interestingly, in this study, the reaction was performed over organosolv lignin from woody eucalyptus under high temperature ( $300^\circ\text{C}$ ) without initial pressurization in the presence of phosphate based catalysts. These catalysts have been reported to show good catalytic cracking of lignin to bio-oil via liquefaction, nevertheless, no study has previously reported the production of high yield and selectivity of syringol from the depolymerization of woody biomass. In addition, it was observed from the present work that the reaction with  $\text{CaP}_2\text{O}_6$  in methanol-water mixture (50/50 wt.%) gains relatively high yield of syringol up to 16.7 % (in aqueous fraction and in residual lignin) with only small amounts of other phenolic compounds (*i.e.* 1,2-benzendiol, benzoic acid, benzaldehyde, and ethanone) produced. From our understanding, no study has previously reported the production of high yield and selectivity of syringol from the depolymerization of woody biomass with additional phosphate based catalysts (*i.e.*  $\text{CoP}_2\text{O}_6$  and  $\text{CaP}_2\text{O}_6$ ). Recently, (Wang et al., 2013) summarized the performance of several solid catalysts for lignin conversion into phenol products, as shown in **Table 7.5**. The activities of these catalysts are also compared to the catalysts studied in this work.

**Table 7.5** Solid catalyzed lignin depolymerization (Wang et al., 2013)

Lignin	Type of Catalysts	Reaction conditions		Major products	Yield (wt.%)
		T (°C)	P (MPa)		
This work organosolv eucalyptus lignin	SBA-15	300	-	Syringol	23.03
This work organosolv eucalyptus lignin	CaP <sub>2</sub> O <sub>6</sub>	300	-	Syringol	16.7
Kraft lignin	(1) Si-Al catalyst/H <sub>2</sub> O/butanol	200-350		Phenols	6.5
	(2) ZrO <sub>2</sub> -Al <sub>2</sub> O <sub>3</sub> -FeO <sub>x</sub>	300	1.1-23		
Organosolv switchgrass lignin	16 wt.% formic acid	350	-	4-Propylguaiacol	7.8
	4 wt.% Pt/C 80 wt.% ethanol			4-Methylguaiacol	5
Acidic hydrolysis spruce lignin	4.4 wt.% formic acid	300	9.6	Guaiacol	2
	0.15 wt.% Pd catalyst			Pyrocatechol	1.8
	0.94 wt.% Nafion SAC-13			Resorcinol	0.5
Enzymatic hydrolysis spruce Lignin	4.4 wt.% formic acid	300	9.6	Guaiacol	1.7
	0.15 Pd catalyst			Pyrocatechol	1.3
	0.94 wt.% Nafion SAC-13			Resorcinol	1
Kraft spruce lignin	4.4 wt.% formic acid	300	9.6	Guaiacol	4.7
	0.15 wt.% Pd catalyst			Pyrocatechol	4.9
	0.94 wt.% Nafion SAC-13			Resorcinol	1.2

**Table 7.5** Solid catalyzed lignin depolymerization (continue) (Wang et al., 2013)

Lignin	Type of Catalysts	Reaction conditions		Major products	Yield (wt.%)
		T (°C)	P (MPa)		
Lignosulfonate	Ni/C, NiLa/C, NiPt/C, NiCu/C, NiPd/C, and NiCe/C	200	5	Guaiacol	10
Birch sawdust lignin	Ni/C	200	-	Propenylguaiacol Propenylsyringol	12 36
Enzymatic hydrolysis corn stalk lignin	Pt/C, Pd/C, Ru/C	200–250	1–6	4-Ethylphenol 4-Ethylguaicol	0.13–3.1 0.06–1.4
Organosolv olive tree pruning lignin	Ni, Pd, Pt, or Ru supported by mesoporous Al-SBA-15	140	-	Diethyl phthalate	1.1
Guaiacyl dehydrogenation oligomers	K10 montmorillonite clay (Al <sub>2</sub> O <sub>3</sub> -4SiO <sub>2</sub> - xxH <sub>2</sub> O)/HCl	100	-	Low-molecular weight products	-

### 7.3 Conclusion

The depolymerization of isolated lignin from eucalyptus wood chips by organosolv fractionation and purification by alkaline precipitation pretreatment was studied. The catalysts MCM-41 and SBA-15 gave the highest yields of syringol, whereas doping  $\text{ZrO}_2$  on these catalysts did not improve the yields. The optimum reaction temperature was 300 °C, and changing the reaction solvent from water to methanol/water solution (50/50, wt/wt) further increased the yield of syringol. For the phosphate-based catalysts, the depolymerization in the presence of  $\text{CaP}_2\text{O}_6$  can be achieved the highest yields of syringol (16.7 wt.% (including syringol in aqueous phase, and extracted syringol from residue lignin)). The characteristic  $\text{CaP}_2\text{O}_6$  catalyst was well-crystallized; whereas, it has low surface area ca. 0.5  $\text{m}^2/\text{g}$  with relatively high acidity. The optimum reaction temperature was 300 °C, and changing the reaction solvent from water to methanol/water solution (50/50, wt/wt) also increased the yield of syringol.

## CHAPTER 8

### SUMMARY AND RECOMMENDATIONS

#### 8.1 Summary

This research specifically studied the transformation of organic compounds into eucalyptus wood chips to sugar and chemicals. Organosolv fractionation was applied as primary step to isolate eucalyptus wood chips to cellulose, hemicellulose, and lignin by one-step with. Then, cellulose and hemicellulose proportion were converted to C<sub>6</sub>- and C<sub>5</sub>-sugars via hydrolysis under hot-compressed water (HCW) condition. Lastly, isolated lignin from the fractionation process was decomposed to monomeric phenolic compounds via depolymerization reaction.

In detail, the single-step aqueous-organosolv process for the fractionation of the eucalyptus wood chips was carried out using a ternary mixture of MIBK:methanol:water with and without the addition of homogeneous and/or heterogeneous acid promoters. It can be concluded that the suitable condition for fractionation process was used eucalyptus wood weight to solvent mixture of 0.167, mixture of MIBK, methanol and water as solvent with the ratio of 25:42:33 (v/v), initial pressure of 20 bars, at 180°C for 60 min presence of 0.008 M H<sub>2</sub>SO<sub>4</sub>. In the presence of acid promoter *i.e.* H<sub>2</sub>SO<sub>4</sub>, higher fractionation performance was observed, from which 13.3% yield of lignin (43% of substrate), 12.2% yield of xylose, 4% yield of xylo-oligosaccharide (77% of substrate) can be extracted from eucalyptus wood chip. Importantly, synthesized solid acid catalyst (*i.e.* AC-H<sub>3</sub>PO<sub>4</sub>; activated carbon phosphonation) can also be applied in the fractionation process instead of H<sub>2</sub>SO<sub>4</sub>; from which the fractionation performance of AC-H<sub>3</sub>PO<sub>4</sub> is comparable to that of H<sub>2</sub>SO<sub>4</sub>. The benefit of AC-H<sub>3</sub>PO<sub>4</sub> is its reusability since the fractionation performance of the reused AC-H<sub>3</sub>PO<sub>4</sub> is identical to that of the fresh H<sub>2</sub>SO<sub>4</sub>. The solid promoters are thus attractive alternatives to the highly corrosive homogeneous acids.

For the hydrolysis, the sulfonated solid carbonaceous acid catalysts showed high hydrolysis performance as reflected by their high catalytic efficiency and selectivity under HCW. Compared to the conventional homogeneous acid catalysts, the developed SO<sub>3</sub>H-Suc can be recycled in consecutive batch process with lower loss of sugars via dehydration

reaction and would be less corrosive to the system, resulting in improved overall economic feasibility of the process. This study also revealed the necessity for biomass pretreatment and/or fractionation prior to the hydrothermal hydrolysis, from which significantly higher yields of sugar can be achieved. Importantly, AC-H<sub>3</sub>PO<sub>4</sub> also showed great hydrolysis performance under HCW, from which high sugar yields with low unwanted by-product formations comparable to sulfonated solid carbonaceous acid catalysts can be achieved. The great benefit of AC-H<sub>3</sub>PO<sub>4</sub> is possible use for both organosolv fractionation (as acid promoter) and hydrothermal hydrolysis (as acid catalyst), which provides high potential for combining fractionation and hydrolysis processes without intermediate material treatment required.

For lignin conversion, isolated lignin from the fractionation process (so-called organosolv lignin, OL) was further treated by alkaline precipitation process (so-called treated organosolv lignin, TOL) to enhance higher solubility in organic solvents (*i.e.* tetrahydrofuran, dimethyl sulfoxide, and methanol) for further benefit the conversion processes. From the characterizations, OL contained small amounts of contaminations (*e.g.* sugars, ash, and sulfur), which can be removed by alkaline precipitation treatment without causing any significant structural change. Elemental analysis indicated highest purity and highest molecular weight for TOL. Results from Mannich reactivity tests revealed that OL contains more active sites than TOL or SL. This may simply be because of the contaminants in OL reacting in the Mannich process, and not with the free C-3 and C-5 lignin sites. Nevertheless, high molecular weight and high residue solid of OL and TOL compared to soda lignin was observed, which probably specifies the presence of condensed lignin. The depolymerization of TOL was then studied.

It was revealed that the best mesostructured silica catalyst was SBA-15, which obtained the highest yield of total syringol of 23.0 wt.% (7.2 wt.% in aqueous fraction and 15.84 wt% in extracted residual lignin) with using a methanol-water mixture (50:50 wt/wt) as the solvent in the presence of high acidity at 300°C for 1 h. From the GC/MS analysis, the main components in aqueous fraction from the reaction in the presence of SBA-15 included high proportion of syringol (72.1 wt%) with slight formations of 1,2-benzenediol, benzaldehyde, and ethanone, whereas the main components extracted from residual lignin were syringol (17.2 wt%) with other multi-compound mixture of polymeric phenolic compounds and high molecular weight of lignin. In addition, the phosphate-based catalysts also were investigated. It was found that the additional CaP<sub>2</sub>O<sub>6</sub> in depolymerization

reaction under hydrothermal process achieved the highest yields of syringol (16.7 %w/w) without char formation (including syringol in aqueous phase, and extracted syringol from residue lignin). Moreover, the  $\text{CaP}_2\text{O}_6$  catalyst was characterized by the XRD analysis to confirm the  $\text{CaP}_2\text{O}_6$  crystalline phases of the catalyst samples, while acid strength of catalyst was in a range of  $+3.3 \leq H_0 \leq +4.8$ . The distribution of phenol products could obtain small molecular products, mainly consisting of five phenols: syringol, 1,2-benzendiol, benzoic acid, benzaldehyde, and ethanone. Overall, the work leads to improvement in lignocellulose conversion process for maximization of biomass utilization in integrated biorefinery applications. From this study, the processes of converting woody eucalyptus to sugar and chemicals can be summarized in **Figure 8.1**.

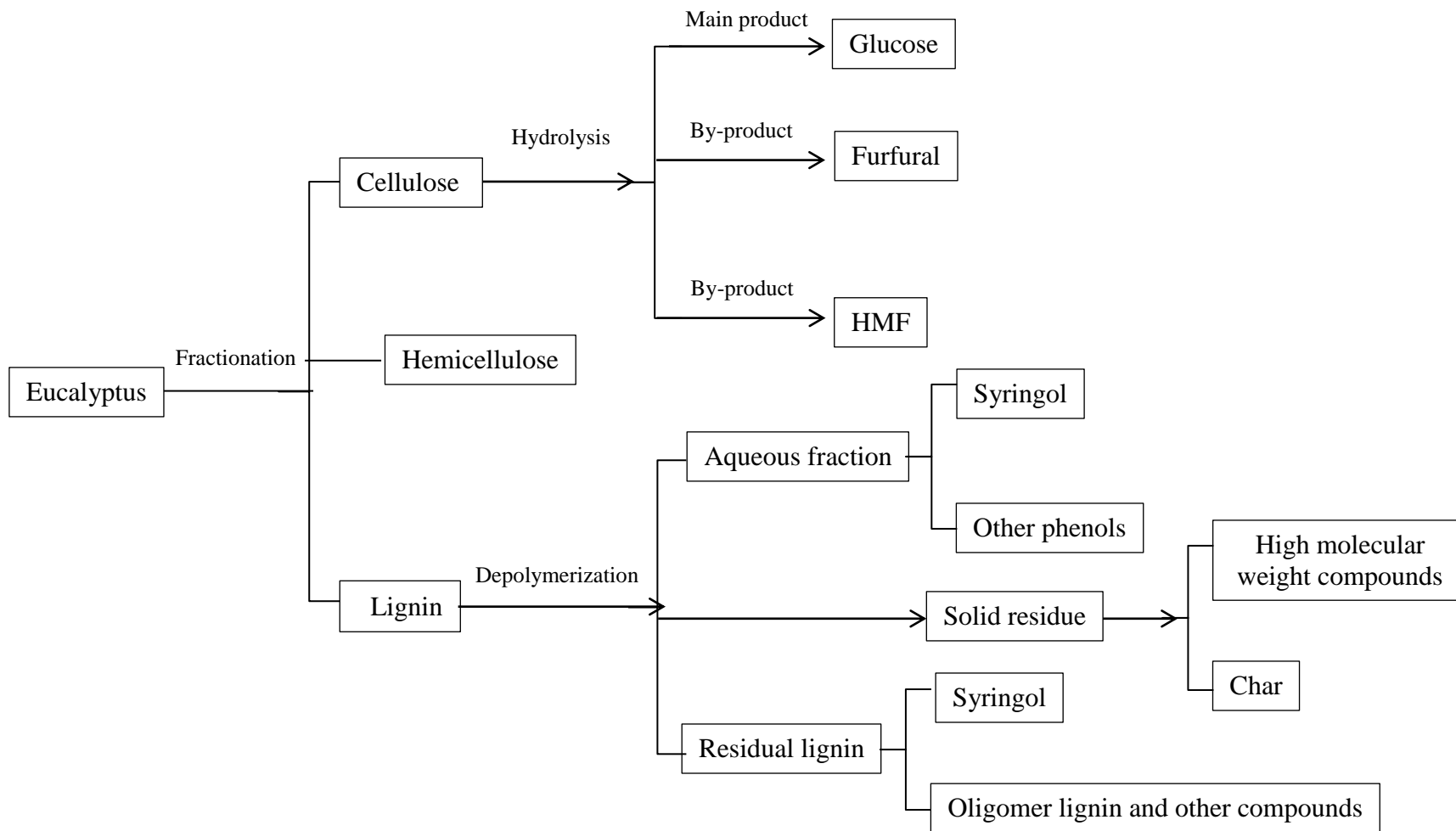


**Figure 8.1** Simplified reaction scheme for the conversion of the eucalyptus into sugars and chemicals.

## 8.2 Recommendations for further studies

- Further catalyst and acid promoter developments are required to improve the product yields from the reactions (*i.e.* fractionation, and hydrolysis) as well as to minimize the leaching of acid groups (*e.g.*,  $-\text{SO}_3\text{H}$ ,  $-\text{PO}_3\text{H}_2$ ) from the surface of carbon-based support (*i.e.* sugars and activated carbon) for prolonged testing.
- Types of solvent and operating conditions for organosolv fractionation should be further optimized to enhance higher yields of isolated lignin and hemicellulose.
- Detailed reaction mechanism of lignin depolymerization should be further investigated for providing a basis to improve phenol production yield.

## REFERENCES

- Aida, T.M., Tajima, K., Watanabe, M., Saito, Y., Kuroda, K., Nonaka, T., Hattori, H., Smith Jr, R.L., Arai, K. 2007. Reactions of d-fructose in water at temperatures up to 400 °C and pressures up to 100 MPa. *The Journal of Supercritical Fluids*, **42**(1), 110-119.
- Akim, L.G., Shevchenko, S.M., Zarubin, M.Y. 1993. <sup>13</sup>C NMR studies on lignins depolymerized with dry hydrogen iodide. *Wood Science and Technology*, **27**(4), 241-248.
- Almendros, G., Martinez, A.T., Gonzalez, A.E., Gonzalez-Vila, F.J., Freund, R., Luedemann, H.D. 1992. CPMAS carbon-13 NMR study of lignin preparations from wheat straw transformed by five lignocellulose-degrading fungi. *Journal of Agricultural and Food Chemistry*, **40**(7), 1297-1302.
- Alriols, M.G., García, A., Llano-ponte, R., Labidi, J. 2010. Combined organosolv and ultrafiltration lignocellulosic biorefinery process. *Chemical Engineering Journal*, **157**(1), 113-120.
- Amendola, D., De Faveri, D.M., Egues, I., Serrano, L., Labidi, J., Spigno, G. 2012. Autohydrolysis and organosolv process for recovery of hemicelluloses, phenolic compounds and lignin from grape stalks. *Bioresour Technol*, **107**, 267-74.
- Ando, H., Ohba, H., Sakaki, T., Takamine, K., Kamino, Y., Moriwaki, S., Bakalova, R., Uemura, Y., Hatate, Y. 2004. Hot-compressed-water decomposed products from bamboo manifest a selective cytotoxicity against acute lymphoblastic leukemia cells. *Toxicology in Vitro*, **18**(6), 765-771.
- Asghari, F.S., Yoshida, H. 2006. Dehydration of fructose to 5-hydroxymethylfurfural in sub-critical water over heterogeneous zirconium phosphate catalysts. *Carbohydrate Research*, **341**(14), 2379-2387.
- Bai, Y.Y., Xiao, L.P., Shi, Z.J., Sun, R.C. 2013. Structural variation of bamboo lignin before and after ethanol organosolv pretreatment. *Int J Mol Sci*, **14**(11), 21394-413.
- Barbier, J., Charon, N., Dupassieux, N., Loppinet-Serani, A., Mahé, L., Ponthus, J., Courtiade, M., Ducrozet, A., Quoineaud, A.-A., Cansell, F. 2012. Hydrothermal conversion of lignin compounds. A detailed study of fragmentation and condensation reaction pathways. *Biomass and Bioenergy*, **46**, 479-491.

- Bauer, S., Sorek, H., Mitchell, V.D., Ibanez, A.B., Wemmer, D.E. 2012. Characterization of *Miscanthus giganteus* lignin isolated by ethanol organosolv process under reflux condition. *J Agric Food Chem*, **60**(33), 8203-12.
- Bautista, F.M., Campelo, J.M., García, A., Luna, D., Marinas, J.M., Quirós, R.A., Romero, A.A. 2003. Influence of acid–base properties of catalysts in the gas-phase dehydration–dehydrogenation of cyclohexanol on amorphous AlPO<sub>4</sub> and several inorganic solids. *Applied Catalysis A: General*, **243**(1), 93-107.
- Beauchet, R., Monteil-Rivera, F., Lavoie, J.M. 2012. Conversion of lignin to aromatic-based chemicals (L-chems) and biofuels (L-fuels). *Bioresour Technol*, **121**, 328-34.
- Berlyn, G. 1972. Lignins: Occurrence, Formation, Structure and Reactions by K. V. SARKANEN; C. H. Ludwig. *American Scientist*, **60**(4), 506-507.
- Billingham, J., Breen, C., Yarwood, J. 1997. Adsorption of polyamine, polyacrylic acid and polyethylene glycol on montmorillonite: An in situ study using ATR-FTIR. *Vibrational Spectroscopy*, **14**(1), 19-34.
- Boeriu, C.G., Bravo, D., Gosselink, R.J.A., van Dam, J.E.G. 2004. Characterisation of structure-dependent functional properties of lignin with infrared spectroscopy. *Industrial Crops and Products*, **20**(2), 205-218.
- Boerjan, W., Ralph, J., Baucher, M. 2003. LIGNIN BIOSYNTHESIS. *Annual Review of Plant Biology*, **54**(1), 519-546.
- Bozell, J.J., Black, S.K., Myers, M., Cahill, D., Miller, W.P., Park, S. 2011a. Solvent fractionation of renewable woody feedstocks: Organosolv generation of biorefinery process streams for the production of biobased chemicals. *Biomass and Bioenergy*, **35**(10), 4197-4208.
- Bozell, J.J., O'Lenick, C.J., Warwick, S. 2011b. Biomass fractionation for the biorefinery: heteronuclear multiple quantum coherence-nuclear magnetic resonance investigation of lignin isolated from solvent fractionation of switchgrass. *J Agric Food Chem*, **59**(17), 9232-42.
- Bozell, J.J., Petersen, G.R. 2010. Technology development for the production of biobased products from biorefinery carbohydrates—the US Department of Energy's "Top 10" revisited. *Green Chemistry*, **12**(4), 539.
- Brebu, M., Tamminen, T., Spiridon, I. 2013. Thermal degradation of various lignins by TG-MS/FTIR and Py-GC-MS. *Journal of Analytical and Applied Pyrolysis*, **104**(0), 531-539.

- Brethauer, S., Wyman, C.E. 2010. Review: Continuous hydrolysis and fermentation for cellulosic ethanol production. *Bioresource Technology*, **101**(13), 4862-4874.
- Brudecki, G., Cybulska, I., Rosentrater, K. 2013. Optimization of clean fractionation process applied to switchgrass to produce pulp for enzymatic hydrolysis. *Bioresour Technol*, **131**, 101-12.
- Buranov, A.U., Mazza, G. 2012. Fractionation of flax shives with pressurized aqueous ethanol. *Industrial Crops and Products*, **35**(1), 77-87.
- Casas, A., Oliet, M., Alonso, M.V., Rodríguez, F. 2012. Dissolution of *Pinus radiata* and *Eucalyptus globulus* woods in ionic liquids under microwave radiation: Lignin regeneration and characterization. *Separation and Purification Technology*, **97**(0), 115-122.
- Chang, V., Holtzapfle, M. 2000. Fundamental factors affecting biomass enzymatic reactivity. *Applied Biochemistry and Biotechnology*, **84-86**(1-9), 5-37.
- Chareonlimkun, A., Champreda, V., Shotipruk, A., Laosiripojana, N. 2010. Reactions of C5 and C6-sugars, cellulose, and lignocellulose under hot compressed water (HCW) in the presence of heterogeneous acid catalysts. *Fuel*, **89**(10), 2873-2880.
- Corma, A., Iborra, S., Velty, A. 2007. Chemical Routes for the Transformation of Biomass into Chemicals. *Chemical Reviews*, **107**(6), 2411-2502.
- Cybulska, I., Brudecki, G., Rosentrater, K., Lei, H., Julson, J. 2012. Catalyzed modified clean fractionation of prairie cordgrass integrated with hydrothermal post-treatment. *Biomass and Bioenergy*, **46**, 389-401.
- Cybulska, I., Brudecki, G.P., Hankerson, B.R., Julson, J.L., Lei, H. 2013. Catalyzed modified clean fractionation of switchgrass. *Bioresour Technol*, **127**, 92-9.
- Daorattanachai, P., Khemthong, P., Viriya-Empikul, N., Laosiripojana, N., Faungnawakij, K. 2012. Conversion of fructose, glucose, and cellulose to 5-hydroxymethylfurfural by alkaline earth phosphate catalysts in hot compressed water. *Carbohydr Res*, **363**, 58-61.
- de la Torre, M.J., Moral, A., Hernández, M.D., Cabeza, E., Tijero, A. 2013. Organosolv lignin for biofuel. *Industrial Crops and Products*, **45**, 58-63.
- Dedsuksophon, W., Faungnawakij, K., Champreda, V., Laosiripojana, N. 2011. Hydrolysis/dehydration/aldol-condensation/hydrogenation of lignocellulosic biomass and biomass-derived carbohydrates in the presence of Pd/WO<sub>3</sub>-ZrO<sub>2</sub> in a single reactor. *Bioresour Technol*, **102**(2), 2040-6.

- Deepa, A.K., Dhepe, P.L. 2014. Solid acid catalyzed depolymerization of lignin into value added aromatic monomers. *RSC Advances*, **4**(25), 12625-12629.
- Dinjus, E., Kruse, A. 2007. Applications of Supercritical Water. in: *High Pressure Chemistry*, Wiley-VCH Verlag GmbH, pp. 422-446.
- Domínguez, J.C., Oliet, M., Alonso, M.V., Gilarranz, M.A., Rodríguez, F. 2008. Thermal stability and pyrolysis kinetics of organosolv lignins obtained from *Eucalyptus globulus*. *Industrial Crops and Products*, **27**(2), 150-156.
- El Hage, R., Brosse, N., Chrusciel, L., Sanchez, C., Sannigrahi, P., Ragauskas, A. 2009. Characterization of milled wood lignin and ethanol organosolv lignin from miscanthus. *Polymer Degradation and Stability*, **94**(10), 1632-1638.
- El Hage, R., Brosse, N., Sannigrahi, P., Ragauskas, A. 2010. Effects of process severity on the chemical structure of Miscanthus ethanol organosolv lignin. *Polymer Degradation and Stability*, **95**(6), 997-1003.
- El Mansouri, N.-E., Salvadó, J. 2007. Analytical methods for determining functional groups in various technical lignins. *Industrial Crops and Products*, **26**(2), 116-124.
- Garrote, G., Domínguez, H., Parajó, J.C. 2001. Generation of xylose solutions from *Eucalyptus globulus* wood by autohydrolysis–posthydrolysis processes: posthydrolysis kinetics. *Bioresource Technology*, **79**(2), 155-164.
- Gedon, S., Fengi, R. 2000. Cellulose Esters, Organic Esters. in: *Kirk-Othmer Encyclopedia of Chemical Technology*, John Wiley & Sons, Inc.
- Gírio, F.M., Fonseca, C., Carvalheiro, F., Duarte, L.C., Marques, S., Bogel-Lukasik, R. 2010. Hemicelluloses for fuel ethanol: A review. *Bioresource Technology*, **101**(13), 4775-4800.
- González, M., Tejado, Á., Peña, C., Labidi, J. 2008. Organosolv Pulping Process Simulations. *Industrial & Engineering Chemistry Research*, **47**(6), 1903-1909.
- Gosselink, R.J.A., Abächerli, A., Semke, H., Malherbe, R., Käuper, P., Nadif, A., van Dam, J.E.G. 2004. Analytical protocols for characterisation of sulphur-free lignin. *Industrial Crops and Products*, **19**(3), 271-281.
- Gu, M., Yu, D., Zhang, H., Sun, P., Huang, H. 2009. Metal (IV) Phosphates as Solid Catalysts for Selective Dehydration of Sorbitol to Isosorbide. *Catalysis Letters*, **133**(1-2), 214-220.

- Guo, F., Fang, Z., Xu, C.C., Smith, R.L. 2012. Solid acid mediated hydrolysis of biomass for producing biofuels. *Progress in Energy and Combustion Science*, **38**(5), 672-690.
- Hara, M. 2010. Biomass conversion by a solid acid catalyst. *Energy & Environmental Science*, **3**(5), 601.
- Harmsen, P. 2010. *Literature Review of Physical and Chemical Pretreatment Processes for Lignocellulosic Biomass*. Wageningen UR, Food & Biobased Research.
- Heitner, C., Dimmel, D., Schmidt, J. 2010. Lignin and Lignans : Advances in Chemistry. 1 ed, Taylor and Francis. Hoboken.
- Huijgen, W.J.J., Reith, J.H., den Uil, H. 2010. Pretreatment and Fractionation of Wheat Straw by an Acetone-Based Organosolv Process. *Industrial & Engineering Chemistry Research*, **49**(20), 10132-10140.
- Ibarra, D., del Río, J.C., Gutiérrez, A., Rodríguez, I.M., Romero, J., Martínez, M.J., Martínez, Á.T. 2005. Chemical characterization of residual lignins from eucalypt paper pulps. *Journal of Analytical and Applied Pyrolysis*, **74**(1-2), 116-122.
- Imman, S., Arnthong, J., Burapatana, V., Laosiripojana, N., Champreda, V. 2013. Autohydrolysis of tropical agricultural residues by compressed liquid hot water pretreatment. *Appl Biochem Biotechnol*, **170**(8), 1982-95.
- Jeong, T.S., Choi, C.H., Lee, J.Y., Oh, K.K. 2012. Behaviors of glucose decomposition during acid-catalyzed hydrothermal hydrolysis of pretreated *Gelidium amansii*. *Bioresour Technol*, **116**, 435-40.
- Jiménez, L., de la Torre, M.J., Bonilla, J.L., Ferrer, J.L. 1998. Organosolv pulping of wheat straw by use of acetone-water mixtures. *Process Biochemistry*, **33**(4), 401-408.
- Johansson, A., Aaltonen, O., Ylinen, P. 1987. Organosolv pulping — methods and pulp properties. *Biomass*, **13**(1), 45-65.
- Joseph, L.M., Aminul, I. 1999. Lignin Chemistry, Technology, and Utilization: A Brief History. in: *Lignin: Historical, Biological, and Materials Perspectives*, Vol. 742, American Chemical Society, pp. 2-99.
- Kamm, B., Kamm, M. 2004. Principles of biorefineries. *Appl Microbiol Biotechnol*, **64**(2), 137-45.
- Kang, S., Li, X., Fan, J., Chang, J. 2013. Hydrothermal conversion of lignin: A review. *Renewable and Sustainable Energy Reviews*, **27**, 546-558.

- Karimi, K., Kheradmandinia, S., Taherzadeh, M.J. 2006. Conversion of rice straw to sugars by dilute-acid hydrolysis. *Biomass and Bioenergy*, **30**(3), 247-253.
- Khemthong, P., Daorattanachai, P., Laosiripojana, N., Faungnawakij, K. 2012. Copper phosphate nanostructures catalyze dehydration of fructose to 5-hydroxymethylfurfural. *Catalysis Communications*, **29**, 96-100.
- Kleinert, M., Gasson, J.R., Barth, T. 2009. Optimizing solvolysis conditions for integrated depolymerisation and hydrodeoxygenation of lignin to produce liquid biofuel. *Journal of Analytical and Applied Pyrolysis*, **85**(1-2), 108-117.
- Klinke, H.B., Ahring, B.K., Schmidt, A.S., Thomsen, A.B. 2002. Characterization of degradation products from alkaline wet oxidation of wheat straw. *Bioresource Technology*, **82**(1), 15-26.
- Kumar, P., Barrett, D.M., Delwiche, M.J., Stroeve, P. 2009. Methods for Pretreatment of Lignocellulosic Biomass for Efficient Hydrolysis and Biofuel Production. *Industrial & Engineering Chemistry Research*, **48**(8), 3713-3729.
- Lan, W., Liu, C.F., Sun, R.C. 2011. Fractionation of bagasse into cellulose, hemicelluloses, and lignin with ionic liquid treatment followed by alkaline extraction. *J Agric Food Chem*, **59**(16), 8691-701.
- Lanzafame, P., Temi, D.M., Perathoner, S., Spadaro, A.N., Centi, G. 2012. Direct conversion of cellulose to glucose and valuable intermediates in mild reaction conditions over solid acid catalysts. *Catalysis Today*, **179**(1), 178-184.
- Laurichesse, S., Avérous, L. 2014. Chemical modification of lignins: Towards biobased polymers. *Progress in Polymer Science*, **39**(7), 1266-1290.
- Lavoie, J.-M., Baré, W., Bilodeau, M. 2011. Depolymerization of steam-treated lignin for the production of green chemicals. *Bioresource Technology*, **102**(7), 4917-4920.
- Lenihan, P., Orozco, A., O'Neill, E., Ahmad, M.N.M., Rooney, D.W., Walker, G.M. 2010. Dilute acid hydrolysis of lignocellulosic biomass. *Chemical Engineering Journal*, **156**(2), 395-403.
- Liguori, L., Barth, T. 2011. Palladium-Nafion SAC-13 catalysed depolymerisation of lignin to phenols in formic acid and water. *Journal of Analytical and Applied Pyrolysis*, **92**(2), 477-484.
- Lora, J.H., Glasser, W.G. 2002. Recent Industrial Applications of Lignin: A Sustainable Alternative to Nonrenewable Materials. *Journal of Polymers and the Environment*, **10**(1-2), 39-48.

- Mansouri, N.-E.E., Salvadó, J. 2006. Structural characterization of technical lignins for the production of adhesives: Application to lignosulfonate, kraft, soda-anthraquinone, organosolv and ethanol process lignins. *Industrial Crops and Products*, **24**(1), 8-16.
- Minowa, T., Inoue, S. 1999. Hydrogen production from biomass by catalytic gasification in hot compressed water. *Renewable Energy*, **16**(1-4), 1114-1117.
- Mosier, N., Wyman, C., Dale, B., Elander, R., Lee, Y.Y., Holtzapfle, M., Ladisch, M. 2005. Features of promising technologies for pretreatment of lignocellulosic biomass. *Bioresource Technology*, **96**(6), 673-686.
- Mousavioun, P., Doherty, W.O.S., George, G. 2010. Thermal stability and miscibility of poly(hydroxybutyrate) and soda lignin blends. *Industrial Crops and Products*, **32**(3), 656-661.
- Mousavioun, P., George, G.A., Doherty, W.O.S. 2012. Environmental degradation of lignin/poly(hydroxybutyrate) blends. *Polymer Degradation and Stability*, **97**(7), 1114-1122.
- Nguyen, T.D.H., Maschietti, M., Belkheiri, T., Åmand, L.-E., Theliander, H., Vamling, L., Olausson, L., Andersson, S.-I. 2014. Catalytic depolymerisation and conversion of Kraft lignin into liquid products using near-critical water. *The Journal of Supercritical Fluids*, **86**, 67-75.
- Nigam, P., Singh, D. 1995. *Process. Biochem.*, **30**, 117.
- Onda, A., Ochi, T., Yanagisawa, K. 2009. Hydrolysis of Cellulose Selectively into Glucose Over Sulfonated Activated-Carbon Catalyst Under Hydrothermal Conditions. *Topics in Catalysis*, **52**(6-7), 801-807.
- Palmqvist, E., Hahn-Hagerdal, B. 2000. Fermentation of lignocellulosic hydrolysates. II: inhibitors and mechanisms of inhibition. *Bioresource Technology*, **74**(1), 25-33.
- Pandey, K.K. 1999. A study of chemical structure of soft and hardwood and wood polymers by FTIR spectroscopy. *Journal of Applied Polymer Science*, **71**(12), 1969-1975.
- Pandey, M.P., Kim, C.S. 2011. Lignin Depolymerization and Conversion: A Review of Thermochemical Methods. *Chemical Engineering & Technology*, **34**(1), 29-41.
- Patil, P.T., Armbruster, U., Martin, A. 2014. Hydrothermal liquefaction of wheat straw in hot compressed water and subcritical water-alcohol mixtures. *The Journal of Supercritical Fluids*, **93**, 121-129.

- Pińkowska, H., Wolak, P., Złocińska, A. 2011. Hydrothermal decomposition of xylan as a model substance for plant biomass waste – Hydrothermolysis in subcritical water. *Biomass and Bioenergy*, **35**(9), 3902-3912.
- Pronyk, C., Mazza, G. 2012. Fractionation of triticale, wheat, barley, oats, canola, and mustard straws for the production of carbohydrates and lignins. *Bioresour Technol*, **106**, 117-24.
- Rencoret, J., Gutierrez, A., Nieto, L., Jimenez-Barbero, J., Faulds, C.B., Kim, H., Ralph, J., Martinez, A.T., Del Rio, J.C. 2011. Lignin composition and structure in young versus adult Eucalyptus globulus plants. *Plant Physiol*, **155**(2), 667-82.
- Roberts, V.M., Stein, V., Reiner, T., Lemonidou, A., Li, X., Lercher, J.A. 2011. Towards quantitative catalytic lignin depolymerization. *Chemistry*, **17**(21), 5939-48.
- Romani, A., Garrote, G., Lopez, F., Parajo, J.C. 2011. Eucalyptus globulus wood fractionation by autohydrolysis and organosolv delignification. *Bioresour Technol*, **102**(10), 5896-904.
- Romaní, A., Garrote, G., López, F., Parajó, J.C. 2011. Eucalyptus globulus wood fractionation by autohydrolysis and organosolv delignification. *Bioresource Technology*, **102**(10), 5896-5904.
- Romaní, A., Ruiz, H.A., Pereira, F.B., Domingues, L., Teixeira, J.A. 2013. Fractionation of Eucalyptus globulus Wood by Glycerol–Water Pretreatment: Optimization and Modeling. *Industrial & Engineering Chemistry Research*, **52**(40), 14342-14352.
- Rubin, E.M. 2008. Genomics of cellulosic biofuels. *Nature*, **454**(7206), 841-845.
- Sanchez, G., Pilcher, L., Roslander, C., Modig, T., Galbe, M., Liden, G. 2004. Dilute-acid hydrolysis for fermentation of the Bolivian straw material Paja Brava. *Bioresource Technology*, **93**(3), 249-256.
- Sannigrahi, P., Ragauskas, A.J. 2013. Fundamentals of Biomass Pretreatment by Fractionation. in: *Aqueous Pretreatment of Plant Biomass for Biological and Chemical Conversion to Fuels and Chemicals*, John Wiley & Sons, Ltd, pp. 201-222.
- Sarkanen, S., Teller, D.C., Abramowski, E., McCarthy, J.L. 1982. Lignin. 19. Kraft lignin component conformation and associated complex configuration in aqueous alkaline solution. *Macromolecules*, **15**(4), 1098-1104.
- Sasaki, M., Takahashi, K., Haneda, Y., Satoh, H., Sasaki, A., Narumi, A., Satoh, T., Kakuchi, T., Kaga, H. 2008. Thermochemical transformation of glucose to 1,6-

- anhydroglucose in high-temperature steam. *Carbohydrate Research*, **343**(5), 848-854.
- Sharma, R.K., Wooten, J.B., Baliga, V.L., Lin, X., Geoffrey Chan, W., Hajaligol, M.R. 2004. Characterization of chars from pyrolysis of lignin. *Fuel*, **83**(11–12), 1469-1482.
- Shukry, N., Fadel, S.M., Agblevor, F.A., El-Kalyoubi, S.F. 2008. Some physical properties of acetosolv lignins from bagasse. *Journal of Applied Polymer Science*, **109**(1), 434-444.
- Singh, S.K., Ekhe, J.D. 2014. Towards effective lignin conversion: HZSM-5 catalyzed one-pot solvolytic depolymerization/hydrodeoxygenation of lignin into value added compounds. *RSC Advances*, **4**(53), 27971-27978.
- Sluiter, J.B., Ruiz, R.O., Scarlata, C.J., Sluiter, A.D., Templeton, D.W. 2010. Compositional Analysis of Lignocellulosic Feedstocks. 1. Review and Description of Methods. *Journal of Agricultural and Food Chemistry*, **58**(16), 9043-9053.
- Suganuma, S., Nakajima, K., Kitano, M., Yamaguchi, D., Kato, H., Hayashi, S., Hara, M. 2010. Synthesis and acid catalysis of cellulose-derived carbon-based solid acid. *Solid State Sciences*, **12**(6), 1029-1034.
- Sun, Y., Cheng, J. 2002. Hydrolysis of lignocellulosic materials for ethanol production: a review. *Bioresource Technology*, **83**(1), 1-11.
- Tamthientrong N., L.N., Ruanglek V., Champreda V., Assabumrungrat S., Wiyarath W., Jongsomjit B. 2011. Sugar production from the hydrolysis of biomass under hot compressed-water in the presence of solid acid catalysts. *Thesis of The Joint Graduate School of Energy and Environment Thailand*.
- Thring, R.W., Chornet, E., Bouchard, J., Vidal, P.F., Overend, R.P. 1990. Characterization of lignin residues derived from the alkaline hydrolysis of glycol lignin. *Canadian Journal of Chemistry*, **68**(1), 82-89.
- Toledano, A., Serrano, L., Labidi, J. 2012. Organosolv lignin depolymerization with different base catalysts. *Journal of Chemical Technology & Biotechnology*, **87**(11), 1593-1599.
- Toor, S.S., Rosendahl, L., Rudolf, A. 2011. Hydrothermal liquefaction of biomass: A review of subcritical water technologies. *Energy*, **36**(5), 2328-2342.
- Van de Vyver, S., Geboers, J., Jacobs, P.A., Sels, B.F. 2011. Recent Advances in the Catalytic Conversion of Cellulose. *ChemCatChem*, **3**(1), 82-94.

- Vanholme, R., Demedts, B., Morreel, K., Ralph, J., Boerjan, W. 2010. Lignin Biosynthesis and Structure. *Plant Physiology*, **153**(3), 895-905.
- Vila, C., Santos, V., Parajó, J.C. 2002. Simulation of an Organosolv Pulping Process: Generalized Material Balances and Design Calculations. *Industrial & Engineering Chemistry Research*, **42**(2), 349-356.
- Wang, H., Tucker, M., Ji, Y. 2013. Recent Development in Chemical Depolymerization of Lignin: A Review. *Journal of Applied Chemistry*, **2013**, 1-9.
- Wang, K., Yang, H., Guo, S., Tang, Y., Jiang, J., Xu, F., Sun, R.-C. 2012. Organosolv fractionation process with various catalysts for improving bioconversion of triploid poplar. *Process Biochemistry*, **47**(10), 1503-1509.
- Warner, G., Hansen, T.S., Riisager, A., Beach, E.S., Barta, K., Anastas, P.T. 2014a. Depolymerization of organosolv lignin using doped porous metal oxides in supercritical methanol. *Bioresour Technol*, **161**, 78-83.
- Warner, G., Hansen, T.S., Riisager, A., Beach, E.S., Barta, K., Anastas, P.T. 2014b. Depolymerization of organosolv lignin using doped porous metal oxides in supercritical methanol. *Bioresour Technol*, **161C**, 78-83.
- Watanabe, M., Inomata, H., Osada, M., Sato, T., Adschiri, T., Arai, K. 2003. *Fuel*, **82**, 545.
- Wikberg, H., Liisa Maunu, S. 2004. Characterisation of thermally modified hard- and softwoods by <sup>13</sup>C CPMAS NMR. *Carbohydrate Polymers*, **58**(4), 461-466.
- Wildschut, J., Smit, A.T., Reith, J.H., Huijgen, W.J. 2013. Ethanol-based organosolv fractionation of wheat straw for the production of lignin and enzymatically digestible cellulose. *Bioresour Technol*, **135**, 58-66.
- Xu, W., Miller, S.J., Agrawal, P.K., Jones, C.W. 2012. Depolymerization and hydrodeoxygenation of switchgrass lignin with formic acid. *ChemSusChem*, **5**(4), 667-75.
- Yamaguchi, D., Hara, M. 2010. Starch saccharification by carbon-based solid acid catalyst. *Solid State Sciences*, **12**(6), 1018-1023.
- Yamaguchi, D., Kitano, M., Suganuma, S., Nakajima, K., Kato, H., Hara, M. 2009. Hydrolysis of Cellulose by a Solid Acid Catalyst under Optimal Reaction Conditions. *The Journal of Physical Chemistry C*, **113**(8), 3181-3188.
- Yang, H., Yan, R., Chen, H., Lee, D.H., Zheng, C. 2007. Characteristics of hemicellulose, cellulose and lignin pyrolysis. *Fuel*, **86**(12-13), 1781-1788.

- Yu, Y., Lou, X., Wu, H.W. 2008. Some recent advances in hydrolysis of biomass in hot-compressed, water and its comparisons with other hydrolysis methods. *ENERGY & FUELS*, **22**(1), 46-60.
- Zakzeski, J., Bruijninx, P.C.A., Jongerius, A.L., Weckhuysen, B.M. 2010. The Catalytic Valorization of Lignin for the Production of Renewable Chemicals. *Chemical Reviews*, **110**(6), 3552-3599.
- Zakzeski, J., Jongerius, A.L., Bruijninx, P.C., Weckhuysen, B.M. 2012. Catalytic lignin valorization process for the production of aromatic chemicals and hydrogen. *ChemSusChem*, **5**(8), 1602-9.
- Zhou, C.H., Xia, X., Lin, C.X., Tong, D.S., Beltramini, J. 2011. Catalytic conversion of lignocellulosic biomass to fine chemicals and fuels. *Chem Soc Rev*, **40**(11), 5588-617.
- Zhou, X.-F. 2014. Conversion of kraft lignin under hydrothermal conditions. *Bioresource Technology*, **170**(0), 583-586.

**APPENDIX  
LIST OF PUBLICATIONS**

## LIST OF PUBLICATIONS

### 1. International Journals

- No.1 Thepparat Klamrassamee, Verawat Champreda, Vasimon Ruanglek, Navadol Laosiripojana. 2013. Comparison of homogeneous and heterogeneous acid promoters in single-step aqueous-organosolv fractionation of eucalyptus wood chips. *Bioresource Technology*, 147, 276-84. (IF-2013: 5.039).
- No.2 Thepparat Klamrassamee, Navadol Laosiripojana, Dylan Cronin, Lalehvasht Moghaddam, Zhanying Zhang, William O. S. Doherty. 2015. Effects of mesostructured silica catalysts on the depolymerization of organosolv lignin fractionated from woody eucalyptus. *Bioresource Technology*, 180, 222-29. (IF-2013: 5.039).

#### Research topics have been submitted for publication

- No.1 Thepparat Klamrassamee, Nutrada Tamthiengtrong, Verawat Champreda, Navadol Laosiripojana. Hydrolysis of pretreated and non-pretreated woody eucalyptus under hot compressed water in the presence of sulfonated carbon-based catalysts
- No.2 Thepparat Klamrassamee, Navadol Laosiripojana, Dylan Cronin, Lalehvasht Moghaddam, William O. S. Doherty. Examine the poor solubility of lignin produced by a single-step aqueous-organosolv fractionation of eucalyptus wood chips.
- No.3 Thepparat Klamrassamee, Navadol Laosiripojana, William O. S. Doherty. Production of phenols from organosolv lignin fractionated woody eucalyptus via depolymerization reaction in the presence of phosphate-based catalysts.

### 2. International Conferences

- No.1 T. Klamrassamee, V. Champreda, V. Ruanglek, S. Assabumrungrat, N. Laosiripojana, Effect of Solvent Type and Acid Adding on Lignin Removal from Eucalyptus Wood Chips via Organosolv Process. AEDCEE 2013: International Conference on Alternative Energy in Developing Countries and Emerging Economics 30-31 May 2013, Bangkok, Thailand.

- No.2 T. Klamrassamee, V. Champreda, W. Wiyarath, and N. Laosiripojana, Comparison of Fractionated Eucalyptus in Organic Solvent Subsequence Hydrolysis Reaction to Sugar Hydrolysis. ICABC 2014: International Conference on Advance in Biology and Chemistry 29-31 July, 2014, Hong Kong.
- No.3 Thepparat Klamrassamee, Navadol Laosiripojana, Dylan Cronin, Lalehvasht Moghaddam, William O.S. Doherty, Characterization of Lignin Extracted from Eucalyptus Wood Chip by Organosolv and subsequent alkaline precipitation processes. SEE 2014: International Conference on Sustainable Energy and Environment Science, Technology, and Innovation for Asean Green Growth 19-21 November, 2014, Bangkok, Thailand.